Neuronal Circuits and Reinforcement Mechanisms Underlying Feeding Behaviour

Zhen Fang Huang Cao

University of Cambridge

Department of Pharmacology

Sidney Sussex College

This dissertation is submitted to the University of Cambridge in accordance with the requirements of the degree of Doctor of Philosophy in the School of the Biological Sciences

Submitted on 30th of September 2014

Summary

**Neuronal Circuits and Reinforcement
Mechanisms Underlying Feeding Behaviour**

By Zhen Fang Huang Cao

Animal survival depends on the brain's ability to detect the energetic state of the body and to alter behaviour in order to maintain homeostasis. Current research in the control of food consumption stresses the importance of identifying and establishing the specific roles of homeostatic neurons, which sense the body's energetic state and elicit complex and flexible food seeking behaviours. Recent developments in optogenetics, molecular genetics, and anatomical techniques have made these investigations possible at the resolution of specific cell types and circuits. These neurons are of particular interest because they serve as key entry points to the identification of downstream circuits and reinforcement mechanisms that control feeding behaviour. This dissertation probes the role of two kinds of homeostatic neurons— agouti-related peptide (AGRP) in the arcuate nucleus (ARC) and leptin receptor (LepRb) neurons in the lateral hypothalamic area (LHA)—in the control of food intake.

First, I examined the role of LepRb neurons in the LHA in feeding. Results from electrophysiological studies indicate that these neurons consist of a subpopulation of homeostatic sensing LHA γ-aminobutyric acid (GABA) expressing neurons. In addition to their response to leptin, these neurons are capable of modulating their activity in response to changes in glucose levels, further substantiating their role as homeostatic sensing neurons. Behavioural studies using optogenetic activation of these neurons show that their elevated activity is capable of reducing body weight, although their role in modulating feeding remains unclear.

Second, I investigated the reinforcement mechanisms employed by AGRP neurons to elicit voracious food consumption and increased willingness to work for food. Conditioned place avoidance studies under optogenetic activation of AGRP

neurons reveal that their increased activity has negative valence and is avoided. In addition, imposition of elevated AGRP neuron activity in an operant task reduced instrumental food seeking with particular sensitivity under high effort requirements. Taken together, these results suggest that AGRP neurons employ a negative reinforcement teaching signal to direct action selection during food seeking and consumption.

Third, I systematically analyzed the contribution of specific AGRP neuron projection subpopulations in AGRP neuron mediated evoked-feeding behaviour. Optogenetic activation studies of AGRP neuron axons in downstream projection regions indicate that several, but not all, subpopulations are capable of independently evoke food consumption. This work reveals a parallel and redundant functional circuit organization for AGRP neurons in the control of food intake. Interestingly, all AGRP neuron subpopulations examined displayed similar modulation by states of energy deficit and signals of starvation, despite their apparent divergence in function.

As a whole, this dissertation extends our understanding of the role of homeostatic neurons in food consumption and uncovers previously unappreciated functional organization and reinforcement mechanisms employed by neuronal circuits that control feeding behaviour.

Declarations

I hereby declare that this dissertation entitled "Neuronal Circuits and Reinforcement Mechanisms Underlying Feeding Behaviour" is the result of my own work and includes nothing which is the outcome of work done in collaboration with others, except where specifically indicated under the Contributions by Collaborators section.

The research in this dissertation was carried out at the Department of Pharmacology, University of Cambridge, under the supervision of Dr. Denis Burdakov and Dr. John Apergis–Schoute; and at Howard Hughes Medical Institute's Janelia Farm Research Campus, under the supervision of Dr. Scott Sternson.

This dissertation does not exceed the word limit set by the School of the Biological Sciences of 60,000 words. The results presented in this thesis were obtained between October 2010 and July 2014, and have not been submitted for any other degree or diploma.

Parts of this dissertation have been published as the following journal articles and conference abstracts:

1. Betley JN*, Huang Cao ZF*, Gong R, Magnus CJ, Sternson SM (2014) Homeostatic neurons for hunger and thirst transmit a negative reinforcement teaching signal. *In review.* (*equal contribution)

2. Betley JN*, Huang Cao ZF*, Ritola KD, Sternson SM (2013) Parallel, redundant circuit organization for homeostatic control of feeding behaviour. *Cell* Dec 5, 155(6): 1337-1350. (*equal contribution)

3. Sternson SM, Betley JN, Huang Cao ZF (2013) Neural circuits and motivational processes for hunger. *Current Opinion in Neurobiology* June, 23(3): 353-360.

4. Huang Cao ZF, Burdakov D, Sarnyai Z (2011) Optogenetics: potentials for addiction research. *Addiction Biology* Oct, 16(4): 519-531.

5. Huang Cao ZF, Betley JN, Sternson SM (2014) A role for negative reinforcement in AGRP neuron-mediated instrumental food seeking. Society for Neuroscience Annual Meeting, Washington DC 2014 (Poster 267.05)

6. Huang Cao ZF, Betley JN, Sternson SM (2013) Anatomical and functional evaluation of AGRP neurons reveals a novel circuit node for feeding. Synapses: from molecules to circuits and behaviour, Cold Spring Harbor Laboratories (Poster).

_____

Zhen Fang Huang Cao

Contributions by Collaborators

Contributions of collaborator to datasets presented in this dissertation are as follows:

Chapter 4

- Datasets shown in section 4.3.2 (Figure 4.6) were collected with the aid of Nicholas J. Betley, where ~50% of the data was collected by him.

- Breeding of all experimental animals used was performed by Janelia Farm Animal Breeding staff.

- Brain sectioning for datasets shown in section 4.3.1 (Figures 4.2-4.4) were performed by Monique Copeland (Janelia Farm Histology Core staff member).

- All fibre implantations for animals used in datasets shown in section 4.3.2 (Figure 4.6) were performed by Janelia Farm Animal Surgery staff.

Chapter 5

- Datasets shown in section 5.3.3 (Figure 5.11 and 5.12) were collected with the aid of Nicholas J. Betley. He analyzed c-Fos intensity in $ACR^{AGRP} \rightarrow aBNST$ and $ARC^{AGRP} \rightarrow PAG$ neuron subpopulations.

- Breeding of all experimental animals used was performed by Janelia Farm Animal Breeding staff.

- A small percentage (~10%) of stereotaxic viral vector injection surgeries were performed by Janelia Farm Animal Surgery staff.

- Brain sectioning for datasets shown in section 5.3.1 (Figures 5.2-5.7) and immunohistochemical staining for ~50% of these datasets were performed by Monique Copeland (Janelia Farm Histology Core staff member).

Acknowledgements

I would like to thank here all the people who have supported me throughout the years as I pursued this research and degree. This work would not have been possible without their unfailing encouragement and constant guidance.

First and foremost, I would like to thank my supervisors, Denis Burdakov and John Apergis-Schoute at the University of Cambridge, and Scott Sternson at Janelia Farm Research Campus. They have been a great source of inspiration for me, and their invaluable mentorship, guidance, and support have helped me become the scientist that I am today. I am forever grateful.

This PhD would not have been possible without the institutional and financial support from the University of Cambridge and Janelia Farm Research Campus, in particular, the Janelia Farm Graduate Scholar Program. I would like to thank everyone that has been involved in the program throughout the years, especially Ulrike Heberlein, Sue Jones, and Maryrose Franko, who have been invaluable in making this program an outstanding opportunity for aspiring scientists like me.

During my time in Cambridge, I had the opportunity to work alongside some incredible researchers in the Burdakov lab: Anne Venner, Mahesh Karnani, and Connie Schoene. I would like to thank them for their support, encouragement, and friendship, as well as being a great source of entertainment and providing me with priceless lessons in the art of patch-clamping. The days of working together in the dark will always be remembered with great fondness.

At Janelia, I was blessed to have some amazing co-workers. I would like to thank all current and former members of the Sternson Lab I have had the opportunity to work with for their constant help and feedback: Nick Betley, Chris Magnus, Pete Lee, Shengjing Xu, Rong Gong, Anne-Kathrin Eiselt, Trace Henry, Helen Su, Yeka Aponte, Deniz Atasoy, and Yunlei Yang. In particular, Nick Betley, whom I had the opportunity of working with in several collaborative projects, has been an amazing resource and teacher throughout the years. Everything I know about immunohistochemistry and microscopy was taught to me by him. I would also like to thank Laura Hart, our lab coordinator, whose incredible ability at getting things done has allowed me to focus on my research, and allowed the lab to function as smoothly

as it does. I would also like to thank my committee members, Josh Dudman and Karel Svoboda, for their invaluable advice and feedback on my research. I certainly would not have been able to accomplish as much as I have without the help from the Vivarium, Surgery, Histology, and Instrument and Design members at Janelia. In particular, I would like to thank Monique Copeland for all of her help with brain sectioning and histology for my projects.

The many friends that have been by my side along the way have provided some of the most memorable moments in this journey. At Janelia, I've had the opportunity to meet some amazingly smart people and shared numerous enlightening conversations. They have been invaluable resources academically, but have also been great friends. I'm glad to have had the opportunity to share some amazing moments with them. Many thanks to all my friends at Sidney Sussex College in Cambridge. They made my time there one of most fun and memorable periods of my life. My friends outside of Janelia have also been a great source of support. Despite the fact that they don't really understand what I do, they continuously insist I do great work and have been an outstanding source of encouragement throughout the years.

Last but not least, I would like to thank my family. My sister is four years younger than I am, but has been there for me and taken care of me like an older sister. I want to thank her for all of her support throughout my life. I hope that I can be an invaluable resource to her as she embarks on her own journey to earn a PhD degree. My mom and dad, I can never thank enough. They have provided me with unquestionable support throughout my education and life. Despite barely having an understanding of what I do, given my poor attempts at explaining it to them in my broken Chinese, they are always my biggest cheerleaders. Thank you for your wisdom, guidance, hard work, and sacrifice. I hope I can be as great a parent one day as you have been for me.

Table of Contents

List of Figures

List of Tables

List of Abbreviations

3V: third ventricle

4V: fourth ventricle

5HT: serotonin

5HT3R: serotonin 3 receptor

AAV: adeno-associated virus

aBNST: anterior subdivisions of the bed nucleus of stria terminalis

ac: anterior commissure

Ach: acetylcholine

aCSF: artificial cerebrospinal fluid

***ad lib*:** *ad libitum*

AGRP: agouti-related peptide

AHP: after-hyperpolarisation potential

αMSH: α-melanocyte stimulating hormone

ANOVA: analysis of variance

AOM: acousto-optic modulator

AP: action potential

Aq: aqueduct

ARC: arcuate nucleus

Arch: archaerhodopsin

BDNF: brain-derived neurotrophic factor

BLA: basolateral nucleus of the amygdala

BMI: body mass index

BNST: bed nucleus of stria terminalis

BSA: bovine serum albumin

CART: cocaine- and amphetamine-regulated transcript

CCK: cholecystokinin

CEA: central nucleus of the amygdala

CEAlc: lateral capsular division of the central nucleus of the amygdala

CGRP: calcitonin-gene related peptide

ChR2: channelrhodopsin-2

CNO: clozapine-n-oxide

CNTF: ciliary neurotrophic factor

CRACM: channelrhodopsin-assisted circuit mapping

CRH: corticotropin-releasing hormone

DA: dopamine

DIC: differential interference contrast

DMH: dorsomedial nucleus of the hypothalamus

DR: dorsal raphe

DREADD: designer receptor exclusively activated by designer drugs

DS: dorsal surface of the brain

DT: diphtheria toxin

DVC: dorsal vagal complex

EGFP: enhanced green fluorescent protein

EM: electron microscopy

EnvA: envelope protein

EYFP: enhanced yellow fluorescent protein

FG: Fluoro-Gold

FLEx: flip-excision

FR: fixed ratio

FS: fast-spiking

fx: fornix

GABA: γ-aminobutyric acid

GFP: green fluorescent protein

GLP-1: glucagon-like peptide 1

Glu: glutamate

GPCR: G-protein coupled receptor

GRP: gastrin-releasing peptide

HA: histamine

i.c.v.: intracerebroventricular

i.p.: intraperitoneal

I_h: hyperpolarisation-activated current

IP: interpeduncular nucleus

IRES: internal ribosome entry site

I-V: input current and membrane potential

JAK: Janus-activated kinase

KD: knock-down

KO: knock-out

LC: locus coeruleus

LepRb: leptin receptor

LHA: lateral hypothalamic area

LHAs: suprafornical subdivision of the lateral hypothalamic area

LS: late-spiking

LTS: low threshold-spiking

MC4R: melanocortin 4 receptor

MCH: melanin-concentrating hormone

NAc: nucleus accumbens

NE: norepinephrine

NLS: nuclear localization signal

NpHR: halorhodopsin

NPY: neuropeptide-Y

NTS: nucleus of the solitary tract

Nts: neurotensin

OX: orexin

OX1: orexin-1 receptor

OX2: orexin-2 receptor

OX-A: orexin A

OXT: oxytocin

PACAP: pituitary adenylate cyclase-activating polypeptide

PAG: periaqueductal grey

PAGvl: ventrolateral periaqueductal grey

PBelo: external lateral subdivision of the parabrachial nucleus

PBN: parabrachial nucleus

PBS: phosphate buffered saline

PKC-δ: protein kinase C-δ

PMV: ventral premammillary nucleus

POMC: proopiomelanocortin

PP: pancreatic polypeptide

PR: progressive ratio

PVH: paraventricular nucleus of the hypothalamus

PVT: paraventricular thalamic nucleus

PYY: peptide YY

RFP: red fluorescent protein

RM: repeated measures

RMg: raphe magnus

ROb: raphe obscurus

RS: regular-spiking

SAD∆G: glycoprotein deleted rabies virus

s.c. : subcutaneous

S.E.M.: standard error of the mean

SF-1: steroidogenic factor-1

shRNA: small hairpin RNA

SIM1: single-minded homolog 1 protein

SNc: substantia nigra compacta

SOCS3: suppressor of cytokine signalling 3

SS: skull surface at Bregma

STAT: signal transducers and activator of transcription

STAT3: signal transducers and activator of transcription 3

TH: tyrosine hydroxylase

TMN: tuberomammillary nucleus of the hypothalamus

TRH: thyrotrophin-releasing hormone

Vgat: vesicular GABA transporter

Vglut2: vesicular glutamate transporter 2

VMH: ventromedial nucleus of the hypothalamus

VTA: ventral tegmental area

WGA: wheat-germ agglutinin

WT: wild-type

Chapter 1

General Introduction

1.1 Introduction

A long standing goal of neuroscience is to understand how the brain directs the output of behaviours essential for survival, in particular, the relationship between brain function and need states such as hunger. Extensive research on the regulation of food intake has revealed that feeding behaviour is regulated by many brain regions, neuropeptides, and neurotransmitters (Bray 2000, Coll et al. 2007, Gao & Horvath 2007, 2008, Morton et al. 2014, Ramos et al. 2005, Sohn et al. 2013, Valassi et al. 2008). Recent studies in this area indicate that appetite can be controlled by multiple molecularly defined neuron populations. These neurons are known as homeostatic interoceptive neurons, as they are capable of integrating peripheral signals of energy status and visceral state in order to coordinate or suppress behavioural responses to seek and consume food (Gao & Horvath 2007, Sternson 2013). The identification of underlying neuronal cell-types that drive food intake remains an area of intense investigation, and it is unclear what downstream circuits of these neurons are important in regulating feeding, and how different circuits and peptides might interact with each other in hunger to direct flexible food-seeking and consumption behaviours. Furthermore, the flexibility of behaviours employed by animals to seek and consume food are believed to be under the influence of motivational mechanisms (Berridge 2004, Bindra 1976, Dickinson 2002, Hull 1943, Schultz 2006), but the exact processes homeostatic neurons employ to direct action selection in hunger remain poorly understood (Berridge 2004, Sternson et al. 2013). In this chapter, I begin with a short historical review on feeding behaviour research and proceed to discuss the technological advancements leading to the current understanding and research focus in the field. Following this, I delineate three major questions arising from recent studies that this dissertation seeks to address, and finish with a brief summary of the aims of this dissertation.

1.2 Homeostasis and feeding behaviour

The concept of an internal regulatory mechanism of the body for survival was first described by Claude Bernard in 1859. Bernard described an internal environment of the body, consisting largely of body fluids. In mammals, the properties of this internal environment usually vary within fixed ranges, and any

deviations outside of these limits jeopardize survival (Bernard 1859). Later on, through a long series of experiments, Walter Cannon would confirm and expand on Bernard's original hypothesis (Cannon 1932). Cannon termed the regulation of this internal environment homeostasis. He states:

> "The constant conditions which are maintained in the body might be termed equilibria. That word, however, has come to have a fairly exact meaning as applied to relatively simple physic-chemical states, in closed systems, where known forces are balanced. The coordinated physiological processes which maintain most of the steady state in the organism are so complex and so peculiar to living beings—involving, as they may, the brain and nerves, the heart, lungs, kidney, and spleen, all working cooperatively—that I have suggested a special designation for these states, homeostasis. The word does not imply something set and immobile, a stagnation. It means a condition—a condition which may vary, but which is relatively constant."

Bernard and Cannon's work focused almost entirely on the physiological and chemical regulators of the internal environment. For example, when animals are placed in a cold external environment, body temperature is maintained by reducing the loss of heat through the decreased activity of sweat glands and constriction of peripheral blood vessels, and increased body heat is produced by burning of stored fat and shivering (Cannon 1932). In contrast, Curt Richter's body of work described the concept of behaviour regulators, and their ability to maintain a constant internal environment (Richter 1943). He indicates:

> "The existence of such behaviour regulators was first established by the results of experiments in which it was found that after elimination of the physiological regulators, the animals themselves made an effort to maintain a constant internal environment or homeostasis."

Animals, for instance, will build nests that vary in size with changing external temperatures, in order to maintain adequate body temperatures (Richter 1943). Moreover, animals in which the pituitary gland has been removed display an inability to produce adequate amounts of body heat and die after 35 days. However, if provided with nest building paper, these animals will build much larger nests than normal animals, in an effort to regulate their body temperature (Richter 1943). Hence, in the absence of physiological regulators, homeostasis can be maintained through behavioural responses. Together, the concepts of homeostasis and

behaviour regulators have guided the study of the control of feeding behaviour and metabolism. Food seeking and consumption behaviours are understood to be the result of an animal's effort to maintain homeostasis under states of reduced energy stores in the body.

1.3 The emerging role of the brain in the control of feeding behaviour

In the early part of the 1900s, the concept that eating started and stopped in response to body signals were mostly driven by notions of peripheral hunger signalling, such as gastric contractions (Cannon 1915, Cannon & Washburn 1912). However, human lesions from tumours (Frohlich 1901) and early lesion studies of the hypothalamus in rats (Anand & Brobeck 1951b, Brobeck et al. 1943, Hetherington & Ranson 1940, 1942) implicated the brain in the regulation of body weight and food intake. Electrolytic lesions of the ventromedial nucleus of the hypothalamus (VMH) in rats increased their body weight and resulted in a significant increase in food consumption (Brobeck et al. 1943), while studies confining the lesions to the lateral hypothalamic area (LHA) resulted in animals that were deemed healthy, but did not eat (Anand & Brobeck 1951b). Studies on the activation of these brain areas with electrical stimulation corroborated these results. Delgado and Anand showed that electrical stimulation of the LHA in rats increased food intake (Delgado & Anand 1953). Conversely, Krasne's electrical and chemical stimulation of the VMH resulted in cessation of eating, even in food deprived animals (Krasne 1962). These results led to the proposal that the control of food intake was focused in the hypothalamus, and brought about the concepts of brain feeding and satiety centres, with the VMH as a feeding centre and the LHA as a satiety centre (Anand & Brobeck 1951a). Further hypothalamic brain lesion studies uncovered additional brain regions involved in the control of food intake, including the dorsomedial nucleus of the hypothalamus (DMH), the arcuate nucleus (ARC) and the paraventricular nucleus of the hypothalamus (PVH), and provided further evidence for this theory (Bellinger et al. 1986, Brecher & Waxler 1949, Epstein 1960, Leibowitz et al. 1981, Marshall et al. 1955, Olney 1969, Olney et al. 1971).

1.4 Peripheral and central nervous system regulators of food intake

Refinement of the understanding of the brain's control of feeding was brought about through pharmacological studies attempting to determine the signals regulating feeding and satiety centres. In order for brain regions to control energy homeostasis and food intake, it must know the state of body energy stores. Therefore, the first theories attempting to describe the regulation of feeding centres pointed towards circulating peripheral signals. Kennedy's lipostatic theory proposed that VMH lesions decreased the effect of negative feedback of signals from adipose tissue, which in turn led to increased feeding (Kennedy 1950). Mayer's glucostatic theory, on the other hand, proposed that glucose utilization by critical cells in the hypothalamus generates a signal to brain areas controlling appetite and food intake. When glucose utilization decreases, hunger is elicited and eating is initiated. Increased glucose utilization, on the other hand, terminated eating (Mayer 1953). Parabiotic studies, where two live animals are joined by suturing such that blood can pass from one animal to the other, also supported the concept of peripheral circulating signals of hunger and satiety (Coleman & Hummel 1969, Davis et al. 1967, Hervey 1959). Early pharmacological studies using systemic and intracerebroventricular (i.c.v.) peripheral circulating factors such as glucose, insulin, and cholecystokinin (CCK), led to observations that the administration of these agents either increased or decreased food consumption (Brief & Davis 1984, Gibbs et al. 1973, Plata-Salaman & Oomura 1986, Smith & Epstein 1969, Strubbe & Mein 1977, Woods et al. 1979), validating prior theories and linking the peripheral system with the brain in the control of food intake.

In addition to peripheral signals, many pharmacological studies also attempted to determine the role of central signals in feeding. Early studies using intra-hypothalamic administration of neurotransmitters and synthetic agonists and antagonists led to observations that the administration of these agents were also capable of modulating food consumption behaviours (Grossman 1960, Leibowitz 1970a, 1970b, Margules 1970). Interestingly, some studies demonstrated that different pharmacological agents applied to the same area could elicit different behaviours (Grossman 1960), or the same agent could elicit opposing feeding behaviours when applied to different regions in the hypothalamus (Leibowitz 1970b). Grossman (1960), for example, showed that infusions of adrenergic agents,

epinephrine or norepinephrine (NE), in the LHA resulted in increased food intake. Infusions of cholinergic agents, acetylcholine (ACh) or carbachol, in the same region, however, resulted in increased water intake (Grossman 1960). In addition, Leibowitz (1970b) showed that infusions of epinephrine in the LHA resulted in a slight reduction of feeding, while infusions in the VMH increased food intake. This was determined to be due to the differential stimulation of α and β adrenergic receptors in these regions, highlighting the importance of receptor type in the modulation of food intake. Food consumption is increased through stimulation of α_1 receptors in the VMH, while inhibition of food intake is mediated through β_1 and β_2 receptors expressed in the LHA (Leibowitz 1970b).

Results such as those observed by Grossman and Leibowitz suggested that distinct neuronal populations within an area might have distinct functions. Concurrently, further studies on the roles of discrete hypothalamic nuclei in the control of food intake started to put into question the theory of feeding and satiety centres. Lesion studies using knife cuts, which severed projections to known feeding and satiety centres, led to similar results as direct lesions to these areas (Sclafani & Berner 1977, Sclafani et al. 1975, Sclafani & Nissenbaum 1988). For instance, overeating and obesity similar to those observed under bilateral parasagittal knife cuts in the medial hypothalamus could be induced by a unilateral parasagittal medial hypothalamus knife cut combined with a contralateral coronal knife cut in the midbrain (Sclafani & Berner 1977). Similarly, pharmacologically ablating dopaminergic axon tracts passing through the LHA (Ungerstedt 1971) and noradrenergic axons passing through the VMH (Ahlskog & Hoebel 1973) was capable of recapitulating the effects observed with lesions of these areas as a whole. Furthermore, electrical stimulation of the LHA did not always result in feeding, but also other behaviours such as drinking or tail-preening (Hoebel 1971, Wise 1974). This led to a movement away from the concept of feeding and satiety centres to a more refined notion of anorexigenic (decrease food intake) vs. orexigenic (increase food intake) signals.

The rise of cloning and molecular genetics techniques in the later parts of the 20th century led to a boom of gene discoveries which identified new neuropeptides, along with their receptors and transcription factors. The ability to create mutant mouse lines with global knock-in or knock-out (KO) of specific peptides and

receptors brought forth the understanding of the role of these newly discovered neuropeptides and receptors in the control of food intake. During the turn of the century, feeding behaviour was believed to be under the control and modulation by numerous peripheral circulating signals, neurotransmitters, and neuropeptides (Bray 2000, Coll et al. 2007, Gao & Horvath 2007, 2008) (Figure 1.1).

Within the central nervous system, pharmacological and genetic studies have identified numerous peptides and neurotransmitters important in the regulation of food intake (Coll et al. 2007, Gao & Horvath 2007, Sohn et al. 2013, Valassi et al. 2008). Monoaminergic neurotransmitters produced outside of the hypothalamus, including NE, dopamine (DA), and serotonin (5HT), have been shown to interact with neuropeptides and hormones in the hypothalamus to control eating behaviour (Halford et al. 2005, Heisler et al. 2006, Lechin et al. 2006, Leibowitz 1970b, Leibowitz et al. 1988, Ramos et al. 2005, Sohn et al. 2013) (Figure 1.1).

Within the hypothalamus, studies have demonstrated that peptides expressed in the LHA, VMH, PVH, DMH, and ARC, are responsible in the modulation of food consumption and metabolism (Figure 1.1). Major roles have been attributed to three peptides: proopiomelanocortin (POMC), agouti-related peptide (AGRP), and neuropeptide-Y (NPY). AGRP and NPY are known to be orexigenic peptides. Direct administration of NPY intro cerebral ventricles or the PVH resulted in robust increases of food intake (Clark et al. 1984, Stanley & Leibowitz 1984). Ectopic expression of AGRP are known to cause an obese phenotype (Klebig et al. 1995), and i.c.v. administration of AGRP increases body weight and food intake in *ad libitum* fed animals (Small et al. 2001). In contrast, POMC is an anorexigenic peptide, as mice and humans lacking POMC develop hyperphagia and obesity (Challis et al. 2004, Krude et al. 1998, Yaswen et al. 1999). Anatomical studies have shown that these peptides are expressed in neurons located in the ARC, where POMC and AGRP are expressed in distinct neuronal populations (POMC neurons and AGRP neurons, respectively) (Gee et al. 1983, Hahn et al. 1998). AGRP neurons also co-express NPY and γ-aminobutyric acid (GABA) (Hahn et al. 1998, Horvath et al. 1997). AGRP and POMC peptides have been identified as two primary components of the melanocortin control of food intake. The melanocortin system consists of melanocortin peptides and G-protein coupled melanocortin receptors (Gantz & Fong 2003). POMC in POMC neurons is cleaved into the melanocortin

peptide α-melanocyte-stimulating hormone (αMSH) (Gantz & Fong 2003), which in turn activates melanocortin 4 receptors (MC4R) to suppresses feeding (Adan et al. 1994, Cowley et al. 2001, Fan et al. 1997). AGRP, on the other hand, is an endogenous antagonist of MC4R, and increases food intake through the inhibition of these receptors (Fan et al. 1997, Gantz & Fong 2003, Hahn et al. 1998, Lu et al. 1994, Ollmann et al. 1997, Yang et al. 1999). Although MC4R is expressed in many brain regions within and outside the hypothalamus (Kishi et al. 2003), activity of MC4R in the PVH has been attributed to be the main pathway for the melanocortin system's regulation of food consumption (Balthasar et al. 2005). NPY does not act directly on the melanocortin system, but exerts its orexigenic effects on NPY receptors (Pronchuk et al. 2002, Yulyaningsih et al. 2011). GABA, in turn, can inhibit αMSH release through projections from AGRP to POMC neurons (Cowley et al. 2001, Horvath et al. 1992) (Figure 1.2).

In the periphery, a long list of circulating peptides, secreted by peripheral organs, has been implicated in the modulation of appetite through their actions on distinct receptors in the brain, in particular the hypothalamus. This includes peptides secreted by the gastrointestinal tract, the pancreas, adipose tissue, the pituitary, thyroid and adrenal glands, as well as other circulating factors such as glucose and free fatty acids (Bray 2000, Coll et al. 2007) (Figure 1.1). Particular attention has been focused on the roles of leptin and ghrelin in the regulation of food intake. Leptin is released from adipose tissue in the body, representing a signal of energy stores, and is an anorexigenic peptide (Ahima et al. 1996, Caro et al. 1996, Considine et al. 1996, Fruhbeck et al. 1998, Havel 1999, Seeley & Woods 2003). Nonsense mutations of the gene encoding leptin in *ob/ob* mutant mice, for example, leads to hyperphagia and extreme obesity (Ingalls et al. 1950, Zhang et al. 1994). Ghrelin, on the other hand, is an orexigenic peptide secreted from the stomach (Date et al. 2000, Dornonville de la Cour et al. 2001, Kojima et al. 1999), and peripheral administration increases food consumption (Asakawa et al. 2001, Nakazato et al. 2001, Tschop et al. 2000, Williams & Cummings 2005, Wren et al. 2001). However, KO of ghrelin does not have a substantial influence on appetite and body weight, indicating that this is one of many orexigenic signals that regulate food consumption (Sun et al. 2003). Leptin and ghrelin's modulation of the melanocortin system, through actions on AGRP and POMC neurons in the ARC, has been attributed to be their major

source of influence on feeding behaviour (Coll et al. 2007, Gao & Horvath 2007, 2008, Oswal & Yeo 2010, van Swieten et al. 2014). Leptin activates POMC neurons and inhibits AGRP neuron activity, which in turn increases and decreases release of αMSH and AGRP respectively, to increase MC4R activation and suppress feeding (Adan et al. 1994, Cowley et al. 2001, Fan et al. 1997, Spanswick et al. 1997, van den Top et al. 2004). Ghrelin, on the other hand, increases food intake by activating AGRP neurons (Cowley et al. 2003, van den Top et al. 2004, Yang et al. 2011) and indirectly inhibiting POMC neuron activity through GABAergic projections from AGRP neurons (Cowley et al. 2001, Horvath et al. 1992) (Figure 1.2). Thus, the brain's control of food intake involves a complex system capable of integrating numerous signals from the periphery with neuropeptides and neurotransmitters in multiple brain regions.
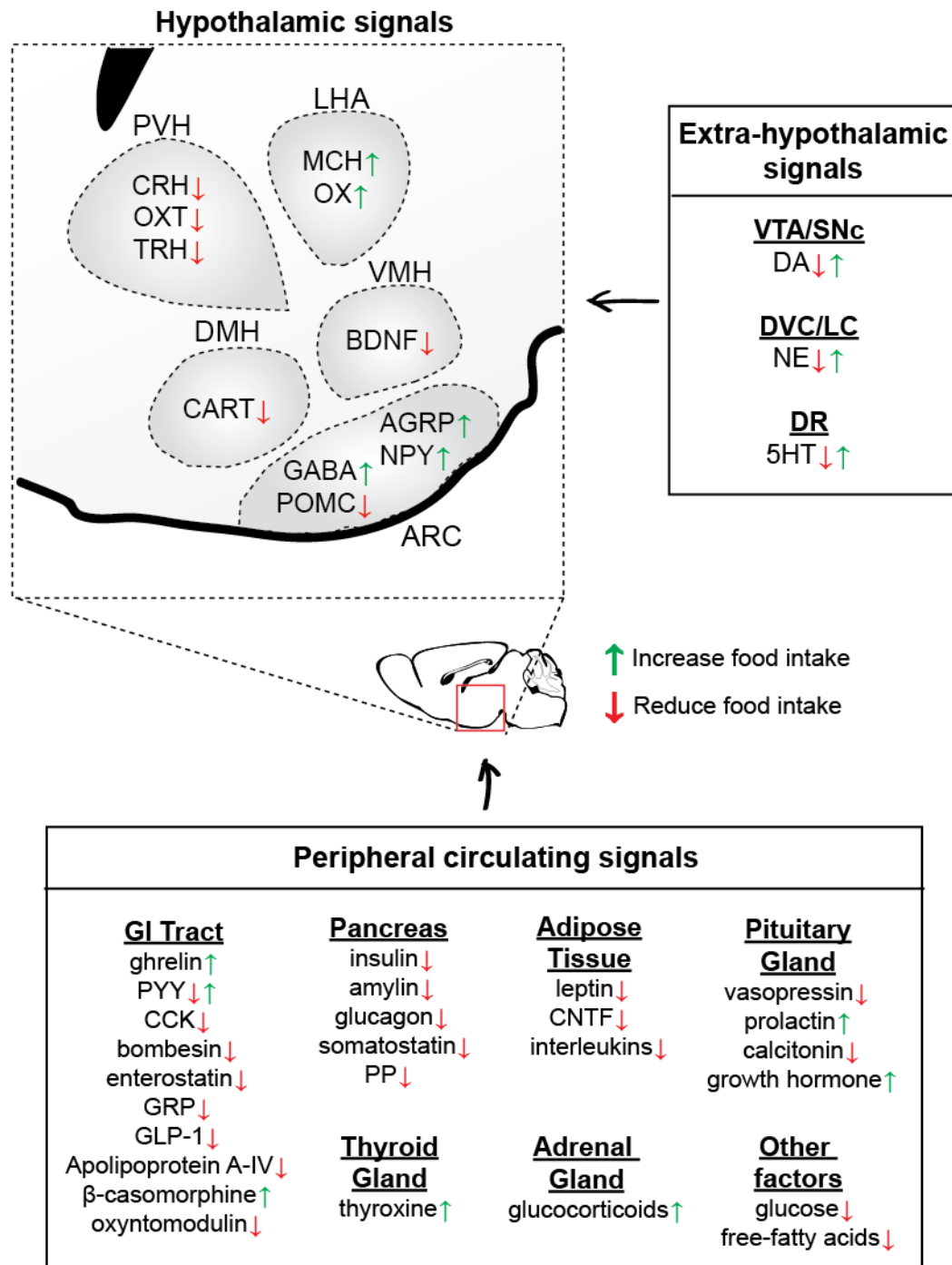
Figure 1.1 Central and peripheral signals that regulate food consumption. Food consumption is regulated by numerous peptides expressed in various hypothalamic nuclei, neurotransmitters expressed outside the hypothalamus, and peripheral circulating signals released from the gastrointestinal tract, pancreas, adipose tissue, thyroid, adrenal and pituitary glands, as well as other circulating factors. Increase in food intake is depicted by green upward pointing arrows, while decrease in food

intake is depicted by red downward pointing arrows. PVH: paraventricular nucleus of the hypothalamus; LHA: lateral hypothalamic area; DMH; dorsomedial nucleus of hypothalamus; VMH: ventromedial nucleus of hypothalamus; ARC: arcuate nucleus; VTA: ventral tegmental area; SNc: substantia nigra compacta; DVC: dorsal vagal complex; LC: locus coeruleus; DR: dorsal raphe; CRH: corticotropin-releasing hormone; OXT: oxytocin; TRH: thyrotrophin-releasing hormone; MCH: melanin-concentrating hormone; OX: orexin; BDNF: brain-derived neurotrophic factor; CART: cocaine-and amphetamine-regulated transcript; AGRP: agouti-related peptide; NPY: neuropeptide-Y; GABA: γ-aminobutyric acid; POMC: proopiomelanocortin; DA: dopamine; NE: norepinephrine; 5HT: serotonin; PYY: peptide YY; CCK: cholecystokinin; GRP: gastrin-releasing peptide; GLP-1: glucagon-like peptide 1; PP: pancreatic polypeptide; CNTF: ciliary neurotrophic factor.
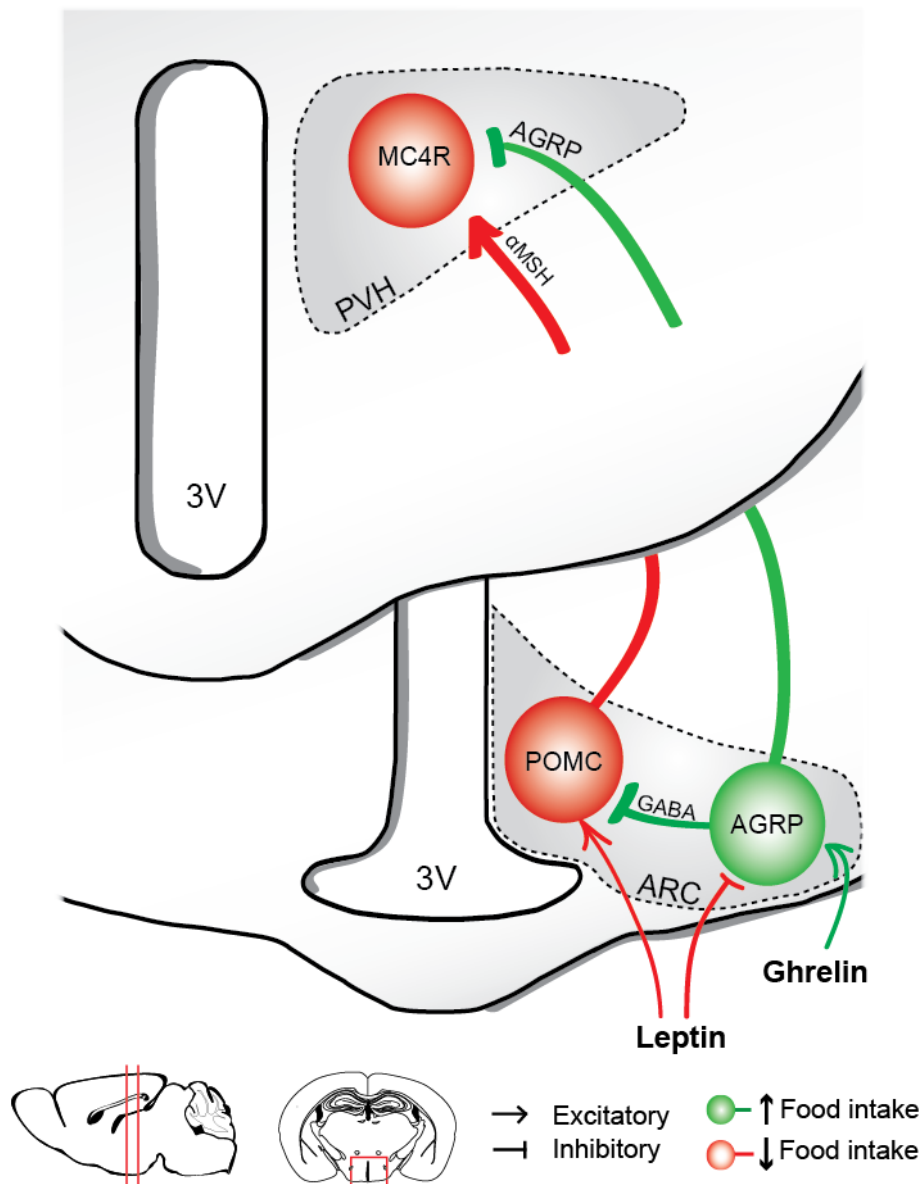
Figure 1.2 The melanocortin system in the control of food intake. In the ARC, anorexigenic POMC neurons and orexigenic AGRP neurons are intermingled. These neurons project to the PVH. POMC neurons release αMSH, which activates anorexigenic MC4R expressing neurons in the PVH to reduce food intake. In contrast, AGRP neurons release AGRP, which antagonizes MC4R to increase feeding. In addition, AGRP neurons can inhibit POMC neurons through GABAergic transmission. In the presence of leptin, POMC neurons are activated and AGRP neurons are inhibited to reduce food intake. Ghrelin, on the other hand, activates AGRP neurons and indirectly inhibits POMC neurons to increase food intake. Red lines and red box in sagittal and coronal section diagrams of the brain, respectively, represent position of regions depicted in the graphic. PVH: paraventricular nucleus of the hypothalamus; ARC: arcuate nucleus; 3V: third-ventricle; POMC: proopiomelanocortin; AGRP: agouti-related peptide; GABA: γ-aminobutyric acid; MC4R: melanocortin 4 receptor; αMSH: α-melanocyte-stimulating hormone. Design of this graphic was based on Figure 4 from (Barsh & Schwartz 2002), but adapted.

1.5 Homeostatic cell-type specific regulation of feeding

The development of molecular genetics techniques brought forth a major push in the identification of signals regulating food intake. However, studies using genetic mouse lines with global KO of peptides or receptors made it difficult to understand their role within specific brain regions, as some peptides might have different functions in different areas of the brain. For example, *ob/ob* and A^y animals, also display other changes not directly related to food intake and metabolism, such as infertility (Granholm et al. 1986, Mounzih et al. 1997). This is most likely due to the disruption of leptin and melanocortin signalling in multiple regions of the brain in these animals, as leptin receptors (LepRb) and MC4Rs are expressed ubiquitously (Kishi et al. 2003, Leshan et al. 2006, Scott et al. 2009). More problematic, however, was the fact that in many studies, genetic KO of peptides known to modulate feeding based on pharmacological experiments did not always elicit the expected behavioural changes, bringing into question whether these peptides are, in fact, regulating food intake. The accumulation of these types of results, therefore, emphasized the need to understand the control of food intake through the investigation of the role of specific cell-types (marked by the expression of a particular peptide or receptor of interest) within defined brain regions.

AGRP neurons are a prime example of a cell-type important in the regulation of food intake. As mentioned before, pharmacological studies had shown that i.c.v. administration of NPY or AGRP, which are expressed in AGRP neurons, resulted in increased food intake (Clark et al. 1984, Small et al. 2001). Surprisingly, mice with KO of the NPY or AGRP gene did not exhibit the expected hypophagia (Erickson et al. 1996, Qian et al. 2002). However, studies using diptheria toxin (DT) dependent cell-type selective and inducible ablation of AGRP neurons led to a rapid and significant decrease in body weight and severe hypophagia in adult mice, demonstrating the necessity of AGRP neurons as a whole in the maintenance of feeding and survival (Gropp et al. 2005, Luquet et al. 2005). This suppression of feeding was, surprisingly, determined to not be due to the removal of AGRP-neuron mediated inhibition of the melanocortin system (Wu et al. 2008). Instead, it was concluded that loss of GABAergic signalling from AGRP neurons was the primary cause, as inactivation of GABA synthesis in AGRP neurons was capable of recapitulating AGRP neuron ablation induced anorexia (Wu et al. 2009).

In addition to the necessity of AGRP neurons in the maintenance of feeding behaviour for survival, studies have also demonstrated that these neurons are homeostatic neurons capable of translating signals of energetic state from the body. Slice recordings, for example, indicate that AGRP neurons have a significantly higher firing rate under states of food deprivation over sated conditions (Takahashi & Cone 2005, Yang et al. 2011). In addition, AGRP neurons show significant expression of the immediate early gene product Fos, a marker of neuronal activity (Bullitt 1990), under food deprivation, in contrast to sated conditions, where Fos expression is very low (Betley et al. 2013). Furthermore, AGRP neuron activity is increased both directly and synaptically by circulating signals of energy deficit, such as ghrelin (Cowley et al. 2003, van den Top et al. 2004, Yang et al. 2011), and are inhibited by signals of energy surplus, including glucose, insulin, and leptin (Fioramonti et al. 2007, Konner et al. 2007, van den Top et al. 2004). AGRP neurons, therefore, are believed to be interoceptive neurons sensitive to starvation, as they are capable of modulating their electrical activity in response to changes in the levels of hormones, metabolites, and neural signals of energy levels in the body (Sternson 2013). These studies demonstrate the importance of investigating feeding behaviour not from the perspective of the role of specific peptides and receptors alone, but from the role of specific homeostatic cell-type populations within brain regions, coupled with differential roles of distinct neurotransmitters expressed in these neurons. Despite the understanding that diverse neuropeptides and receptors are important in feeding, there is still a lack of understanding of the role of neurons that express these peptides as a whole in the control of food consumption behaviours.

.

1.6 Optogenetic and chemogenetic approaches in the study of feeding behaviour

The use of genetic tools to conditionally ablate cell-type specific neurons, as presented above, provide obvious utility in the study of feeding behaviour. However, perturbations of homeostatic interoceptive neurons without temporal control make it difficult to evaluate the exact role of these neurons in feeding behaviour. AGRP neuron ablation in neonatal mice with DT, for example, showed very modest effects on body weight loss and no hypophagia, in contrast to lesions in adult mice (Luquet et al. 2005). In addition, pharmacological manipulations that reversed loss of feeding after AGRP neuron ablation could be discontinued after ~2 weeks, at which point animals would continue to consume food without the treatment (Wu et al. 2009). Hence, compensatory mechanisms often make genetic cell-ablation methods unsuitable neuron manipulation techniques when phenotype evaluation must be performed chronically.

The recent development of chemogenetic and optogenetic tools for fast neuronal activation or inhibition in intact vertebrates allows for acute cell manipulations while avoiding any developmental compensation effects. This has significantly enabled the study of homeostatic neurons and their role in feeding. Chemogenetic tools, the most common being the designer receptors exclusively activated by designer drugs (DREADD) system, allow for the quick and reversible manipulation of neuronal activity through the activation of synthetic receptor-ligand pairs. The DREADD system involves the use of engineered G-protein coupled receptors (GPCRs), hM3D for excitation and hM4D for inhibition, activated by the application of the cognate ligand clozapine-n-oxide (CNO) (Armbruster et al. 2007, Conklin et al. 2008, Nichols & Roth 2009, Pei et al. 2008). Optogenetic tools allow ultra-fast manipulations of neuronal activity through ion channels engineered to be activated by different wavelengths of light. Excitation of neurons can be achieved through the use of the cation channel channelrhodopsin-2 (ChR2) and its variants, which are activated by blue light (470 nm) (Boyden et al. 2005) (Figure 1.3A). Optogenetic inhibition of cells is achieved using halorhodopsin (NpHR), a chloride channel, or Archaerhodopsin (Arch), a proton pump (Chow et al. 2010, Gradinaru et al. 2010, Zhang et al. 2007). Due to the use of light as the activating source for these

channels, optogenetic approaches further refine temporal precision of neuronal activity manipulations, down to milliseconds, and allows for manipulations of firing frequency patterns, from a single action potential up to 40 Hz (Boyden et al. 2005). This creates an advantage over chemogenetic tools, which requires the diffusion of cognate ligands and have minutes-long latency (Alexander et al. 2009).

Many techniques are available for the expression of these channels and receptors. The most commonly used method consists of delivering the genes through the use of viral vectors and stereotaxic surgery procedures (Zhang et al. 2010). It is common practice to fuse a fluorescent reporter protein, such as mCherry or tdTomato, with the channel in order to visually confirm the successful expression of the channels in the neurons of interest (Aponte et al. 2011, Atasoy et al. 2008). To render cell-type specificity, genes can be expressed under the control of a particular promoter of interest, in combination with the Cre-dependent flip-excision (FLEx) switch mechanism (Atasoy et al. 2008, Gradinaru et al. 2009, Schnutgen et al. 2003, Wang et al. 2007, Zhao et al. 2008). In addition, transgenic mouse lines where ChR2 is under conditional Cre-dependent expression have been created (Madisen et al. 2012), allowing for selective breeding with mouse lines expressing Cre under specific promoters of interest to achieve cell-type selective expression of ChR2 (Fig 1.3B-C). This particular method provides greater control over the uniformity of expression of these channels across animals compared to viral injections, in which expression levels are much more variable.

Optogenetic and chemogenetic tools, therefore, allow for neuronal activity manipulations *in vivo* to help elucidate the relationship between changes in neuronal activity patterns and behaviour. For DREADDs, CNO can be delivered through intraperitoneal (i.p.) injections or intracranially through implanted cannulas (Alexander et al. 2009, Atasoy et al. 2012, Krashes et al. 2011, Stachniak et al. 2014). Light delivery for optogenetic activation or inhibition *in vivo* is achieved through the implantation of optic fibres in brain regions of interest (Zhang et al. 2010). In addition, ChR2 assisted circuit mapping (CRACM) techniques facilitate the systematic interrogation of functional synaptic connectivity of cell-type specific neurons (Petreanu et al. 2007). Prior methods for determining synaptic connectivity included the reconstruction of axonal and dendritic arbours (Binzegger et al. 2004, Gilbert 1983) as well as the use of paired recordings (Holmgren et al. 2003,

Thomson et al. 2002). However, reconstruction studies are not capable of determining cell-type specificity nor the strength of functional connections. Paired recordings methods, although capable of estimating connection probabilities, cannot be used to determine long-range synaptic connections, as cells bodies are severed from axons during the preparation of brain slices. Since ChR2 is expressed in both cell bodies as well as projections, it is possible to excite severed axons of a defined cell type and record responses in postsynaptic cells in structures far apart from the original location of the cell bodies (Atasoy et al. 2008, Atasoy et al. 2012, Petreanu et al. 2007) (Figure 1.3D-E). Additionally, synaptic transmission studies using paired recordings can activate nearby cells and axon fibres, creating artefacts. Since photoactivation of presynaptic axons can induce neurotransmitter release, the use of specific channel or receptor blockers in combination with photoactivation can help determine the neurotransmitters responsible for the observed postsynaptic effect (Atasoy et al. 2012, Bass et al. 2010, Schoenenberger et al. 2011, Schone et al. 2012, Stuber et al. 2010, Tecuapetla et al. 2010). Therefore the combination of use of the Cre-Lox system, retrograde and anterograde viral vectors, and spatial targeting of viral delivery or channel/receptor activating agents (CNO or light), allows for highly specific neuronal manipulations to further the understanding of the relationship between the activity of cell-type specific neurons, its functional synaptic circuitry, and feeding behaviour.
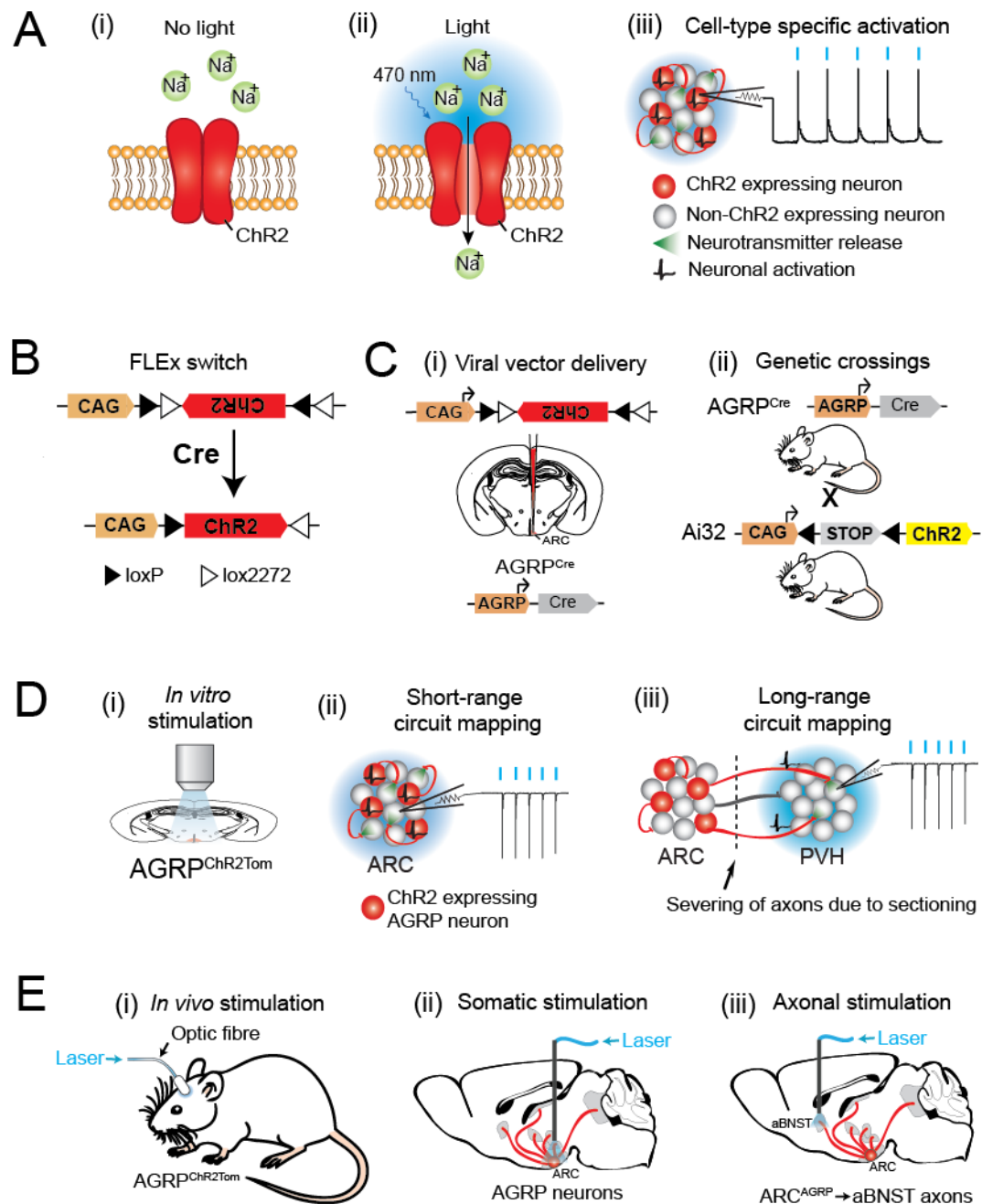
Figure 1.3 Optogenetic approaches for the study of neuronal circuits controlling feeding behaviour. (A) ChR2 is a photosensitive transmembrane cation channel. (i) In the absence of light, the channel remains closed. (ii) In the presence of blue light of 470 nm wavelength, the channel opens and allows influx of cations, with particular preference for Na⁺. (iii) Under a pulsed-light (blue bars) protocol, ChR2-expressing neurons are depolarized and action potentials are triggered with millisecond precision, releasing neurotransmitters. **(B)** Viral vector constructs using a Cre-dependent FLEx switch recombination mechanism includes a promoter, such as

the synthetic promoter CAG, and an inverted ChR2 and fluorescent marker gene, such as tdTomato (red box), double-floxed by two orthogonal lox recognition sequences, such as loxP and lox2272. In the presence of Cre, the ChR2-tdTomato sequence is inverted and lox sites are excised to allow for stable expression of the gene. **(C)** Cell-type specific expression of ChR2 can be achieved using two common methods. (i) Viral vector delivery method involves the targeted injection of a viral vector containing the ChR2 expressing construct into the desired brain region of a transgenic mouse expressing Cre in desired neurons. For ChR2 expression in AGRP neurons, viral vector is delivered into the ARC of AGRP^{Cre} mice, which express Cre under the AGRP promoter. (ii) Expression can also be achieved through genetic crossings between transgenic Cre-expressing mouse lines, such as AGRP^{Cre}, and constitutive ChR2-expressing mouse lines, such as Ai32, which expresses ChR2 fused to an enhanced yellow fluorescent protein (EYFP, yellow box) in the presence of Cre. **(D)** Schematics for CRACM approach for circuit mapping. (i) *In vitro* stimulation for CRACM studies can be achieved by delivering light through a microscope objective to the desired region. (ii) For short-range synaptic connectivity studies between molecularly defined neurons, pulsed-light delivery activates ChR2 expressing neurons to release neurotransmitters, eliciting post-synaptic potentials in patch-clamped post-synaptic neurons. (iii) Light delivery is also capable of activating ChR2-expressing axons severed from cell bodies for long-range synaptic connectivity studies. **(E)** Schematics for *in vivo* optogenetic studies. (i) For *in vivo* light stimulation, an optic fibre is implanted in the brain for light delivery from a laser. (ii) The optic fibre can be targeted to the brain region containing ChR2-expressing neurons for somatic stimulation, or (iii) to brain regions containing ChR2-expressing neuron axons, for projection specific stimulation. ChR2: channelrhodopsin-2; ARC: arcuate nucleus; PVH: paraventricular nucleus of the hypothalamus; aBNST: anterior subdivisions of the bed nucleus of stria terminalis; AGRP: agouti-related peptide; EYFP: enhanced yellow fluorescent protein; CRACM: channelrhodopsin-assisted circuit mapping.

1.7 The control of food intake through extended feeding circuits

Recently, chemogenetic and optogenetic tools have enabled the examination of the sufficiency of AGRP neurons to elicit feeding behaviour, and unravelled an AGRP neuron mediated circuit for the control of feeding. AGRP neuron activation using hM3D led to an increase in food consumption as well as motivation to work for food in well-fed mice, while inhibition with hM4D resulted in significant reduction in food intake during the dark period (Krashes et al. 2011). Activation of AGRP neurons using ChR2 elicited voracious food consumption in well-fed mice within minutes of photostimulation onset, eating as much as 24 hr food deprived mice in daylight hours, when food consumption is usually very low (Aponte et al. 2011). The magnitude and duration of the feeding responses were dependent on AGRP neuron activity levels, as food consumption levels increased while latencies to initiate feeding decreased with increased number of photoexcitable neurons and stimulation frequency, and ongoing photostimulation was required for sustained food consumption (Aponte et al. 2011). These results conclusively established a causal role for these neurons in the control of food intake. In addition to increasing food consumption, photoactivation of AGRP neurons also increased an animal's motivation to work for food in operant tasks (Atasoy et al. 2012, Krashes et al. 2011). Therefore, homeostatic neurons can play a role in engaging motivational mechanisms to direct food seeking and consumption, which is not a role generally attributed to the hypothalamus.

Melanocortin systems has been held as one of the main models for the control of food intake, where AGRP neurons are believed to exert its orexigenic effects through the suppression of melanocortin signalling by anorexigenic POMC neurons, as well as through direct inhibition of PVH neurons through MC4R (Coll et al. 2007, Gao & Horvath 2007, 2008). Prior studies using CRACM had demonstrated that both AGRP neurons and POMC neurons were functionally connected to PVH neurons (Atasoy et al. 2008). However, as with AGRP neuron ablation studies, AGRP neuron evoked-feeding was found not to be mediated by the inhibition of melanocortin receptors, since photoactivation of AGRP neurons in A^y animals, which have elevated levels of AGRP and constitutively blocks MC4R receptors (Miller et al. 1993), still displayed evoked feeding behaviours (Aponte et al. 2011). *In vitro* interrogations of the functional connectivity of AGRP neurons in the ARC using

CRACM, where whole-cell patch clamp recordings of fluorescently labelled POMC neurons were coupled with optogenetic activation of ChR2 expressing AGRP neurons, demonstrated that AGRP neurons inhibit POMC neurons through GABAergic transmission (Atasoy et al. 2012). However, *in vivo* evaluation of this synaptically functional circuit and its role in AGRP neuron evoked food consumption indicated that this circuit is involved in long-term (hours to days) but not short term (minutes to hours) regulation of appetite. Simultaneous optogenetic activation of AGRP and POMC neurons was performed *in vivo* such that AGRP neuron inhibition of POMC would be overridden by ChR2 activation of POMC neurons. This, however, did not eliminate nor diminish evoked food intake (Atasoy et al. 2012). Direct activation of POMC neurons, however, did reduce food intake overnight, but not acutely (Aponte et al. 2011). Therefore, these results suggested that the melanocortin pathway regulates long-term food intake, while acute evoked feeding was mediated through other AGRP neuron circuits.

Outside of the ARC, AGRP neurons project to many hypothalamic and extra-hypothalamic brain regions (Betley et al. 2013, Haskell-Luevano et al. 1999). *In vitro* interrogation of long-range AGRP circuits to two areas known to be important for feeding, the PVH and the parabrachial nucleus (PBN), demonstrated the presence of GABA-mediated inhibitory functional connections between AGRP neurons and postsynaptic neurons in these regions (Atasoy et al. 2012). *In vivo* interrogation of the function of these diverging circuits in evoked-feeding behaviour using region specific AGRP neuron axonal photoactivation showed that activation of $ARC^{AGRP} \rightarrow PVH$ elicited feeding. A combination of optogenetic and pharmacological techniques indicated that the $ARC^{AGRP} \rightarrow PVH$ circuit evoked feeding by inhibition through both GABA and NPY signalling. In addition, chemogenetic inhibition of PVH neurons expressing the single-minded homolog 1 protein (SIM1) was capable of recapitulating both the increase in food intake as well as the increase in lever pressing behaviour observed under AGRP neuron photostimulation, indicating SIM1 neurons in the PVH were the downstream targets of AGRP neurons mediating $ARC^{AGRP} \rightarrow PVH$ circuit evoked food consumption (Atasoy et al. 2012). Further studies interrogating the downstream circuits from the PVH important in the regulation of acute food consumption identified the ventrolateral periaqueductal grey (PAGvl) and the dorsal raphe (DR) as the third-order node. Chemogenetic silencing

of PVH^{SIM1} neuron projections to the PAGvl/DR region was demonstrated to be sufficient to elicit evoked food consumption in a similar fashion as activation of AGRP neurons and inhibition of PVH^{SIM1} neurons (Stachniak et al. 2014) (Figure 1.4).

Interestingly, photoactivation of ARC$^{AGRP}\rightarrow$PBN axons did not elicit an evoked feeding response. Studies attempting to establish the circuits regulating the observed anorexic phenotype after AGRP neuron ablation, however, determined that the removal of inhibition in the PBN was the underlying cause of the hypophagia, as administration of GABA receptor agonists directly into the PBN rescued the anorexia phenotype (Wu et al. 2009). In a series of elegant studies, Palmitter's group found that serotonergic inputs from the raphe magnus (RMg) and raphe obscurus (ROb) to the nucleus of the solitary tract (NTS) increase glutamatergic output of this region. In turn, this increases glutamatergic output from the PBN, which results in mimicking of gastrointestinal malaise to suppress feeding (Wu et al. 2012). AGRP neuron's inhibitory inputs to the PBN, therefore, are thought to promote normal food consumption by suppressing gastrointestinal malaise (Wu et al. 2012). This circuit was deemed the primary cause for the anorexia phenotype observed in AGRP neuron ablated mice. Recent studies using chemogenetic and optogenetic techniques for acute cell-type selective activation and inhibition further demonstrated that excitatory output of the PBN is mediated by calcitonin-gene related peptide (CGRP) expressing neurons, which in turn excite protein kinase C-δ (PKC-δ) expressing neurons in the central nucleus of the amygdala (CEA) to inhibit food intake (Cai et al. 2014, Carter et al. 2013). PKC-δ neurons were found to exert their anorexigenic influence on feeding through intra-CEA inhibition (Cai et al. 2014) (Figure 1.4). This set of studies, therefore, exemplifies how the use of chemogenetic and optogenetic tools can be applied to unravel circuits for feeding. Of particular note, they underscore the utility of employing homeostatic neurons as entry points and their projections as blueprints to uncover downstream nodes for the systematic mapping of brain feeding circuits. Additionally, these results reveal the divergence in roles of downstream circuits of homeostatic neurons in the control of feeding behaviour, highlighting the importance of studying feeding through the systematic interrogation of distinct downstream projections of homeostatic neurons and extended brain circuits.
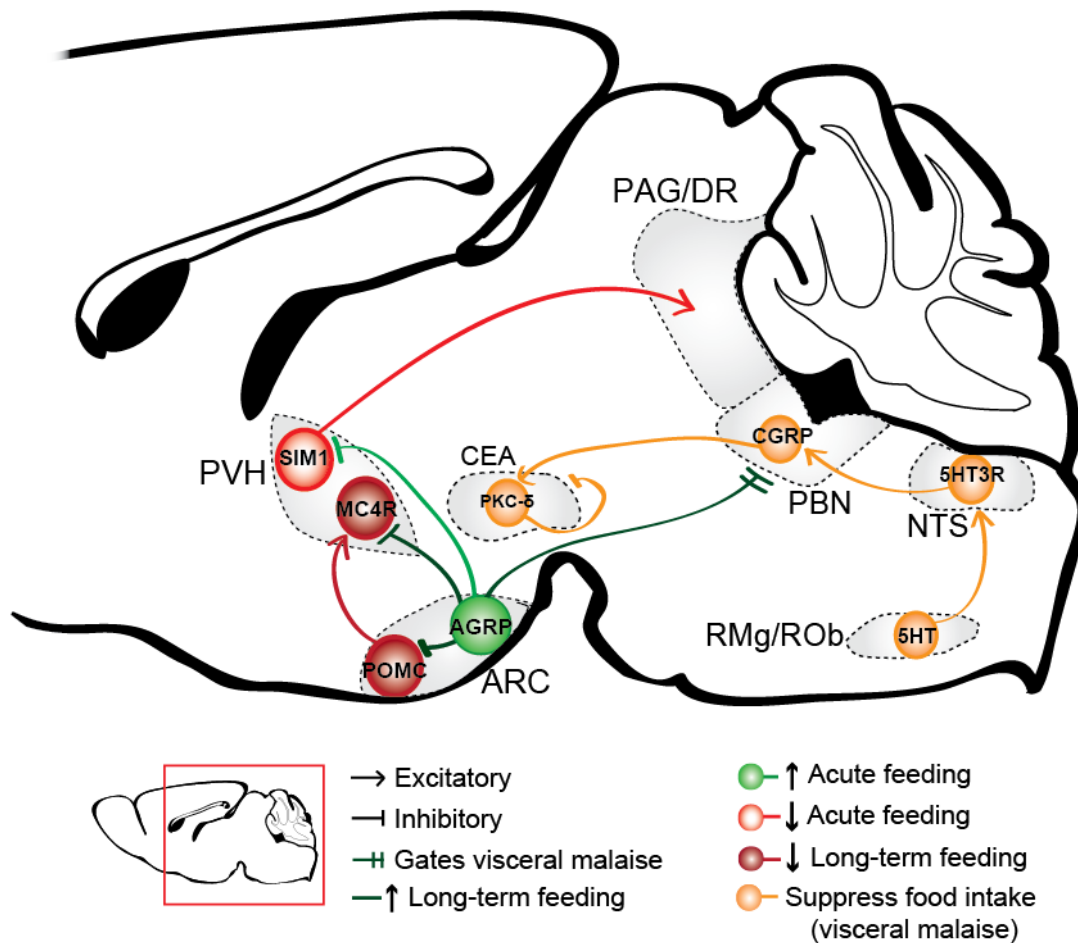
Fig 1.4 AGRP neuron modulated neural circuits for feeding and anorexia. POMC neurons in the ARC activate MC4R neurons in the PVH to reduce long-term food consumption. AGRP neurons inhibit MC4R and POMC neurons to increase long-term food intake. In addition, AGRP neurons inhibit PVH^{SIM1} neurons projecting to the PAG/DR regions to elicit acute feeding. Food intake is suppressed by a visceral malaise circuit where 5HT released from 5HT neurons in the RMg/ROb region activate 5HT3R receptor neurons in the NTS. These in turn activate glutamatergic neurons in the PBN to increase excitatory output from the PBN and inhibit food intake. The activity of this circuit is constrained by inhibitory inputs to the PBN from AGRP neurons in the ARC to allow for normal feeding. Excitatory output of the PBN is mediated by CGRP neurons, which activates PKC-δ expressing neurons in the CEA. PKC-δ neurons reduce food intake by inhibition of other neurons within the CEA. Red box in sagittal brain section diagram represents area depicted in this graphic. ARC: arcuate nucleus; CEA: central nucleus of the amygdala; PBN: parabrachial nucleus; NTS: nucleus of the solitary tract; RMg: raphe magnus nucleus; ROb: raphe obscurus nucleus; PVH: paraventricular nucleus of the hypothalamus; PAG: periaqueductal grey; DR: dorsal raphe; AGRP: agouti-related peptide; Glu: glutamate; 5HT: serotonin; 5HT3R: serotonin 3 receptor; CGRP: calcitonin gene related peptide; PKC-δ : protein kinase C-δ, POMC: proopiomelanocortin; MC4R: melanocortin 4 receptor; SIM1: single-minded homolog 1 protein.

1.8 Outstanding questions in the study of feeding behaviour

The understanding of feeding through the view of cell-type specific control of feeding as well as the rising importance of the control of feeding through organized circuitry in the brain brings forth three outstanding questions in the field: 1) the identification and understanding of the role of other putative homeostatic neurons and their circuits in the control of feeding behaviour; 2) the motivational properties engaged by homeostatic neurons to drive food seeking and food consumption, and 3) the role of divergent projections and downstream circuits of homeostatic neurons in the control of feeding behaviour.

1.8.1 Identification of homeostatic neurons and their circuits for the control of food intake

Studies on the role of AGRP neurons in feeding by different groups highlight the importance of identifying homeostatic interoceptive neurons for the study of the control of food consumption. Despite the understanding that diverse neuropeptides and receptors are important in feeding, there has been a lack of understanding of the role of neurons that express these peptides as a whole in the control of food consumption behaviours. Of particular interest are LepRb expressing neurons. Although there is significant evidence of the importance of leptin signalling in the brain for the modulation of feeding behaviour (Coll et al. 2007, Figlewicz & Benoit 2009, Gao & Horvath 2007, 2008, Oswal & Yeo 2010, van Swieten et al. 2014), leptin has also been implicated in the control of other processes, such as reproduction, stress, learning and memory, and bone density regulation, to name a few (Elias 2014, Irving & Harvey 2014, Quiros-Gonzalez & Yadav 2014, Xu 2014). The issue arises from the fact that LepRbs are expressed ubiquitously in the brain (Leshan et al. 2006, Scott et al. 2009). Therefore, different LepRb expressing neuron populations in distinct brain regions might have differing roles. Given the role of the hypothalamus in the control of feeding, LepRb expressing neurons in hypothalamic areas can be viewed as homeostatic interoceptive neurons, like AGRP and POMC neurons in the ARC. Of particular interest are LepRb neurons in the LHA, as direct

leptin administration into this area reduces food intake (Leinninger et al. 2009). Direct manipulations of the activity of these neurons to elucidate their role in feeding behaviour, however, have not been performed. The role of LHA^{LepRb} neurons and their circuits in feeding behaviour is addressed in chapter 3.

1.8.2 Motivational mechanisms engaged by homeostatic neurons to direct food seeking and consumption

Studies on the role of AGRP neurons in feeding do not only demonstrate that activation of AGRP neurons induce food consumption, but also increase an animal's motivation to work for food through flexible behaviours (Atasoy et al. 2012, Krashes et al. 2011). Thus, AGRP neuron evoked feeding is not solely a reflection of the initiation of motor patterns controlling feeding, but also posses motivational properties to direct food consumption. This is not particularly surprising as it has been shown that animals in a state of energy deficit will work much harder for food in an operant task than animals fed *ad libitum* (Hodos 1961). In addition, hormones that regulate AGRP neuron activity, such as ghrelin and leptin, can also influence the willingness of an animal to work for food (Figlewicz et al. 2006, Overduin et al. 2012). The motivational processes engaged by AGRP neurons, however, have not been reported.

Under states of energy deficit, flexible goal-directed behaviours employed to acquire food are learned through reinforcement processes that evaluate the results of actions to determine the future probability of emission of these actions (Berridge 2004, Bindra 1976, Freud 2001, Hull 1943, Olds 1969, 1976). Negative reinforcement was classically viewed as a mechanism for hunger to influence motivation, where actions that result in elimination of an unpleasant state generated by hunger were reinforced (Berridge 2004, Freud 2001, Hull 1943). Positive reinforcement mechanisms reflect the pursuit of rewards from the environment (Bindra 1976), and hunger has been understood to enhance the rewarding value of food through the increase in their perceived palatability (Rolls et al. 1983, Rolls & Rolls 1997, Stoeckel et al. 2007, Yeomans & Mobini 2006) as well as nutritive properties (Ackroff et al. 2009, de Araujo et al. 2008, Sclafani & Nissenbaum 1988, Yiin et al. 2005). Modulation of sensory sensitivity by hunger has also been proposed

to modulate behavioural responding in invertebrates (Chalasani et al. 2010, Inagaki et al. 2012, Root et al. 2011, Sengupta 2013), but it is unclear whether this mechanisms extends to mammals, as studies in rodents, primates, and humans show inconsistent results (Albrecht et al. 2009, Brosvic & Hoey 1990, Kawai et al. 2000, Pasquet et al. 2006, Rolls et al. 1983, Rolls & Rolls 1997, Savigner et al. 2009, Shin et al. 2008, Stafford & Welbeck 2011, Yaxley et al. 1988, Yaxley et al. 1985, Yeomans & Mobini 2006, Zverev 2004). The reinforcement mechanisms engaged by AGRP neurons in the modulation of feeding behaviour is addressed in chapter 4.

1.8.3 Divergence of roles of homeostatic neurons' downstream circuits in the control of feeding

The study of the role of diverging long-range axonal projections of AGRP neurons in feeding demonstrate the use of this approach to uncover downstream regions important in the coordination of feeding behaviour, as axonal projections of these feeding related homeostatic neurons can serve as a blueprint to unravel the feeding circuits in the brain. However, most studies employing this type of approach have focused on linear relationships between homeostatic neurons and one or two downstream projections, despite the fact that these neurons display broad axonal arborisation throughout the brain (Atasoy et al. 2012, Carter et al. 2013, Jennings et al. 2013, Krashes et al. 2014). AGRP neurons, for example, send significant projections to many regions in the brain, both within and outside of the hypothalamus (Betley et al. 2013, Haskell-Luevano et al. 1999). In addition, the dissociation of function of $ARC^{AGRP} \rightarrow PVH$ and $ARC^{AGRP} \rightarrow PBN$ circuits (Atasoy et al. 2012) indicates that different projections might have different functions. Therefore, to fully understand the role of AGRP neurons in feeding, the role of individual axonal projections in evoked feeding must be systematically examined. This issue is addressed in chapter 5.

1.9 Aims of thesis

This thesis aims to further the understanding of the role of homeostatic interoceptive neurons in the control of feeding behaviour. As a whole, I hypothesize that homeostatic neurons in the brain, in particular the hypothalamus, are in a position to translate peripheral signals of energetic state through changes in their activity. These neurons are not necessarily just consummatory neurons, but may also have the capability of engage motivational processes to direct flexible appetitive food seeking actions, where the changes in their activity can serve as teaching signals for action selection. Their ability to direct behavioural flexibility is likely conferred by the anatomical and functional organization of their downstream projections, whereby different projections might modulate distinct aspects of feeding behaviour. Each chapter attempts to address one of the three issues discussed in the previous section and test the above hypothesis, and are outlined as follows:

Chapter 3: Here I investigate the role of LHA^{LepRb} neurons in feeding using a combination of optogenetic and behavioural manipulations to establish the causal relationship between the elevated activity of these neurons and the modulation of feeding responses. Given that direct leptin infusion in the LHA reduces food intake and leptin is known to depolarize LHA^{LepRb} neurons (Leinninger et al. 2009), I hypothesize that the elevated activity of these neurons will lead to a reduction in food intake. In addition, electrophysiological studies were performed to further understand the electrophysiological properties of these neurons, including their responses to signals of energetic state. I postulate that LHA^{LepRb} neuron activity is modulated by signals of energy deficit and surfeit, given that the LHA is viewed as an energy sensing brain region (Burdakov et al. 2005a, Burdakov et al. 2013, Karnani et al. 2011, Yamanaka et al. 2003). Furthermore, CRACM methods were employed to determine the functional synaptic connectivity of these neurons with two known downstream projection regions, the ventral tegmental area (VTA) and the LHA. Due to the GABAergic nature of LHA^{LepRb} neurons (Leinninger et al. 2009), I expect to observe inhibitory postsynaptic responses during optogenetic activation of LHA^{LepRb} neurons in the LHA and VTA.

Chapter 4: Here I examine the reinforcement mechanism employed by AGRP neurons to coordinate feeding behaviour as well as direct action selection in food

seeking. These studies employed optogenetic techniques in combination with complex behavioural paradigms. Recent data studies show that silencing of AGRP neurons under hunger is reinforcing (Betley et al. 2014). Therefore, conditioned place aversion tests were employed to determine whether elevated AGRP neuron activity possess a negative valence. A number of operant conditioning studies, including progressive ratio and fixed ratio lever pressing tasks, were used to determine the effect of maintaining elevated AGRP neuron activity on action selection in food seeking behaviour. I posit that AGRP neuron activity carries a negative valence and serves as a negative reinforcement teaching signal for action selection, where actions that do not reduce AGRP neuron activity are diminished, while actions that do are reinforced.

Chapter 5: Here I systematically evaluate the role of six major AGRP neuron projections subpopulations in AGRP neuron mediated evoked-feeding behaviour. This was accomplished through the use of optogenetic activation of region-specific AGRP neuron axons during feeding assays to measure the effect of activation of distinct AGRP neuron subpopulations in feeding. In addition, anatomical and pharmacological techniques were employed to understand the regulation of these projection specific subpopulations by states of energy deficit and starvation signals. Given prior evidence that activation of AGRP neuron projections to the PBN does not elicit feeding, I propose that some, but not all, AGRP neuron subpopulations are capable of recapitulating feeding observed under AGRP somatic stimulation, which might be due to their differential regulation by signals of energy deficit.

Chapter 2

General Methods

2.1 Animals

All animal procedures conducted at the University of Cambridge were carried out in accordance with the Animal's Act, 1986 (Scientific procedures). Animals (LepRb^{Cre}, LepRb^{Tom}, and LepRb^{ChR2Tom} mouse lines, see Table 2.1) were bred and kept in the Combined Animal Facility, University of Cambridge. All animal procedures conducted at Janelia Farm Research Campus were carried out in accordance with U.S. National Institutes of Health guidelines for animal research and were approved by the Institutional Animal Care and Use Committee at Janelia Farm Research Campus. At Janelia Farm, animals (LepRb^{Cre}, LepRb^{ChR2Tom}, Ai32, Ai9, AGRP^{Cre}, AGRP^{ChR2EYFP}, and AGRP^{ChR2Tom} mouse lines, see Table 2.1) were housed in the Janelia Farm Vivarium. Mice were housed in standard conditions on a 07:00 to 19:00 light cycle (University of Cambridge) or 06:00 to 18:00 light cycle (Janelia Farm Research Campus) with *ad libitum* food and water.

At the University of Cambridge, LepRb^{Cre} and LepRb^{Tom} experimental animals were generated in house through homozygote/homozygote breeding pairs. At Janelia Farm Research Campus, LepRb^{Cre} animals were generated through homozygote/homozygote breeding pairs. AGRP^{Cre} experimental mice were generated through breeding of homozygote AGRP^{Cre} with C57BL/6J animals acquired from The Jackson Laboratory. Resulting pups were genotyped for Cre to determine the presence of transgene. AGRP^{ChR2EYFP} experimental mice were generated by breeding homozygote AGRP^{Cre} with homozygote Ai32 animals. Resulting pups were genotyped for Cre, wild-type (WT) ROSA, and YFP-1 to determine the presence of transgene. All genotyping was conducted by Transnetyx, Inc. A summary of transgenic mouse lines used in all studies, including their expression description, generation, and use is provided in Table 2.1.

Line Name	Expression and Generation	Use
Ai9	B6.Cg-*Gt(ROSA)26Sor$^{tm9(CAG-tdTomato)Hzw}$*/J is a Cre-dependent reporter mouse line for the expression of red fluorescent protein tdTomato, generated through a targeted mutation of the *Gt(ROSA)26Sor* locus with a loxP-flanked STOP cassette preventing transcription of *CAG* promoter driven tdTomato (Madisen et al. 2010). Original breeding pair was obtained from The Jackson Laboratory.	For the generation of LepRb^{Tom} mouse line.
Ai32	B6;129S-*Gt(ROSA)26Sor$^{tm32(CAG-COP4*H134R/EYFP)Hze}$*/J is a Cre-dependent reporter mouse line for the expression of membrane localized enhanced channelrhodopsin (ChR2), ChR2 (H134R), fused to an enhanced yellow fluorescent protein (EYFP). The line was generated through a targeted mutation of the *Gt(ROSA)26Sor* locus with a loxP-flanked STOP cassette preventing transcription of *CAG* promoter driven ChR2 (H134R)-EYFP (Madisen et al. 2012). Original breeding pair was obtained from The Jackson Laboratory.	For the generation of AGRP^{ChR2EYFP} mouse line
LepRb^{Cre}	B6.129-*Lepr$^{tm2(cre)Rck}$*/J mouse line expresses Cre under the *Lepr* promoter. A targeting vector containing an internal ribosome entry site (IRES), nuclear localization signal (NLS) and Cre was inserted immediately 3' of the stop codon in the last exon of the *Lepr* gene (DeFalco et al. 2001). Original breeding pair was obtained from The Jackson Laboratory.	For the generation of LepRb^{Tom} mouse line and LepRb^{ChR2Tom} experimental animals.
LepRb^{Tom}	Express tdTomato in leptin receptor (LepRb) neurons. They were generated by crossing LepRb^{Cre} mice with Ai9 mice. Original breeding pair was obtained from Dr. Lora Heisler (currently at: University of Aberdeen).	Used in Chapter 3, sections 3.3.1 and 3.3.2
LepRb^{ChR2Tom}	Express membrane localized ChR2 (H134R), fused to tdTomato in LepRb neurons in the lateral hypothalamic area (LHA). These animals were generated through targeted LHA injections of AAV1.CAGGS.Flex.ChR2-tdTomato.WPRE.SV40 viral vector in LepRb^{Cre} mice.	Used in Chapter 3, sections 3.3.3 and 3.3.4.
AGRP^{Cre}	*AGRP$^{tm1(cre)Lowl}$*/J animals express Cre under the *AGRP* promoter. A targeting vector containing IRES and Cre was inserted immediately downstream of the stop codon in exon 3 of the *AGRP* gene (Tong et al. 2008). Original breeding pair was obtained from The Jackson Laboratory.	For the generation of AGRP^{ChR2EYFP} mouse line and AGRP^{ChR2Tom} and AGRP^{EGFP} experimental animals.

Table 2.1 Transgenic mouse lines used for all studies. Line name corresponds to name used in this dissertation, which might be different from their common name. *Table continued on next page.*

Line Name	Expression and Generation	Use
AGRP^ChR2EYFP	Express membrane localized ChR2 (H134R) fused to EYFP in agouti-related peptide (AGRP) neurons. They were generated by crossing AGRP^Cre mice with Ai32 mice. Mouse line was generated in-house at Janelia Farm Research Campus.	Used in all sections of Chapter 4, and in Chapter 5, section 5.3.3.
AGRP^ChR2Tom	Express membrane localized ChR2 (H134R) fused to tdTomato fluorescent reporter protein in AGRP neurons. These animals were generated through targeted arcuate nucleus (ARC) injections of rAAV2/10-CAG-FLEX-rev--ChR2-tdTomato viral vector in AGRP^Cre mice.	Used in Chapter 5, section 5.3.1 and 5.3.2.
AGRP^EGFP	Express a green fluorescent reporter protein (EGFP) in AGRP neurons in the ARC. These animals were generated through targeted ARC injections of rAAV2/9-*CAG*-FLEX-EGFP viral vector in AGRP^Cre mice.	Used in Chapter 4, section 4.3.2.

Table 2.1 continued

2.2 Viral constructs

Three Cre-recombinase dependent adeno-associated viruses (AAV) were used to achieve conditional expression of channelrhodopsin (ChR2) and enhanced green fluorescent protein (EGFP) in targeted cell populations. All AAV vectors use a Cre-dependent flip-excision (FLEx) switch mechanism were two pairs of anti-parallel and heterotypic loxP-type recombination sites flank the coding sequence (Atasoy et al. 2008). Under the presence of Cre, a synthetic promoter CAG, which includes a cytomegalovirus enhancer element, a promoter with the first exon and first intron of the chicken β-actin gene, and a splice acceptor of rabbit β-globin gene, directs expression of transgene encoded in the viral vector (Miyazaki et al. 1989, Niwa et al. 1991). All viral vectors were obtained from the University of Pennsylvania Vector Core. A summary of all viral vector constructs used, including their titre and expression, can be found in Table 2.2.

Viral construct	Titre	Express
AAV1.CAGGS.Flex.ChR2tdTomato.WPRE.SV40 (Addgene18917)	1.42×10^{13}	Membrane-bound ChR2(H134R) fused to tdTomato
rAAV2/10-CAG-FLEX-rev-ChR2 tdTomato (Addgene18917)	3×10^{13}	Membrane-bound ChR2(H134R) fused to tdTomato
rAAV2/9-*CAG*-FLEX-EGFP	7×10^{12}	EGFP

Table 2.2 Adeno-associated viral vectors used for transgene delivery. Titre is reported as genomic copies per ml.

2.3 Electrophysiology

2.3.1 Preparation of acute brain slices

Mice were euthanized by cervical dislocation during the light phase and rapidly decapitated. After decapitation, the brain was quickly removed and incubated shortly (~2 min) in cold (<4º C) oxygenated (95% O_2 and 5% CO_2) sucrose slicing solution. A block of brain tissue was glued to the stage of a vibratome (Campdem Vibroslice, Campdem Instruments Ltd. or Leica VT1200s, Leica Biosystems) and thick sections were sliced while immersed in ice-cold oxygenated sucrose slicing solution. Sections were then transferred into oxygenated artificial cerebrospinal fluid (aCSF), were they were allowed to recover at 35º C for one hour and then maintained at room temperature (21-24º C). Sections were used for recording within 8 hours of slicing. aCSF was oxygenated continuously throughout experiments. For recordings in the lateral hypothalamic area (LHA), 250 µm coronal sections were used. For recordings in the ventral tegmental area (VTA), 250 µm coronal sections or 300 µm horizontal sections were used. Contents of sucrose slicing solution and aCSF are listed in Table 2.3. All chemicals used were purchased from Sigma-Aldrich.

Sucrose slicing solution		aCSF	
Sucrose	110	NaCl	125
NaCl	52.5	KCl	2.5
KCl	2.5	NaH_2PO_4	1.2
NaH_2PO_4	1.25	$NaHCO_3$	21
$NaHCO_3$	26	$MgCl_2$	2
$MgCl_2$	5	$CaCl_2$	2
$CaCl_2$	1	D-(+)-Glucose	1
D-(+)-Glucose	25	Ascorbic acid	0.4
Ascorbic acid	0.4	Sodium pyruvate	0.15
Kynurenic acid	0.1		

Table 2. 3 Extracellular perfusion solutions for *in vitro* experiments.
Concentrations are reported in mM.

2.3.2 Whole-cell patch clamp recordings

An EPC-10 amplifier and Patchmaster software (HEKA Elektronik) were used to perform whole-cell patch clamp recordings from acute brain slices. Patch pipettes with tip resistance of 3-5 MΩ (with KCl intracellular solution) or 5-8 MΩ (with K-Gluconate intracellular solution) were pulled from thin-walled borosilicate glass capillaries with an internal filament (outer diameter 1.5 mm, inner diameter 1.12 mm, Drummond Scientific Company) using a DMZ-Universal puller (Zeitz Instruments). Slices were placed in a submerged-type chamber and anchored with a nylon string grid stretched over platinum wire. Brain slices were perfused continuously with oxygenated aCSF at a rate of ~2 ml per min and all recordings were made at 37º C. Visualization of living cells in brain slices was performed using an Olympus BX50WI microscope with an Olympus LUMPlanFI-IR 40x/0.8 numerical aperture objective (Olympus), a mercury lamp, and an mCherry filter set (Chroma Technology Corp.) for visualisation of tdTomato marked cells. Recording pipettes were advanced under positive pressure towards identified cells in the slice, and pressure was released and slight suction applied to form a GΩ seal. The membrane was then ruptured by suction to gain access to the cell. Only cells with series resistance <25 MΩ were used for experiments and analysis. KCl intracellular solution was used for all ChR2-

assisted circuit mapping (CRACM) experiments. For all other experiments, K-Gluconate intracellular solution was used. Contents of KCl and K-Gluconate solutions are listed in Table 2.4. All chemicals used were purchased from Sigma-Aldrich.

KCl		K-Gluconate	
KCl	130	K-Gluconate	120
HEPES	10	KCl	10
EGTA	0.1	HEPES	10
NaCl	2	EGTA	0.1
$MgCl_2$	2	$MgCl_2$	2
K_2ATP	5	K2-ATP	4
		Na_2ATP	1

Table 2.4 Intracellular pipette solutions for *in vitro* experiments. Concentrations are reported in mM. Solutions were neutralized to pH 7.3 with KOH.

2.4 Stereotaxic surgeries

Mice at least 6 weeks of age were anaesthetized with isoflurane (~0.5% in O_2), and placed into a stereotaxic apparatus (David Kopf Instruments). The skull was exposed via a small incision in the scalp and small holes were drilled on the skull for virus or dye injections and fibre ferrule implantation. A pulled glass pipette (Drummond Scientific Company) with 20-40 μm tip diameter was inserted into the brain and virus or dye was delivered using an infusion pump (Harvard Apparatus Ltd) at a speed of 120 nl per min or a manual pump (Narishige International USA) at ~50 nl per min. If no fibre ferrule was implanted, scalp incision was closed with Vetbond (3M). Fibre ferrules, made by capping an optic fibre (200 μm diameter core, multimode, NA 0.48, ThorLabs) with a 1.25 mm OD zirconia ferrule (Precision Fiber Products), were implanted ~0.3-0.4 mm above target region. Grip cement (Denstply) was used to anchor the ferrule capped fibres to the skull. Pre-operative analgesia (buprenorphine, 0.1 mg/kg, subcutaneous (s.c.) injection) and postoperative analgesia (ketoprofen, 5 mg/kg, s.c., immediately after surgery completion and for the following 2 days) was provided. Animals were single-housed post-surgery and

allowed to recover for at least 5 days before the start of any experiment. Coordinates used for all target areas are listed in Table 2.5.

Target region	Anterior/Posterior	Medial/Lateral	Dorsal/Ventral
LHA	- 1.4 mm	± 1.1 mm	5.0 mm (SS)
ARC	- 1.3 mm	± 0.3 mm	5.8 mm (DS)
aBNST	0.62 mm	± 0.65 mm	4.4 mm (SS)
PVH	0.7 mm	± 0.15 mm	4.6 mm (SS)
LHAs	- 1.3 mm	± 1.0 mm	4.7 mm (SS)
PVT	1.1 mm	0.0 mm	3.0 mm (SS)
CEA	-1.2 mm	± 2.5 mm	4.35 mm (SS)
PAG	-4.5 mm	± 0.5 mm	2.8 mm (SS)
PBN	-5.8 mm	± 0.9 mm	3.5 mm (SS)

Table 2.5 Coordinates for target regions. Anterior/Posterior and Medial/Lateral coordinates were measured from Bregma and the midline, respectively. Dorsal/Ventral coordinates were measured from the dorsal surface of the brain (DS) or skull surface at Bregma (SS). LHA: lateral hypothalamic area; ARC: arcuate nucleus; aBNST: anterior subdivisions of the bed nucleus of stria terminalis; PVH: paraventricular nucleus of the hypothalamus; LHAs: suprafornical subdivision of the lateral hypothalamic area; PVT: paraventricular thalamic nucleus; CEA: central nucleus of the amygdala; PAG: periaqueductal grey; PBN: parabrachial nucleus

2.5 Optogenetic stimulation

2.5.1 *In vitro* slice photostimulation

To stimulate ChR2, a LAMBDA DG-4 fast switcher (Sutter Instruments) with a xenon lamp and ET470/40 nm bandpass filter was used. Blue light (10 mW/mm^2) was delivered *via* a 40x/0.8 NA objective for whole-field pulsed-light stimulation. Ten-second pulsed light stimulations at varying frequencies (1 Hz, 5 Hz, and 20 Hz) and varying pulse durations (1 ms and 5 ms) were used.

2.5.2 *In vivo* photostimulation

For optical delivery of light pulses with millisecond precision to multiple mice, the output beam of a diode laser (473 nm, Altechna Co. Ltd. or OptoEngine LLC) was controlled using an acousto-optic modulator (AOM) (Quanta Tech, OPTO-ELECTRONIC) to generate light pulses that were launched into a single fibre port (PAF-X-5, Thorlabs) and a 6-way laser beam splitter (Fibersense). Optical fibres (200 µm diameter core, multimode, NA 0.37 or 0.48, Doric Lenses Inc.) were coupled to beam splitters using a fibre coupler (ADAFC4, Thorlabs). These were then coupled to final optical fibres with 1.25 OD zirconium ferrules (Doric Lenses Inc.) inside sound attenuating chambers (described below in section 2.6.1) through single fibre or double fibre commutators (Doric Lenses Inc.) for unilateral or bilateral stimulation, respectively, installed inside chambers. Light was delivered to the brain by coupling optical fibres to ferrule capped fibres implanted into animals with a zirconium sleeve (Precision Fiber Products). Using these components, multiple animals could be simultaneously photostimulated. For all *in vivo* photostimulation experiments, the same pulse protocol was used: 10 ms pulses, 20 pulses for 1 s, repeated every 4 seconds for the duration of the stimulation. Software controlling AOMs was custom written in LabView (National Instruments).

2.5.3 Irradiance calculation

Irradiance at target regions (I_z) were estimated using previously described relationship of light scattering and absorption in the brain as a function of distance (Aravanis et al. 2007) with the following formula:

$$I_z = \left(\frac{P_{laser}}{\pi r_{fib}{}^2}\right)\left(f_{laser\_coupling}\right)\left(\frac{\rho^2}{(Sz+1)(z+\rho^2)}\right) \, ,$$

where P_{laser} is the power of laser used, the radius of the optic fibre (r_{fib}) = 100 µm, the laser coupling fraction ($f_{laser\_coupling}$) = 0.9, the scattering coefficient (S) = 11.2 mm^{-1}, z is the distance of target from fibre tip (mm) and

$$\rho = r_{fib}\sqrt{\left(\frac{n_{tis}}{NA_{fib}}\right)^2 - 1} \, ,$$

where the tissue refractive index (n_{tis}) = 1.36 as calculated for gray matter and fibre NA (NA_{fib}) is 0.48. Using this relationship, unless otherwise noted, the light power exiting the fibre tip (10-15 mW) was estimated to correspond to irradiances >2.0 mW/mm^2 at target regions, which was sufficient to drive a behavioural response, as ChR2 activation threshold is ~1 mW/mm^2 (Aravanis et al. 2007, Lin et al. 2009).

2.6 Behaviour set-up

All behavioural studies were conducted using adult animals >8 weeks old. Due to the large variety and complexity of behavioural paradigms, only behavioural set ups are described below. Exact protocols for each behavioural paradigm are described within each results chapter.

2.6.1 Food consumption and lever press studies

Behavioural testing of food intake measurements and lever press studies was performed using automated feeding cages (Coulbourn Instruments) housed inside custom made sound attenuating chambers as described by The Neurogenetics and Behavior Center at Johns Hopkins University (see http://nbc.jhu.edu/facilities/manuals.html). Feeding cages were equipped with a food hopper and an automatic pellet dispenser which delivered 20 mg food pellets (described below in section 2.6.2). During free feeding tests, food pellets were available *ad libitum* but provided one by one by the automatic pellet dispenser. Pellet removal from the food hopper was sensed by the offset of a beam break and an additional pellet was delivered after a 5 s delay. For all lever pressing experiments, two retractable levers, one active and one inactive, were available at either side of the food hopper. Levers were extended upon the start of the testing session. After reaching lever press criteria, levers retracted and a 20 mg pellet was delivered into the food hopper. Five seconds after pellet removal from the hopper, levers were extended and available for pressing again. This protocol was adopted in order to ensure lever pressing behaviour was goal-directed (towards obtaining food) and not a measure of general behavioural activation. Lever pressing on the inactive lever was also monitored for this purpose. Food consumption and lever pressing

behaviour was recorded continuously during test sessions using Graphic State software (Coulbourn Instruments).

2.6.2 Food pellets

All food pellets used in behavioural experiments were irradiated 20 mg pellets (Test Diet). Unless otherwise noted, grain pellets were used for all food consumption tests as well as lever press training sessions. Grape and citrus pellets were used for lever pressing experiments (as described in Chapter 4). Grain pellets were of identical composition to the food in the home cages (product code: UTUM). Grape pellets were of the same composition as grain pellets with added 1% saccharine and grape flavouring. Citrus pellets were of the same composition as grain pellets with added 1% saccharine and citrus flavouring.

2.6.3 Conditioned place avoidance studies

Conditioned place avoidance studies were conducted in a custom-made two-chambered apparatus with visual (black and white sides) and textural cues (the flooring on the black side was paired with a plastic grid (3 mm holes) and the white side was paired with the soft textured side of a Kimtech Science bench top protector #7546, Kimberly Clark). The floor was back-lit at a luminance of ~100 Lux units using a tuneable LED that provided uniform distribution of the light over the entire length of the floor. A video camera (Basler Inc) was mounted overhead to record the mouse's position. Video recordings were performed at 3.75 Hz frame rate with gVision software (Lott 2010). Mouse position was tracked offline using Ctrax (Branson et al. 2009). The entire apparatus was place in a sound isolation chamber similar to that described by The Neurogenetics and Behavior Center at Johns Hopkins University. These conditions were chosen such that 1) no population side bias was observed, 2) mice explored both chambers readily, and 3) the initial preference of individual mice was stable over 5 days of exposure in the absence of conditioning, suggesting that mice can differentiate context and do not exhibit spontaneous changes in their original preference.

2.7 Immunohistochemistry

Mice were perfused with 4% paraformaldehyde in 0.1 M phosphate buffer fixative (pH 7.4). Tissue was post-fixed in this solution for 3-4 hrs and washed overnight in phosphate buffered saline (PBS) (pH 7.4). Brain slices (20-100 μm thick) were incubated overnight at 4⁰ C with primary antibodies diluted in PBS with 1% bovine serum albumin (BSA) and 0.1% triton X-100. Slices were then washed 3 times and incubated with species appropriate and minimally cross reactive fluorophore-conjugated secondary antibodies for 2 hours at room temperature (~21⁰ C). Slices were rinsed in PBS 2 times and mounted onto Superfrost mounting slides (Thermo Scientific) for imaging using hardset Vectashield (H1400, Vector Laboratories). Antibodies used and their concentrations are listed in Table 2.6. All chemicals used were purchased from Sigma-Aldrich.

Antibody	Dilution	Company
Mouse anti-TH	1:1,000	Millipore
Rabbit anti-RFP	1:1,000	Rockland Immuno
Goat anti-AGRP	1:3,000	Neuromics
Guinea-pig anti-RFP	1:20,000	Covance
Rabbit anti-Fos (Lot C1010)	1:5,000	Santa Cruz Biotechnology
Rabbit anti-POMC	1:2,000	Phoenix Pharmaceuticals
Sheep anti-GFP	1:1,000	AbD Serotec
Guinea-pig anti-FG	1:500	Protos Biotech
Species specific fluorophore-conjugated secondary antibodies (FITC, Cy3, Cy5)	1:500	Jackson ImmunoResearch

Table 2.6 Primary and secondary antibodies used for immunohistochemical studies. TH: tyrosine hydroxylase; RFP: red fluorescent protein; AGRP: agouti-related peptide; POMC: proopiomelanocortin; GFP: green fluorescent protein; FG: Fluoro-Gold.

2.8 Imaging

Epifluorescent images were taken using a Zeiss Axioskop2 (Zeiss) with a 10x or 20x objective (Chapter 3). Differential interference contrast (DIC) and fluorescent images of patched neurons were taken using an Olympus BX50WI microscope with a 40x/0.8 numerical aperture objective (Chapter 3). Whole brain slice epifluorescent images were taken using an Olympus MVX10 with a DP71 camera and MV Plano 2xC objective to record fibre position (Chapters 3, 4, and 5). Whole brain slice epifluorescent images for dye injection localization and agouti-related peptide (AGRP) peptide or transgene expression mapping (Chapters 4 and 5) were taken using a 20x objective on an automated panoramic slide scanner (Perkin Elmer). Confocal images were taken for measurements of transgene penetrance and transgene expression patterns (Chapters 4 and 5) using a Zeiss LSM 510 microscope with a 65x objective (Zeiss), and images for Fos immunoreactivity measurements were taken using a 20x objective (Chapter 3, 4, 5).

2.9 ChR2 expression calculations

2.9.1 ChR2 penetrance in AGRP^{ChR2EYFP} animals

To verify the expression of ChR2 in AGRP neurons, hypothalamic brain slices of AGRP^{ChR2EYFP} animals were co-immunostained for green fluorescent protein (GFP) and AGRP. In addition, separate brain sections were co-immunostained for GFP and proopiomelanocortin (POMC) to verify specificity of ChR2 expression. Whole brain slice epifluorescent images were taken to visualize AGRP peptide, POMC peptide, and transgene expression (marked by GFP) using a 20x objective on an automated panoramic slide scanner in known AGRP neuron projection fields. Confocal images of axonal varicosities in target regions were imaged using a 65x objective with a z-stack of 5 optical sections of 0.5 μm depth. A total of 6 images per projection field was taken and analyzed from brain sections of three animals (2 images per section, 1 section per animal). Colocalization of GFP and AGRP or POMC was determined by manually inspecting at random 100 AGRP or POMC

boutons per image analyzed, and colocalization of GFP was determined for each bouton.

2.9.2 ChR2 penetrance in virally transduced neurons

To quantify ChR2 penetrance in virally transduced AGRP neuron projection fields in AGRP^{ChR2Tom} animals, the colocalization of the ChR2-fused fluorescent protein reporter tdTomato and AGRP immunoreactivity was calculated. Brain slices were co-immunostained for AGRP and the tdTomato fluorescent protein. Confocal images of axonal varicosities in target regions were imaged at 65x with a z-stack of 5 optical sections of 0.5 μm depth in the projection field area directly under the implanted optical fibre in one 50 μm brain slice. The percentage of AGRP-containing boutons transduced with ChR2-tdTomato was calculated using automated varicosity detection in Vaa3D (Peng et al. 2010) and confirmed by manual inspection, as described previously (Atasoy et al. 2012).

2.10 Fos intensity distribution calculations

Confocal images (z-stack with 1 μm optical sections through the thickness of the section, ~50 μm) of brain tissue stained for Fos were obtained with a 20x objective, maintaining individual pixel intensities in the linear range for Fos-immunofluorescence from tissue taken from a food deprived mouse, and those settings were applied to all other conditions. Average fluorescent pixel intensity per nuclei was calculated using the histogram function of Adobe Photoshop (Adobe Systems Inc.).

2.11 Statistics

Electrophysiological data extraction, plotting and analysis were carried out using MiniAnalysis 6.0.7 (Synaptosoft Inc), Matlab 2013b (Mathworks) and Igor Pro 6.3 (Wavemetrics). Data extraction and plotting for all behavioural studies were carried out using Matlab 2013b. P-values for pair-wise comparisons were calculated

by unpaired or paired two-tail student's t-test. P-values for comparisons across more than two groups were calculated using one-way or two-way analysis of variance (ANOVA) or repeated measures (RM) ANOVA. Individual *post-hoc* statistical comparisons were corrected for multiple comparisons using the Holm-Sidak correction method. Analyses of distributions were performed using the Mann-Whitney Rank sum test, or the Kruskal-Wallis one-way ANOVA on ranks test for comparisons of more than 2 distributions. All statistical analyses were performed using SigmaPlot (Systat). Data are shown as means ± standard error of the mean (S.E.M.). Statistical significance was defined as having a p-value <0.05.

Chapter 3

Lateral Hypothalamic Leptin Receptor

Neurons are Anorexigenic

3.1 Introduction

The concepts of homeostasis (Cannon 1932) and behavioural regulation of energy balance (Richter 1943) have guided the study of the control of feeding behaviour by the brain. Research today indicates that signals conveying the energetic state of the body are capable of modulating homeostatic sensing neurons to modulate food consumption and food seeking actions (Sternson et al. 2013). Therefore, the identification of homeostatic neurons in the brain and their circuits is an important step to fully understand how the brain directs food consumption behaviour. One such group of neurons requiring further investigation are leptin receptor (LepRb) neurons in the lateral hypothalamic area (LHA).

3.1.1 Leptin and LepRb control of food intake

Leptin is a 16kDa non-glycosylated polypeptide, product of the *ob* gene, produced and secreted by white adipose cells into the bloodstream (Caro et al. 1996, Considine et al. 1996, Havel 1999). Leptin is considered a signal that represents the availability of internal energy stores (Ahima et al. 1996, Seeley & Woods 2003), as circulating leptin concentrations correlate with both body mass index (BMI) and total body fat (Caro et al. 1996, Considine et al. 1996). Leptin enters the brain through active transport across the blood brain barrier or diffusion through regions such as the median eminence adjacent to the arcuate nucleus (ARC) of the hypothalamus (Bjorbaek et al. 1998, Caro et al. 1996). In the brain, leptin acts through LepRb (also known as Ob-Rb) (Lee et al. 1996, Lollmann et al. 1997, Tartaglia et al. 1995). LepRb is expressed widely throughout the brain, with the highest levels of expression found in the hypothalamus, including the ARC, the dorsomedial nucleus of the hypothalamus (DMH), the ventromedial nucleus of the hypothalamus (VMH), the LHA, and the ventral premammillary nucleus (PMV) (Leshan et al. 2006, Scott et al. 2009). Leptin binding to LepRb creates a conformational change in the structure of the receptor (Hegyi et al. 2004), which activates the Janus-activated kinase/ signal transducers and activators of transcription (JAK/STAT) pathway, phosphorilating signal transducer and activator of transcription 3 (STAT-3) to promote expression of suppressor of cytokine signalling 3 (SOCS3) gene and anorexigenic genes such as

proopiomelanocortin (POMC), while inhibiting expression of orexigenic genes such as agouti-related peptide (AGRP) (Bjorbak et al. 2000).

Leptin is known to be an anorectic peptide, as leptin inhibits food consumption and promotes energy expenditure when food is plentiful (Gao & Horvath 2007, 2008). Most of what is known about leptin and its role in feeding was brought to light through the study of the *ob/ob* and *db/db* mouse lines. Both mutant mouse lines arose at random within mice colonies at The Jackson Laboratory. These animals are hyperphagic and severely overweight in comparison to their wild-type (WT) counterparts (Hummel et al. 1966, Ingalls et al. 1950). It was later discovered that the *ob* gene encodes leptin (Zhang et al. 1994) leading to the understanding that *ob/ob* animals lacked leptin (Zhang et al. 1994), while *db/db* mice lacked functional LepRb (Chen et al. 1996). Lack of functional LepRb is also responsible for the observed obese phenotype of Zucker *fa/fa* rats (Chua et al. 1996). Humans with inherited mutations of genes encoding leptin or LepRb also display severe obesity (Farooqi et al. 2003, Montague et al. 1997, Pelleymounter et al. 1995). Further manipulations of leptin levels in mutant and WT mice established the role of leptin in feeding. Intracerebroventricular (i.c.v.) administration of leptin i.c.v. lowered food intake in both WT and *ob/ob* animals (Mistry et al. 1997). Administration of leptin i.c.v. in rats also lowered self-administration of sucrose (Figlewicz et al. 2006). Moreover, transplantation of leptin responsive hypothalamic cells into the hypothalamus of *db/db* mice reduced the obesogenic phenotype of these animals (Czupryn et al. 2011).

3.1.2 LepRb neurons in the brain

Since leptin is an important signal that conveys the energetic state of an animal, and has been shown to modulate feeding, LepRb expressing neurons in the brain can be viewed as putative homeostatic interoceptive neurons. Because LepRb is expressed widely throughout the brain (Leshan et al. 2006, Scott et al. 2009), however, the exact LepRb neurons and circuits that play a role in the modulation of feeding behaviour is still poorly understood. In the ARC, LepRb is known to be expressed in AGRP and POMC neurons (Coll et al. 2007, Elmquist et al. 2005, Oswal & Yeo 2010). In the presence of leptin, AGRP neuron activity is suppressed

and expression of AGRP and NPY is reduced, while POMC neurons are activated and synthesis of POMC and secretion of α-melanocyte stimulating hormone (αMSH) is increased, leading to a decrease in food intake (Cowley et al. 2001, Schwartz et al. 2000, van den Top et al. 2004). However, data also suggests that the action of leptin on these neurons accounts for only a fraction of leptin's action in the control of feeding behaviour (Dhillon et al. 2006, Dimicco & Zaretsky 2007, Leinninger et al. 2009, Myers et al. 2009). For example, leptin depolarizes and increases firing rate of LepRb neurons in the VMH that co-express steroidogenic factor-1 (SF-1), and knock-out (KO) of LepRb VMH^{SF-1} neurons increases body weight (Dhillon et al. 2006). In addition, LepRb is also expressed in the ventral tegmental area (VTA), and direct leptin infusion to the VTA is sufficient to decrease food intake and hyperpolarize VTA dopamine (DA) neurons in anesthetized animals (Hommel et al. 2006). This indicates that other LepRb neuron populations and their circuits are also important in the regulation of feeding behaviour. Pharmacological and genetic studies (Davis et al. 2011, Leinninger et al. 2009), in addition to the role of the LHA as an energy sensing brain region (Burdakov et al. 2005a, Burdakov et al. 2013, Karnani et al. 2011, Yamanaka et al. 2003), indicates that LHA^{LepRb} neurons are putative homeostatic neurons.

3.1.3 LHA^{LepRb} neurons

LepRb expressing neurons in the LHA are intermingled with orexin (OX) and melanin-concentrating hormone (MCH) neurons and are modulated by leptin (~ 33% depolarized, ~22% hyperpolarized) (Leinninger et al. 2009). LHA^{LepRb} neurons are known to be inhibitory as they express γ-aminobutyric acid (GABA), and a subpopulation of these neurons (~60%) express neurotensin (Nts) and galanin (Laque et al. 2013, Leinninger et al. 2009, Leinninger et al. 2011). Intra-LHA infusion of leptin was sufficient to suppress food intake and weight gain in normal rats (Leinninger et al. 2009), and KO of LepRb specifically in Nts expressing LHA neurons led to an increase in body weight and reduced oxygen consumption, indicating that LHA^{LepRb} neurons play a role in the regulation of energy balance through the modulation of food consumption and activity/energy expenditure (Leinninger et al. 2011). In addition, knock-down (KD) of LepRb in the LHA of rats

using a small hairpin RNA (shRNA) approach led to an increase in consumption of a high-fat diet and body weight when maintained on this diet (Davis et al. 2011). Therefore, LHA^{LepRb} neurons are potential homeostatic interoceptive neurons that may play a role in feeding.

Tracing studies using traditional neuronal tracers, Cre-inducible expression of trans-synaptic wheat-germ agglutinin (WGA) tracer, and Cre-inducible expression of fluorescent dyes, indicate that LHA^{LepRb} neurons, including LHA$^{LepRb-Nts}$ neurons, project prominently within the LHA onto OX neurons to modulate expression of OX (Leinninger et al. 2009, Leinninger et al. 2011, Louis et al. 2010). In addition, labelled axons can also be observed in the VTA, and LepRb KO in LHA^{Nts} neurons reduced evoked DA release in the nucleus accumbens (NAc) (Leinninger et al. 2009, Leinninger et al. 2011, Louis et al. 2010). Very little is still known about LHA^{LepRb} neurons, however. Despite being responsive to leptin, it is unclear whether these neurons are capable of sensing changes in other signals of energetic state, such as glucose. Moreover, direct manipulations of the activity of these neurons have not been performed to determine their role in feeding, and functional synaptic connectivity with the VTA and LHA is yet to be established.

3.1.4 Experimental aims

The experiments detailed in this chapter aim to further understand the functional role of LHA^{LepRb} neurons in the control of feeding behaviour. Specific aims may be summarized as follows: 1) to electrophysiologically characterize and classify LHA^{LepRb} neurons; 2) to determine whether LHA^{LepRb} neurons are responsive to other signals of energetic state, such as OX and glucose; 3) to determine the effect of activation of LHA^{LepRb} neurons in the modulation of food consumption; and 4) to evaluate the functional synaptic connectivity between LHA^{LepRb} neurons and VTA neurons, as well as other intra-LHA neurons.

3.2 Methods specific to the chapter

3.2.1 Electrophysiological properties

Whole-cell patch clamp recordings were conducted in brain slices of LepRb^{Tom} animals (P14-P25). All cells that yielded stable recordings and had action potentials that overshoot 0 mV were considered healthy and analyzed.

Spontaneous firing frequency (Hz): spontaneous firing was recorded using a 30 sec current clamp protocol at 0 pA current injection.

Resting membrane potential (mV) and input resistance (MΩ): resting membrane potential and membrane resistance were determined from a 1 sec depolarizing voltage step protocol (-80 mV to 0 mV with 10 mV steps) from a holding potential of -90 mV with a 1 sec pre- and post-stimulation recording.

Action potential (AP) parameters and maximum initial firing frequency: cells were depolarized from a -60 mV holding potential using a 1 sec current injection step protocol (10-150 pA) with a 1 sec pre- and post-stimulus interval in current clamp mode. AP parameters were analyzed using the first AP elicited at the smallest injected current to produce spiking (Young & Sun 2009). The exact definitions of all electrophysiological parameters analyzed are described in Table 3.1.

Electrophysiological parameter	Definition
AP threshold (mV)	the first peak of the third derivative of the AP voltage trace
AP half width (ms)	the width of the AP half-way between the threshold value and the peak of the AP
After-hyperpolarisation potential (AHP, mV)	the difference between the threshold value and the most negative potential following the spike
AP peak amplitude (mV)	the difference between the threshold value and the peak of the AP
AP (10-90) (mV)	amplitude of AP between 10-90% of the AP rising phase (portion of the AP between the threshold value and the peak)
AP max rise slope (10-90)	slope of spike rising phase between 10-90% of the AP rising phase
AP rise time (10-90) (ms)	Time difference between 10-90% of the AP rising phase
AP decay slope (90-10):	slope of spike decay phase between 90-10% of the AP decay phase (portion of the AP between the peak and the AHP)
AP decay time (10-90) (ms)	difference between the 10-90% of the AP decay phase
Maximum initial firing frequency	the reciprocal of the first inter-spike-interval (ISI) as measured following the highest injected current before spike inactivation was observed
Spontaneous firing frequency (Hz)	was determined using the last 20 s of the 30 s current clamp recording at 0 pA current injection
Input resistance (MΩ)	the slope of the best fit line between -80 mV and -60 mV in the current/voltage curve
Resting membrane potential (mV)	the extrapolated voltage at which the current/voltage curve crosses 0 pA
Membrane capacitance (pF):	determined in voltage clamp using a 10 mV, 10 ms positive square test pulse and neutralizing the outward current transient due to charging of membrane capacitance by the C-slow capacitance compensation circuit of HEKA EPC10, providing estimates for capacitance

Table 3.1 Definitions of electrophysiological parameters measured.

3.2.2 Classification of LHA^{LepRb} neurons

Fast-spiking (FS) cells were classified according to their maximum initial firing frequency and AP half-width. To determine whether cells were late-spiking (LS), low-threshold spiking (LTS), or regular-spiking (RS), spike frequency was calculated during a 500 ms window before a 1 sec hyperpolarizing step to -90 mV (X) and a 250 ms window after (Y). Spike ratio was defined as $\frac{2y}{x}$. Classification criteria are based on previous criteria used to classify GABA neurons in the LHA (Karnani et al. 2013) and are described in Table 3.2.

Cell type	Classification criteria
Fast Spiking (FS)	If maximum initial firing frequency was greater than 200 Hz and spike half-width less than 0.6 ms
Regular Spiking (RS)	Spike ratio between 0.5 and 1.5
Low-Threshold Spiking (LTS)	Spike ratio greater than 1.5
Late Spiking (LS)	Spike ratio less than 0.5

Table 3.2 Classification criteria for FS, RS, LTS, and LS neurons

3.2.3 Leptin, Glucose and OX responses

All experiments were conducted in acute brain slices of adult LepRb^{Tom} animals (>8 weeks). Long-duration current-clamp recordings were carried out with long-term application of leptin (500 nM, Bachem), glucose (4 mM, Bachem) or orexin-A (OX-A) (500 nM, Bachem) in artificial cerebrospinal fluid (aCSF). A 3-5 min baseline recoding was taken before application of pharmacological agents. Leptin, glucose or OX-A was applied for up to 10 min, followed by 10-20 minutes of washout. For glucose recordings using synaptic blockers, 50 µM AP5 ((2R)-amino-5-phosphonovaleric acid), 10 µM CNQX (6-cyano-7-nitroquinoxaline-2,3-dione), 50 µM TTX (tetrodotoxin), and 3 µM gabazine (S-R95531) was added to aCSF. In these experiments, glucose concentrations were increased from 1 mM to 2.5 mM first.

After a washout period of 10-20 min, glucose concentrations were increased from 1 mM to 5 mM. Breaks in current clamp traces correspond to moments when recording was paused to take voltage clamp measurements. Voltage clamp ramps from -120 mV to 20 mV at a rate of 0.1 mV/ ms were taken before and during application of glucose or OX-A. Changes in membrane potential after application of glucose or OX-A were determined using these voltage clamp ramps, where membrane potential was determined as the voltage were current injection equals 0 pA. Change in membrane potential was defined as the difference between the pre-application membrane potential and application membrane potential. Cells with a change in membrane potential > 2 mV where considered to show a response (depolarizing if positive change, hyperpolarizing if negative change), as noise in recordings were measured to be below that threshold. Cells with a change in membrane potential < 2 mV were classified as non-responsive.

3.2.4 Effect of LHA ^{LepRb} neuron activation on food intake

LepRb^{ChR2Tom} animals, where LepRb^{Cre} animals were bilaterally injected with of AAV1.CAGGS.flex.ChR2.tdTomato.SV40 directly into the LHA at 4 sites, 45 nl at each site (Bregma, anterior/posterior: -1.4 mm, medial/lateral: ±1.1 mm, dorsal/ventral: -5.0 and -5.2 from skull surface at Bregma) for channelrhodopsin (ChR2) expression, were used for LHA^{LepRb} neuron photostimulation. For behavioural studies, a fibre ferrule was implanted over the LHA (see Table 2.5 for coordinates used). For all *in vivo* photostimulation experiments in this chapter, the same pulse protocol was used: 10 ms pulses, 20 Hz for 1 s, repeated every 4 seconds.

3.2.4.1 Overnight feeding suppression

LepRb^{ChR2Tom} animals were habituated to behaviour chambers overnight. The next day, food consumption was measured for 22 hrs starting at the onset of the dark period (6 pm) without photostimulation as a baseline. The following day, food consumption was measured for 22 hrs starting at the onset of the dark period. On this test day, animals received photostimulation for the duration of the test (22 hrs).

Body weight was measured prior to the test, and after the test. During all feeding tests, animals had *ad libitum* access to 20 mg grain pellets and water.

3.2.4.2 Feeding suppression under food restriction

LepRb^{ChR2Tom} animals were food restricted for 24 hrs and then placed in behaviour chambers during the light period where animals received unlimited access to food (20 mg grain pellets). Amount of food consumed over a 1 hr period was measured as a baseline. After this test, animals were removed from chambers and returned to homecage and provided a small amount of food (~1 g), maintaining food restriction. The following day, animals were returned to the behaviour chambers during the light period and allowed to consume food for 1 hr. During this period of time, animals were photostimulated and food consumption was measured. Animals had *ad libitum* access to water.

3.2.5 CRACM studies

Whole- cell patch-clamp recordings in brain slices of LepRb^{ChR2Tom} animals were carried out for channelrhodopsin assisted circuit mapping (CRACM) experiments. For LHA^{LepRb}→VTA studies, non-infected cells in the VTA were patched in the vicinity of LHA^{LepRb} neuron axons expressing ChR2-tdTomato. For LHA^{LepRb}→LHA studies, non-infected cells in the LHA were patched in the vicinity of LHA^{LepRb} neuron axons expressing ChR2-tdTomato. Ten-second pulsed-light stimulations at varying frequencies (1 Hz, 5 Hz, or 20 Hz) and varying pulse durations (1 ms or 5 ms) were carried out in voltage clamp. Recordings in voltage clamp were carried out at a holding potential of -70 mV.

3.3 Results

3.3.1 Electrophysiological properties of LHA^{LepRb} neurons indicate that they are predominantly LHA ^{GABA} LTS neurons

The electrophysiological properties of LHA^{LepRb} neurons were investigated in order to determine whether these neurons are distinct from OX and MCH neurons, as well as to determine whether they represent a distinct subpopulation of LHA^{GABA} neurons. All experiments were conducted in acute brain slices of LepRb^{Tom} animals.

3.3.1.1 Verification of LepRb^{Tom} animals

To verify the appropriate labelling of LepRb neurons in LepRb^{Tom} animals, immunohistological analysis of expression of tdTomato was performed by staining hypothalamic brain slices of LepRb^{Tom} animals with anti-red fluorescent protein (RFP) antibody. Immunohistological analysis of the tdTomato expression in the hypothalamus of LepRb^{Tom} animals (n=3 animals) reveals an appropriate pattern of expression for LepRb neurons. High levels of tdTomato immunoreactivity was observed in the ARC, LHA, DMH, VMH, and PMV (Figure 3.1A-D), consistent with previous reports of LepRb expression in the hypothalamus (Leshan et al. 2006, Scott et al. 2009). In addition, whole-cell patch clamp recordings of tdTomato labelled neurons in the presence of synaptic blockers indicate that these neurons were responsive to leptin (500 nM, 4 of 6 cells recorded were depolarized and/or increased firing rate, Fig 3.1E-I), consistent with previous reports indicating LHA^{LepRb} neurons show depolarization responses to leptin (Leinninger et al. 2009). Therefore, LHA^{LepRb} neurons are appropriately labelled by tdTomato in LepRb^{Tom} animals, making them suitable for use in the study of electrophysiological properties of LHA^{LepRb} neurons.
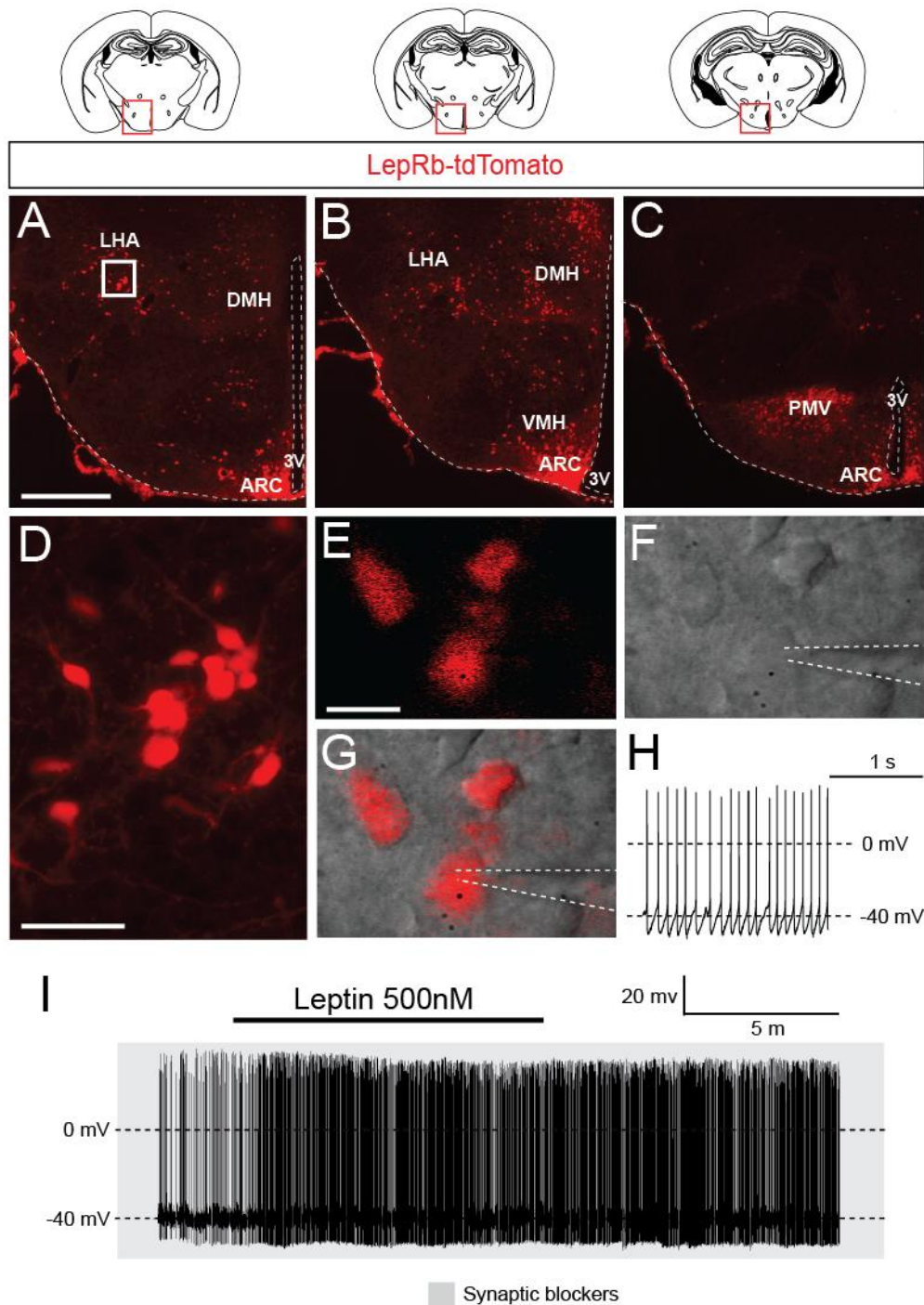
Figure 3.1 tdTomato appropriately marks LepRb neurons in the hypothalamus of LepRb^(Tom) animals. (A-C) Diagrams and epifluorescence images of tdTomato (red) expression in (A) anterior, (B) medial, and (C) posterior hypothalamus of LepRb^(Tom) animals. Red boxes in coronal brain section diagrams represent regions shown. Scale bar: 500 μm. **(D)** Inset from (A) showing high magnification epifluorescent image of tdTomato expressing LepRb neurons (red) in the LHA. Scale

bar: 50 µm. **(E-G)** (E) Epifluorescence, (F) DIC, and (G) merged image of a LepRb neuron labelled by tdTomato (red) patched in the LHA. Dotted white line marks location of patch pipette. Scale bar: 20 µm. **(H)** Sample trace of whole-cell current clamp recording of spontaneous firing in LHA^{LepRb} neurons. **(I)** Sample trace of whole-cell current clamp recording of LHA^{LepRb} neuron displaying an increase in firing in response to 500 nM leptin application (4/6 neurons recorded showed modulatory responses to leptin). LHA: lateral hypothalamic area; DMH: dorsomedial nucleus of the hypothalamus, ARC: arcuate nucleus; 3V: third ventricle; VMH: ventromedial nucleus of the hypothalamus, PMV: ventral premammillary nucleus of the hypothalamus.

3.3.1.2 Firing properties of LHA^{LepRb} neurons

Whole-cell patch clamp recordings were conducted in brain slices of LepRb^{Tom} animals to determine electrophysiological properties of LHA^{LepRb} neurons. tdTomato labelled neurons around the fornix (fx) were patched randomly and recorded. All LHA^{LepRb} neurons recorded (n=14) were found to be spontaneously firing (Figure 3.1E-H) making them distinct from MCH neurons, which do not fire spontaneously (van den Pol et al. 2004). Spontaneous firing frequencies recorded were between 4.65 Hz and 25.3 Hz, with a mean firing frequency of 10.25 ± 1.79 Hz. The average resting membrane potential of these cells was determine to be -44.89 ± 1.92 mV, which is consistent with the general resting membrane potential of spontaneously firing cells. In addition, LHA^{LepRb} neurons have an average membrane capacitance of 15.68 ± 2.09 pF, consistent with other LHA^{GABA} neurons (Karnani et al. 2013) and in contrast to OX neurons, which are considerably larger (Williams et al. 2011). Input resistance was variable, ranging from 372.04 MΩ to 1287.08 MΩ, with an average input resistance of 801.50 ± 79.14 MΩ. Action potential parameters were also determined in LHA^{LepRb} neurons (Table 3.3). For all AP parameters recorded other than AP threshold, LHA^{LepRb} neurons display similar AP characteristics to other LHA^{GABA} neurons (Karnani et al. 2013).

General electrophysiological properties		Action potential properties	
Spontaneous firing frequency (Hz)	10.25 ± 1.79	*AP threshold (mV)*	-28.05 ± 1.35
Input resistance (MΩ)	801.50 ± 79.14	*AP half width (ms)*	0.7 ± 0.05
Resting membrane potential (mV)	-44.8929 ± 1.92	*AHP (mV)*	-25.03 ± 1.44
Membrane capacitance (pF):	15.68 ± 2.09	*AP peak amplitude (mV)*	74.65 ± 2.63
Maximum initial firing frequency	148.2 ± 53.85	*AP (10-90) (mV)*	69.34 ± 2.45
		AP max rise slope (10-90)	365.64 ± 40.60
		AP rise time (10-90) (ms)	0.21 ± 0.02
		AP decay slope (90-10):	-133.52 ± 18.11
		AP decay time (10-90) (ms)	0.6 ± 0.05

Table 3.3 Electrophysiological characteristics of LHA^{LepRb} neurons. Values are mean ± S.E.M.

3.3.1.3 Classification of LHA^{LepRb} neurons

The LHA contains four subtypes of GABAergic neurons: FS, RS, LS and LTS (see Table 3.2) (Karnani et al. 2013). Because LHA^{LepRb} neurons are known to be GABAergic (Leinninger et al. 2009), recorded LHA^{LepRb} neurons were classified according to their electrophysiological properties to determine whether they represent a specific subtype of LHA^{GABA} neurons. FS GABAergic neurons both in the cortex and in the LHA display narrow APs (Karnani et al. 2013, Young & Sun 2009). Based on this previously described category, no LHA^{LepRb} cells recorded (n=14) were found to be FS neurons (Figure 3.2A-B). To determine whether LHA^{LepRb} neurons are LS, LTS or RS neurons, responses to hyperpolarizing current steps were recorded and changes in firing frequency after release from inhibition was determined. LTS neurons show increases in firing when comparing firing rates before and after the hyperpolarizing step. LS neurons show a slow ramp depolarization back to baseline, resulting in a decrease in firing rate compared to initial firing rate. RS neurons do not display any changes in firing rate after the hyperpolarisation step (Karnani et al. 2013, Young & Sun 2009). Approximately 86% of neurons recorded (12 out of 14 cells recorded) displayed an increase in firing rate after hyperpolarisation, indicating that the most LHA^{LepRb} neurons are LHA^{GABA} LTS neurons (Fig 3.2C-E). This suggests that LHA^{LepRb} neurons can be modulated with smaller inputs and provide more temporarily precise inhibition (Karnani et al. 2013).
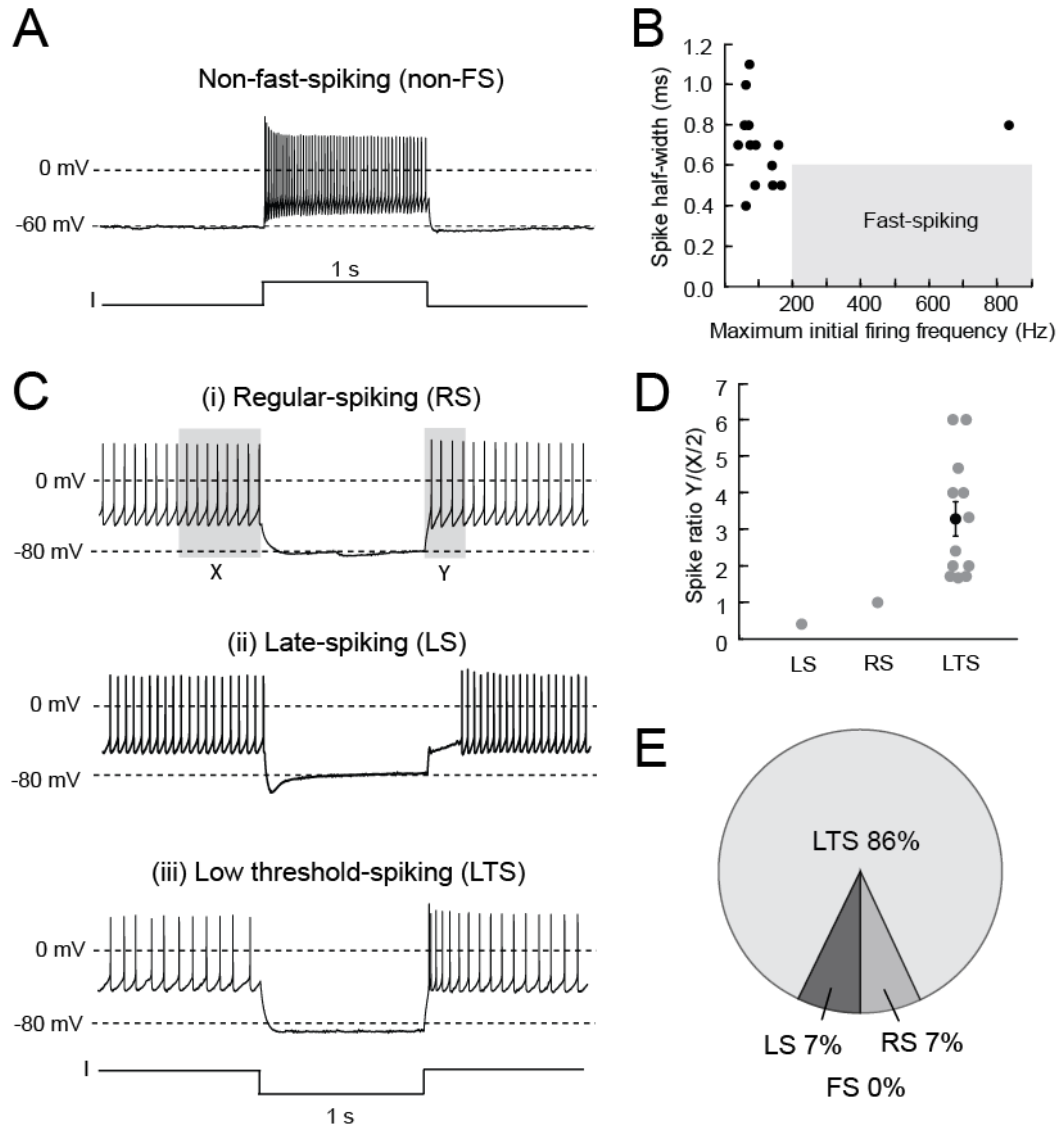
Figure 3.2 LHA^{LepRb} neurons are LHA^{GABA} LTS neurons. (A) Representative trace of maximum firing of a typical non-FS LHA^{LepRb} neuron during a depolarizing step. **(B)** Scatter plot of AP spike half-width over maximum initial firing frequency of all LHA^{LepRb} neurons recorded (n=14), none of which fall under the FS category. **(C)** Representative traces of RS (top), LS (middle), and LTS (bottom) LHA^{LepRb} neurons during a hyperpolarizing current step. **(D)** Spike ratio, calculated from X (500 ms) and Y (250 ms) time windows shown in top panel of (C) for LS (n=1), RS (n=1) and LTS (n=12) LHA^{LepRb} neurons recorded. Grey circles represent individual cells, black circle and error bars represents mean ± S.E.M. **(E)** Fractions for each cell type (n=14 total). FS: fast-spiking; RS: regular-spiking; LS: late-spiking; LTS: low-threshold-spiking.

3.3.2 Glucose and OX modulates LHA^{LepRb} neurons' membrane potential

Because LHA^{LepRb} neurons are putative homeostatic interoceptive neurons based on their responsiveness to leptin, I investigated whether other signals of energetic state might also modulate their activity. Previous studies have shown that LHA neurons, including GABAergic neurons, are sensitive to glucose (Burdakov et al. 2005b, Karnani et al. 2013, Williams & Mitchell 2008, Yamanaka et al. 2003). Here, I investigated whether LHA^{LepRb} neurons, which are GABAergic (Leinninger et al. 2009), are also responsive to changes in glucose concentration. Changes in membrane potential in response to a 1 mM to 4 mM (low to high) change in extracellular glucose were recorded in current-clamp mode with a holding potential of -60 mV (imposed by sustained current injection), with no synaptic blockers present. This change in glucose concentration led to variable responses in LHA^{LepRb} neurons recorded. Fifty percent of neurons recorded showed a hyperpolarisation response to increased glucose levels (5 out of 10 cells recorded), with a maximum hyperpolarisation response of 21.3 mV (Figure 3.3A-B). In addition, 30 percent of cells showed a depolarizing response to glucose (3 out of 10 cells recorded), with a maximum depolarization of 8.6 mV (Figure 3.3C-D). In order to determine whether depolarisation and hyperpolarisation responses were a result of direct glucose action on LHA^{LepRb} neurons, changes in membrane potential from 1 mM to 2.5 mM and 1 mM to 5 mM extracellular glucose were recorded in the presence of synaptic blockers. Two of four cells recorded showed a hyperpolarizing response to glucose concentrations (Figure 3.3E-G), indicating that glucose can directly inhibit some LHA^{LepRb} neurons. No depolarization responses were observed, however, potentially due to the low number of recordings performed. Therefore, it is still unclear whether depolarization responses observed in the absence of synaptic blockers are a result of direct or indirect action of glucose on these neurons.

Since LHA^{LepRb} neurons are intermingled with OX neurons (Leinninger et al. 2009), and both orexin-1 (OX1) and orexin-2 (OX2) receptors are expressed in the LHA (Jacob 2005), I investigated whether LHA^{LepRb} neurons can be modulated by OX, as OX is known to be an orexigenic peptide (Hara et al. 2001, Rodgers et al. 2000, Rodgers et al. 2001). Similar to glucose studies, changes in membrane potential were measured during a 500 nM OX-A application in current clamp mode with 0 pA current injections and no synaptic blockers. LHA^{LepRb} neurons displayed

variable responses to OX-A application. Fifty percent of neurons showed a hyperpolarizing response (5 out of 10 cells recorded), with a maximum depolarization of 21.52 mV (Figure 3.4A-B). In addition, 20% of neurons showed a depolarizing response (2 out of 10 cells recorded, Figure 3.4C-D). Therefore, LHA^{LepRb} neurons are capable of being modulated by several signals of energy status, including leptin, glucose, and OX. However, it is unclear whether modulatory responses to OX are direct or indirect, as recordings in the presence of synaptic blockers were not conducted.
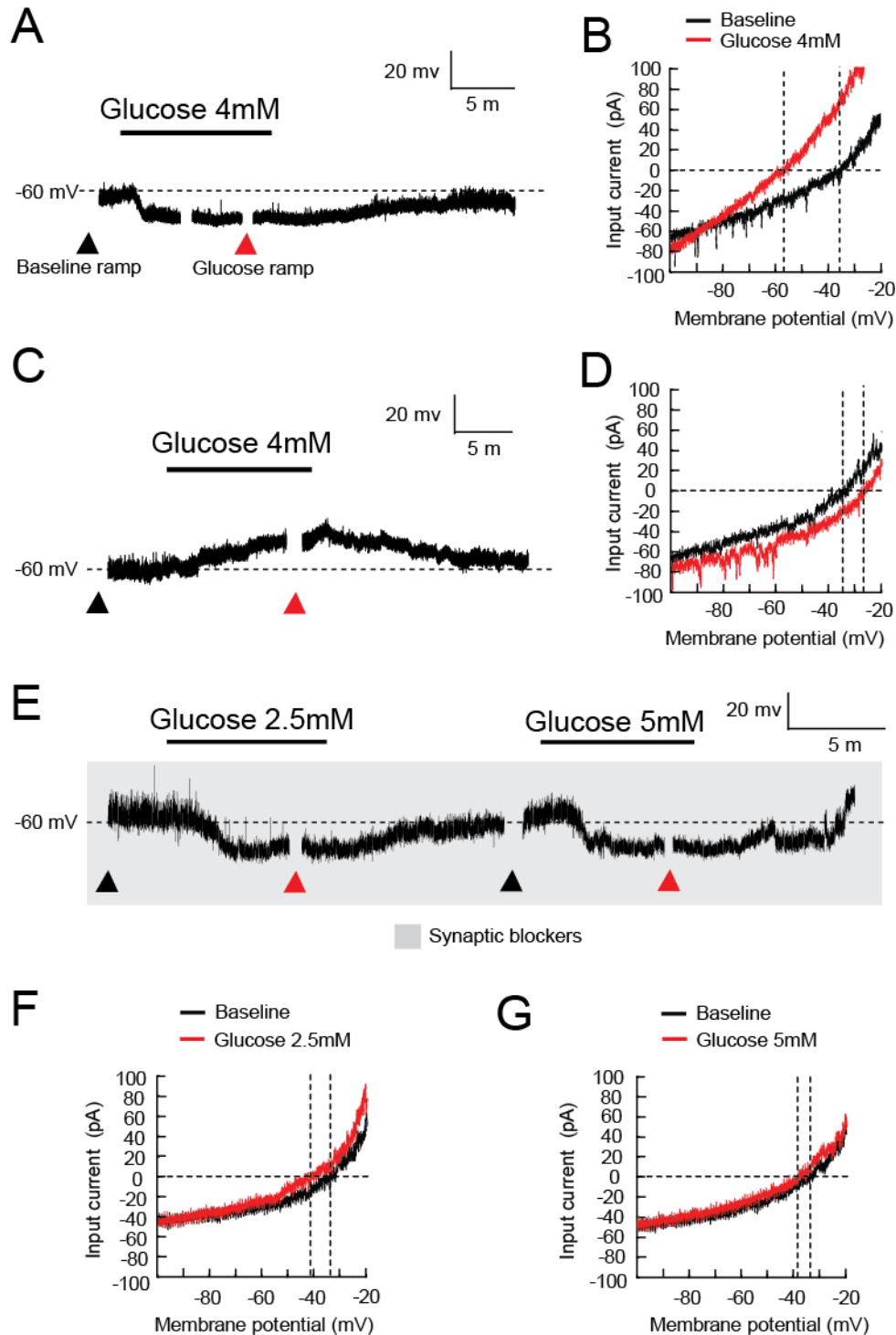
Figure 3.3 Glucose directly inhibits LHA^{LepRb} neurons. (A) Sample trace of a whole-cell current clamp recording of an LHA^{LepRb} neuron showing a hyperpolarizing response to 4 mM glucose application without synaptic blockers (5/10 cells recorded showed similar responses) **(B)** Plot of input current and membrane potential (I-V) relationship under baseline (black) and glucose application (red) conditions for (A).

(C) Sample trace of a whole-cell current clamp recording of an LHA^{LepRb} neuron showing a depolarizing response to 4 mM glucose application without synaptic blockers (3/10 neurons recorded showed similar responses). **(D)** I-V plot of baseline (black) and glucose application (red) conditions for (C). **(E)** Sample trace of a whole-cell current clamp recording of LHA^{LepRb} neuron showing hyperpolarizing responses to 2.5 mM and 5 mM glucose application with synaptic blockers (grey box, 2/4 neurons recorded showed similar responses). **(F, G)** I-V plots of baseline conditions (black) and 2.5 mM (F) and 5 mM (G) glucose application conditions (red) for (E). Breaks in recorded traces represent time points for ramps under baseline conditions (black triangles) and under glucose application (red triangles). Vertical dashed lines in I-V plots show where traces are at 0 pA current, indicating membrane potential of cell during baseline and glucose application conditions. Total of neurons recorded: 10 without synaptic blockers, 4 with synaptic blockers.
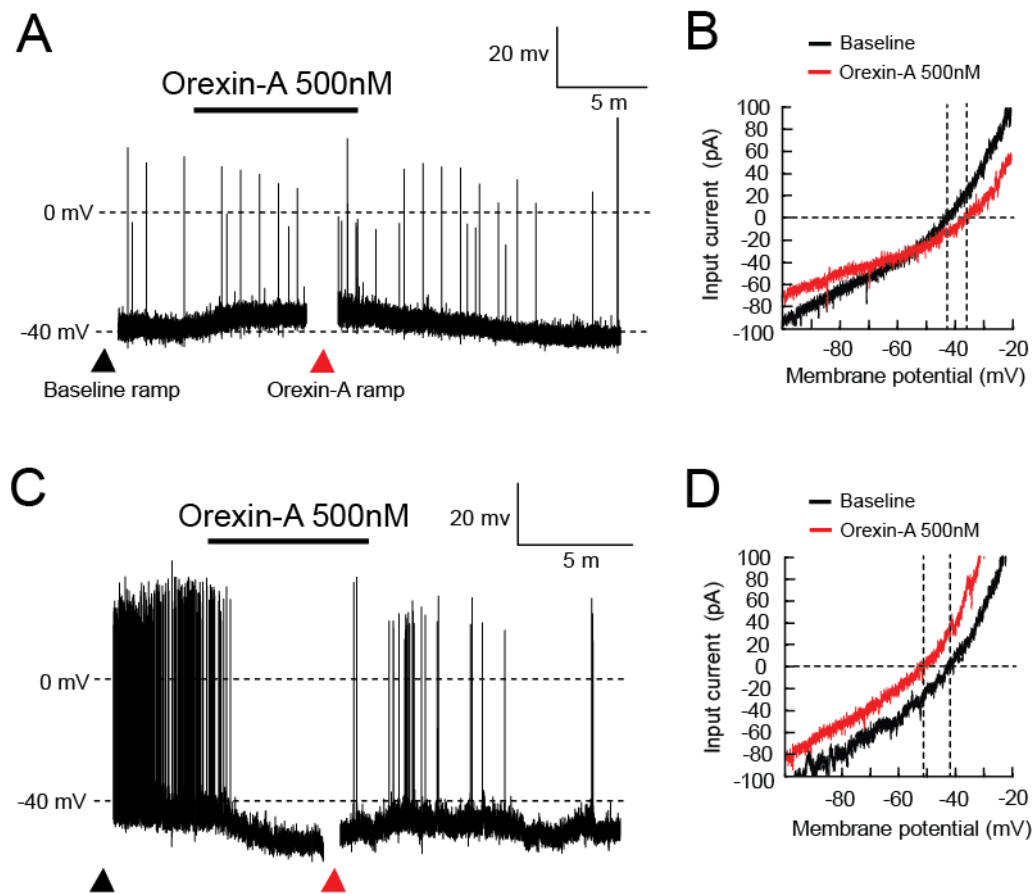
Figure 3.4 LHA^{LepRb} neurons are modulated by OX. (A) Sample trace of a whole-cell current clamp recording of an LHA^{LepRb} neuron showing a depolarizing response to 500 nM orexin-A application without synaptic blockers (5/10 cells recorded showed similar responses). **(B)** Plot of input current (I) and membrane potential (V) relationship under baseline (black) and glucose application (red) conditions for (A). **(C)** Sample trace of a whole-cell current clamp recording of an LHA^{LepRb} neuron showing a hyperpolarizing response to 500 nM orexin-A application without synaptic blockers (2/10 cells recorded showed similar responses). **(D)** I-V plot of baseline (black) and glucose application (red) conditions for (C). Breaks in recorded traces represent time points for ramps under baseline conditions (black triangles) and under orexin-A application (red triangles). Vertical dashed lines in I-V plots show where traces are at 0 pA current, indicating membrane potential of cell during baseline and orexin-A application conditions. Total neurons recorded: 10.

3.3.3 Activation of LHA^{LepRb} neurons suppresses feeding and reduces body weight

To directly test LHA^{LepRb} neuron's role in feeding, I used optogenetic activation of LHA^{LepRb} neurons. All behavioural experiments on the role of LHA^{LepRb} neurons in feeding were conducted in LepRb^{ChR2Tom} animals, were LHA^{LepRb} neurons were rendered photoexcitable through delivery of a viral construct expressing membrane-bound ChR2 fused to a tdTomato reporter in the LHA of LepRb^{Cre} animals (Figure 3.5A).

3.3.3.1 ChR2 expression and functionality validation

To validate the appropriate expression of ChR2, immunohistochemical analysis of tdTomato expression was conducted by staining hypothalamic brain sections of LepRb^{ChR2Tom} animals (n=3 animals) with RFP antibody. Visualization of ChR2-tdTomato infected LHA^{LepRb} cells demonstrate that injection site chosen for viral delivery was appropriate as no tdTomato labelled cells were found outside the LHA. Infected cells were found across 500 μm rostro-caudally in the LHA, between -1.2 mm and -1.5 mm from Bregma. Cell bodies were most abundant between -1.3 mm and -1.4 mm from Bregma, near the fx, where injections were made (Figure 3.5B-C).

Light activation of ChR2-tdTomato expressing LHA^{LepRb} neurons was tested in order to determine functionality of ChR2 (Figure 3.5D-H). First, cells were tested with a single light stimulus of increasing duration (from 1 ms to 39 ms, in 2 ms increments) in both current clamp and voltage clamp to determine minimum stimulus duration required to elicit an action potential and inward current at -60 mV holding potential. Analysis shows that all stimulus durations tested were capable of eliciting current in ChR2-tdTomato expressing cells (Figure 3.5I). In addition, the difference between light stimulus onset and current detection was measured for 1 ms or 5 ms pulse durations of a 10 s stimulus of 1 Hz frequency in currently clamp mode. Delay times recorded were consistent with previous reports (Boyden et al. 2005), where average delay for 1 ms and 5 ms pulse stimulus was 3.88 ± 0.14 ms and 4.28 ± 0.25

ms respectively, with no statistically significant difference in response delays between 1 ms and 5 ms pulses (paired t-test, n=5, p= 0.16; Figure 3.5J).

Second, light stimulation of different frequencies were tested in current clamp and voltage clamp mode in order to determine whether they could reliably elicit action potentials and inward currents for behavioural studies. Cells (n=5) were stimulated with a 10 s pulsed-light stimulus (light pulse duration of 1 ms or 5 ms) protocol of 1 Hz, 5 Hz, or 20 Hz frequency. Recordings were made in both voltage clamp (-60 mV holding potential) and current clamp (0 pA current injection). Recordings indicate that ChR2-tdTomato cells reliably fired at all frequencies tested, with 0% spike failure (Figure 3.5K-L). Current amplitudes, however, were reduced under the 5 Hz and 20 Hz frequency protocols, but not the 1 Hz protocol (Figure 3.5L). For 20 Hz frequency stimulation, current amplitudes were reduced by nearly 70% from initial current amplitude (first elicited AP, Figure 3.5M). This phenomenon is due to ChR2 inactivation, and is consistent with previous reports of ChR2 functionality (Boyden et al. 2005, Ishizuka et al. 2006).
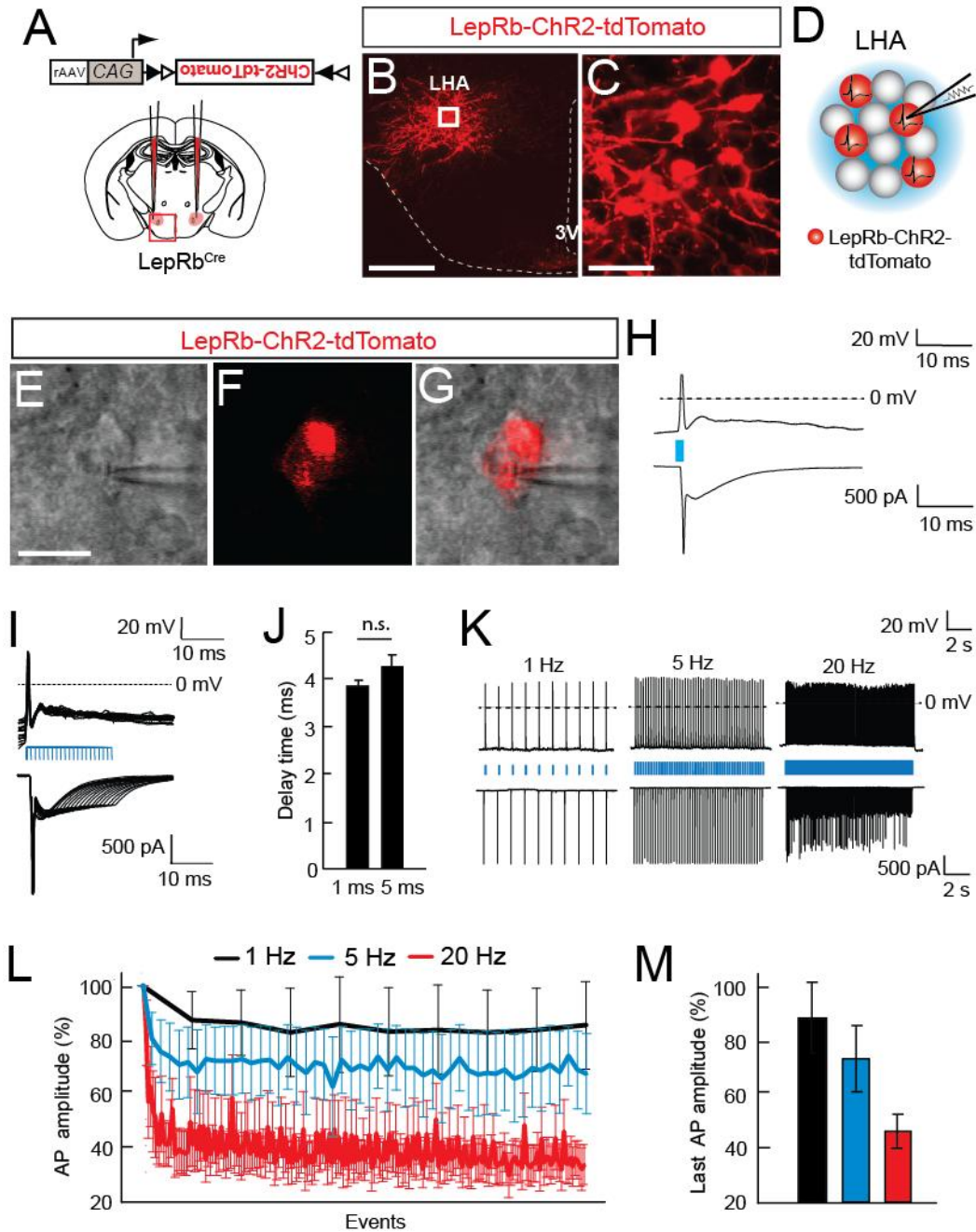
Figure 3.5 ChR2 in LHA[LepRb] neurons of LepRb[ChR2Tom] animals are functional.
(A) Schematic of viral vector delivery for expression of ChR2 in LHA[LepRb] neurons. Viral vector (top) uses a FLEx-switch to express ChR2-tdTomato under the synthetic CAG promoter. Viral vector was bilaterally injected into the LHA of LepRb[Cre] mice (bottom). **(B)** Epifluorescence image of ChR2-tdTomato (membrane-bound, red) expression in LHA of LepRb[ChR2Tom] animals. Red box in (A) represents region shown. Scale bar: 500 μm. **(C)** Inset from (B) showing high magnification epifluorescence image of ChR2-tdTomato (membrane-bound) expressing LHA[LepRb] neurons (red). Scale bar: 50 μm. **(D)** Schematic of functional validation of ChR2 experiments.

Whole-cell patch clamp recordings of ChR2-tdTomato expressing LHA^{LepRb} neurons were conducted under photostimulation. **(E-F)** (E) Epifluorescence, (F) DIC, and (G) merged image of a ChR2-tdTomato (membrane-bound expressing) LepRb neuron (red) patched in the LHA. Scale bar: 20 μm. **(H)** Sample trace of a 1 ms light stimulus elicited action potential in current clamp (top) and inward current in voltage clamp (bottom). **(I)** Sample traces of variable light stimulus durations (1 ms to 30 ms durations, with 2 ms increase) elicited action potentials in current clamp (top) and inward currents in voltage clamp (bottom). **(J)** Average delay time between light stimulus onset and current detection with 1 ms or 5 ms light pulse durations (paired t-test). **(K)** Sample traces of a 10 s pulsed light stimulus of 1 Hz (left), 5 Hz (middle), and 20 Hz (right) frequency with 5 ms pulse duration in current clamp (top) and voltage clamp (bottom). **(L)** Percent amplitude of APs elicited under a 10 s pulsed (5 ms duration) light stimulus of 1 Hz (black), 5 Hz (blue) and 20 Hz (red) frequency. **(M)** Percent amplitude of the last AP elicited under a 10 s pulsed (5 ms duration) light stimulus of 1 Hz (black), 5 Hz (blue), and 20 Hz (red) frequency. Total neurons recorded: 5. Values are mean ± S.E.M. n.s $p>0.05$. LHA: lateral hypothalamic area; 3V: third ventricle.

3.3.3.2 Effect of LHA^{LepRb} neuron activation on feeding

In order to determine whether activation of LHA^{LepRb} neurons can reduce feeding, ChR2 expressing LHA^{LepRb} neurons in LepRb^{ChR2Tom} mice were photostimulated. Feeding was measured in a 22 hr assay, starting at the onset of the dark period (6 pm to 4 pm on the following day, Figure 3.6A-D). Baseline measurements of feeding over 22 hrs indicate that mice consumed an average of 5.86± 1.72 g of food. Under photostimulation, however, average food consumption in 22 hrs was reduced to 2.27± 0.52 g, though this change was not statistically significant (paired t-test, n=4, p=0.08; Figure 3.6E-F). A closer look at food consumption during different periods of the 22 hrs measured show a trend in reduction in food consumption during the second portion of the dark period (12 am to 6 am). However, no statistically significant interaction was observed between condition (stimulation vs no stimulation) and time block (two-way RM ANOVA, n=4, interaction: condition x time block F(3,9)=0.6, p=0.629) and comparisons between groups in this time period was only marginally significant (post hoc multiple comparisons with Holm-Sidak correction, n=4, p=0.048; Figure 3.6G, Table 3.4), potentially due to variability and low sample number. Body weight, however, was significantly reduced after 22 hrs of LHA^{LepRb} neuron activation, from 22.6 ± 1.6 g to 19.9 ± 0.9 g (paired t-test, n=4, p=0.036; Figure 3.6H), representing a ~10% body weight reduction. These data indicate that increased activity of LHA^{LepRb} neurons plays a role in the regulation of body weight, and suggest these neurons might be regulating food consumption to a lesser degree.

I also tested whether activation of LHA^{LepRb} neurons might be sufficient to reduce elevated feeding effects induced by food restriction. For this, LepRb^{ChR2Tom} animals (from the same cohort as in previous 22 hr food consumption experiment) were food deprived for 24 hours and then tested for re-feeding in a 1 hr feeding assay under photostimulation (Figure 3.7A-C). On average, baseline measurements indicate that animals will consume about 0.93 ± 0.15 g of food in 1 hr under food deprivation. However, photostimulation did not reduce food intake in food deprivation conditions (paired t-test, n=4, p=0.437; Figure 3.7D-E). To confirm that photostimulation activated LHA^{LepRb} neurons in these animals, Fos expression was assessed in ChR2-tdTomato expressing LHA^{LepRb} neurons following photostimulation for 1 hr. Immunohistochemical analysis of Fos expression indicates that LHA^{LepRb}

neurons were in fact activated by photostimulation during behavioural experiments, as Fos staining was observed in these neurons, validating the experimental manipulation (Figure 3.7F-K). This indicates that leptin signalling alone is not sufficient to diminish food consumption under global states of energy deficit, and other signals of energy deficit and neuronal circuits might have a stronger influence over food intake under more severe states of energy deficit.
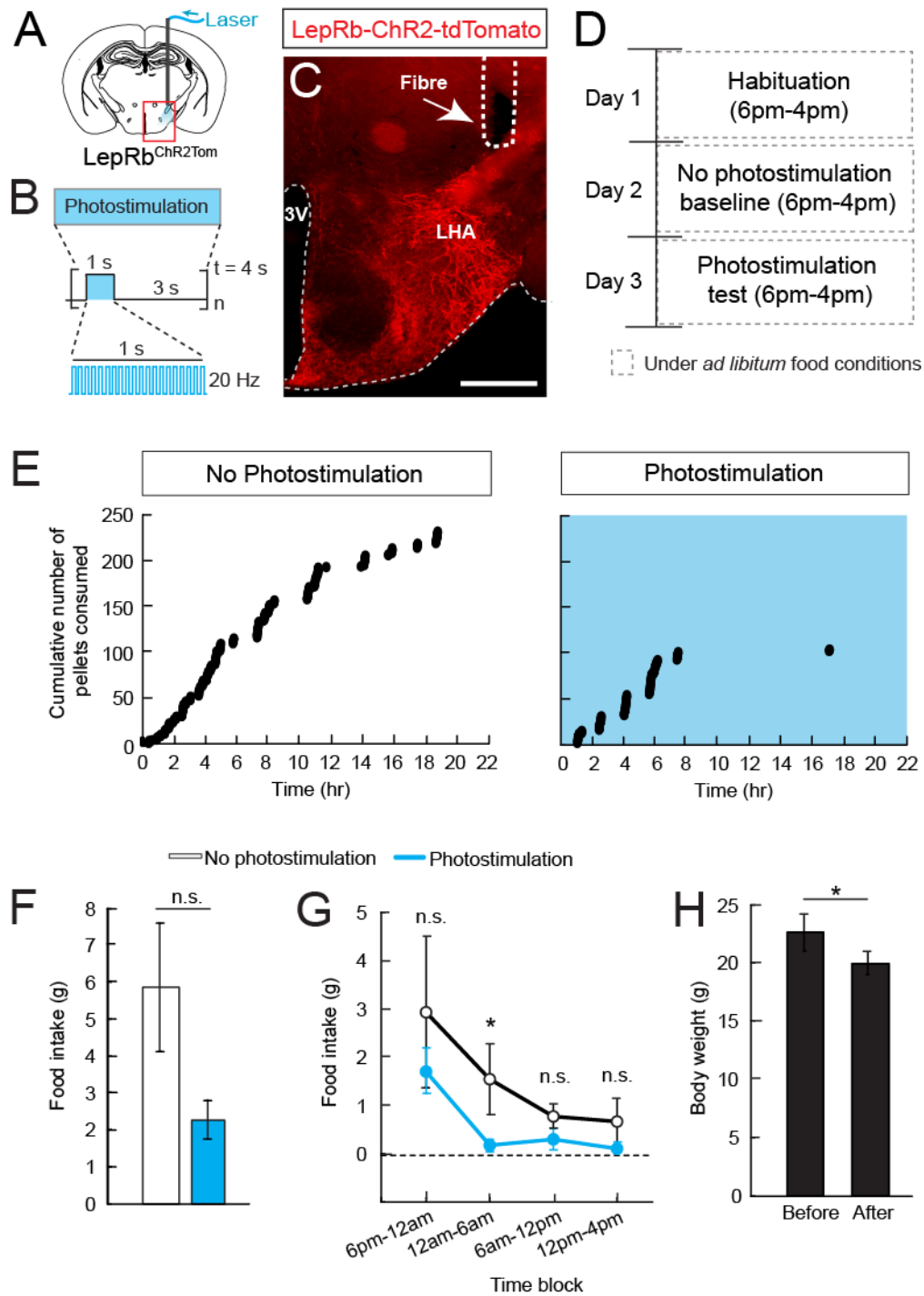
Figure 3.6 Chronic activation of LHA^{LepRb} neurons reduces food intake and body weight. (A) Diagram of fibre placement position in LepRb^{ChR2Tom} animals for LHA^{LepRb} neuron photoactivation. **(B)** Schematic of photostimulation protocol used. **(C)** Epifluorescence image of membrane-bound ChR2-tdTomato (red) expression in LHA of LepRb^{ChR2Tom} animals and fibre placement (dashed line). Red box in coronal brain section diagram in (A) represents region shown. Scale bar: 500 μm. **(D)**

Experimental design schedule. Animals were habituated for one day and then tested for food intake under a no photostimulation baseline condition and a photostimulation condition on consecutive days. Food intake was measured over 22 hours. Experiment was conducted in *ad libitum* fed animals. **(E)** Representative trace of cumulative number of pellets (20 mg) consumed over time (22 hrs) without photostimulation (left) and with photostimulation of LHA^{LepRb} neurons (right). **(F)** Total food intake during no photostimulation baseline (white) and photostimulation test (cyan) over 22 hrs (n=4, paired t-test). **(G)** Food intake during no photostimulation baseline and photostimulation conditions over 22 hrs, separated into four time blocks (n=4). Statistical comparisons are across conditions for each time block (see Table 3.4). **(H)** Body weight before and after 22 hr photostimulation (n=4, paired t-test). Values are mean ± S.E.M. n.s. p>0.05; * p<0.05. LHA: lateral hypothalamic area; 3V: third ventricle.

Figure panel	Sample size	Statistical test	Values
F	4	Paired t-test	p= 0.082
G	4	Two-Way RM ANOVA	
		Factor 1: Condition (No photostimulation vs. Photostimulation)	F(3,9)=0.6, p=0.082
		Factor 2: Time block	F(3,9)=10.5, p=0.003
		Interaction: Condition x Time block	F(3,9)=0.6, p=0.629
		Post hoc multiple comparisons with Holm-Sidak corrections	
		Time block 6pm-12am	p=0.074
		Time block 12am-6am	p=0.048
		Time block 6am-12pm	p=0.467
		Time block 12pm-4pm	p=0.391
H	4	Paired t-test	p=0.036

Table 3.4 Statistical values for Figure 3.6.
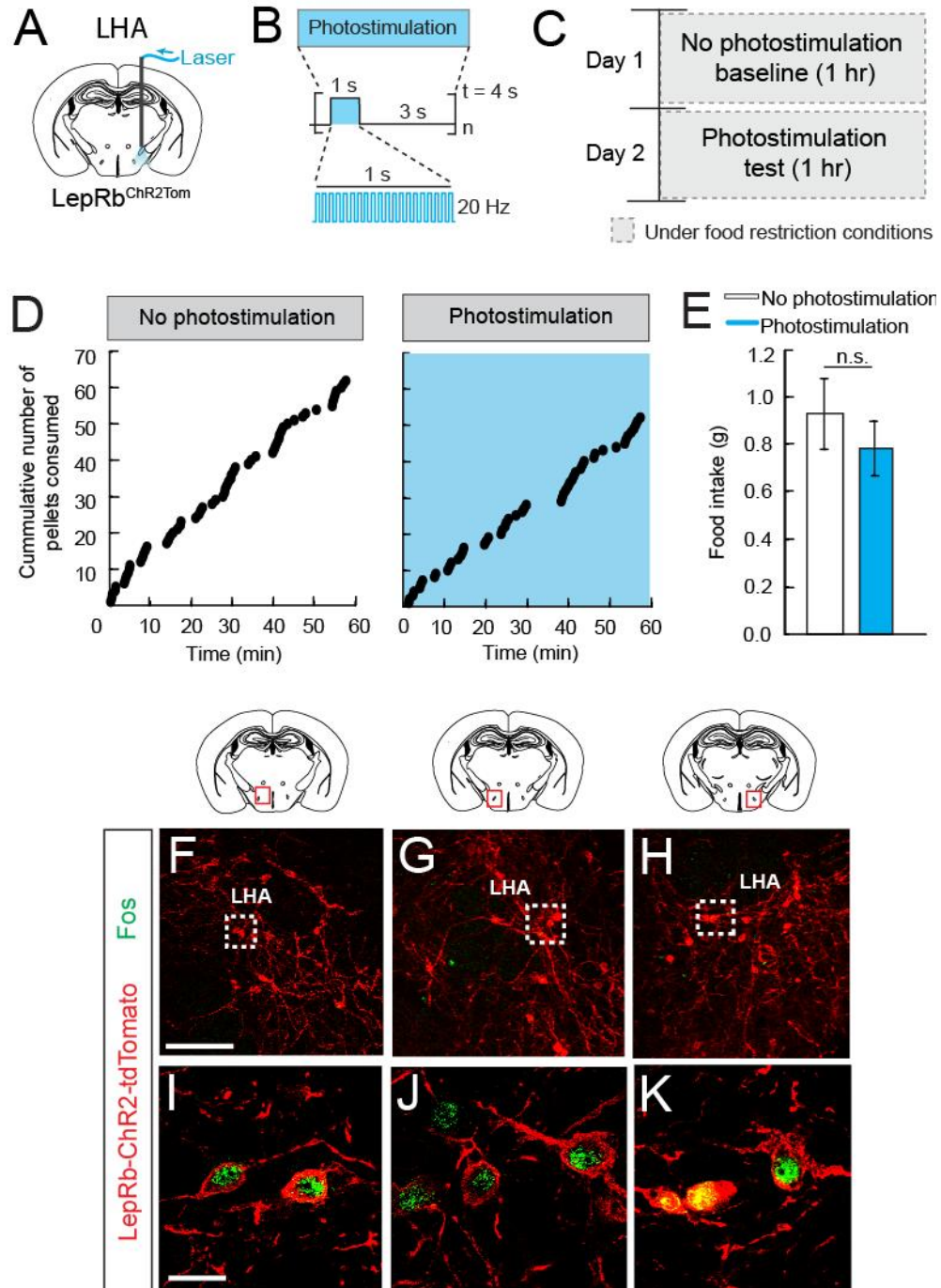
Figure 3.7 Elevated LHA^LepRb neuron activity does not suppress food deprivation induced feeding. (A) Diagram of fibre placement position in LepRb^ChR2Tom animals for LHA^LepRb neuron photoactivation (same animals as in Figure 3.6). **(B)** Schematic of photostimulation protocol used. **(C)** Experimental design schedule. Animals were tested for food intake under a no photostimulation baseline condition and photostimulation condition on consecutive days. Food intake was measured over 1 hour. Experiment was conducted in food restricted animals.

(D) Representative trace of cumulative number of pellets (20 mg) consumed over time (1 hr) without photostimulation (left) and with photostimulation (right) of LHA^{LepRb} neurons under food restriction conditions. **(E)** Total food intake during no photostimulation baseline and photostimulation condition over 1 hr (n=4, paired t-test). **(F-H)** Diagrams and single plane confocal images of ChR2-tdTomato (membrane-bound) expressing LepRb neurons (red) in (F) anterior, (G) medial, and (H) posterior LHA. Red boxes in coronal brain section diagrams represent regions shown. Scale bar: 100 µm. **(I-K)** Single plane confocal images of insets of (F-H), respectively, showing Fos expression (green) in membrane-bound ChR2-tdTomato expressing LepRb neurons (red) in the LHA. Scale bar 20 µm. Values are mean ± S.E.M. n.s. p>0.05. LHA: lateral hypothalamic area.

3.3.4 Functional connectivity between LHA^{LepRb} neurons and downstream projection regions (LHA and VTA) are not observed

Given that activation of LHA^{LepRb} neurons are capable of modulating food consumption and body weight, downstream projections of LHA^{LepRb} neurons would also be important nodes in this circuit in the control of feeding. Anatomical studies have shown that LHA^{LepRb} neurons project to the VTA and within the LHA (Leinninger et al. 2009, Leinninger et al. 2011, Louis et al. 2010). To better understand the role of LHA^{LepRb} neuron circuitry, I used CRACM techniques to determine the functional synaptic connectivity of these neurons to the VTA and LHA.

For functional connectivity studies between LHA^{LepRb} neurons and other LHA neurons, acute brain sections of LepRb^{ChR2Tom} animals were used. Non-tdTomato labelled neurons (n=10) were patched at random in the LHA (Figure 3.8A). Immediately after breaking into the cell, cells were hyperpolarized from resting membrane potential (0 pA current injection, usually around -40 mV) to -90 mV using a 1 sec current injection step protocol (10 pA steps) in order to determine the presence of hyperpolarisation-activated current (I_h). Presence of I_h was used to identify putative OX neurons (Burdakov et al. 2005a) (Figure 3.8B), which are believed to be the downstream targets of LHA^{LepRb} neurons in the LHA (Leinninger et al. 2009, Leinninger et al. 2011, Louis et al. 2010). Following this, ChR2 expressing projections of LHA^{LepRb} cells were optically stimulated using a 10 s pulsed-light protocol at 1 Hz, 5 Hz, and 20 Hz (1 ms or 5 ms pulse duration), and inward currents of LHA neurons were recorded in voltage clamp mode at -70 mV holding potential. A total of 10 cells were recorded, but no recorded cell displayed light-activated currents under photostimulation (Figure 3.8C). Therefore, no functional connectivity was observed.

As with the LHA, functional connectivity studies between LHA^{LepRb} neurons and VTA neurons were performed in acute brain sections of LepRb^{ChR2Tom} animals. Immunohistological analysis of the tdTomato reporter protein (enhanced through staining with anti-RFP antibody) indicates that ChR2 expressing LHA^{LepRb} neuron axons are present in the VTA, in the vicinity of DA neurons, which were identified with tyrosine hydroxylase (TH) immunoreactivity (Figure 3.9A-B), consistent with previous reports (Leinninger et al. 2009, Leinninger et al. 2011). Whole-cell patch-

clamp recording were performed on VTA cells that were observed to be in the vicinity of ChR2-tdTomato expressing LHA^{LepRb} axons (Figure 3.9C). Immediately after breaking into the cell, presence of I_h was determined in the same manner as in the LHA. $I_h(-)$ cells in the VTA are known to be GABAergic, while $I_h(+)$ cells can be either GABAergic or DAergic (Margolis et al. 2006). ChR2 expressing axons of LHA^{LepRb} neurons were optically stimulated using a 10 second pulsed light protocol at 1 Hz, 5 Hz, and 20 Hz (1 ms or 5 ms pulse duration), and inward currents of VTA neurons were recorded in voltage-clamp mode at -70 mV holding potential. A total of 38 cells were recorded in both coronal and horizontal sections. Although both $I_h(+)$ and $I_h(-)$ cells were recorded (n=19 of each), suggesting both GABA and DA neurons were sampled, no recorded cells showed light-activated synaptic currents (Fig 3.9D-G), so functional connectivity was not established in this study.
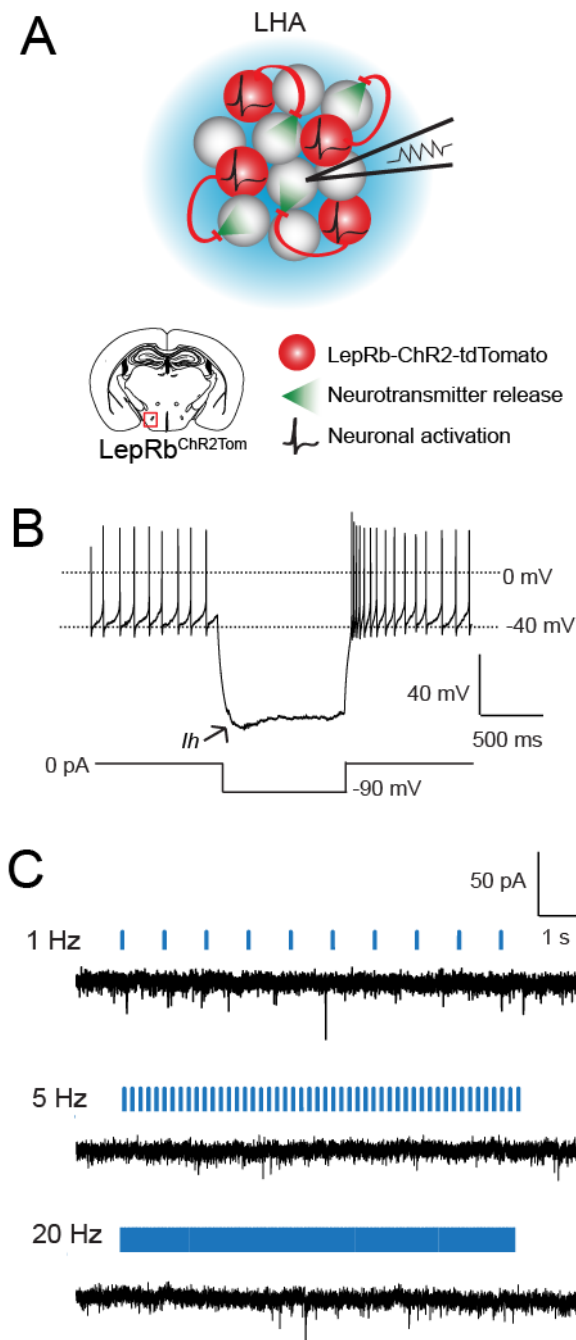
Figure 3.8 Functional synaptic connectivity between LHA^{LepRb} neurons and unlabelled LHA neurons is not observed. (A) Schematic of experimental design. Non-ChR2-tdTomato expressing neurons in hypothalamic brain slices of LepRb^{ChR2Tom} animals where patched under light stimulation. Red box in coronal brain section diagram depicts area where neurons were patched. **(B)** Sample trace of a whole-cell patch clamp recording of a non-ChR2-tdTomato expressing I_h(+) neuron in the LHA in response to a hyperpolarizing current under current clamp. Presence of I_h suggests this is a putative orexin neuron (Burdakov et al. 2005a) **(C)** Sample traces of responses to a 10 s pulsed-light stimulus of 1 Hz (top), 5 Hz (middle), and 20 Hz (bottom), with a 5 ms pulse duration, in voltage clamp, from cell shown in (C). Total neurons recorded: 10. LHA: lateral hypothalamic area.
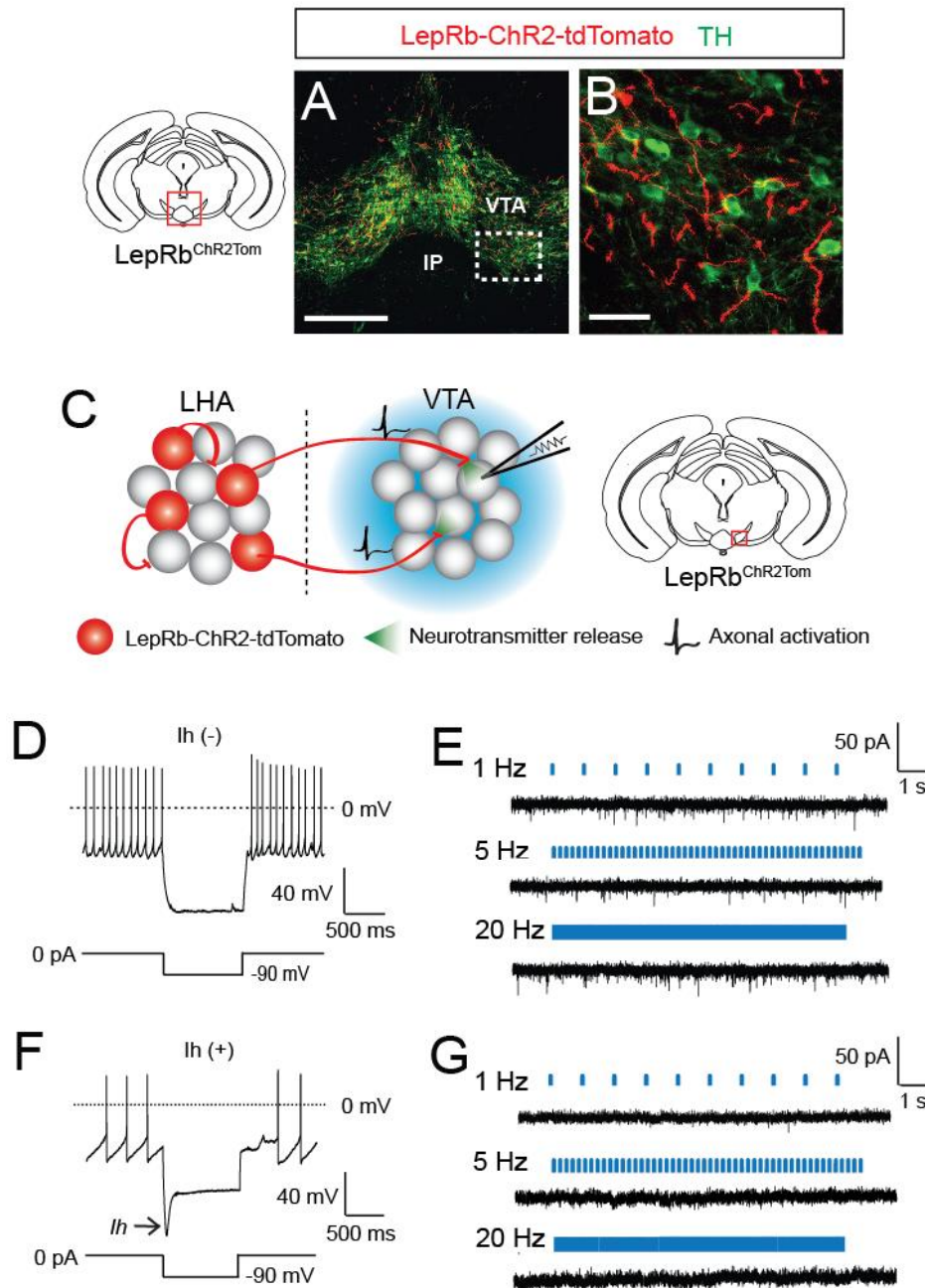
Figure 3.9 LHA^LepRb neurons do not appear to be functionally connected to VTA neurons. (A) Diagram and epifluorescence image showing ChR2-tdTomato LHA^LepRb neuron axons (red) present in the VTA of LepRb^ChR2Tom animals, in proximity to DA neurons, which are marked by TH (green) immunoreactivity. Red box in coronal brain section diagram depicts area shown. Scale bar: 500 μm. **(B)** Epifluorescence image of inset of (A). Scale bar: 50 μm. **(C)** Schematic of experimental design. VTA neurons in proximity to ChR2-tdTomato expressing LHA^LepRb neuron axons in midbrain brain slices of LepRb^ChR2Tom animals where patched under light stimulation. Red box in coronal brain section diagram depicts

area where neurons were patched. **(D, F)** Sample traces of a whole-cell patch clamp recording of an (D) I_h(-) and an (F) I_h(+) VTA neuron in response to a hyperpolarizing current under current clamp. I_h(-) neurons are GABAergic neurons, while I_h(+) neurons are either GABAergic or DAergic (Margolis et al. 2006) **(E, G)** Sample traces of responses to a 10 s pulsed light stimulus of 1 Hz (top), 5 Hz (middle), and 20 Hz (bottom), with a 5 ms pulse duration, in voltage clamp, from cells shown in (D) and (F), respectively. Total neurons recorded: 38 LHA: lateral hypothalamic area; IP: interpeduncular nucleus; VTA: ventral tegmental area; TH: tyrosine hydroxylase.

3.4 Discussion

In the LHA, LepRb neurons are putative homeostatic interoceptive neurons capable of modulating feeding behaviour. However, direct tests of the role of these neurons in feeding and functional connectivity to downstream projection regions had not been previously evaluated. Using a combination of electrophysiological, optogenetic, and behavioural techniques, I set up to broaden the understanding of the role of these neurons and their circuits in the regulation of feeding processes.

3.4.1 LHA^{LepRb} neurons are LHA^{GABA} LTS neurons capable of sensing signals of energetic state

LepRb neurons in the LHA are known to be modulated by leptin and express GABA (Leinninger et al. 2009). In addition, histological analysis indicates that they are distinct from two other major populations in the lateral hypothalamus: OX and MCH neurons (Leinninger et al. 2009). My studies on the electrophysiological properties of LHA^{LepRb} neurons corroborate histological studies, as LHA^{LepRb} neurons possess distinct electrical properties from OX and MCH neurons. LHA^{LepRb} neurons were shown to be spontaneously firing, making them distinct from MCH neurons, which are generally silent (van den Pol et al. 2004). In addition, LHA^{LepRb} neurons are significantly smaller than OX neurons, measured by their membrane capacitance (Williams et al. 2011). Further analysis of electrical properties of LHA^{LepRb} neurons indicate that these neurons constitute a subtype of GABA neurons in the LHA: LTS neurons (Karnani et al. 2013). Although the number of neurons recorded for analysis was small (n=14), LHA^{LepRb} neurons recorded were sampled randomly and should, therefore, be a representative population. However, studies with greater sample sizes should be conducted to verify that LHA^{LepRb} neurons are, in fact, LTS neurons. Due to these electrophysiological properties, these neurons have the potential of being modulated by smaller inputs and provide inhibition with greater temporal precision (Karnani et al. 2013).

In addition, a subset of LHA^{LepRb} neurons is sensitive to changes in glucose concentration. Hyperpolarisation responses to increased glucose concentrations are due to direct action of glucose on LHA^{LepRb} neurons, as this response was observed under the presence of synaptic blockers. Some neurons were also depolarized, although it is unclear whether this is a direct or indirect effect. The exact mechanisms of glucose induced hyperpolarisation in LHA^{LepRb} neurons is also unclear at this point, and should be further investigated. OX-A was also shown to modulate the activity of LHA^{LepRb} neurons, by either depolarizing or hyperpolarizing these neurons. Given that these studies were conducted without the use of synaptic blockers, it is unclear at this point whether OX mediated changes in activity are due to the direct action of OX on LHA^{LepRb} neurons. This modulation by OX, however, indicate the potential presence of circuit loops between LepRb and OX neurons in the LHA, as LHA^{LepRb} neurons have been shown, through anatomical studies, to project within the LHA to OX neurons (Leinninger et al. 2009, Leinninger et al. 2011, Louis et al. 2010). This loop can, therefore, serve as either a feed-forward or feedback mechanisms for the output of LHA synaptic transmission to downstream circuits outside of the LHA. Due to the low number of neurons recorded for glucose and OX experiments, however, these studies should be repeated in order to confirm the results presented here. Nonetheless, these preliminary findings support the notion that LHA^{LepRb} neurons constitute another set of homeostatic neurons which are modulated by signals of an animal's physiologic state, including leptin, glucose, and OX.

3.4.2 Regulation of feeding and body weight by LHA^{LepRb} neurons

Although pharmacological studies of leptin's action in the modulation of food consumption in the LHA suggests a role in feeding for LHA^{LepRb} neurons (Leinninger et al. 2009), studies using direct manipulations of the activity of LHA^{LepRb} neurons had not been performed to date. In the studies presented in this chapter, I directly tested the relationship between increased LHA^{LepRb} neuron activity and feeding using optogenetic approaches. Though the experimental cohort used was small, activation of LHA^{LepRb} neurons led to a significant decrease in body weight, and a trend towards a reduction in food intake. Due to variability in food intake between animals

and low number of animals in my study, however, these studies should be replicated in order to confirm these results. Elevated LHA^{LepRb} activity did not reduce elevated feeding under food restriction, however, indicating that this particular circuit is not sufficient to suppress this feeding response, and other circuits might have a greater role in driving this behaviour. Recently, a study indicated that activation of glutamatergic neurons in the LHA, marked by the vesicular glutamate transporter 2 (Vglut2), acutely inhibited food consumption in food restricted animals (Jennings et al. 2013). These results, along with the ones presented in this chapter, highlights the complexity and specificity of neuronal control over the modulation of food intake, where different neuronal cell-types within a brain region can regulate feeding in different contexts.

3.4.3 Functional LHA^{LepRb} neuron circuit connectivity

Homeostatic neurons that are important in the regulation of food consumption and body weight can serve as entry points to aid in unravelling the neural circuits that control feeding behaviour (Sternson 2013). Since LHA^{LepRb} neurons are capable of modulating feeding, its downstream projection targets provide a map of potential feeding nodes involved in the regulation of food intake. Although anatomical studies had demonstrated the presence of LHA^{LepRb} axons in the LHA and VTA (Leinninger et al. 2009, Leinninger et al. 2011, Louis et al. 2010), functional connectivity had not been tested. Traditionally, these studies are conducted using paired electrophysiological recordings in slice (Holmgren et al. 2003, Thomson et al. 2002). However, this technique produces low yields of recorded pairs and cannot be used for long range projections as cell bodies are severed from axons during slice preparation.

Here, I used CRACM techniques to determine connectivity between LHA^{LepRb} neurons and other LHA and VTA neurons. Although immunohistochemical analysis indicated that LHA^{LepRb} neuron axons are present in the VTA in proximity to DA neurons, photoactivation tests failed to establish connectivity between these neurons and VTA neurons. Recordings within the LHA also failed to yield functional connections. Although the number of recordings performed here in each area was not exhaustive, these results suggests that functional connectivity between LHA^{LepRb}

neurons with both VTA and LHA is low, despite the observance of axonal projections in these two areas (Leinninger et al. 2009, Leinninger et al. 2011, Louis et al. 2010). This phenomenon is not unheard of. For example, although CRACM studies testing the functional connectivity of ARC^{AGRP}→paraventricular nucleus of the hypothalamus (PVH) and ARC^{POMC}→PVH circuits show synaptic connectivity between the PVH and ARC through both AGRP and POMC neurons (Atasoy et al. 2008), it was reported that connectivity between POMC neurons and postsynaptic PVH neurons displayed very low connectivity probabilities (~5%) compared to AGRP neurons (~50%) (Atasoy et al. 2014). Ultrastructure electron microscopy (EM) reconstructions, however, indicated that POMC neuron release sites were generally located more distantly from post-synaptic neuron soma, compared to AGRP neuron release sites (Atasoy et al. 2014). This was suggested to account for the lower functional connectivity observed under CRACM studies, as subcellular location of a synaptic input can strongly influence its ability to perturb post-synaptic cell activity (Williams & Mitchell 2008, Williams & Stuart 2003). Distal targeting might be insufficient to influence neuron excitability on its own, but can act with coincident activity from other inputs to gate neuron excitability (Stuart & Hausser 2001). EM studies like the one employed by Atasoy et al. (2014), therefore, can provide more conclusive evidence demonstrating synaptic connectivity between LHA^{LepRb} neurons and the VTA and LHA, and determine whether structural aspects of the connectivity such as those observed in ARC^{POMC}→PVH circuitry might contribute to the lack of observed functional connectivity.

Furthermore, procedural variables in my recordings itself might not be appropriate to capture functional connectivity of LHA^{LepRb} neurons. Circuit mapping studies using ChR2 have been shown to be effective in releasing and observing post-synaptic effects of fast neurotransmitters such as glutamate (Glu) or GABA (Atasoy et al. 2008, Atasoy et al. 2012, Holloway et al. 2013, Schone et al. 2012, Xia et al. 2011) as well as smaller neurotransmitters such as DA (Stuber et al. 2010), but have in some cases failed to detect effects of larger peptide mediated modulatory effects. For example, circuit connectivity studies between OX neurons and histamine (HA) neurons in the tuberomammillary nucleus of the hypothalamus (TMN) using CRACM protocols, similar to those employed in studies presented here, observed fast post-synaptic excitation in HA neurons attributed to the release and transmission

of Glu from OX neurons, but failed to show any post-synaptic effects due to OX (Schone et al. 2012). Upon further inspection, however, it was noted that a late excitation attributed to OX transmission was observed, and was more prominent when using longer photostimulation protocols (20-30 s) (Schone et al. 2014). In addition, studies interrogating the functional connectivity of AGRP neurons and downstream projection targets showed GABAergic modulation of postsynaptic neurons in the PVH, but not neuropeptide-Y (NPY) (Atasoy et al. 2012). Behavioural studies, however, indicated that both NPY and GABA were important in AGRP neuron's ability to evoke feeding (Atasoy et al. 2012). Circuit mapping studies presented here were conducted with the expectation of observing GABAergic inputs to LHA^{LepRb} targets, due to initial reports indicating these neurons were GABAergic (Leinninger et al. 2009). Further studies have shown that at least a cohort of LHA^{LepRb} neurons also express Nts and galanin (Laque et al. 2013, Leinninger et al. 2011). Although it is believed that neurotransmitters and peptides are generally co-expressed and co-released in axonal boutons (Eccles 1976, Eccles et al. 1954), there has been evidence of segregation of peptide and neurotransmitters in boutons (Samano et al. 2012). Lack of observed functional connectivity of LepRb neurons, then, could also be due to the inability of current protocols to capture slower and more subtle post-synaptic modulatory effects elicited by peptides such as Nts, so further studies should be conducted. Given that behavioural effects under photoactivation of LHA^{LepRb} neurons are not observed acutely, but over a 22 hr period, it is likely slow peptidergic signalling by LHA^{LepRb} neurons are functionally relevant.

3.4.4 Modulation of motivationally directed appetitive behaviours and reinforcement mechanisms

A pressing question not addressed in these studies is the role of LHA^{LepRb} neurons in the modulation of motivated appetitive behaviours and reinforcement mechanisms that direct action selection in feeding behaviour. Although, i.c.v. injections of leptin has been shown to modulate DA dependent motivated appetitive behaviours through lever press studies, the exact circuitry involved in regulating this behaviour is still unknown (Figlewicz et al. 2006). Because LHA^{LepRb} neurons are

believed to modulate the DAergic system through alterations of TH mRNA expression in the VTA as well as DA content in the NAc, these neurons are in a good position to regulate DA dependent appetitive behaviours (Leinninger et al. 2009, Leinninger et al. 2011). Interestingly, a recently study indicated that mice would nose-poke for photoactivation of LHA neurons that project to the VTA, and this was believed to be mediated by LHA^{Nts} neuron inputs to the VTA (Kempadoo et al. 2013). However, direct testing of LHA^{Nts}→VTA circuit in self-stimulation studies were not carried out. In addition, this is not believed to be mediated by Nts expressing LHA^{LepRb} neurons, as post-synaptic potentials observed in the VTA were glutamatergic, and LHA$^{LepRb-Nts}$ neurons are believed to be GABAergic. This is not surprising as only ~30 % of Nts expressing neurons in the LHA were found to also express LepRb (Leinninger et al. 2011). The role of LHA$^{LepRb-Nts}$ neurons was not tested by the group, as all recordings were conducted in the presence of a GABA-A receptor blocker (Kempadoo et al. 2013). Despite the current lack of evidence for functional connectivity between LHA^{LepRb} neurons and the VTA, future studies can take advantage of new optogenetic tools to manipulate neuronal activity in specific projection areas (Atasoy et al. 2012, Jennings et al. 2013) to unravel their role in the modulation of motivationally dependent behaviours. In particular, it would be interesting to determine how GABAergic LHA$^{LepRb-Nts}$ and glutamatergic LHA^{Nts} inputs to the VTA might differentially modulate post-synaptic neurons in this region to affect appetitive behaviours.

3.5 Conclusion

LepRb neurons in the brain are believed to be important regulators of food intake. Through direct cell-type specific manipulation of neuronal activity, data presented in this chapter show that LHA^{LepRb} neurons are capable of modulating body weight, but their role in the food intake remain unclear. In addition, these neurons comprise primarily of LHA^{GABA} LTS neurons, and are homeostatic neurons capable of detecting and signalling information about body energy status, as their activity is modulated by glucose, leptin, and OX. Limited studies probing the functional downstream circuitry of these neurons have failed to detect functional connectivity between these neurons and postsynaptic neurons in the VTA and LHA, two projection areas known to receive LHA^{LepRb} neuron projections based on anatomical studies. Nonetheless, these studies serve as a basis for further interrogation of these neurons' circuit connectivity and their role in the modulation of feeding behaviour.

Chapter 4

AGRP Neurons Employ a Negative

Reinforcement Teaching Signal

4.1 Introduction

Animals use a broad range of behaviours and expend considerable effort in order to regulate energetic requirements for survival. The use of a diverse and flexible set of goal-directed behaviours under states of homeostatic need such as hunger underscores the important relationship between homeostatic regulation and the control of motivated appetitive behaviours. A major challenge for the investigation of the motivational underpinnings of physiological needs like hunger is the existence of diverse pathways that are concurrently engaged during the slow process of energy deprivation (Gao & Horvath 2007). Because homeostatic neurons are capable of sensing circulating signals of energetic state and modulate food consumption and food seeking behaviours (Sternson 2013), modulations of the activity of specific homeostatic neuron populations and their circuits can aid unravel the relationship between distinct motivational processes and specific neuronal circuits that participate in the regulation of feeding behaviour.

4.1.1 Positive and negative reinforcement properties engaged in feeding behaviour

Under states of physiological need, including hunger, flexible goal-directed behaviours employed to acquire food are learned through processes that evaluate the result of actions to influence their probability of being repeated. Thorndike's "Law of Effect" indicates that responses that lead to favourable consequences increase in frequency, while those that present unfavourable or neutral consequences become less frequent (Thorndike 1898). Skinner further developed this concept into his theory of reinforcement (Skinner 1938). Both positive and negative reinforcement mechanisms have each been proposed to underlie and drive behaviours associated with state of energy deficit (Bindra 1976, Hull 1943) (Figure 4.1).

Early behavioural theories assumed that need-based hunger directed behaviours through a negative reinforcement mechanism, where deviation from homeostasis leads to an unpleasant internal state, and cues or actions associated with eliminating that need are reinforced (Berridge 2004, Freud 2001, Hull 1943) (Figure 4.1A). This aversive motivating condition has been called "drive" (Hull 1943).

However, a direct test of negative reinforcement with electrical stimulation-evoked feeding failed to show aversive properties and the presence of an aversive internal state (Margules & Olds 1962, Olds 1976). In addition, negative reinforcement mechanisms do not explain reinforcement in the absence of a homeostatic need (Berridge 2004, Dickinson 2002). Therefore, the absence of direct experimental evidence in animals has led to scepticism about whether negative reinforcement contributes a major role in hunger overall, hedonic or homeostatic (Berridge 2004, Dickinson 2002).

Positive reinforcement theory indicates that outcomes that increase positive affect are reinforced. Although positive reinforcement can operate in the absence of hunger (Yiin et al. 2005), under states of energy deficit, internal or external cues and actions associated with food consumption are strengthened due to an increase in positive valence of outcomes (Berridge 2004) (Figure 4.1B). Hunger can modulate the incentive value of food, in part, by changing the perceived qualities of food. For example, under states of hunger, human subjects report higher palatability for food-related odours (Yeomans & Mobini 2006) and taste cues (Rolls et al. 1983, Rolls & Rolls 1997, Stoeckel et al. 2007). The orexigenic hormone ghrelin also increases the reported palatability of food (Druce et al. 2006). In addition, hunger can also modulate the post-ingestive properties of food. For example, rodents develop a preference for non-nutritive flavours paired with intragastric infusions of caloric sugars, fats and amino acids under hunger (Yiin et al. 2005). Mice genetically engineered to be unable to perceive sweet taste can also develop a preference for sucrose (de Araujo et al. 2008). Since animals in a state of energy deficit will work much harder for food in an operant task than animals fed *ad libitum* (Hodos 1961), and hormones such as leptin and ghrelin, can also influence the willingness of an animal to work for food (Figlewicz et al. 2006, Overduin et al. 2012), it is believed that increased willingness to work for food under hunger is due to the increase of perceived palatability or nutritive value of food rewards.

However, directly distinguishing the role of positive and negative reinforcement in food consumption and action selection during food seeking under states of need-based hunger has been difficult, as food consumption can be viewed as increasing reward or as reducing a negative state. One approach to address this issue is by analyzing the reinforcement properties associated with changes in

electrical activity of cell-type specific homeostatic neurons (Sternson et al. 2013). For homeostatic neurons that increase food consumption, positive and negative reinforcement can be distinguished in the absence of food, by whether increased activity of these neurons is reinforcing (positive) or whether reduction of their activity is required for reinforcement (negative).
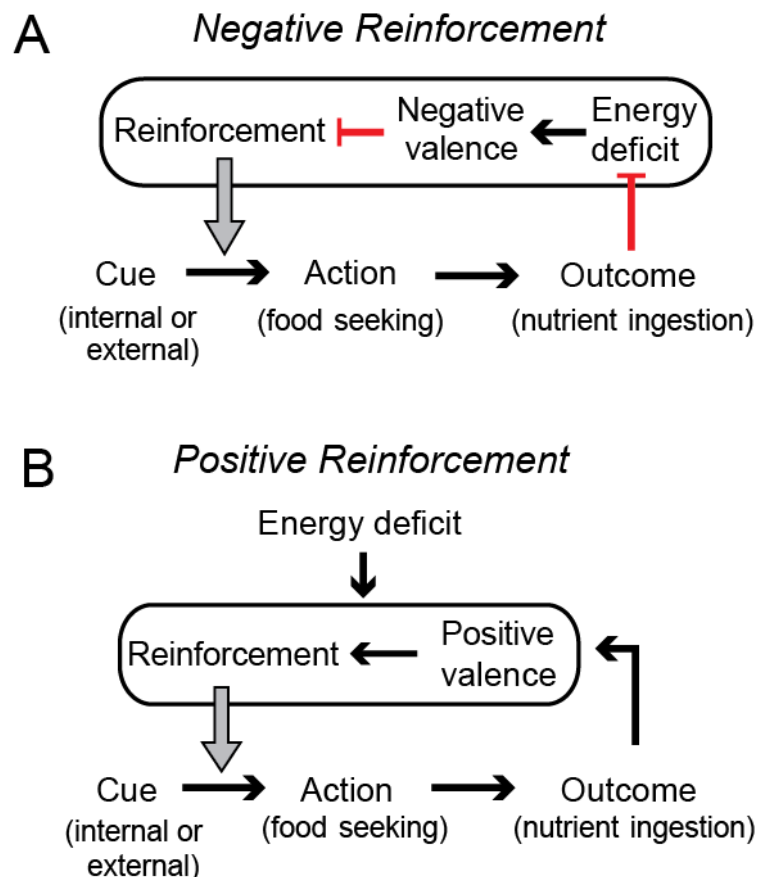
Figure 4.1 Positive and negative reinforcement processes in homeostatic hunger. (A) Negative reinforcement model of food-seeking increases behavioural responding by reducing an energy deficit internal state that has negative valence. The relationship between internal or external cues and food-seeking actions is strengthened by nutrient ingestion outcomes that reduce energy deficit and the associated negative valence (red bar arrows are inhibitory). Conversely, the relationship between internal or external cues and food-seeking actions is weakened if outcomes do not reduce energy deficit and the associated negative valence. **(B)** Positive reinforcement model of food-seeking. The relationship between internal or external cues and food-seeking actions is strengthened by outcomes that result in nutrient ingestion, which has intrinsic positive valence (Yiin et al. 2005). Grey block arrow represents reinforcement process increasing the probability of performing food-seeking actions. Energy deficit is not necessary for positive reinforcement but enhances the value of outcomes associated with nutritive food.

4.1.2 AGRP neurons and the control of food consumption

Studies investigating the functional importance of agouti-related peptide (AGRP) neurons in the arcuate nucleus (ARC) have shown that they are vital in feeding behaviour. AGRP neuron activity is increased both directly and synaptically by circulating signals of energy deficit, such as ghrelin (Cowley et al. 2003, van den Top et al. 2004, Yang et al. 2011), and are inhibited by signals of energy surplus, including glucose, insulin, and leptin (Fioramonti et al. 2007, Konner et al. 2007, van den Top et al. 2004). AGRP neurons also display elevated activity under food deprivation, as Fos expression is significantly elevated compared to sated states (Betley et al. 2013), and firing rate is significantly higher under food deprivation compared to well-fed conditions (Yang et al. 2011). In addition, ablation of AGRP neurons in adult animals using diphtheria toxin (DT) leads to aphagia (Luquet et al. 2005). Inhibition of their electrical activity leads to a suppression of feeding (Krashes et al. 2011), while channelrhodopsin (ChR2) activation of AGRP neurons evokes acute food intake in sated animals during the light period, with amounts consumed similar to those of animals that have been food deprived for 24 hrs (Aponte et al. 2011). Activation of these neurons specifically directs behaviours towards food consumption, as water consumption was only initiated after feeding bouts (Aponte et al. 2011). Thus, AGRP neurons can transduce circulating signals of metabolic state intro electrical activity to modulate feeding behaviour.

As with food deprivation, AGRP neuron activation not only influences food consumption, but also food seeking and effort. During AGRP neuron stimulation, mice show elevated breakpoints in a progressive ratio task to obtain food by either nose poking (Krashes et al. 2011) or lever pressing (Atasoy et al. 2012). Thus, AGRP neuron activity evoked feeding is not solely a reflection of the initiation of motor patterns controlling feeding, but also posses motivational properties to direct flexible food-seeking actions. Consequently, AGRP neurons can serve as a sensory neuron entry point for the investigation of motivational processes and downstream circuit nodes that regulate feeding behaviour (Sternson et al. 2013).

4.1.3 Reinforcement mechanisms engaged by AGRP neurons

Despite lack of direct experimental evidence for negative reinforcement in hunger, human subjects report that energy deficit is unpleasant and eating can be directed towards alleviating this feeling (Keys et al. 1950, Stunkard & Rush 1974, Wadden et al. 1986). Thus, negative reinforcement processes might still play a role in hunger regulated behaviours, although the neural processes that elicit food seeking and negative emotions associated with homeostatic hunger states have not been identified to date.

Recently, a study by Betley et al. (2014) attempted to determine the reinforcement capability of AGRP neuron inhibition under hunger states. Because energy deficit leads to food-seeking through elevated AGRP neuron activity (Cowley et al. 2003, Takahashi & Cone 2005, van den Top et al. 2004) and ingestion of nutrients reverses this (Fioramonti et al. 2007, van den Top et al. 2004, Yang et al. 2011), the group tested whether silencing AGRP neurons in the absence of food would be reinforcing. Using a conditioned place preference paradigm, the study showed that chemogenetic cell-type specific silencing of AGRP neurons under food restriction was reinforcing, as animals displayed a preference for the chamber associated with AGRP neuron silencing (Betley et al. 2014). In addition, a conditioned taste preference paradigm also demonstrated that animals preferred the flavour of a non-nutritive food associated with AGRP neuron silencing under hunger (Betley et al. 2014). These results are consistent with a negative reinforcement teaching signal that can direct an animal's actions and food consumption choices. Nevertheless, it is unclear whether activation of AGRP neurons can induce a negative internal affect, and how disruption of this negative reinforcement mechanism might affect behavioural modulation of food seeking and consumption behaviours.

4.1.4 Experimental Aims

The experiments detailed in this chapter aim to further understand the reinforcement properties engaged by AGRP neurons to promote and direct food seeking and food consumption behaviours. Specific aims may be summarized as follows: 1) to determine whether activation of AGRP neurons has a negative valence, consistent with a negative reinforcement mechanism for directing behaviour; and 2) to determine the behavioural consequences of the disruption of negative reinforcement mechanisms engaged by AGRP neurons in relation to food seeking and food consumption.

4.2 Methods specific to the chapter

4.2.1 *In vivo* photostimulation

For all behavioural studies, adult AGRP^{ChR2EYFP} animals (>8 weeks) were used. Adult AGRP^{EGFP} animals were also used as controls for one study. For behavioural studies, a fibre ferrule was implanted over the ARC of all animals used (see Table 2.5 for coordinates used). For all *in vivo* photostimulation experiments in this chapter, the same pulse protocol was used: 10 ms pulses, 20 Hz for 1 s, repeated every 4 seconds.

4.2.2. Fos expression under differing conditions

Brain tissue of AGRP^{ChR2EYFP} animals were collected from *ad libitum* fed mice, after 24 hrs of food deprivation, or after 1 hr of AGRP neuron photostimulation, and stained for Fos. At least 100 neurons were examined in the same fashion for each condition to determine Fos intensity distributions (see section 2.10).

4.2.3 AGRP neuron evoked feeding in AGRP^{ChR2EYFP} animals

AGRP^{ChR2EYFP} mice with implanted fibre ferrules over the ARC were allowed to acclimate to the behavioural cages overnight before initiating the photostimulation protocols, and were tested for evoked feeding behaviour during the early light period. During the test, animals had *ad libitum* access to 20 mg grain pellets and water. Food intake was recorded during a pre-photostimulation baseline for 1 hr, followed by a 1 hr of AGRP neuron photostimulation. Latency to feed was defined as the time elapsed between the onset of photostimulation and the initiation of the first bout of feeding. A feeding bout was defined as the consumption of a minimum of five pellets with inter-pellet-intervals less than 2.4 min (Aponte et al. 2011). Several post hoc tests were performed in order to determine inclusion of an animal to the final analysis. Fibre transmittance was measured after removal from brain. Animals with less than 50% fibre transmittance were excluded from analysis. Fibre placement was also determined. Animals with off-target fibre placement were excluded from

analysis. For all of the experiments described below, animals were pre-screened for evoked food consumption as described here. Animals that consumed at least 0.7 g of food were considered to have suitable optical fibre placement.

4.2.4 Conditioned place avoidance

Conditioned place avoidance was conducted in a two chambered apparatus. AGRP^{ChR2EYFP} animals pre-screened for feeding (consumed 0.7 g of food in an *ad libitum* AGRP neuron photostimulation evoked feeding test, as described above in section 4.2.3) were used for the experimental group, while AGRP^{EGFP} animals were used for the control group. All animals were given an acclimatization session (15 min) to the apparatus the day before testing initial preference. The initial preference was tested by placing the mouse in the preference chamber for 1800 s and its position was video recorded. Position of animals was tracked offline using these video recordings and the initial side preference was determined. After this initial preference test, animals under optogenetic neuron photostimulation (both experimental group and control group) were conditioned with a two-step protocol alternating passive conditioning with an active avoidance place preference test. The active avoidance place preference protocol alone was less reliable for conditioning avoidance, likely related to the minutes long latency (Aponte et al. 2011) of AGRP neuron activation to induce food-seeking and consumption. Therefore, some prior experience with AGRP neuron activity on one of the sides appears to be required, despite the fact that this exposure alone did not significantly alter place preference.

Passive conditioning sessions involved separate exposure to each side of the apparatus (1800 s each), where the initially less preferred side was not paired with intracranial light pulses, and the initially more preferred side was paired with intracranial light pulses to photostimulate neurons expressing ChR2. Control animals, which only expressed an enhanced green fluorescent protein (EGFP), also experienced intracranial light pulses on the initially more preferred side to ensure that the light pulse protocol used is not aversive on its own. Passive conditioning was followed by active avoidance place preference testing on the subsequent day, in which mice were allowed free access to both sides of the chamber (900 s) while the

position of the mouse was recorded and photostimulation was applied only when the mouse entered the side of the chamber also paired with photostimulation during passive conditioning (photostimulation ceased as soon as the mouse crossed to the other side). This allowed the mouse to adjust its behaviour to avoid elevated AGRP neuron activity. After 7 days of this protocol (morning: active avoidance, afternoon: passive conditioning), mice received one more passive conditioning session, and the next day were given free access to the chamber for 1800 s and allowed to explore the chamber without any photostimulation events (extinction) while the position of the mouse was recorded. The experimental schedule is summarized in Table 4.1

Session	Day 1	Day 2-8	Day 9
Morning	Initial preference measurement *(1800 s)*	Active avoidance session *(900 s)*	Place preference in extinction *(1800 s)*
Afternoon	Passive conditioning *(1800 s on each side of chamber)*	Passive conditioning *(1800 s each side of chamber)*	

Table 4.1 Conditioned place avoidance training and experimental schedule.

4.2.5 Lever pressing experiments

AGRP^{ChR2EYFP} animals were used for all lever pressing tasks. Animals pre-screened for evoked feeding (consumed 0.7 g of food in an *ad libitum* AGRP neuron photostimulation evoked feeding test, as described above in section 4.2.3) were used for all AGRP neuron photostimulation groups. Mice that did not reach this criterion were used for control groups (food restriction groups). All lever press training was conducted under food restriction, where animals were maintained at ~85% body weight. Food rewards during training consisted of 20 mg grain pellets. Food rewards were switched to 20 mg grain pellets with 1% saccharine and grape or orange flavouring during testing to allow comparison of reinforcing effects of food consumption outside of the testing session (i.e., influence of flavoured pellets vs.

regular chow consumption in the homecage). All animals received exposure to these pellets in their homecages (50 pellets) the night prior to the start of tests to limit any effects on behaviour from neophobia. All training and tests were conducted in operant conditioning chambers during the light period.

4.2.5.1 Progressive Ratio 7 reinforcement schedule for feeding

Training

All mice were trained to lever press for food at a fixed ratio (FR) 1 ratio overnight for one night. While food restricted, mice were then trained on daily, 30 min FR1 sessions until reaching learning criteria (earning 18 pellets in a 30 min session for 3 consecutive days). They were then trained with 2 hr sessions for two days on a progressive ratio (PR) schedule where the required number of presses for each subsequent reward increases by 3 (PR3). Mice were then trained on a PR7 schedule for one day in a 2 hr session.

PR Test

Following training, mice were tested on a PR7 test for 15 consecutive days. PR7 was used to ensure that mice would exert high levels of effort for food and to limit satiation at low levels of effort. PR7 test sessions were 2 hrs; however, mice were only allowed to press for food for the first 40 min of each session. After training, mice in the food restriction group were kept on food restriction and tested on a PR7 schedule for 15 consecutive days. Mice were then returned to *ad libitum* food for 2 days to allow their body weight to recover, and tested on a PR7 schedule under *ad libitum* fed conditions. Mice were tethered to a dummy fibre (no photostimulation) during testing to ensure that this tether does not interfere with lever pressing activity or with food consumption.

For the AGRP neuron photostimulation groups, mice were returned to *ad libitum* food intake for 2 days after training, before initiating testing. All mice were tested under well-fed conditions (absence of energy deficit) with photostimulation on a PR7 schedule for 15 consecutive days. During test sessions, one group of mice

received photostimulation for the whole length of the session (120 min) in order to fully dissociate cessation of photostimulation from lever pressing and food consumption. Within this group, some mice were provided regular chow in their home cages, while others were maintained on the same food used as rewards during the test session for the duration of the experiment. These two subgroups were ultimately combined for statistical analysis because no difference in lever pressing was observed between them. A second group received photostimulation only during the first 40 min of the session, when the mice were allowed to press for food. Mice in both photostimulation groups were also tested in the absence of photostimulation after the 15 day test sessions.

For all groups, mice that did not earn at least 5 food rewards on the first day of PR7 test were removed from the experiment as low lever pressing is most likely due to aversion to novel food (from switching to flavoured food reward between training and testing phases); this applied to one mouse from the food restriction group. Food rewards during test sessions consisted of 20 mg grain pellets with 1% saccharine and grape flavouring. Breakpoint was defined as the last ratio completed before 5 min passed without earning a reward. For the rate of lever pressing analysis, lever presses were divided into two blocks: first 10 minutes (low-effort work requirement) and rest of session (high-effort work requirement). The first 10 min were chosen as low-effort work requirement conditions since average breakpoint time was greater than 10 min for all groups.

4.2.5.2 Fixed Ratio 100 reinforcement schedule for feeding.

Training

All mice were trained to lever press for food at an FR1 ratio overnight for one night. While food restricted, mice were trained on daily, 30 min FR1 sessions until reaching learning criteria (earning 18 pellets in a 30 min session for 3 consecutive days). They were then trained with one 40 minute session (one session per day) for each of the following fixed ratio schedules on consecutive days: FR5, FR15, FR30,

FR60, and FR100. Only animals that pressed at least 500 times on the FR100 schedule were used for testing.

FR Test

Following training, mice were tested on FR100 test for 15 consecutive days. FR100 was used to ensure that mice would exert high levels of effort for food and to limit satiation at low levels of effort. FR100 test sessions were 2 hrs; however, mice were only allowed to press for food for the first 40 min of each session to mimic the PR7 study. Food rewards during test sessions consisted of 20 mg grain pellets with 1% saccharine and grape flavouring. As with PR7 experiment, after training, mice in the food restriction group were kept on food restriction and tested on a FR100 schedule for 15 consecutive days. Mice were then returned to *ad libitum* food for 2 days to allow their body weight to recover, and tested on a FR100 schedule under *ad libitum* fed conditions. Mice were tethered to a dummy fibre (no photostimulation) during testing to ensure that this tether does not interfere with lever pressing activity or with food consumption. For the AGRP neuron photostimulation group, mice were returned to *ad libitum* food intake for 2 days after training, before initiating testing. All mice were tested under well-fed conditions (absence of energy deficit) with photostimulation on an FR100 schedule for 15 consecutive days. During test sessions, mice received photostimulation for the whole length of the session (120 min). Mice were also tested in the absence of photostimulation after the 15 day test sessions.

To study the effects on lever pressing of elevated AGRP neuron activity under food restriction in an FR100 reinforcement schedule for feeding, the experiment was conducted as described above, using animals from the same cohort. Animals were retrained on lever pressing with one 40 min session (one session per day) for each of the following fixed ratio schedules on consecutive days: FR5, FR15, FR30, FR60, and FR100. Following training, the experimental procedure was exactly as described above for the food restriction group. For AGRP neuron photostimulation group, animals were not returned to *ad libitum* food consumption. Instead, all photostimulated sessions were tested while animals were maintained on food restriction. Food pellets used in this test contained a different flavour cue (citrus instead of grape) from those used for the experiment described above to avoid any

associations with experience in the prior experiment. All other procedures were identical to those described above.

4.2.6 Photostimulation induced weight gain

AGRP^{ChR2EYFP} mice that consumed 0.7 g of food or more during an *ad libitum* AGRP neuron photostimulation evoked feeding test were used for this experiment. All mice were trained to lever press under a PR7 schedule under food restriction as described in section 4.2.5.1 above. Food rewards during training consisted of 20 mg grain pellets. After training, mice were then returned to *ad libitum* food for 2 days before testing began. Food rewards were switched to 20 mg grain pellets with 1% saccharine and grape flavouring during PR7 testing to allow comparison of reinforcing effects of food consumption outside of the testing session (i.e., influence of flavoured pellets vs. regular chow consumption in the homecage), mirroring the protocol used in the PR7 reinforcement assay (section 4.2.5.1 above). All mice received exposure to these pellets in their homecages (50 pellets) the night prior to the start of tests to limit neophobia. Mice were then tested on a PR7 task under well fed conditions during photostimulation of AGRP neurons. The PR7 reinforcement session was 2 hrs long but levers were only available for the first 40 min of the session. Photostimulation was given during the entire length of the session (120 min) in order to fully dissociate cessation of photostimulation from lever pressing and food consumption.

Next, mice underwent the weight gain induction period. Weight gain was induced in one group of mice through daily, 2 hr photostimulation sessions (22 days) until weight gain matched that of the 120 min photostimulation group in the PR7 test (~28%). A second group did not receive photostimulation, but were tethered to an optic fibre and served as controls for natural weight gain and any potential decline in lever pressing due to the time elapsed between tests. During these sessions, mice did not lever press for food. Mice in both groups were allowed to consume a number of rewards (20 mg grain pellets with 1% saccharine and grape flavouring) in order to ensure any changes in lever pressing on the post weight gain PR7 test was not due to the novelty of the food or neophobia. The number of rewards provided during the weight gain stimulation sessions each day was matched to the average number of rewards earned by the 120 min photostimulation group in the PR7 test. After ~28%

weight gain in the photostimulated group, well fed mice were then tested again on a PR7 task under AGRP neuron stimulation (120 min), and without AGRP neuron photostimulation on the following day.

4.2.7 Repeated daily AGRP neuron evoked free feeding assay

Three groups of mice were tested for 15 consecutive daily sessions for food consumption in a free feeding assay: 1) food restriction, 2) *ad libitum* fed with AGRP neuron photostimulation, and 3) *ad libitum* fed without AGRP neuron photostimulation. The photostimulation group received AGRP neuron photostimulation for the whole duration of the testing session (2 hours) each day. Food restriction and *ad libitum* fed group were tethered to an optic fibre, but did not receive any light stimulation. Sessions were 2 hrs long but mice were only allowed to consume food during the first 40 minutes of the session (mimicking lever pressing studies). Food rewards consisted of 20 mg grain pellets with 1% saccharine and grape flavouring to distinguish any reinforcing effects of food consumption outside of the testing session (regular chow consumption in the homecage). All mice received exposure to these pellets in the homecage (50 pellets) the night prior to the start of tests. AGRP^{ChR2EYFP} mice that consumed 0.7 g of food or more during an *ad libitum* AGRP neuron photostimulation evoked feeding test were used for the AGRP neuron photostimulation group. Mice that did not reach this criterion were used for the food restriction and *ad libitum* fed no photostimulation groups.

4.3 Results

4.3.1 Optogenetic manipulations of AGRP neurons for the study of motivational processes in feeding

To study the motivational properties of AGRP neuron circuit, optogenetic techniques were employed to allow for the rapid, cell-type specific activity manipulations of AGRP neurons. Previous studies have shown that the amount of food consumed in AGRP neuron evoked feeding behaviours is dependent on the number of AGRP neurons activated by photostimulation (Aponte et al. 2011). Therefore, in order to reduce variability in neuronal activation and behavioural effects, which is more prominent under viral transduction of ChR2 due to variability in infection levels, cell-type selective expression of ChR2 in AGRP neurons was achieved by crossing AGRP^{Cre} animals (Tong et al. 2008) with Ai32 animals, a Cre-dependent mouse line for the expression of membrane-localized ChR2 with a fused enhanced yellow fluorescent protein (EYFP) marker (Madisen et al. 2012). The resulting mouse line, AGRP^{ChR2EYFP}, express ChR2 specifically in AGRP neurons.

4.3.1.1 Validation of ChR2 expression in AGRP^{ChR2EYFP} animals

To verify the expression of ChR2 in AGRP neurons, hypothalamic brain slices of AGRP^{ChR2EYFP} animals were stained for green fluorescent protein (GFP). Under visual inspection of brain slices of AGRP^{ChR2EYFP} mice, ChR2-EYFP only labelled cell bodies in the ARC (n=3 animals). In addition, projections were only observed in previously described AGRP neuron projection regions (Betley et al. 2013, Haskell-Luevano et al. 1999), suggesting appropriate expression pattern of this mouse line (Figure 4.2A-D, I-L). Validation of cell-type specific expression and penetrance levels of ChR2 in AGRP^{ChR2EYFP} mice was performed by analyzing colocalization of ChR2-EYFP with endogenous AGRP in axonal terminals of seven major projection fields: anterior subdivisions of the bed nucleus of stria terminalis (aBNST), paraventricular nucleus of the hypothalamus (PVH), paraventricular thalamic nucleus (PVT), suprafornical subdivision of the lateral hypothalamic area (LHAs), central nucleus of

the amygdala (CEA), periaqueductal grey (PAG), and parabrachial nucleus (PBN) (Betley & Sternson 2011, Haskell-Luevano et al. 1999) (4.2E-H, N-P). Analysis of colocalization shows that AGRP^{ChR2EYFP} mouse line expresses ChR2-EYFP in ~97% of AGRP peptide immunoreactive boutons across all projection areas examined (Figure 4.2Q). In addition, colocalization of ChR2-EYFP with proopiomelanocortin (POMC), the second major population of neurons in the ARC, was measured to determine expression specificity. Colocalization was also measured in major AGRP axonal projections, which are also major targets of POMC neurons (Betley et al. 2013) (Figure 4.3A-P). The analysis showed that ChR2-EYFP is minimally co-expressed in POMC neurons, as only ~1.4% of POMC immunoreactive boutons were colocalized with ChR2-EYFP across all projection areas examined (Figure 4.3Q). This indicates that AGRP^{ChR2EYFP} mouse line displays high ChR2 penetrance in AGRP neurons with minimal expression in other cell-types.
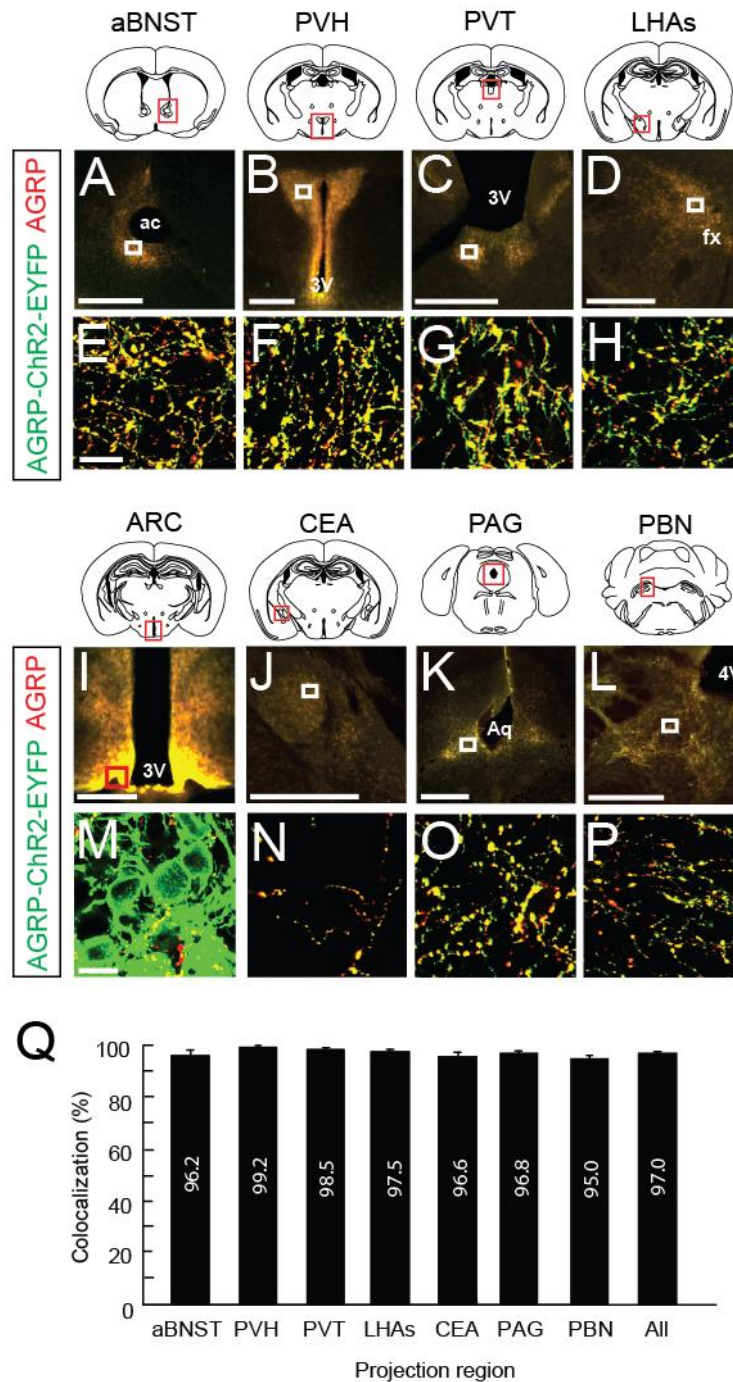
Figure 4.2 AGRP[ChR2EYFP] animals display high penetrance of ChR2 expression in AGRP neurons. (A-D, I-L) Diagrams and epifluorescence images showing colocalization of membrane-bound ChR2-EYFP (green) and AGRP (red) immunoreactivity in major AGRP neuron projection regions in AGRP[ChR2EYFP] mice: (A) aBNST, (B) PVH, (C) PVT, (D) LHAs, (I) ARC, (J) CEA, (K) PAG, and (L) PBN. Red boxes coronal brain section diagrams represent regions shown. Scale bars: 500 μm. **(E-H, M-P)** Insets of (A-D, I-L), respectively, showing single confocal plane of

AGRP (red) and membrane-bound ChR2-EYFP (green) containing boutons. Scale bars: 10 µm. **(Q)** Percent colocalization of ChR2-EYFP containing boutons with AGRP containing boutons in all projection regions analyzed (n=100 AGRP boutons counted per projection region). aBNST: anterior subdivisions of the bed nucleus of stria terminalis; PVH: paraventricular nucleus of the hypothalamus; PVT: paraventricular thalamic nucleus; LHAs: suprafornical subdivision of the lateral hypothalamic area; ARC: arcuate nucleus; CEA: central nucleus of the amygdala; PAG: periaqueductal grey; PBN: parabrachial nucleus; ac: anterior commissure; 3V: third ventricle; fx: fornix; Aq: aqueduct; 4V: fourth ventricle.
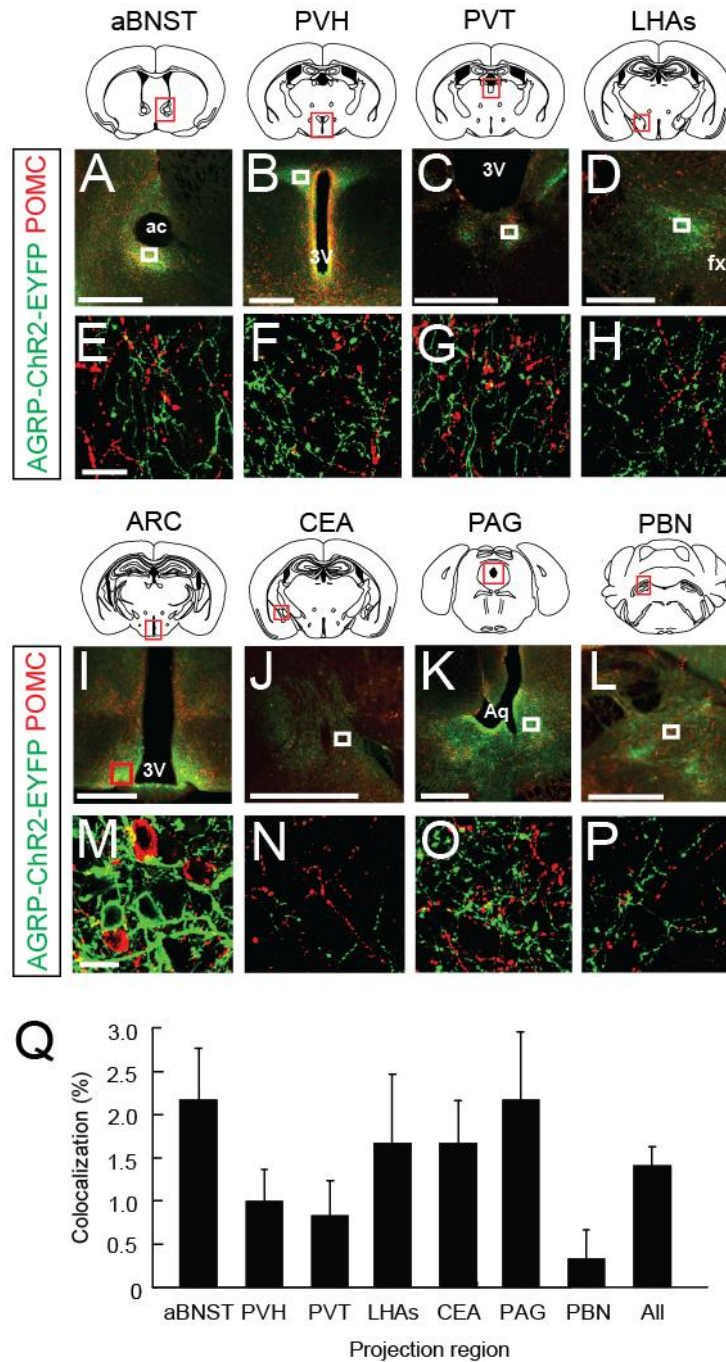
Figure 4.3 ChR2 in AGRP^{ChR2EYFP} animals is not expressed in POMC neurons. **(A-D, I-L)** Diagrams and epifluorescence images showing colocalization of membrane-bound ChR2-EYFP (green) and POMC (red) immunoreactivity in major AGRP neuron projection regions in AGRP^{ChR2EYFP} mice: (A) aBNST, (B) PVH, (C) PVT, (D) LHAs, (I) ARC, (J) CEA, (K) PAG, and (L) PBN. Red boxes coronal brain section diagrams represent regions shown. Scale bars: 500 μm. **(E-H, M-P)** Insets of (A-D, I-L), respectively, showing single confocal plane of POMC (green) and membrane-bound ChR2-EYFP (green) containing boutons. Scale bars: 10 μm. **(Q)**

Percent colocalization of ChR2-EYFP containing boutons with POMC containing boutons in all projection regions analyzed (n=100 AGRP boutons counted per projection region). aBNST: anterior subdivisions of the bed nucleus of stria terminalis; PVH: paraventricular nucleus of the hypothalamus; PVT: paraventricular thalamic nucleus; LHAs: suprafornical subdivision of the lateral hypothalamic area; ARC: arcuate nucleus; CEA: central nucleus of the amygdala; PAG: periaqueductal grey; PBN: parabrachial nucleus; ac: anterior commissure; 3V: third ventricle; fx: fornix; Aq: aqueduct; 4V: fourth ventricle.

4.3.1.2 Functional validation of ChR2 in AGRP^{ChR2EYFP} animals *in vivo*

To test the functionality of ChR2 expressed in AGRP^{ChR2EYFP} animals, I determined the ability of photostimulation of the ARC to produce Fos expression in ChR2 expressing AGRP neurons, and whether Fos expression levels are similar to those observed in AGRP neurons under food deprivation conditions (Betley et al. 2013). Brain slices of AGRP^{ChR2EYFP} animals that were either under *ad libitum* food, 24 hr food deprivation, or receiving 1 hour of *in vivo* AGRP neuron photostimulation were stained for Fos. Immunohistochemical analysis showed Fos expression in AGRP neurons under 24 hr food deprivation and 1 hr *in vivo* photostimulation conditions, but not under *ad libitum* fed conditions (Figure 3.4A-I). In addition, analysis of Fos intensity distributions of 100 randomly selected AGRP neurons per condition (from 2 animals per condition) show no significant differences between the food deprived and photostimulated conditions (Mann-Whitney rank sum test between food deprivation and photostimulation conditions only, n=100 neurons per condition, p=0.170, Fig 4.4J), indicating that ChR2 in AGRP neurons of AGRP^{ChR2EYFP} animals is functional and photostimulation is capable of activating these neurons.
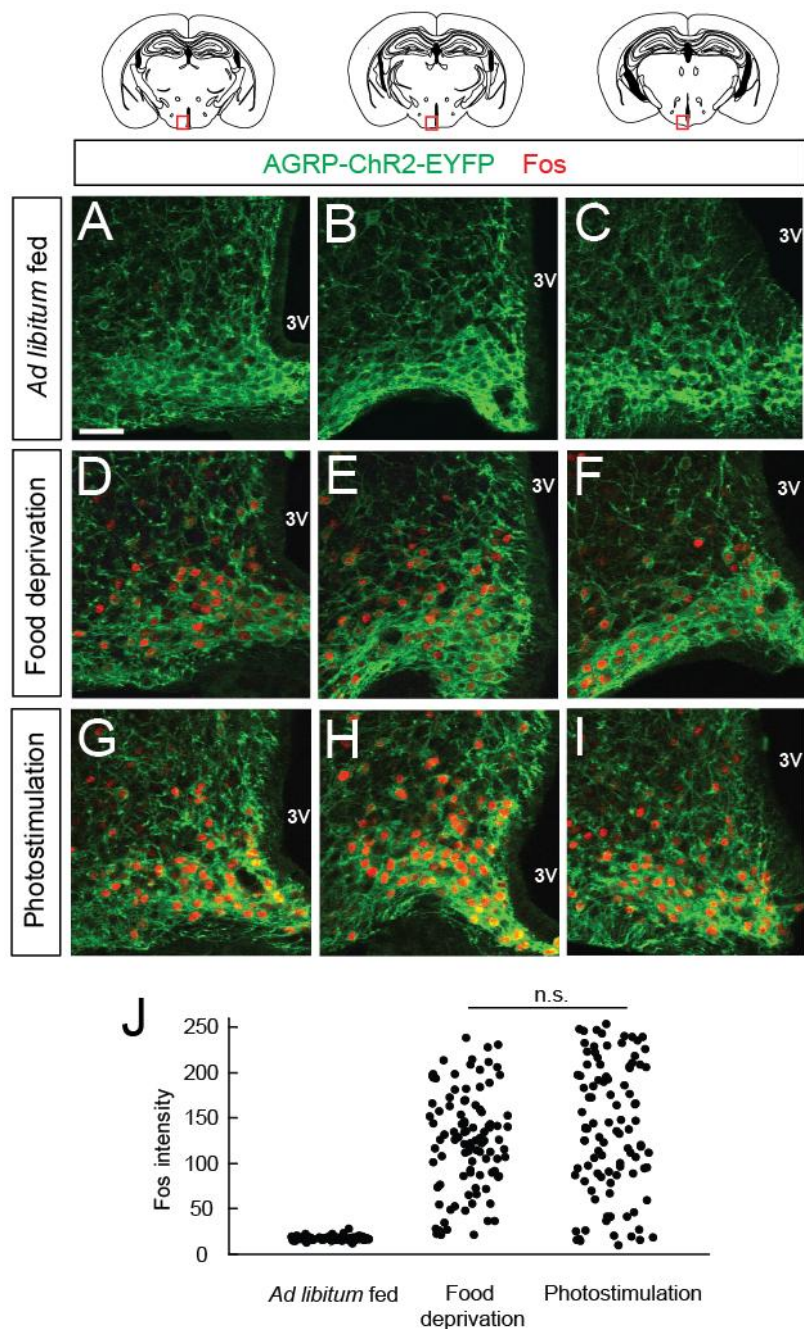
Figure 4.4 Optogenetic stimulation of AGRP neurons in AGRP^{ChR2EYFP} animals induced Fos expression similar to food deprivation. (A-C) Single plane confocal image showing no Fos (red) immunoreactivity in membrane-bound ChR2-EYFP expressing AGRP neurons(green) in the (A) anterior, (B) medial, and (C) posterior ARC of *ad libitum* fed AGRP^{ChR2EYFP} animals. Scale bar: 50 µm. **(D-F)** Single plane confocal image of Fos (Red) immunoreactivity in membrane-bound ChR2-EYFP expressing AGRP neurons (green) in the (D) anterior, (E) medial, and (F) posterior ARC of 24 hr food deprived AGRP^{ChR2EYFP} animals. **(G-I)** Single plane confocal image showing Fos (red) immunoreactivity in membrane-bound ChR2-EYFP

expressing AGRP neurons (green) in the (A) anterior, (B) medial, and (C) posterior ARC of 1 hr AGRP neuron photostimulated AGRP^{ChR2EYFP} animals. Red boxes in coronal brain section in diagrams represent areas shown. **(J)** Scatter plots showing distribution of Fos immunofluorescence intensity measured in the nucleus of AGRP-ChR2-EYFP labelled neurons from three groups of mice: *Ad libitum* fed, 24 hr food deprived, and 1 hr AGRP neuron photostimulated (Mann-Whitney rank sum test between food restriction and photostimulation conditions only, n=100 neurons per group, from 3 animals in each group,). n.s. p>0.05. 3V: third ventricle.

4.3.1.3 AGRP neuron evoked feeding in AGRP^{ChR2EYFP} animals

To determine whether AGRP^{ChR2EYFP} animals are suitable for behavioural studies, I tested whether optogenetic activation of AGRP neurons in these animals results in an evoked-feeding response as previously reported with activation of AGRP neurons using viral expression of ChR2 (Aponte et al. 2011, Atasoy et al. 2012) (Figure 4.5A-C). Results indicate that photostimulation of AGRP neurons in well-fed AGRP^{ChR2EYFP} animals elicited an evoked-feeding response (Figure 4.5D). Consistent with prior reports (Aponte et al. 2011), photostimulated animals consumed on average 0.94 ± 0.12 g in 1 hr, a significant increase over a 1 hr pre photostimulation baseline, where animals only consumed 0.09 ± 0.03 g (paired t-test, n=6, p=0.001, Fig 4.5E). In addition, latency from the onset of photostimulation to the first bout of food consumption was on average 3.2 ± 0.9 min, which is within the range of previously reported latencies (~6 min) (Aponte et al. 2011). Therefore, AGRP^{ChR2EYFP} present similar behavioural responses under AGRP neuron activation as previously reported and are suitable for use in behavioural studies.
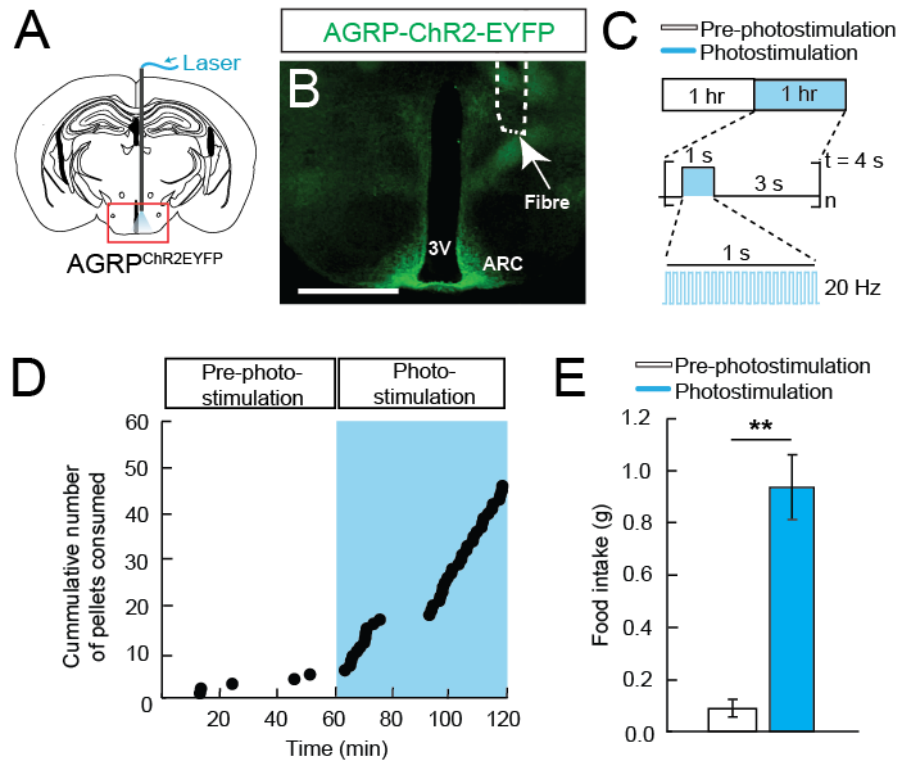
Figure 4.5 Photoactivation of AGRP neurons in elicits evoked feeding response in AGRP^ChR2EYFP animals. (A) Diagram of fibre placement position in AGRP^ChR2EYFP animals for AGRP neuron photoactivation. **(B)** Epifluorescence image of membrane-bound ChR2-EYFP (green) expression in the ARC of AGRP^ChR2EYFP animals and fibre placement (dashed line). Red box in coronal brain section diagram in (A) represents region shown. Scale bar: 1 mm. **(C)** Schematic of experimental design and photostimulation protocol used. Food intake was measured for 1 hr pre photostimulation and 1 hr under AGRP neuron photostimulation in *ad libitum* fed animals during the light period. **(D)** Cumulative number of pellets (20 mg) consumed over time for pre photostimulation baseline (1 hr, white background) and under AGRP neuron photostimulation (1 hr, cyan background). **(E)** Total food intake during pre photostimulation baseline (white) and under AGRP neuron photostimulation (cyan) (n=6, paired t-test). Values are mean ± S.E.M. ** p<0.01. ARC: arcuate nucleus, 3V: third ventricle.

4.3.2 AGRP neuron stimulation has a negative valence and is avoided

Prior studies indicate that suppression of AGRP neuron activity under hunger is reinforcing, suggesting that AGRP neurons might engage a negative reinforcement mechanism to direct food consumption behaviours (Betley et al. 2014). If AGRP neurons motivate food-seeking and consumption *via* a negative reinforcement mechanism, then increased AGRP neuron activity is expected to signal negative valence. This would direct the selection of behaviours that resulted in a reduction of AGRP neuron activity, and therefore, alleviation from the associated negative valence. To test this hypothesis independently of the reinforcing properties of nutrient ingestion (Yiin et al. 2005), the reinforcement characteristics of AGRP neuron activation in the absence of food consumption or energy deficit were examined using a conditioned place avoidance paradigm.

AGRP^{ChR2EYFP} mice, as well as control AGRP^{EGFP} mice, were passively and actively (active avoidance) conditioned each day for 7 days. Under passive conditioning sessions, animals received exposure to AGRP neuron photostimulation on one side of a two-chamber apparatus, and no photostimulation to the other side. In active avoidance sessions, animals were allowed to freely explore both sides of the conditioning apparatus. AGRP neuron photostimulation was triggered whenever the mouse entered the side of the chamber previously exposed to photostimulation under passive conditioning, and terminated when animals exited it. The protocol allowed animals to use a behavioural response distinct from food intake to shut off elevated AGRP neuron activity (Figure 4.6A-D). Over the course of 7 days, mice showed avoidance of the side paired with AGRP neuron photostimulation compared to controls, which do not show this response (two-way RM ANOVA, n=12 per group, interaction: group x session $F_{(7, 154)}$= 3.3, p=0.003; Figure 4.6E-F, Table 4.2). This effect was more robust for the second half of the active aversion session (two-way RM ANOVA, n=12 per group, interaction: group x session $F_{(7, 154)}$ = 3.8, p<0.001; Figure 4.6G, Table 4.2.), which is likely related to the minutes-long latency of AGRP neuron stimulation to evoke feeding (Aponte et al. 2011). In a subsequent extinction test in the absence of photostimulation, mice continued to avoid the side previously associated with elevated AGRP neuron activity (unpaired t-test, n=12 per group, p=0.025; Figure 4.6H). This shows that elevated AGRP neuron activity has a negative valence, which can be used to reinforce behavioural responses to avoid it,

further supporting a negative reinforcement motivational mechanism for food seeking during AGRP neuron activation. Under energy deficit, elevated AGRP neuron activity elicits an internal state with negative valence, which mice learn to avoid. In the presence of food, animals would be motivated to eat as nutrient ingestion normally suppresses these neurons and eliminates this negative internal state.
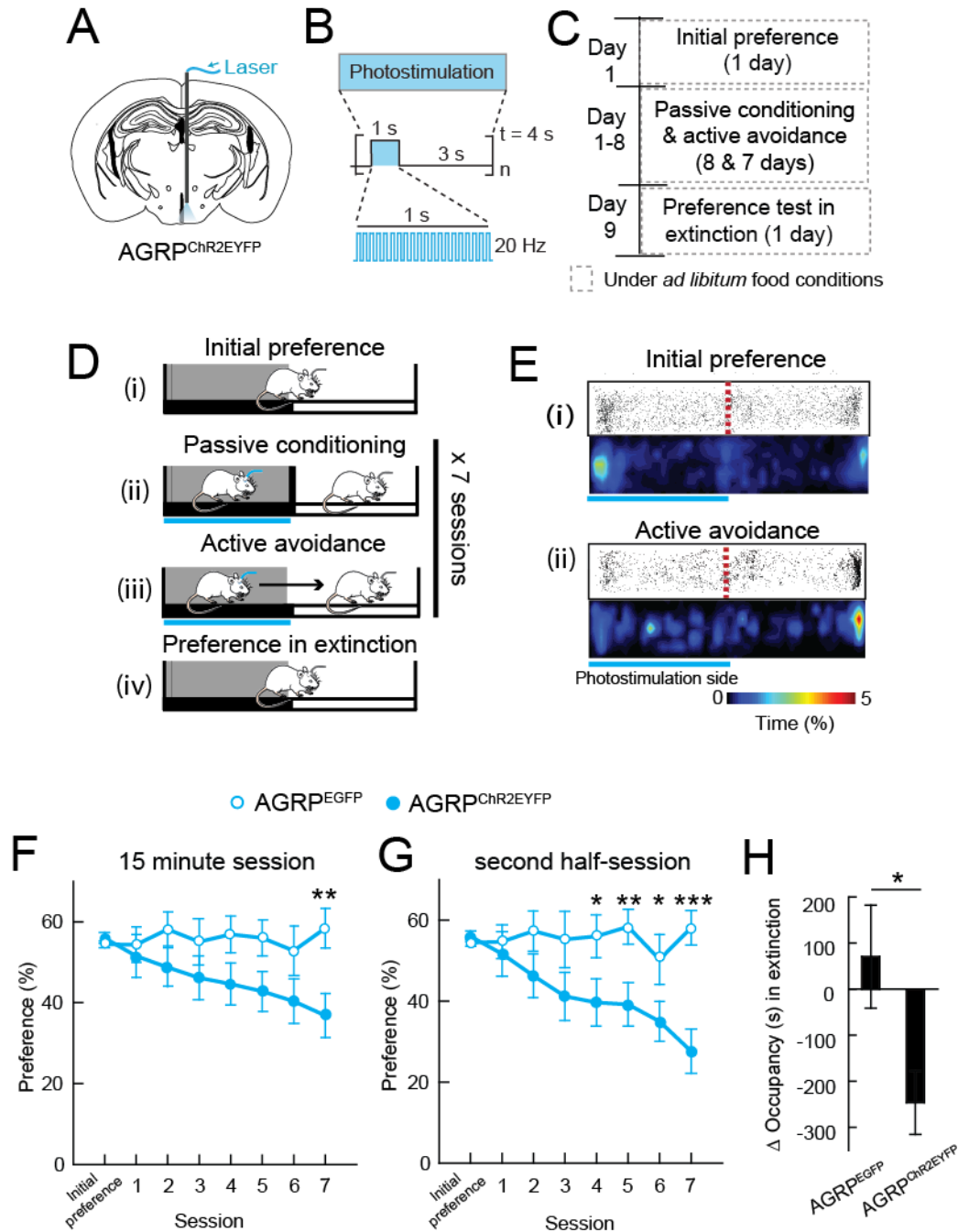
Figure 4.6 Elevated AGRP neuron activity is actively avoided. (A) Diagram of fibre placement position in AGRP[ChR2EYFP] animals for AGRP neuron photoactivation. **(B)** Schematic of photostimulation protocol used. **(C)** Schematic of experimental design schedule. Initial preference was measured, followed by passive conditioning and active avoidance protocols over 7 days, with a final passive conditioning session and a preference test in extinction. Experiment was conducted under *ad libitum* food conditions for all animals during the light period. **(D)** Experimental design for each conditioned place aversion experimental step. (i) Initial place preference was

measured in a 2-chamber apparatus. Animals received no photostimulation and had access to the entire apparatus. (ii) Under passive conditioning sessions, mice were separately exposed to each side of the chamber (30 min each, with or without light delivery). Photostimulation side is indicated by cyan bar. (iii) In active conditioning sessions, animals had access to the entire apparatus. Light was delivered upon entering the side of the chamber previously conditioned with stimulation, and the mouse's exit from that side terminated photostimulation. (i) and (iii) were repeated over 7 days. (iv) A preference test in extinction was subsequently performed, where the animal had full access to both sides of the chamber and no photostimulation. **(E)** For a representative AGRP^{ChR2EYFP} mouse, scatter plots tracking mouse position (top) and corresponding heat map (bottom) showing percentage of occupancy times in photostimulation (cyan bar) and no photostimulation side, revealing a change from the (i) initial preference to the side of the chamber paired with the cessation of AGRP neuron photostimulation during (ii) last active avoidance test. **(F, G)** Percent occupancy time on photostimulation side for AGRP^{EGFP} control (open circles, n=12) and AGRP^{ChR2EYFP} experimental group (filled circles, n=12) during (F) 15-min active avoidance sessions and (G) the second half of each active avoidance session. Statistical comparisons are across groups for each session (see Table 4.2). **(H)** Change in occupancy time on the previously photostimulated side for AGRP^{EGFP} control (n=12) and AGRPChR2EYFP (n=12) experimental group during a 30 min preference test in extinction (unpaired t-test). Values are mean ± S.E.M. * $p < 0.05$; ** $p < 0.01$; *** $p < 0.001$.

Figure panel	Sample size	Statistical test	Values
F	12 per group	Two-Way RM ANOVA Factor 1: Group (AGRP^{ChR2EYFP} vs. AGRP^{EGFP})	F(1,154)=3.0, p=0.097
		Factor 2: Session	F(7,154)=2.3, p=0.029
		Interaction: Group x Session	F(7,154)=3.3, p=0.003
		Post hoc multiple comparison with Holm-Sidak corrections	
		Session 7	p=0.003
G	12 per group	Two-Way RM ANOVA Factor 1: Group (AGRP^{ChR2EYFP} vs. AGRP^{EGFP})	F(1,154)=6.4, p=0.019
		Factor 2: Session	F(7,154)=3.2, p=0.004
		Interaction: Group x Session	F(7,154)=3.8, p<0.001
		Post hoc multiple comparison with Holm-Sidak corrections	
		Session 4	p=0.025
		Session 5	p=0.009
		Session 6	p=0.035
		Session 7	p<0.001
H	12 per group	Unpaired t-test	p=0.025

Table 4.2 Statistical values for Figure 4.6

4.3.3 Disruption of negative reinforcement reduces instrumental food seeking

If AGRP neurons induce food seeking due to the learned contingency between actions that results in nutrient ingestion and reduction of AGRP neuron activity, then food seeking actions that fail to reduce AGRP neuron activity are expected to diminish in intensity over time. To examine the role of negative reinforcement for AGRP neuron-mediated food-seeking, I sought to prevent reduction of AGRP neuron activity during and following a food-seeking task by imposing elevated AGRP neuron activity in the absence of other homeostatic need signals. AGRP neuron activation in *ad libitum* fed mice increases lever pressing for food on a progressive ratio task as much as food restriction (Atasoy et al. 2012). However, if AGRP neuron activity is predominantly mediating food seeking behaviours through negative reinforcement, then previously reinforced lever pressing actions would gradually decrease because nutrient ingestion would no longer be capable of reducing elevated AGRP neuron activity (Figure 4.7A). This would be analogous to behavioural extinction, as the reinforcer, in this case decrease in AGRP neuron activity, is withheld, even though food is still delivered and consumed. Alternatively, if AGRP neuron activity predominantly influences food seeking by a positive reinforcement process associated with the enhancement of positive valence of food consumption, then lever pressing would be expected to remain elevated (Figure 4.7B).

To test this, I compared three groups of animals that were trained to lever press on a PR7 food reinforcement schedule under food restriction. After learning the contingency between lever pressing and food delivery, they were tested for 15 days in a PR7 paradigm. In this test, animals were allowed to lever press for food for 40 min, and then remained in the testing chamber for another 80 min. (Figure 4.8A-C). One group (n=7) was maintained under food restriction and showed steady lever press responses over 15 sessions (Figure 4.8D). The other two groups were re-fed to *ad libitum* and were tested for instrumental food seeking during AGRP neuron photostimulation. One group received photostimulation only while animals had access to levers to earn food rewards (40 min, n=12). For a second group, photostimulation was continued after the levers and food access were withdrawn (120 min, n=11) in order to fully dissociate cessation of photostimulation from lever pressing and food consumption. In the first session, both groups of mice responded

to AGRP neuron photostimulation with high lever presses and food consumption, similar to mice in the food restriction group (one-way ANOVA, n= 7 food restriction, 12 photostimulation (40 min), 11 photostimulation (120 min), $F_{(2, 27)} = 0.741$, p=0.486; Figure 4.8D). In subsequent sessions, however, both groups of *ad libitum* fed photostimulated AGRP^{ChR2EYFP} mice showed a progressive decline in lever presses (two-way RM ANOVA, n= 7 food restriction, 12 photostimulation (40 min), 11 photostimulation (120 min), interaction: groups x session $F(28, 378)= 2.12$, p<0.001; Figure 4.8D, Table 4.3), with the 120 min photostimulation group showing the most dramatic effect. The 40 min photostimulation group displayed an intermediate effect in decline in lever presses between the food restricted and 120 min photostimulated group, indicating that the magnitude of reduced lever pressing for food was sensitive to the duration of AGRP neuron photostimulation in the behavioural session (Figure 4.8D). In addition, little or no lever pressing was observed on the inactive lever through the entire experiment for all groups, indicating that lever pressing was goal-directed and decline in lever pressing was not due to switching of activity to a different lever (data not shown). Comparisons between the first (session 1) and last (session 15) sessions of testing show that food restricted animals do not change their lever pressing, and both sessions remain elevated over an *ad libitum* fed, no photostimulation (*Ad lib*) session tested (post hoc multiple comparisons with Holm-Sidak correction, n=7, session 1 vs. session 15 p=0.839, session 1 vs. *Ad lib* session p=0.021, session 15 vs. *Ad lib* session p=0.02; Figure 4.8F, Table 4.3). In contrast 120 min photostimulation group show a statistically significant decline in lever presses between the first and last sessions of testing, with the level of lever pressing on the last session being comparable to the *Ad lib* session (post hoc multiple comparisons with Holm-Sidak correction, n=11, session 1 vs. session 15 p<0.001, session 15 vs. *Ad lib* session p=0.33; Figure 4.8F, Table 4.3). The 40 min photostimulation group also displayed a reduction in lever pressing between session 1 and session 15, but lever presses on session 15 remained elevated over the *Ad lib* session (post hoc multiple comparisons with Holm-Sidak correction, n=12, session 1 vs. session 15 p=0.006, session 15 vs. *Ad lib* session p=0.009; Figure 4.8F, Table 4.3).

Analysis of number of pellets earned showed similar patterns. The food restricted group showed no changes in numbers of pellets earned between the first

and last session of testing (post hoc multiple comparisons with Holm-Sidak correction, n=7, session 1 vs. session 15 p=1.000; Figure 4.8G, Table 4.3), while both 120 min photostimulation (post hoc multiple comparisons with Holm-Sidak correction, n=11, session 1 vs. session 15 p<0.001; Table 4.3) and 40 min photostimulation group (post hoc multiple comparisons with Holm-Sidak correction, n=12, session 1 vs. session 15 p=0.002; Table 4.3) showed a significant decline (Fig 4.8G). Further analysis between food restriction and 120 min photostimulation group shows that there is a statistical significant difference in lever pressing over multiple sessions of the test (two-way RM ANOVA, n= 7 food restriction, 11 photostimulation (120 min), group $F_{(1,224)}$= 5.4 p=0.033, session $F_{(14,224)}$= 2.9 p<0.001, interaction $F_{(14,224)}$= 3.5, p<0.001; Figure 4.8D, Table 4.3). This experiment indicates that elevated AGRP neuron activity during and following instrumental responding for food reduced the level of effort expended to seek and consume food. This is in accord with a model where AGRP neuron activity serves predominantly as a negative reinforcement teaching signal for food seeking behaviours (Figure 4.7A). One caveat to this interpretation is the observance of AGRP neuron photostimulation induced body weight (Figure 4.8E), which would lead to an alternative hypothesis where long term metabolic changes can influence motivation for food seeking. This issue is addressed in the next section.
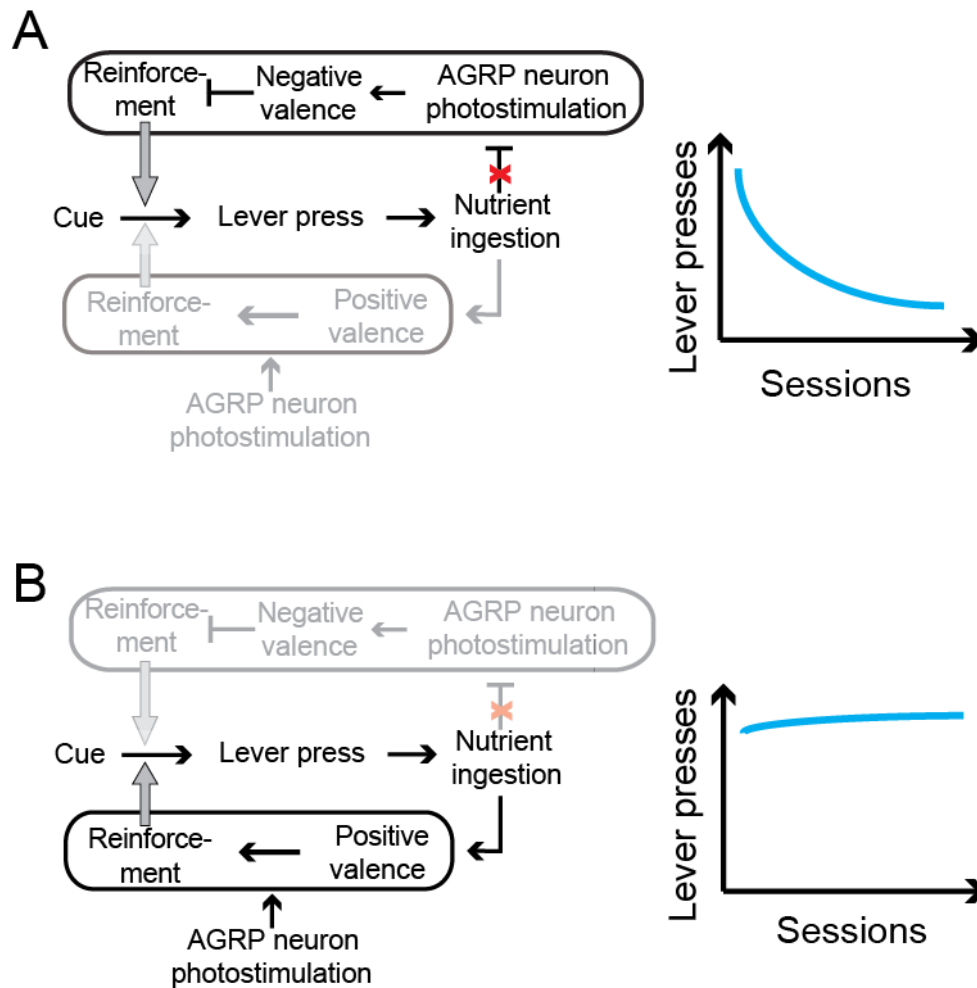
Figure 4.7 Prediction of outcomes under AGRP neuron-mediated negative reinforcement signal disruption. (A) Model that combines concerted negative and positive reinforcement for AGRP neuron-mediated food seeking and ingestion. If AGRP neurons operate primarily via negative reinforcement, under conditions of elevated AGRP neuron activity imposed by photostimulation, previously reinforced actions (lever press) are predicted to decrease (schematic, right) as nutrient ingestion no longer reduces AGRP neuron activity and negative valence. Although ingested nutrients are intrinsically positively reinforcing (greyed-out pathway), this is insufficient to compensate for loss of negative reinforcement. **(B)** As an alternative hypothesis, if AGRP neurons predominantly mediate reinforcement through the enhancement of the positive valence of nutrients instead of through negative reinforcement (greyed-out pathway), then previously reinforced actions that lead to nutrient ingestion under states of energy deficit would remain elevated (schematic, right).
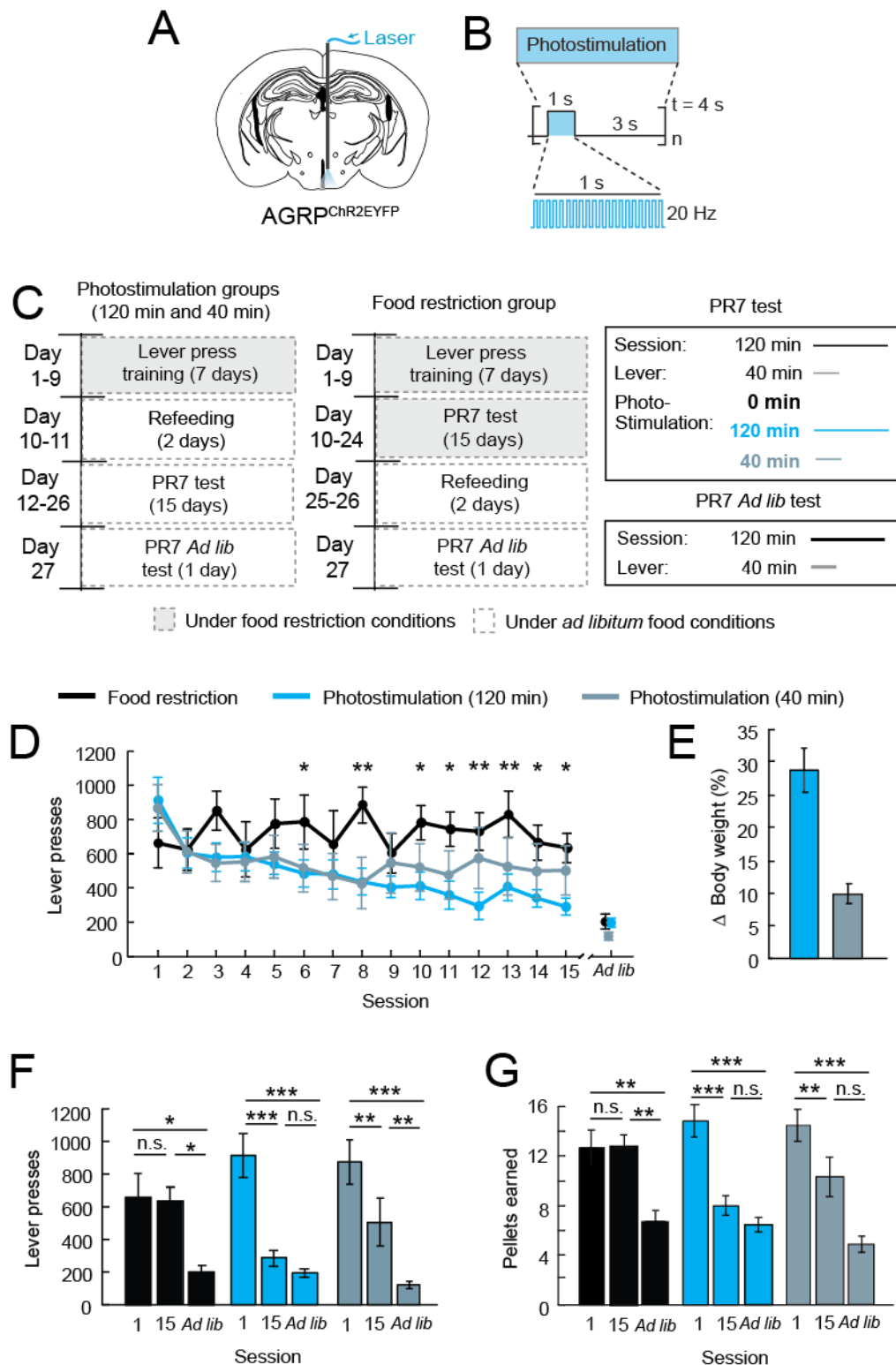
Figure 4.8 Disruption of AGRP neuron mediated negative reinforcement reduces instrumental responding for food. (A) Diagram of fibre placement position in AGRP^{ChR2EYFP} animals for AGRP neuron photoactivation. **(B)** Schematic

of photostimulation protocol used. **(C)** Schematic of experimental design schedule. AGRP[ChR2EYFP] mice were trained in energy deficit to lever press with a PR7 reinforcement schedule for food pellets. PR7 reinforcement testing was performed over 15 sessions on three groups: food restriction (black), *ad libitum* fed AGRP neuron photostimulation (120 min, cyan) and *ad libitum* fed AGRP neuron photostimulation (40 min, grey). After the 15th test session, a test session was performed for all groups without photostimulation and under *ad libitum* food (*Ad lib*) conditions. During test sessions (120 min for all groups), levers were available for the first 40 min. Food restriction group did not receive photostimulation. The AGRP neuron photostimulation (120 min) group received intracranial light pulses for the entire 120-min session, while the AGRP neuron photostimulation (40 min) group received intracranial light pulses only during the 40 min period when the lever was available. All tests were conducted during the light period. **(D)** Lever presses in each session during PR7 test for food restriction (black, n = 7), *ad libitum* fed AGRP neuron photostimulation (120 min) (cyan, n = 11), and *ad libitum* fed AGRP neuron photostimulation (40 min, n = 12) mice. Statistical comparisons are across groups, between food restriction and photostimulation (120 min) groups only, for each session (see Table 4.3). **(E)** Weight gain for the 120 min (cyan, n=11) and 40 min (grey, n=12) AGRP neuron photostimulation groups in PR7 experiment after 15 sessions. Weight gain is due to eating after the test session when the mouse is returned to the homecage and is associated with long-lasting effects from release of AGRP (Hagan et al. 2000). Previous experiments have shown that AGRP is not responsible for the acute feeding behaviour investigated in this study (Aponte et al. 2011, Atasoy et al. 2012, Krashes et al. 2013). However, metabolic changes associated with weight gain could be an alternative cause of reduced instrumental food seeking shown in (D). **(F, G)** (F) Lever presses and (G) pellets earned from first (1), last (15) and *ad libitum* (*Ad lib*) PR7 test sessions for food restriction (black), AGRP neuron photostimulation (120 min) (cyan) and AGRP neuron photostimulation (40 min) (grey) groups. Statistical comparisons are within groups (see Table 4.3). Values are mean ± S.E.M. n.s. p>0.05; * p<0.05; ** p<0.01; *** p<0.001.

Figure panel	Sample size	Statistical test	Values
D	Food Restriction group: 7 Photostimulation (120 min) group: 11 Photostimulation (40 min) group: 12	Two-Way RM ANOVA Factor 1: Group (Food restriction Photostimulation (120 min), Photostimulation (40 min))	$F_{(2,378)}=1.2$, $p=0.315$
		Factor 2: Session	$F_{(14,378)}=3.9$, $p<0.001$
		Interaction: Group x Session	$F_{(28,378)}=2.1$, $p<0.001$
D	Food Restriction group: 7 Photostimulation (120 min) group: 11	Two-Way RM ANOVA Factor 1: Group (Food restriction vs. Photostimulation (120 min) only)	$F_{(1,224)}=5.4$, $p=0.033$
		Factor 2: Session	$F_{(14,224)}=2.9$, $p<0.001$
		Interaction: Group x Session	$F_{(14,224)}=3.5$, $p<0.001$
		Post hoc multiple comparison with Holm-Sidak corrections	
		Session 6	$p=0.045$
		Session 8	$p=0.003$
		Session 10	$p=0.014$
		Session 11	$p=0.011$
		Session 12	$p=0.004$
		Session 13	$p=0.005$
		Session 14	$p=0.029$
		Session 15	$p=0.022$
F	Food Restriction group: 7	One-Way RM ANOVA	$F_{(2,12)}=6.6$, $p=0.012$
		Post hoc multiple comparison with Holm-Sidak corrections	
		Session 1 vs. Session 15	$p=0.839$
		Session 1 vs. *Ad lib* Session	$p=0.021$
		Session 15 vs. *Ad lib* Session	$p=0.02$
	Photostimulation (120 min) group: 11	One-Way RM ANOVA	$F_{(2,20)}=33.1$, $p<0.001$
		Post hoc multiple comparison with Holm-Sidak corrections	
		Session 1 vs. Session 15	$p<0.001$
		Session 1 vs. *Ad lib* Session	$p<0.001$
		Session 15 vs. *Ad lib* Session	$p=0.332$

Table 4.3 Statistical values for Figure 4.8. *Table continued on next page.*

Figure panel	Sample size	Statistical test	Values
F	Photostimulation (40 min) group: 12	One-Way RM ANOVA	$F_{(2,22)}=19.2$, $p<0.001$
		Post hoc multiple comparison with Holm-Sidak corrections	
		Session 1 vs. Session 15	$p=0.006$
		Session 1 vs. *Ad lib* Session	$p<0.001$
		Session 15 vs. *Ad lib* Session	$p=0.009$
G	Food Restriction group: 7	One-Way RM ANOVA	$F_{(2,12)}=11.5$, $p=0.002$
		Post hoc multiple comparison with Holm-Sidak corrections	
		Session 1 vs. Session 15	$p=1.000$
		Session 1 vs. *Ad lib* Session	$p=0.004$
		Session 15 vs. *Ad lib* Session	$p=0.003$
	Photostimulation (120 min) group: 11	One-Way RM ANOVA	$F_{(2,20)}=38.1$, $p<0.001$
		Post hoc multiple comparison with Holm-Sidak corrections	
		Session 1 vs. Session 15	$p<0.001$
		Session 1 vs. *Ad lib* Session	$p<0.001$
		Session 15 vs. *Ad lib* Session	$p=0.145$
	Photostimulation (40 min) group: 11	One-Way RM ANOVA	$F_{(2,22)}=33.4$, $p<0.001$
		Post hoc multiple comparison with Holm-Sidak corrections	
		Session 1 vs. Session 15	$p=0.002$
		Session 1 vs. *Ad lib* Session	$p<0.001$
		Session 15 vs. *Ad lib* Session	$p=0.145$

Table 4.3 continued

4.3.4 Decline in willingness to work for food is experience dependent

An increase in body weight was observed during the multi-session AGRP neuron stimulation protocol (Figure 4.8E) likely due to a long-acting effect of released AGRP (Hagan et al. 2000) following photostimulation. However, this is not responsible for the acute food consumption under investigation here, which is due to the release of neuropeptide-Y (NPY) and γ-aminobutyric acid (GABA) (Aponte et al. 2011, Atasoy et al. 2012, Krashes et al. 2013). Weight gain was dependent on the length of photostimulation provided in each session, as the 120 min photostimulation group displayed a larger percent weight gain (~28%) than the 40 min photostimulation group (~ 10%) by the end of the 15 session test. Since the level of decline in lever pressing was less prominent in the 40 min photostimulation group, it is possible that the decline in willingness to work for food is due to long-term metabolic changes induced by chronic AGRP neuron photostimulation, as changes in metabolism can lead to changes in motivation to work for food (Atalayer et al. 2010, Finger et al. 2010).

In order to rule out this possibility, I dissociated AGRP stimulation and weight gain from the lever pressing action. AGRP^{ChR2EYFP} animals were trained to lever press under food restriction and then tested on a PR7 schedule under *ad libitum* fed conditions with photostimulation for one day, with a similar protocol to the 120 min photostimulation group in the study previously described. After this, one group of animals received 120 min of photostimulation per session for 22 days to induce weight gain (Induced weight gain group, n=6) but were not subjected to the lever press task. A second group of animals was not photostimulated (controls, n=6). At the end of this protocol, animals were tested again on a PR7 test in order to determine whether weight gain alone can reduce lever pressing (Figure 4.9A-C). AGRP neuron photostimulation induced weight gain group gained ~30% of body weight following the weight gain induction protocol, which was statistically significant from natural weight gain observed in the control group (unpaired t-test, n=6 per group, p<0.001; Figure 4.9D). However, for both groups, there was no significant difference in lever pressing between the first (session 1) and second (session 2) PR7 test, and lever pressing remained elevated over an *Ad lib* session (post hoc multiple comparisons with Holm-Sidak correction, n=6 per group, control group: session 1 vs.

session 2 p=0.359, session 2 vs. *Ad lib* session p=0.042; induced weight gain group: session 1 vs. session 2 p=0.104, session 2 vs. *Ad lib* session p<0.001; Figure 4.9E, Table 4.4). In addition, percent lever press change between the two groups was not significantly different (unpaired t-test, n=6 per group, p=0.386; Figure 4.9F). Therefore, body weight gain and long-term metabolic changes are not responsible for the suppression in responding observed in the prior PR7 study. Instead, decline in lever pressing is dependent on the animal experiencing both the act of lever pressing and photostimulation concurrently. The learned association between lever pressing and the inability of this action paired with food consumption to reduce AGRP neuron activity leads the animal to abandon this behavioural strategy.
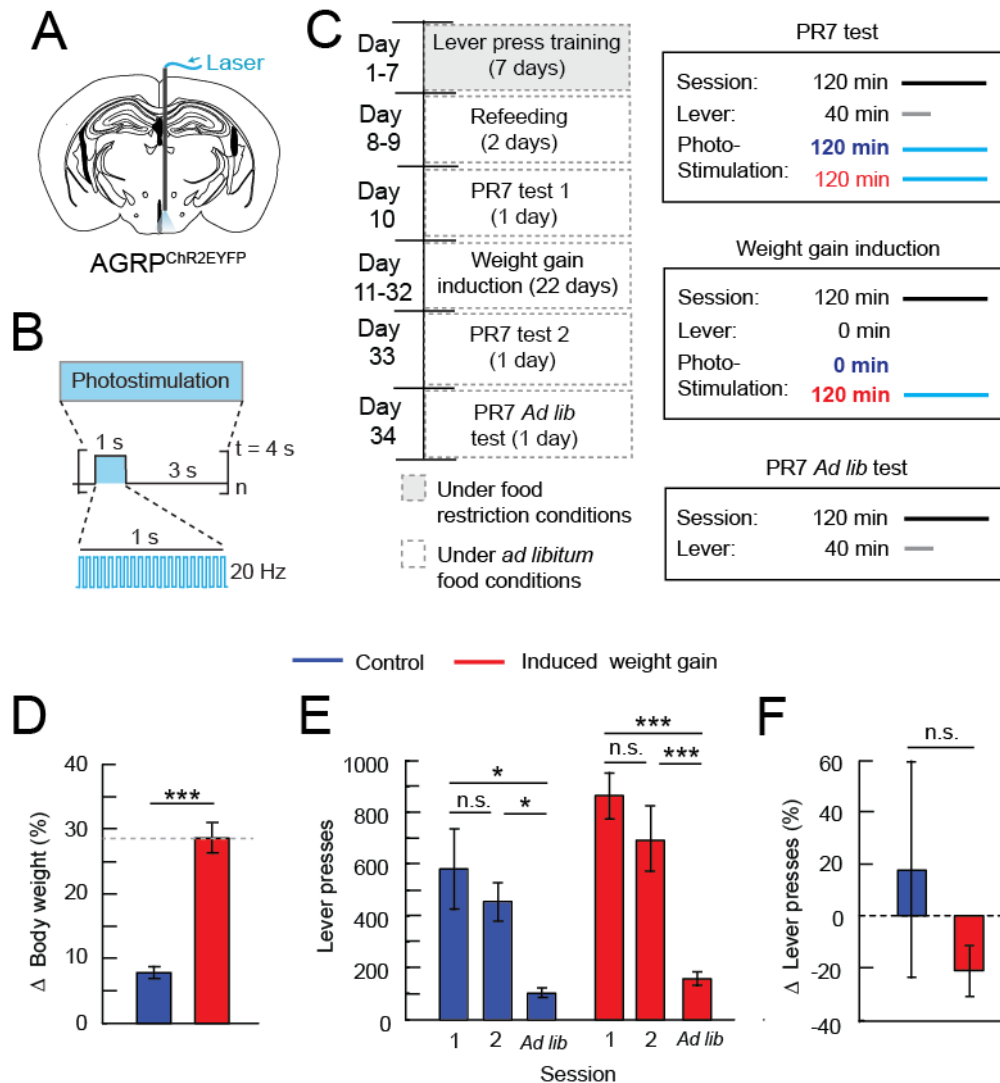
Figure 4.9 AGRP neuron stimulation associated body weight increase does not suppress AGRP neuron-evoked food seeking. (A) Diagram of fibre placement position in AGRP^{ChR2EYFP} animals for AGRP neuron photoactivation. **(B)** Schematic of photostimulation protocol used. **(C)** Schematic of experimental design schedule. AGRP^{ChR2EYFP} mice were trained under food deprivation to lever press under a PR7 schedule for food pellets. After training, both groups were *ad libitum* re-fed, and the mice were divided into two groups: 1) control mice with no induction of weight gain (blue) and 2) the induced weight gain group (red). Both groups were then tested on a PR7 reinforcement schedule under AGRP neuron photostimulation conditions (PR7 test 1). Following this session, a photostimulation-induced weight gain protocol was initiated for the second group. Mice received one 2-h experimental session per day, where they were photostimulated for the whole experimental session and body weight was monitored daily. During these sessions, levers were not available, but free food was provided during these sessions (the amount of food was matched in quantity to the average amount of food acquired by the 120 min photostimulation

group under the PR7 experiment from Fig. 4.8 for the corresponding session). The photostimulation-induced weight grain protocol was conducted for 22 consecutive days, which was required for percent body weight gain to be comparable to levels acquired by the 120-min AGRP neuron photostimulation group in the PR7 experiment (~28%) from Fig 4.8. Control mice were tethered to a fibre but did not receive photostimulation, otherwise they received the same experimental manipulation as induced weight gain mice (access to the same amount of food), and their body weight was also monitored. After the induced weight gain group achieved ~28% weight gain, a second PR7 test was conducted for both groups in the same manner as the first one. A final no photostimulation, *ad libitum* fed test session (PR7 *Ad lib* test) was also conducted. All tests were conducted during the light period. **(D)** Percent body weight change from initial body weight for control (blue, n=6) and induced weight gain (red, n=6) mice after weight gain induction protocol. Grey dotted line: percent body weight change for mice in the photostimulation (120 min) in PR7 experiment from Fig. 4.8 (unpaired t-test). **(E)** Lever presses for control (blue) and AGRP neuron photostimulation-induced weight gain (red) groups on first (1) and second (2) PR7 test, prior and after weight gain induction protocol, respectively, and a no photostimulation, *ad libitum* fed (*Ad lib*) PR7 test. Statistical comparisons are within groups (see Table 4.4). **(F)** Percent lever press change between first and second PR7 test sessions for control (blue, n=6) and induced weight gain (red, n=6) mice (unpaired t-test). Values are mean ± S.E.M. n.s. p>0.05; * p<0.05; *** p<0.001.

Figure panel	Sample size	Statistical test	Values
D	6 per group	Unpaired t-test	p<0.001
E	Control group: 6	One-Way RM ANOVA	F(2,10)=7.3, p=0.011
		Post hoc multiple comparison with Holm-Sidak corrections	
		Session 1 vs. Session 2	p=0.359
		Session 1 vs. *Ad lib* Session	p=0.012
		Session 2 vs. *Ad lib* Session	p=0.042
	Induced weight gain group: 6	One-Way RM ANOVA	F(2,10)=28.6, p<0.001
		Post hoc multiple comparison With Holm-Sidak corrections	
		Session 1 vs. Session 2	p=0.104
		Session 1 vs. *Ad lib* Session	p<0.001
		Session 2 vs. *Ad lib* Session	p<0.001
F	6 per group	Unpaired t-test	p=0.386

Table 4.4 Statistical values for Figure 4.9

4.3.5 Negative reinforcement disruption is most sensitive under high effort requirements

Further analysis of the food seeking behaviour of mice during AGRP neuron stimulation revealed that cost/energy expenditure may also play an important role in the modulation of actions. In the PR7 study, breakpoint ratio was also affected by extended AGRP neuron photostimulation. Food restriction animals show no change in breakpoint ratio between the first and last sessions of the test (post hoc multiple comparisons with Holm-Sidak correction, n=7, session 1 vs. session 15 p=0.211; Figure 4.10A, Table 4.5). In contrast, breakpoint ratio was significantly reduced between the first and last sessions of the test for 120 min photostimulated group (post hoc multiple comparisons with Holm-Sidak correction, n=11, session 1 vs. session 15 p=0.002; Figure 4.10A, Table 4.5), and 40 min photostimulated group (post hoc multiple comparisons with Holm-Sidak correction, n=12, session 1 vs. session 15 p=0.007; Figure 4.10A, Table 4.5).

Given that in a PR task subsequent pellets require an increased number of lever presses to be emitted, this means that pellets earned in latter parts of the test are more costly. Therefore, the rate of lever pressing can be compared between the early periods of the test, where pellets are cheap, and the latter periods of the test, where pellets are more expensive, to understand the role of cost and effort in AGRP neuron mediated negative reinforcement. Here I analyzed the lever press rate in the first 10 min of the session (low effort/cost) versus the rest of the session (high effort/cost) between the first and last sessions of the test. For animals under food restriction, low effort lever pressing rate increased, while high effort lever pressing rate remained unchanged (post hoc multiple comparisons with Holm-Sidak correction, n=7, session 1 vs. session 15: First 10 min p=0.009, rest of session p=0.234; Figure 4.10B-C, Table 4.4). Under photostimulation, however, the lever pressing rate for food pellets requiring high ratio responses was most strongly diminished under AGRP neuron stimulation, but lever pressing that required low levels of effort were only modestly reduced (post hoc multiple comparisons with Holm-Sidak correction: 120 min photostimulation group: n=11, session 1 vs. session 15: First 10 min p=0.006, rest of session p<0.001; 40 min photostimulation group: n=12, session 1 vs. session 15: First 10 min p=0.078, rest of session p=0.002; Figure 4.10B-C, Table 4.4). These experiments, then, suggest that high effort

motivated responding is most sensitive to disruption of negative reinforcement in AGRP-mediated food seeking.

To directly test this hypothesis, I tested whether elevated AGRP neuron activity would disrupt food consumption or lever pressing under a repeated *ad libitum* feeding test (low/no effort) and under an FR100 schedule lever pressing task (high effort). For the repeated *ad libitum* feeding test, AGRP^{ChR2EYFP} animals were tested for food consumption under *ad libitum* fed conditions with AGRP neuron photostimulation, under food restriction conditions, or under *ad libitum* fed unphotostimulated conditions for 15 sessions. For each session, animals had access to *ad libitum* food and water for the first 40 min of the test, after which animals remained in the behaviour chambers for an additional 80 min. Animals in the photostimulation group (n=6) received photostimulation spanning the whole 2 hrs of the session (Figure 4.11A-C). Pellet consumption during this test remained elevated throughout the test for both the photostimulation group and the food restriction group (n=6), while the unphotostimulated group (n=6) consumed very low levels of food throughout the test (post hoc multiple comparisons with Holm-Sidak correction, n= 6 per group, food restriction vs. photostimulation $p=0.26$, food restriction vs. *ad libitum* fed $p<0.001$, photostimulation vs. *ad libitum* fed $p<0.001$; Figure 4.11D, Table 4.6), indicating that disruption of AGRP neuron-mediated negative reinforcement does not reduce food seeking and consumption actions under low effort requirements. These results also suggest that reduced food seeking observed in the PR7 schedule study was not due to a developed aversion to the food reward, nor diminished effectiveness of repeated sessions of extended AGRP neuron photostimulation.

For the high effort FR100 study, animals were trained to lever press under food deprivation. Following this, one group of animals was kept on food restriction (n=7) and tested on an FR100 schedule over 15 sessions. FR100 was chosen as a high effort schedule as this ratio is higher than the breakpoint ratio for all animals on the first day of the PR7 study. As with the PR7 experiment, animals were allowed to lever press for food for 40 minutes, and then remained in the testing chamber for another 80 minutes. AGRP neuron photostimulation group (n=6) was returned to *ad libitum fed* conditions before starting the 15 session FR100 schedule test. As with food restricted animals, this groups of animals were allowed to earn pellets during the first 40 min of the session, but were photostimulated for the entire session length

(120 min) (Figure 4.12A-C). Consistent with previous results, photostimulated animals show a slow progressive decline in lever pressing and pellets earned throughout the experiment, but food restricted animals show an increase in lever pressing (two-way RM ANOVA, n= 7 food restriction, 6 photostimulation, interaction: group x session $F_{(14,154)}$= 3.163 p<0.001; Figure 4.12D, Table 4.7). Lever pressing and pellets earned was significantly reduced on the last session compared to the first session of testing for the photostimulation group (post hoc multiple comparisons with Holm-Sidak correction, n=6, lever presses: session 1 vs. session 15 p=0.007; pellets earned: session 1 vs. session 15 p=0.006; Figure 4.12E-F, Table 4.7). However, the food restricted group showed an increase in these measures, not observed under the PR7 schedule study (post hoc multiple comparisons with Holm-Sidak correction, n=7, lever presses: session 1 vs. session 15 p=0.002, pellets earned: session 1 vs. session 15 p=0.004; Figure 4.12E-F, Table 4.7). This indicates that other feeding circuits and signals play a significant role in food seeking and consumption under food restriction conditions, and AGRP neuron stimulation only plays a partial role in this effect in hunger. This effect was better observed under a high fixed ratio schedule. Together, this set of results indicates that high cost/effort motivated responding is most sensitive to the disruption of negative reinforcement in AGRP neuron mediated food seeking. Other factors appear sufficient to mediate low effort responding directed towards *ad libitum* food consumption, such as deprivation state-insensitive positive reinforcement from ingested nutrients (Yiin et al. 2005).
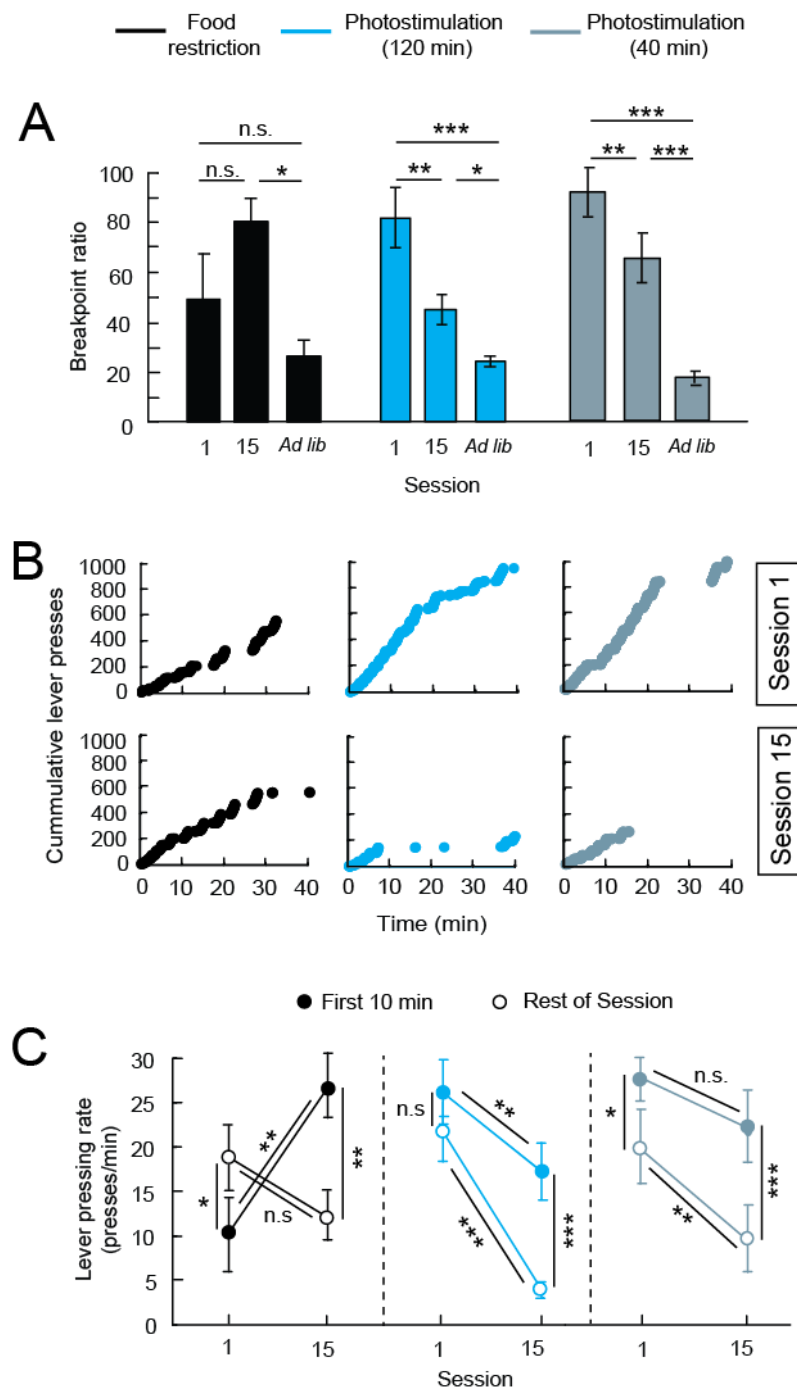
Figure 4.10 Maintenance of high effort responding is most sensitive to disruptions of AGRP neuron mediated negative reinforcement. (A) Breakpoint ratio from first (1), last (15) and no photostimulation *ad libitum fed* (*Ad lib*) PR7 test sessions for food restriction (black), AGRP neuron photostimulation (120 min) (cyan) and AGRP neuron photostimulation (40 min) (grey) groups from Figure 4.8. **(B)** Representative traces of cumulative lever pressing responses during first (1) and last (15) PR7 test sessions for food restriction (black), AGRP neuron photostimulation

(120 min) (cyan), and AGRP neuron photostimulation (40 min) (grey) groups from Figure 4.8. **(C)** Rate of lever pressing during first 10 minutes of session (low effort, filled circles) and rest of session (high effort, open circles) on first (1) and last (15) session of PR7 test for food restriction (black), AGRP neuron photostimulation (120 min) (cyan) and AGRP neuron photostimulation (40 min) (grey) groups from Figure 4.8. Statistical comparisons are within groups (see Table 4.5). Values are mean ± S.E.M. n.s. p>0.05; * p<0.05; ** p<0.01; *** p<0.001.

Figure panel	Sample size	Statistical test	Values
A	Food Restriction group: 7	One-Way RM ANOVA	$F_{(2,12)}=4.5$, $p=0.035$
		Post hoc multiple comparison with Holm-Sidak corrections	
		Session 1 vs. Session 15	$p=0.211$
		Session 1 vs. *Ad lib* Session	$p=0.227$
		Session 15 vs. *Ad lib* Session	$p=0.033$
	Photostimulation (120 min) group: 11	One-Way RM ANOVA	$F_{(2,20)}=19.5$, $p<0.001$
		Post hoc multiple comparison with Holm-Sidak corrections	
		Session 1 vs. Session 15	$p=0.002$
		Session 1 vs. *Ad lib* Session	$p<0.001$
		Session 15 vs. *Ad lib* Session	$p=0.039$
	Photostimulation (40 min) group: 12	One-Way RM ANOVA	$F_{(2,22)}=35.0$, $p<0.001$
		Post hoc multiple comparison with Holm-Sidak corrections	
		Session 1 vs. Session 15	$p=0.007$
		Session 1 vs. *Ad lib* Session	$p<0.001$
		Session 15 vs. *Ad lib* Session	$p<0.001$
C	Food Restriction group: 7	Two-Way RM ANOVA	
		Factor 1: Time block (First 10 min vs. Rest of session)	$F_{(1,6)}=1.3$, $p=0.291$
		Factor 2: Session	$F_{(1,6)}=1.4$, $p=0.284$
		Interaction: Time block x Session	$F_{(1,6)}=16.7$, $p=0.006$
		Post hoc multiple comparison with Holm-Sidak corrections	
		Session 1: First 10 min vs. Rest of session	$p=0.044$
		Session 15: First 10 min vs. Rest of session	$p=0.003$
		First 10 min: Session 1 vs. Session 15	$p=0.009$
		Rest of Session: Session 1 vs. Session 15	$p=0.234$

Table 4.5 Statistical values for Figure 4.10. *Table continued on next page*

Figure panel	Sample size	Statistical test	Values
C	Photostimulation (120 min) group: 11	Two-Way RM ANOVA	
		Factor 1: Time block (First 10 min vs. Rest of session)	$F_{(1,10)}=27.9$, $p<0.001$
		Factor 2: Session	$F_{(1,10)}=34.2$, $p<0.001$
		Interaction: Time block x Session	$F_{(1,10)}=7.6$, $p=0.021$
		Post hoc multiple comparison with Holm-Sidak corrections	
		Session 1: First 10 min vs. Rest of session	$p=0.076$
		Session 15: First 10 min vs. Rest of session	$p<0.001$
		First 10 min: Session 1 vs. Session 15	$p=0.006$
		Rest of Session: Session 1 vs. Session 15	$p<0.001$
	Photostimulation (40 min) group: 12	Two-Way RM ANOVA	
		Factor 1: Time block (First 10 min vs. Rest of session)	$F_{(1,11)}=11.2$, $p=0.006$
		Factor 2: Session	$F_{(1,11)}=14.3$, $p=0.003$
		Interaction: Time block x Session	$F_{(1,11)}=2.3$, $p=0.156$
		Post hoc multiple comparison with Holm-Sidak corrections	
		Session 1: First 10 min vs. Rest of session	$p=0.027$
		Session 15: First 10 min vs. Rest of session	$p<0.001$
		First 10 min: Session 1 vs. Session 15	$p=0.078$
		Rest of Session: Session 1 vs. Session 15	$p=0.002$

Table 4.5 continued
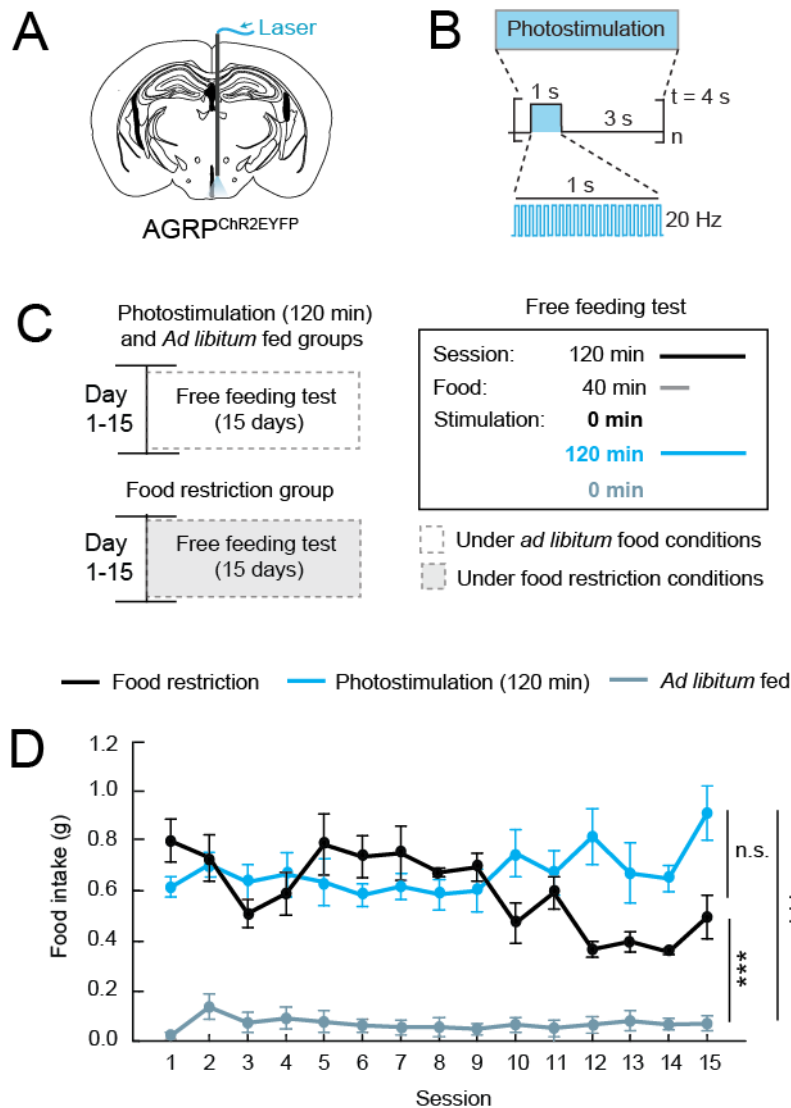
Figure 4.11 Free food consumption is not reduced with repeated daily AGRP neuron photostimulation sessions. (A) Diagram of fibre placement position in AGRP^ChR2EYFP animals for AGRP neuron photoactivation. **(B)** Schematic of photostimulation protocol used. **(C)** Schematic of experimental design schedule. Three groups of AGRP^ChR2EYFP mice were tested on a 15 session free feeding protocol (no lever pressing required) either under food restriction (black), *ad libitum* fed with AGRP neuron photostimulation (120 min) (cyan), or *ad libitum* fed without AGRP neuron photostimulation (grey) conditions. On each day, mice received one 2-hour session, where food was freely available for the first 40 minutes of the session. AGRP neuron photostimulation (120 min) group received photostimulation for the entire 2 hour session (cyan). The two other groups, food restriction (black) and *ad libitum* fed (grey) groups, did not receive photostimulation. All tests were performed during the light period. **(D)** Food intake for each session of the free feeding experiment for food restriction (black, n=6), *ad libitum* fed AGRP neuron photostimulation (120 min) (cyan, n=6), and *ad libitum* fed (grey, n=6) groups. Statistical comparisons are across groups (see Table 4.6). Values are mean ± S.E.M. n.s. $p>0.05$; *** $p<0.001$.

Figure panel	Sample size	Statistical test	Values
D	Food restriction group: 6 *Ad libitum* fed group: 6 Photostimulation (120 min) group: 6	Two-Way RM ANOVA Factor 1: Group (Food restriction, *Ad libitum* fed, Photostimulation) Factor 2: Session Interaction: Group x Session	 $F_{(2,210)}=50.6$, $p<0.001$ $F_{(14,210)}=2.4$, $p=0.004$ $F_{(28,210)}=5.4$, $p<0.001$
		Post hoc multiple comparison with Holm-Sidak corrections Food restriction vs. Photostimulation Food restriction vs. *Ad libitum* fed Photostimulation vs. *Ad libitum* fed	 $p=0.260$ $p<0.001$ $p<0.001$

Table 4.6 Statistical values for Figure 4.11

.
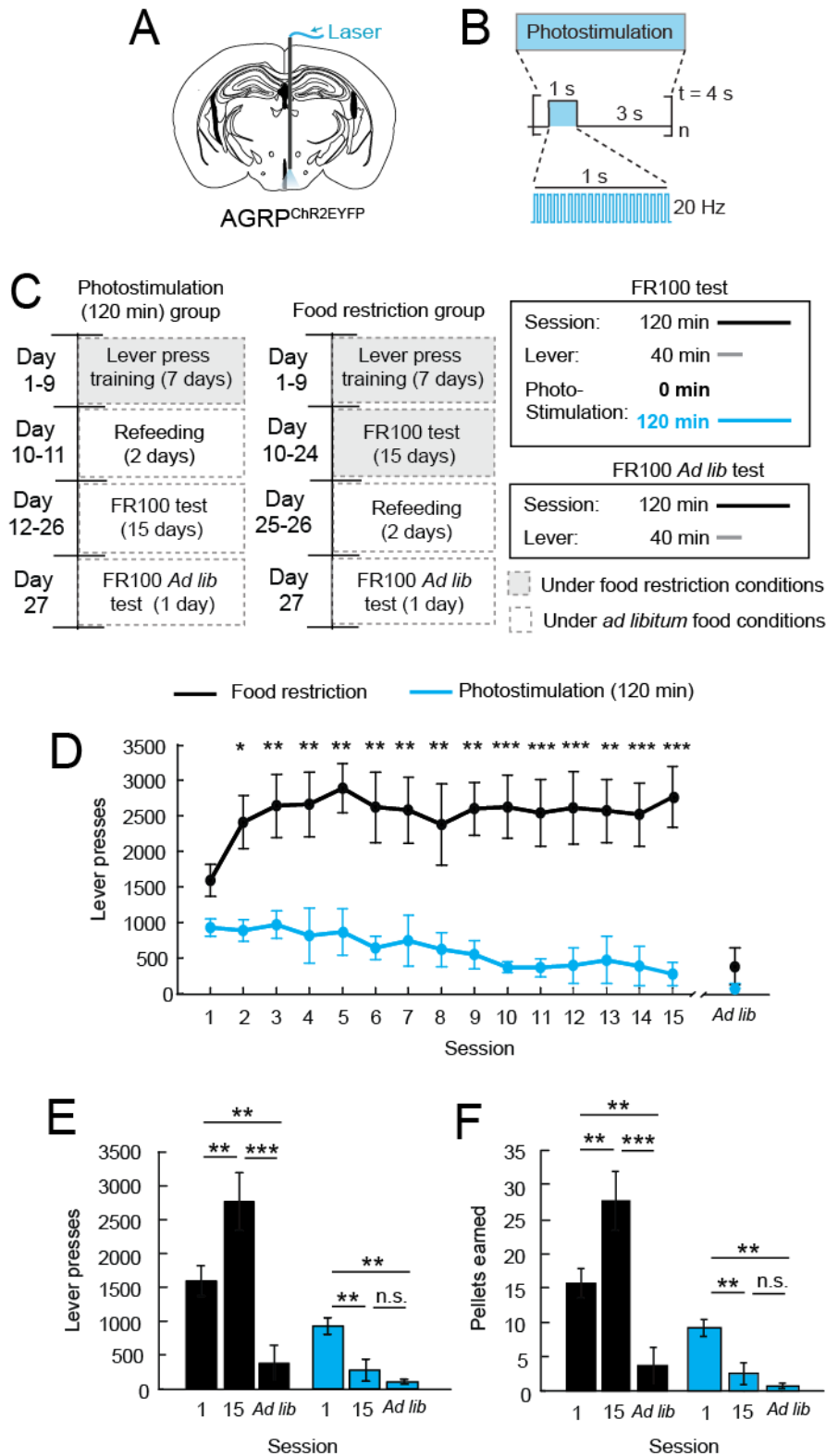
Figure 4.12 Instrumental responding for food under a fixed high cost schedule diminished under disruption of AGRP neuron negative reinforcement signal.
(A) Diagram of fibre placement position in AGRP^{ChR2EYFP} animals for AGRP neuron photoactivation. **(B)** Schematic of photostimulation protocol used. **(C)** Schematic of

experimental design schedule. AGRP^{ChR2EYFP} mice were trained in energy deficit to lever press with an FR100 reinforcement schedule for food pellets. FR100 reinforcement testing was performed over 15 sessions (FR100 test) on two groups: food restriction (black) and *ad libitum* fed AGRP neuron photostimulation (120 min) (cyan). After the 15th test session, a no photostimulation *ad libitum* fed session (FR100 *Ad lib* test) was performed for all groups. During test sessions (120 min for all groups), levers were available for the first 40 minutes. Food restriction group did not receive photostimulation. The AGRP neuron photostimulation (120 min) group received intracranial light pulses for the entire 120-min session. All tests were conducted during the light period. **(D)** Lever presses in each session during FR100 test for food restriction (black, n=7) and ad *libitum* fed AGRP neuron photostimulation (120 min) (cyan, n = 6) groups. Statistical comparisons are across groups for each session (see Table 4.7). **(E, F)** (E) Lever presses and (F) pellets earned from first (1), last (15) and a no photostimulation, *ad libitum* fed (*Ad lib*) FR100 test sessions for food restriction (black) and AGRP neuron photostimulation (120 min) (cyan) groups. Statistical comparisons are within groups (see Table 4.7). Values are mean ± S.E.M. n.s. p>0.05; * p<0.05; ** p<0.01; *** p<0.001.

| Figure panel	Sample size	Statistical test	Values
D	Food restriction group: 7 Photostimulation (120 min) group: 6	Two-Way RM ANOVA Factor 1: Group (Food restriction, Photostimulation) Factor 2: Session Interaction: Group x Session	$F(1,154)=16.4$, $p=0.002$ $F(14,154)=1.7$, $p=0.65$ $F(14,154)=3.2$, $p<0.001$
		Post hoc multiple comparison with Holm-Sidak corrections Session 2 Session 3 Session 4 Session 5 Session 6 Session 7 Session 8 Session 9 Session 10 Session 11 Session 12 Session 13 Session 14 Session 15	 $p=0.011$ $p=0.006$ $p=0.003$ $p=0.001$ $p=0.002$ $p=0.003$ $p=0.004$ $p=0.001$ $p<0.001$ $p<0.001$ $p<0.001$ $p=0.001$ $p<0.001$ $p<0.001$
E	Food restriction group: 7	One-Way RM ANOVA	$F(2,12)=31.0$, $p<0.001$
		Post hoc multiple comparison with Holm-Sidak corrections Session 1 vs. Session 15 Session 1 vs. *Ad lib* Session Session 15 vs. *Ad lib* Session	 $p=0.002$ $p=0.004$ $p<0.001$
	Photostimulation (120 min) group: 6	One-Way RM ANOVA	$F(2,10)=12.8$, $p=0.002$
		Post hoc multiple comparison with Holm-Sidak corrections Session 1 vs. Session 15 Session 1 vs. *Ad lib* Session Session 15 vs. *Ad lib* Session	 $p=0.007$ $p=0.002$ $p=0.357$

Table 4.7 Statistical values for Figure 4.12. *Table continued on next page*

Figure panel	Sample size	Statistical test	Values
F	Food restriction group: 7	One-Way RM ANOVA	$F_{(2,12)}=31.5$, $p<0.001$
		Post hoc multiple comparison with Holm-Sidak corrections	
		Session 1 vs. Session 15	$p=0.004$
		Session 1 vs. *Ad lib* Session	$p=0.002$
		Session 15 vs. *Ad lib* Session	$p<0.001$
	Photostimulation (120 min) group: 6	One-Way RM ANOVA	$F_{(2,10)}=13.5$, $p=0.001$
		Post hoc multiple comparison with Holm-Sidak corrections	
		Session 1 vs. Session 15	$p=0.006$
		Session 1 vs. *Ad lib* Session	$p=0.002$
		Session 15 vs. *Ad lib* Session	$p=0.313$

Table 4.7 continued

4.3.6 Disruption of AGRP neuron negative reinforcement signal alone is insufficient to direct behaviour under global state of energy deficit

PR7 and FR100 schedule studies indicate that disruption of AGRP neuron mediated negative reinforcement teaching signal in the absence of other homeostatic signals can disrupt the previously learned contingency between learned actions that lead to nutrient ingestion and the reduction of AGRP neuron activity induced negative internal state. In order to determine the sufficiency of AGRP neuron mediated negative reinforcement signal in action selection under homeostatic hunger states, I tested whether maintaining elevated AGRP neuron activity under food deprivation is sufficient to reduce lever pressing under an FR100 schedule. Animals previously tested on the FR100 schedule study described above were retrained to lever press under food restriction. Following this training, animals were maintained on food restriction and tested on an FR100 schedule using the same protocol as before. One group was tested without photostimulation (food restriction group, n=7), and the second received photostimulation through the entire session (120 min, photostimulation group, n=6, Figure 4.13A-C). Throughout the experiment, lever pressing was not diminished for either group (two-way RM ANOVA, n= 7 food restriction, 6 photostimulation, group $F_{(1,154)}=2.058$ p=0.179, session $F_{(14, 154)}=1.956$ p=0.025, interaction: group x session $F_{(14,154)}=1.730$ p=0.055; Figure 4.13D, Table 4.8), and lever presses and pellets earned did not change between the first (session 1) and last session (session 15) of testing for either group (post hoc multiple comparisons with Holm-Sidak correction, food restricted group: n=7, lever presses: session 1 vs. session 15 p=0.632, pellets earned: session 1 vs. session 15 p=0.603; photostimulation group: n=6, lever presses: session 1 vs. session 15 p=0.722, pellets earned: session 1 vs. session 15 p=0.743; Figure 4.13E-F, Table 4.8). This indicates that under global states of energy deficit, other hunger circuits and systems are capable of maintaining reinforced behaviours despite maintenance of elevated AGRP neuron activity.
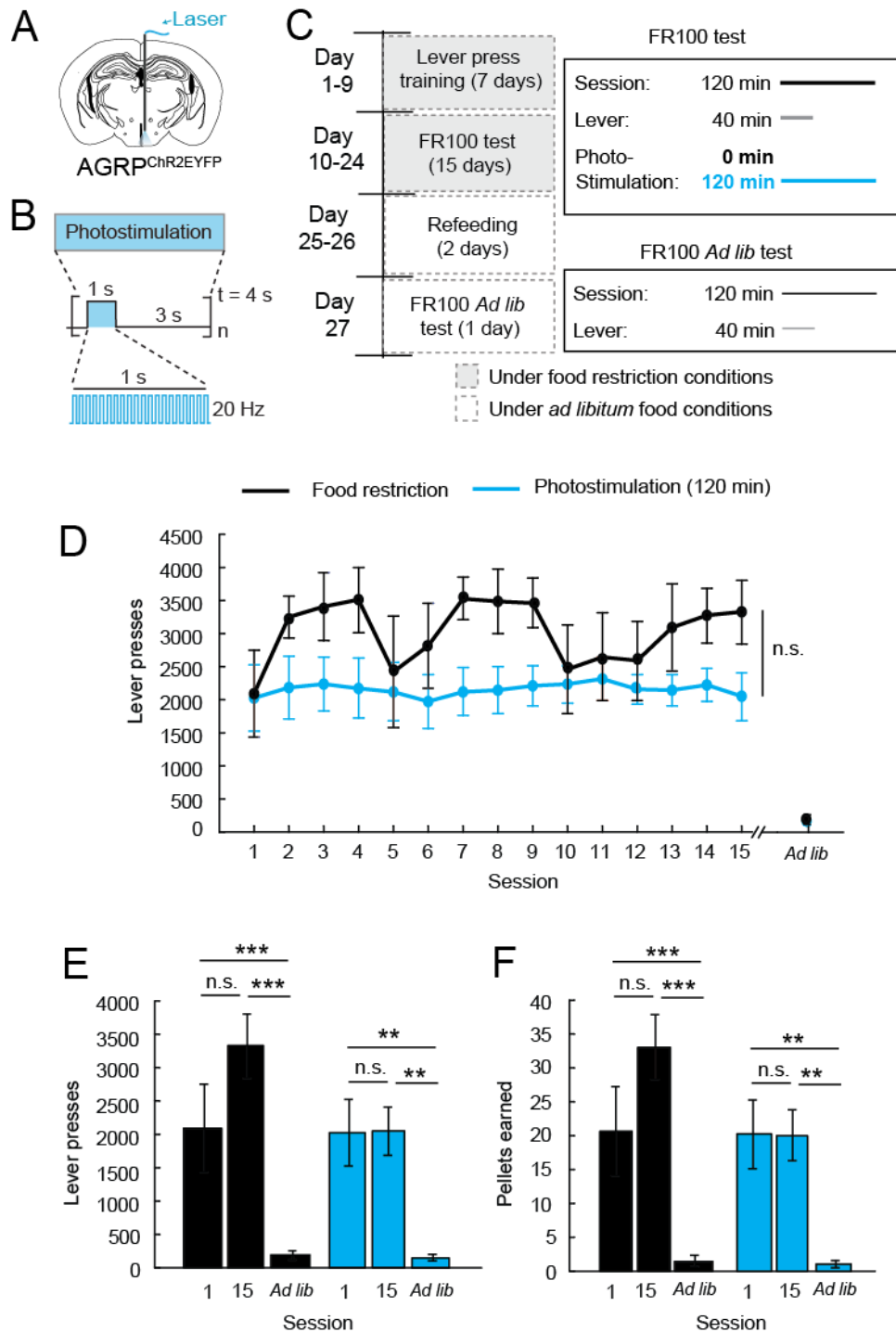
Figure 4.13 AGRP neuron negative reinforcement disruption does not diminish instrumental food seeking under food deprivation. (A) Diagram of fibre placement position in AGRP^{ChR2EYFP} animals for AGRP neuron photoactivation. **(B)** Schematic of photostimulation protocol used. **(C)** Schematic of experimental design schedule. AGRP^{ChR2EYFP} mice were trained in energy deficit to lever press with an

FR100 reinforcement schedule for food pellets. FR100 reinforcement testing was performed over 15 sessions (FR100 test) on two groups: food restriction (black) and food restriction with AGRP neuron photostimulation (120 min) (cyan) groups. After the 15th test session, a no photostimulation *ad libitum* fed session (FR100 *Ad lib* test) was performed for all groups. During test sessions (120 min for all groups), levers were available for the first 40 minutes. Food restriction group did not receive photostimulation. The AGRP neuron photostimulation (120 min) group received intracranial light pulses for the entire 120-min session. All tests were conducted during the light period. **(D)** Lever presses in each session during FR100 test for food restriction (black, n = 7) and ad *libitum* fed AGRP neuron photostimulation (120 min) (cyan, n = 6) groups. Statistical comparisons are between groups (see Table 4.8). **(E, F)** (E) Lever presses and (F) pellets earned from first (1), last (15) and a no photostimulation, *ad libitum* fed (*Ad lib*) FR100 test sessions for food restriction (black) and AGRP neuron photostimulation (120 min) (cyan) groups. Statistical comparisons are within groups (see Table 4.8). Values are mean ± S.E.M. n.s. $p > 0.05$; * $p < 0.05$; ** $p < 0.01$; *** $p < 0.001$.

| Figure panel	Sample size	Statistical test	Values
D	Food restriction group: 7 Photostimulation (120 min) group: 6	Two-Way RM ANOVA Factor 1: Group (Food restriction vs. Photo-stimulation (120 min)) Factor 2: Session Interaction: Group x Session	 $F(1, 154)=2.1, p=0.179$ $F(14,154)=2.0, p=0.025$ $F(14,154)=1.7, p=0.055$
E	Food restriction group: 7	One-Way RM ANOVA	$F(2,12)=37.0, p<0.001$
		Post hoc multiple comparison with Holm-Sidak corrections Session 1 vs. Session 15 Session 1 vs. *Ad lib* Session Session 15 vs. *Ad lib* Session	 $p=0.632$ $p<0.001$ $p<0.001$
	Photostimulation (120 min) group: 6	One-Way RM ANOVA	$F(2,10)=14.4, p=0.001$
		Post hoc multiple comparison with Holm-Sidak corrections Session 1 vs. Session 15 Session 1 vs. *Ad lib* Session Session 15 vs. *Ad lib* Session	 $p=0.722$ $p=0.002$ $p=0.002$
F	Food restriction group: 7	One-Way RM ANOVA	$F(2,12)=38.8, p<0.001$
		Post hoc multiple comparison with Holm-Sidak corrections Session 1 vs. Session 15 Session 1 vs. *Ad lib* Session Session 15 vs. *Ad lib* Session	 $p=0.603$ $p<0.001$ $p<0.001$
	Photostimulation (120 min) group: 6	One-Way RM ANOVA	$F(2,10)=14.4, p=0.001$
		Post hoc multiple comparison With Holm-Sidak corrections Session 1 vs. Session 15 Session 1 vs. *Ad lib* Session Session 15 vs. *Ad lib* Session	 $p=0.743$ $p=0.002$ $p=0.002$

Table 4.8 Statistical values for Figure 4.13

4.4 Discussion

Need states such as hunger are capable of modulating behaviour in order to ensure an organism's survival. However, uncovering the underlying motivational processes of physiological needs has been challenging due to the broad range of neural circuits that are engaged in the process (Gao & Horvath 2007). Given AGRP neuron's role in feeding regulation (Aponte et al. 2011, Krashes et al. 2011, Luquet et al. 2005), they are expected to induce some of the motivational characteristic of deprivation-induced hunger (Sternson et al. 2013). Therefore, understanding the mechanisms in which AGRP neuron circuits mediate food related behaviours can provide insights into the reinforcement mechanisms engaged in homeostatic hunger to direct behaviour. Here, I set out to further investigate the reinforcement mechanism employed by AGRP neurons to direct feeding behaviour using an array of behavioural techniques in combination with optogenetic stimulation of AGRP neurons.

4.4.1 AGRP neurons engage a negative reinforcement teaching signal to direct behaviour

The studies presented here, along with recent studies by Betley et al. (2014), show that negative reinforcement contributes substantially to the motivational effects of AGRP neurons in the modulation of feeding behaviour. Elevated AGRP neuron activity leads to an aversive internal state which is avoided, while suppression of AGRP neuron activity is reinforcing and can direct food consumption choices. A negative reinforcement mechanism also suggests an explanation for how simple activity patterns imposed on AGRP neurons can selectively evoke complex food seeking and consumption responses. AGRP neurons have extensive physiological and visceral effects (Krashes et al. 2011, Luquet et al. 2005), and animals can use such homeostatic deficit states as discriminative internal cues to select actions appropriate to satisfy the deficit (Davidson 1987, Webb 1955). An internal state with negative valence motivates action by driving the animal to explore possibilities to exit the state (Hull 1943) and imposing a cost on not acting or on performing actions that do not lead to nutrient ingestion. Consistent with this, disruption of AGRP neuron

negative reinforcement gradually reduced previously reinforced food seeking actions, indicating that negative reinforcement appears to dominate over any potential direct influence AGRP neurons may have on positive reinforcement. In this framework, starvation-sensitive AGRP neurons condition animals to prefer places and flavours and to perform actions that lead to nutrient ingestion because these are outcomes that naturally suppress circulating starvation signals. Therefore, homeostatic AGRP neurons transmit a relatively simple motivational output, and their respective visceral consequences could lead to a central representation of the specific need, with the complexity of the corresponding food-seeking behaviours determined by previously learned responses that minimize homeostatic negative reinforcement signals.

4.4.2 Positive and negative reinforcement in homeostatic feeding

Positive reinforcement processes must also play a role in the regulation of action selection in feeding behaviour, as elevated AGRP neuron activity alone in states of food restriction was unable to disrupt the contingency between learned actions and outcomes. Positive reinforcement processes in hunger are likely mediated through coordinated activity across multiple systems, including other homeostatic neuron circuits and hormones such as ghrelin, leptin, and insulin. Moreover, the motivational effects from manipulations of AGRP neuron activity are different from related perturbations in the lateral hypothalamus that also lead to avid food consumption but exhibit rewarding properties (Jennings et al. 2013, Olds & Milner 1954). This may reflect mechanistic differences between homeostatic and hedonic motivation for food, which are primarily distinguished by appetite for nutritive food arising from a need state or highly palatable food consumed even in the absence of a need, respectively (Saper et al. 2002). Although the motivational mechanisms underlying homeostatic need states such as hunger have been a longstanding area of investigation (Berridge 2004, Bindra 1976, Dickinson 2002, Freud 2001, Hull 1943), the ability to isolate a negative reinforcement process for hunger is based on recent methods that allow for manipulation of neuronal activity in specific homeostatic neurons. This suggests a model where physiological need states lead to elevated activity of specialized need-sensitive neurons such as AGRP, which signal negative valence about the internal state, thereby biasing an animal

towards actions that diminish their activity and imposing a cost on actions that do not. Energy deficit can also regulate behaviour through enhancement of outcomes associated with the deficit, such as nutrient ingestion, and cues associated with such outcomes under positive reinforcement. Therefore, under homeostatic hunger, negative and positive reinforcement processes are expected to operate in a concerted manner by controlling state-driven and incentive-driven responding, respectively (Figure 4.14).
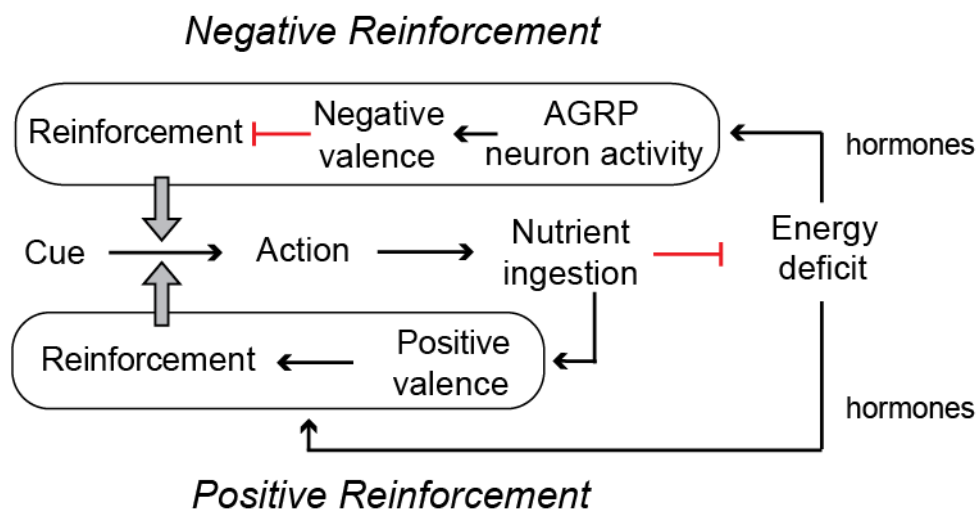
Figure 4.14 Homeostatic control of feeding behaviour through concerted negative and positive reinforcement mechanisms. Energy deficit states act through both negative and positive reinforcement processes to direct feeding behaviour. Energy deficit, through hormonal signals, increases activity in specialized homeostatic cells, such as AGRP neurons, that signal negative valence. The relationship between internal or environmental cues and actions that reduce energy deficit and homeostatic neuron activity is strengthened while the relationship is weakened if the negative internal state persists. Concurrently, cues and actions that lead to intrinsically reinforcing outcomes, such as nutrient ingestion, are also reinforced through positive reinforcement mechanisms. Through hormonal signals, energy deficit modulates positive reinforcement by enhancing the positive valence of outcomes associated with food consumption.

4.4.3 Circuits mediating negative valence of AGRP neuron activity

Because of limited prior evidence for the participation of homeostatic neurons in negative reinforcement, the circuits that mediate the negative valence of AGRP neuron activity are not yet known. Dopamine (DA) neurons have been intensively examined for behavioural modulation during positive reinforcement. However there is substantial evidence that DA neurons also participate in aversive learning and motivation (Bromberg-Martin et al. 2010, King et al. 2009, McCutcheon et al. 2012, Salamone et al. 2009, Volman et al. 2013). A number of brain regions can mediate reward and aversion by increasing or decreasing ventral tegmental (VTA) or substantia nigra compacta (SNc) DA neuron activity, respectively. Other manipulations such as activating VTA^{GABA} neurons or excitatory lateral habenula neurons suppress DA neuron activity and are also aversive (Stamatakis & Stuber 2012, van Zessen et al. 2012). Therefore, suppression of DA neurons may participate in this negative reinforcement process. In my studies, disruption of AGRP neuron-mediated negative reinforcement gradually reduced previously reinforced food-seeking actions in an analogous fashion to food restricted animals lever pressing for non-nutritive rewards, or with neuroleptic administration, both of which are correlated with reduced DA receptor signalling (Beeler et al. 2012b, Wise 1974). In addition, this disruption most prominently affected high effort, but not low effort, food-seeking nor *ad libitum* food consumption, indicating this negative reinforcement influences cost/benefit analysis of action-outcome contingencies, an important factor in the reinforcement process to direct behaviour (Salamone et al. 2009, Salamone et al. 1997). The DA system has also been widely implicated in playing a role in cost/benefit analysis in appetitive behaviours, as interference with DA transmission can modulate effort-related choice behaviour (Beeler et al. 2010, Beeler et al. 2012a, Salamone et al. 2009, Salamone et al. 1994), and tonic DA is believed to convey information about costs and benefits in instrumental tasks (Ostlund et al. 2011).

Recently, negative reinforcement has been demonstrated in rodents for approach to cues associated with alleviation of pain by analgesia (King et al. 2009), which requires neurons in the VTA and is associated with DA neuron activation (Navratilova et al. 2012). In addition, withdrawal symptoms associated with drug addiction have been proposed to negatively reinforce drug-seeking behaviours (Koob 2013). Withdrawal is suggested to operate as an opponent process to positive

reinforcement that is based, in part, on suppression of DA neuron function, and relapse to drug consumption provides concomitant relief from the aversive feelings of lowered DA signalling in the nucleus accumbens (NAc) (Koob & Le Moal 1997). This DA deficiency theory (Figlewicz 2003, Kenny 2011) has also been proposed as an explanation for the development of food addiction (Randolph 1956, Smith & Robbins 2013). Interestingly, manipulations that reduce DA neuron activity or neurotransmission and lead to aversion also reduce consumption of palatable sucrose solutions, which differs from behavioural profile associated with AGRP neuron activation (Stamatakis & Stuber 2012, van Zessen et al. 2012). In addition, these manipulations lead to extremely rapid aversive learning, while avoidance responses from AGRP neuron activation are prominent but considerably less acute, suggesting potential differences in the mechanisms with previously described avoidance responses. Regulation of other systems, such as the serotonergic system, has also been proposed to contribute to negative reinforcement learning (Cools et al. 2011, Dayan & Huys 2009).

Reinforcement learning, whether through positive or negative reinforcement, also requires the ability of an animal to form associations between cues, actions and outcomes. Several areas in the brain have been implicated in the control of reinforcement learning through their involvement in the acquisition of Pavlovian and instrumental conditioning. The basolateral amygdala (BLA) and orbitofrontal cortex seems to be required for the monitoring of current value of reward under Pavlovian conditioning or instrumental choice behaviour respectively (Cardinal et al. 2002). The NAc influences instrumental conditioning by allowing a Pavlovian conditioned cue to affect the level of instrumental responding. The prelimbic cortex is required for learning of action-outcome contingencies (Cardinal et al. 2002). Consequently, AGRP neuron mediated negative reinforcement may engage these areas of the brain for the selection of actions to direct food consumption. Direct anatomical interactions of AGRP neurons with downstream brain areas show limited connectivity with these reinforcement circuits (Betley et al. 2013, Haskell-Luevano et al. 1999). However, AGRP neurons may interact with these areas through secondary nodes. For example, AGRP neurons project prominently to the LHA (Betley et al. 2013), which in turn innervates the VTA and NAc (Hahn & Swanson 2010). AGRP neurons also project to the CEA, which is highly interconnected with the BLA (Dong et al.

2001). Further studies manipulating the projections nodes of AGRP neurons can provide insights into the downstream brain regions and circuits important in mediating this AGRP neuron negative reinforcement signal.

4.5 Conclusions

Hunger is a powerful modulator of behaviour, but understanding the underlying reinforcement mechanisms engaged during states of energy deficit have been challenging. In these studies, I demonstrated that AGRP neurons use a negative reinforcement teaching signal to direct food seeking action selection and food consumption choices. In addition, disruption of this teaching signal also led to the disruption of formerly learned contingencies between actions and outcomes in relation to food consumption. Furthermore, high effort motivated behavioural responding is most sensitive to this disruption. Together, these studies show a prior unrecognized role for negative reinforcement in the regulation of behaviour under homeostatic hunger states.

Publication arising from data from this chapter:

Betley JN*, **Huang Cao ZF***, Gong R, Magnus CJ, Sternson SM (2014) Homeostatic neurons for hunger and thirst transmit a negative reinforcement teaching signal. *In review.* **(*equal contribution)**

Chapter 5

Parallel and Redundant Functional

Organization of AGRP Neurons

5.1 Introduction

The control of feeding behaviour requires the coordination of flexible goal-directed actions in order to ensure an organism's survival. Because states of energy deficit can direct and modulate behaviour towards food consumption (Berridge 2004, Bindra 1976, Hodos 1961), homeostatic neuron circuits and the reinforcement processes they employ can play a crucial role in the control of action selection (Sternson 2013). Therefore, relationships between the structural organization and function of these circuits can provide a critical framework for understanding how the brain controls feeding.

5.1.1 Unravelling the circuits underlying the control of feeding behaviour

A classic view of behaviours essential for survival, such as feeding behaviour, is that their circuits are organized hierarchically, with a behaviour control node that can elicit complex behaviour using divergent projections to multiple brain regions that coordinate discrete motor patterns (Swanson 2000, Tinbergen 1989). Consistent with the prediction of dedicated circuit components, complex behaviours such as feeding can be evoked selectively by exogenous activation or inhibition of discrete brain regions and cell-types within these regions (Delgado & Anand 1953, Jennings et al. 2013). In a seminal study, Delgado and Anand (1953) demonstrated that electrical stimulation of the lateral hypothalamus resulted in increased food consumption. In addition, a wide range of neurons have been implicated to play a role in the modulation of feeding behaviour (Gao & Horvath 2007). Therefore, the brain regions and neurons that elicit feeding can serve as entry points to reveal the underlying neural circuits that control this behaviour (Sternson et al. 2013).

Extensive anatomical analysis, using axon-tracing techniques, indicates that brain regions functionally associated with feeding behaviour have extremely diverse projection targets (Chronwall 1985, Eskay et al. 1979, Geerling et al. 2010, Hahn & Swanson 2010, Luiten & Room 1980, Makara & Hodacs 1975, Swanson & Sawchenko 1983), as might be expected for the control of complex, flexible behaviours. Due to this complexity, the classical tools of lesions, pharmacological injections, and electrical stimulation have been too non-specific for comprehensive

neural circuit analysis of the brain regions that have the capability to coordinate these behavioural responses. To overcome many of these limitations, molecular genetics, anatomical, and functional approaches using optogenetic and chemogenetic tools (Betley & Sternson 2011, Shapiro et al. 2012, Yizhar et al. 2011) have been applied to investigate the circuits that elicit feeding behaviour. For example, channelrhodopsin (ChR2)-mediated photoexcitation of axons has been used with agouti-related peptide (AGRP) neuron projections (Atasoy et al. 2012), as well as projections from other cell populations (Cai et al. 2014, Carter et al. 2013, Jennings et al. 2013), to relate anatomically and molecularly defined neural circuit projections to a behavioural response. However, most studies to date have only evaluated the contribution of one or two projection circuits, despite the fact that these neurons display broad axonal arborisation throughout the brain. A more complete picture would involve understanding the functional contribution of separate axon projections to the behavioural response, as well as the anatomical relationship between these diverging circuits.

5.1.2 Understanding the neural circuits underlying AGRP neuron mediated negative reinforcement signal

In the previous chapter, studies that aimed to understand the motivational mechanisms engaged by starvation sensitive signals using manipulations of AGRP neuron activity demonstrated that a negative reinforcement mechanism contributes to the motivational effects of AGRP neuron activity in the regulation of food consumption and flexible food seeking behaviours. Increased AGRP neuron activity elicits a negative affective state. This negative affective state motivates action by pushing an animal to select actions that alleviate the unpleasant state by imposing a cost on not acting or performing actions that do not lead to nutrient ingestion.

The brain circuits that mediate this negative reinforcement teaching signal, and therefore, the negative valence of AGRP neuron activity and the coordination of complex food seeking actions, however, are still poorly understood. Because AGRP neurons project widely throughout the brain (Betley et al. 2013, Haskell-Luevano et al. 1999), the downstream circuit connections of these neurons can provide a

blueprint to identify motivationally important brain regions in the control of feeding behaviour.

5.1.3 AGRP neuron circuit

Activation of AGRP neurons under well-fed conditions lead to voracious feeding (Aponte et al. 2011), but this response is not mediated through the melanocortin system, either by antagonism of melanocortin 4 receptors (MC4R) outside of the arcuate nucleus (ARC) (Aponte et al. 2011) or through intra-ARC inhibitory projections to proopiomelanocortin (POMC) neurons (Atasoy et al. 2012). Examination of two long-range AGRP neuron circuits using optogenetic photoexcitation of $ARC^{AGRP} \rightarrow$ paraventricular nucleus of the hypothalamus (PVH) and $ARC^{AGRP} \rightarrow$ parabrachial nucleus (PBN) axonal projections demonstrated that only activation of $ARC^{AGRP} \rightarrow PVH$ circuit was sufficient to recapitulate the acute evoked feeding behaviour previously observed under AGRP neuron somatic photostimulation (Atasoy et al. 2012). These results indicated that within a specific cell-type population, diverging axonal projection-based circuits can have differential roles in the regulation of behaviour, bringing into question the anatomical organization of homeostatic neurons such as AGRP neurons.

Neuronal projections can have three possible anatomical organization structures: one-to-all, one-to-many, or one-to-one arrangements. In a one-to-all structure, every neuron would project to every target region through extensive axon collateralization. For a one-to-many arrangement, two scenarios can be envisioned. In one, groups of neurons project to a defined subset of target regions with related functions. A second scenario would suggest each neuron projects to several, but not all, target regions stochastically. Functionally, this stochastic one-to-many configuration would be similar to a one-to-all structural arrangement. Alternatively, in a one-to-one model, each projection field is a separate communication channel that originates from a group of neurons that do not send collateral projections to other target regions (Figure 5.1A).

Recent anatomical studies using viral tracing techniques indicate that AGRP neurons employ a one-to-one projection specific anatomical organization, as

opposed to a one-to all, or one-to-many configuration. In these studies, Betley et al. (2013) used an envelope protein (EnvA) pseudotyped and glycoprotein deleted rabies (SADΔG) viral vector modified to express mCherry for cell-type and axon-selective neuron tracing. AGRP neurons were engineered to co-express the EnvA receptor, making them competent for transduction by the SADΔG viral vector through targeted injections into discrete axon projection fields. Axonally transduced AGRP neurons expressed high levels of mCherry in cell bodies as well as axons within rabies virus injected projection field, but other AGRP neuron projection sites showed very low or undetectable levels of mCherry expression, indicating the lack of collateralization of axons to multiple brain regions. These results indicate that AGRP neurons can be further subdivided into projection-specific subpopulations. In addition, it was determined that these projection-specific AGRP neuron subpopulations have wide numerical differences in their representation within this molecularly defined population, and they are distributed topographically in the ARC based on their axon projection targets (Betley et al. 2013) (Figure 5.1B).

This one-to-one anatomical circuit configuration, along with functional studies demonstrating the inability of ARC^{AGRP}→PBN axonal activation to evoke food intake (Atasoy et al. 2012), raise basic questions about the functional importance of AGRP neuron subpopulations and their circuits, in particular, pertaining to their contribution in AGRP neuron-mediated evoked-feeding responses. The prioritization of these subpopulations can, therefore, guide the discovery of downstream brain regions important for the negative reinforcement teaching signal engaged by AGRP neurons to coordinate food seeking and food consumption behaviours.
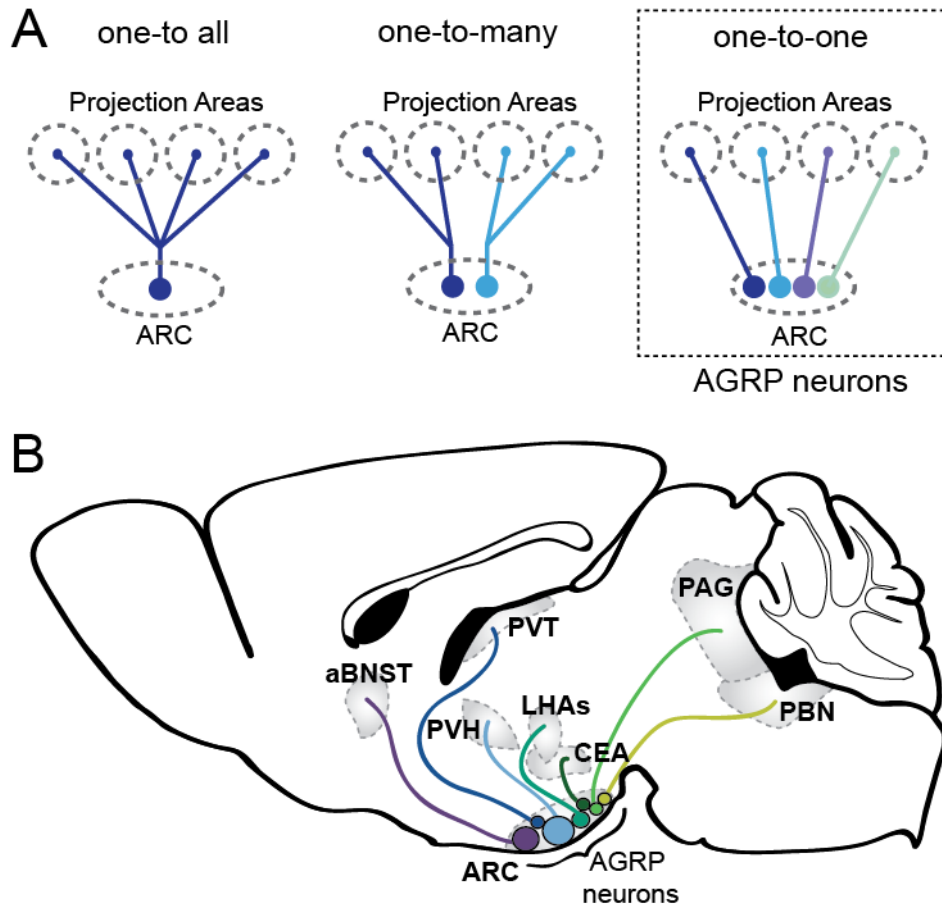
Figure 5.1 One-to-one anatomical circuit configuration of AGRP neurons. (A) Potential configurations for cell-type specific anatomical circuit organization: one-to-all (left), one-to-many (centre), one-to-one (right). AGRP neurons employ a one-to-one anatomical organization. Different shading denotes different hypothetical subpopulations. **(B)** AGRP neurons can be subdivided into distinct projection-specific subpopulations. Distinct AGRP neuron subpopulations are represented by circles and their projections are represented by lines linking circles to projection areas in different colours (trajectory of lines does not necessarily represent actual axonal trajectory). Size of AGRP neuron subpopulations relative to whole AGRP population is represented by size of circles where known (sizes are not proportional). Approximate distribution of AGRP neuron subpopulations along anterior-posterior axis of ARC is represented by position of circles where known. aBNST: anterior subdivisions of the bed nucleus of stria terminalis; PVH: paraventricular nucleus of the hypothalamus; PVT: paraventricular thalamic nucleus; LHAs: suprafornical subdivision of the lateral hypothalamic area; ARC: arcuate nucleus; CEA: central nucleus of the amygdala; PAG: periaqueductal grey; PBN: parabrachial nucleus.

5.1.4 Experimental Aims

The experiments detailed in this chapter aim to determine and prioritize the functional importance of AGRP neuron projection-based subpopulations. Specific aims may be summarized as follows: 1) to determine which AGRP neuron subpopulations contribute to the observed evoked feeding response under AGRP neuron activation; 2) to determine whether feeding insufficient subpopulations may contribute to feeding responses by facilitating and enhancing feeding under conditions that favour food consumption; and 3) to determine whether AGRP neuron subpopulations might be differentially regulated by states and signals of energy deficit.

5.2 Methods specific to the chapter

5.2.1 ChR2 expression and *in vivo* photostimulation

All feeding studies used AGRP[ChR2Tom] animals, where AGRP[Cre] animals received bilateral injections of rAAV2/10-CAG-FLEX-rev-ChR2tdtomato at four sites in the ARC, 125-400 nl at each site (Bregma, anterior/posterior: -1.3 mm, medial/lateral: ±0. 25 mm, dorsal/ventral: -5.85 and -5.95 from dorsal surface of the brain). Large volume injections were performed to increase transgene penetrance. AGRP neuron subpopulation photostimulation was achieved through AGRP neuron axonal photoactivation in target regions. Ferrule capped fibres were implanted at target regions of interest: anterior subdivisions of the bed nucleus of stria terminalis (aBNST), PVH, paraventricular thalamic nucleus (PVT), suprafornical subdivision of the lateral hypothalamic area (LHAs), central nucleus of the amygdala (CEA), and periaqueductal grey (PAG) (see Table 2.5 for coordinates used).

5.2.2 Daytime *ad libitum* food consumption tests

Mice were allowed to acclimate to the behavioural cages overnight before initiating photostimulation protocols and were tested for evoked feeding behaviour during the early light period. During all feeding tests, animals had *ad libitum* access to 20 mg grain pellets and water. Food intake was recorded during a pre-stimulus baseline for 1 hr, followed by a 1 hr AGRP neuron axonal photostimulation period. Latency to feeding was defined as the time when first bout of feeding was initiated after the onset of photostimulation. A bout was defined as the consumption of a minimum of five pellets with inter-pellet-intervals less than 2.4 min (Aponte et al. 2011). Evoked feeding was tested over 2 consecutive days, either unilaterally or bilaterally. All animals were naïve to photostimulation during the first day of testing. Several post-hoc tests were performed in order to determine inclusion of an animal in the final analysis. Fibre transmittance was measured after removal from the brain. For animals that did not show feeding responses, animal with fibres presenting less than 50% fibre transmittance were excluded from analysis. Fibre placement was also

determined. Animals with off target fibre placements were excluded from analysis. Transgene penetrance analysis was also conducted to verify ChR2-tdTomato expression in ARC^{AGRP} neurons.

5.2.3 Early dark period *ad libitum* food consumption tests

Mice were allowed to acclimate to the behavioural cages overnight before initiating tests. During all feeding sessions, animals had *ad libitum* access to 20 mg grain pellets and water. Feeding was recorded during the first hour of the dark period (6-7pm). On the first day of the test, animals were tethered to an optic fibre but no photostimulation was delivered to measure baseline food consumption. On the second day of testing, animals were tethered to an optic fibre and photostimulation was provided but light was prevented from entering the brain by blocking light output at the junction of the optic fibre and implanted ferrule capped fibre. This testing day was termed "mock stimulation", and was conducted as a control for any increase or decrease in feeding due to presence of light alone. Axonal photostimulation was performed on the third day of testing. After these tests, all animals were verified for transgene penetrance, fibre transmittance, and fibre placement to determine inclusion in analysis.

5.2.4 Fos immunoreactivity in AGRP neuron subpopulations

Retrograde dye labelling was performed to label specific projection-based subpopulations of AGRP neurons by injecting a 4% Fluoro-Gold (FG) solution (75 nl, Flourochrome LLC, Denver, CO) in AGRP neurons target regions (aBNST, PVH, PVT, LHAs, CEA, PAG, PBN, see Table 2.5 for coordinates used) in AGRP^{ChR2EYFP} animals, which express membrane-bound ChR2 and fused enhanced yellow fluorescent protein (EYFP) in AGRP neurons. EYFP was used to identify AGRP neurons in the ARC. Six days were allowed for retrograde transport. Brain tissue was collected and processed after 24 hrs of food deprivation or 3 hrs after an i.p. injection of ghrelin (1 mg/kg) and stained for Fos. At least 20 neurons were examined for Fos expression intensity in the same fashion for each projection region tested under food deprivation or ghrelin administration.

5.3 Results

5.3.1 Multiple AGRP neuron subpopulations are capable of independently evoke feeding

To determine the influence of different AGRP neuron projection subpopulations (Betley et al. 2013) in AGRP neuron evoked feeding behaviour, I photoactivated, either unilaterally or bilaterally, prominent axon projections in a total of six target regions of interest in AGRP^ChR2Tom mice and measured their food intake. The regions included intra-hypothalamic (PVH and LHAs) as well as extra-hypothalamic (aBNST, PVT, CEA, PAG) regions across the brain. Immediately after the last test, animals were perfused and brains removed and fixed for Fos expression analysis in ChR2-tdTomato-expressing AGRP neurons and transgene penetrance analysis. Presence of Fos expression indicates that AGRP neuron subpopulations were appropriately activated through axonal photostimulation.

5.3.1.1 Role of intra-hypothalamic projecting AGRP neuron subpopulations in feeding

5.3.1.1.1 ARC ^{AGRP}→PVH circuit

The PVH is known to be an important area for feeding behaviour (Aravich & Sclafani 1983, Balthasar et al. 2005, Krashes et al. 2014, Leibowitz 1978). AGRP neurons project prominently to this area and activation of these projections are known to increase feeding (Atasoy et al. 2012). Here I tested the role of AGRP$_{PVH}$ neurons in evoked feeding as a positive control to my studies (Figure 5.2A-C). Unilateral activation of ARC^{AGRP}→PVH axonal projections showed a significant increase in feeding over pre-stimulation period (paired t-test, n=7, p<0.001; Figure 5.2D-E). On average, animals naïve to photostimulation consumed 0.66 ± 0.06 g of food in 1 hr on the first session of testing. A second session of testing showed similar results (paired t-test, n=6, p=0.003; Figure 5.2E). In addition, latency to the first bout of feeding was within the range of latencies reported for AGRP neuron somatic and

ARC^{AGRP}→PVH axonal photoactivation (Aponte et al. 2011, Atasoy et al. 2012) (Figure 5.2F). ChR2-tdTomato transgene penetrance analysis shows that virus infection was capable of infecting at least 50% of axons in the PVH in all the animals tested, and near maximal feeding response can be achieved at the minimum infection percent of ~50% (Figure 5.2G-I). In addition, significant Fos labelling was observed in ChR2-tdTomato-expressing AGRP neurons across the ARC, indicating appropriate activation by photostimulation (Figure 5.2J-O). Therefore, these results are consistent with prior reports of PVH as an important projection region for AGRP neuron evoked-feeding response (Atasoy et al. 2012).
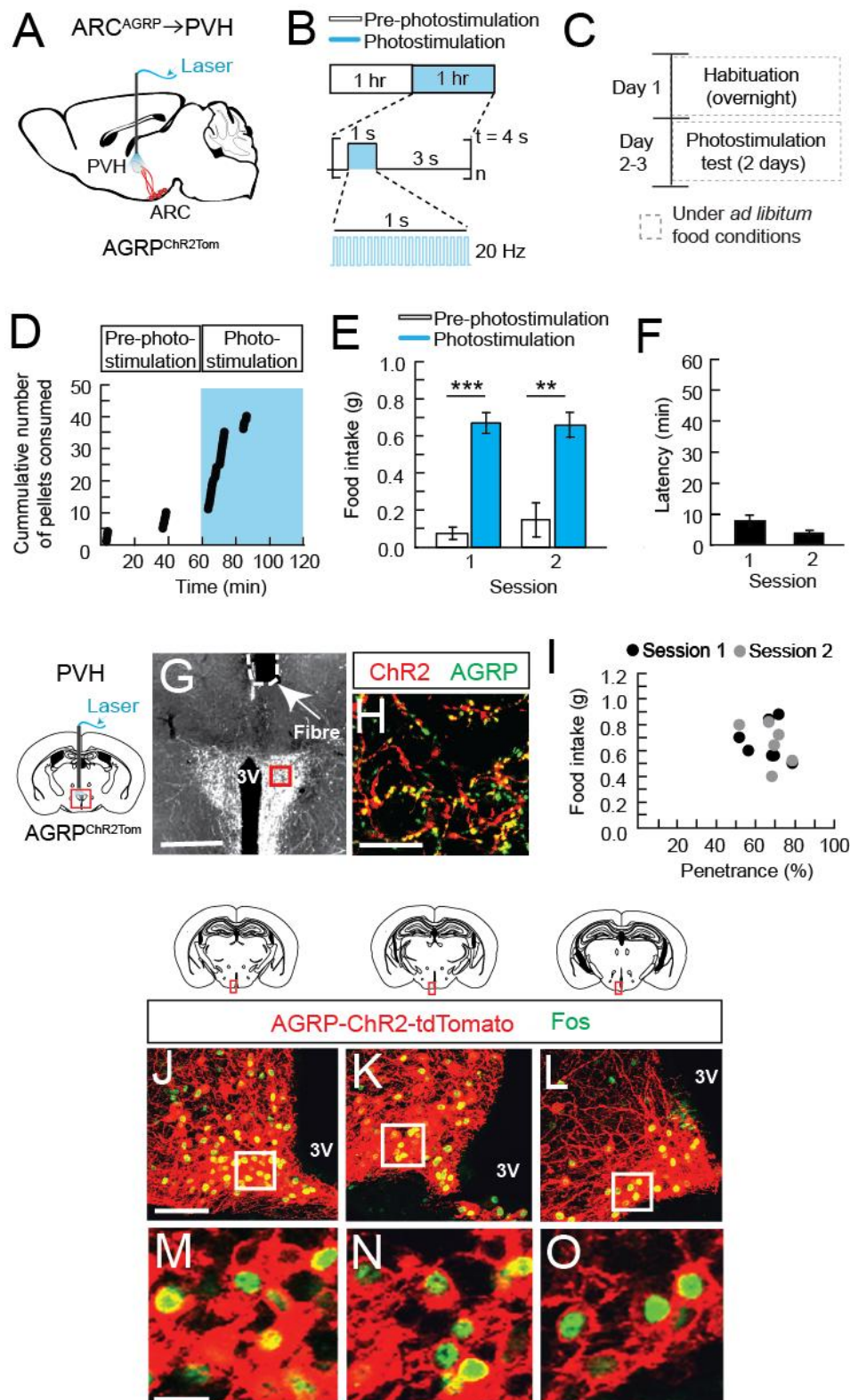
Figure 5.2 Optogenetic activation of ARC^AGRP→PVH neurons evokes food consumption. (A) Diagram of sagittal brain section depicting activation of

ARC$^{AGRP}\rightarrow$PVH circuit in AGRP^{ChR2Tom} animals. **(B)** Schematic of photostimulation test protocol. Food intake was measured for a one hour pre-photostimulation baseline (white) and during one hr ARC$^{AGRP}\rightarrow$PVH axonal photostimulation test (cyan). **(C)** Schematic of experimental design schedule. Animals received one overnight habituation session followed by 2 photostimulation tests conducted in 2 consecutive days. Photostimulation tests were conducted under *ad libitum* fed conditions during the light period. **(D)** Representative example of cumulative number of pellets (20 mg) consumed over time for pre-photostimulation baseline (1 hr, white shading) and ARC$^{AGRP}\rightarrow$PVH axonal photostimulation (1 hr, cyan shading). **(E)** Total food intake during pre-photostimulation baseline (white) and ARC$^{AGRP}\rightarrow$PVH axonal photostimulation (cyan) for each session tested. (n= 7 session 1, 6 session 2, paired t-test for each session). **(F)** Latency to initiate first bout of feeding after photostimulation onset for each session tested. (n= 7 session 1, 6 session 2). **(G)** Diagram and epifluorescence image of optical fibre placement (white dotted line) and ChR2-tdTomato-expressing ARC$^{AGRP}\rightarrow$PVH axon projections. Red box in coronal brain section diagram represents region shown. Scale bar, 500 μm. **(H)** Single plane confocal image showing AGRP (green) and ChR2-tdTomato (red) immunofluorescence containing boutons in the PVH. Red box in (G) shows approximate imaging position for transgene penetrance analysis. Scale bar: 10 μm. **(I)** Food intake as a function of ChR2-tdTomato penetrance for each animal tested in each session (session 1: black, session 2: grey). **(J-L)** Diagrams and confocal images of a z-stack depicting ChR2-tdTomato (membrane-bound, red) and Fos (green) expression in AGRP neurons in (J) anterior, (K) medial, and (L) posterior ARC after one hr of ARC$^{AGRP}\rightarrow$PVH axon projection photostimulation. Red boxes in coronal brain section diagrams represent region shown. Scale bar: 200 μm. **(M-O)** Single plane confocal images of insets of (J-L), respectively, showing Fos (green) expression in ChR2-tdTomato (membrane-bound) expressing AGRP neurons (red). Scale bar 10 μm. Values are mean ± S.E.M. ** $p<0.01$; *** $p<0.001$. ARC: arcuate nucleus; PVH: paraventricular nucleus of the hypothalamus; 3V: third ventricle.

5.3.1.1.2 ARC^{AGRP}→LHAs circuit

The lateral hypothalamic area (LHA) has been widely implicated in having a role in feeding (Anand & Brobeck 1951b, Delgado & Anand 1953, Jennings et al. 2013, Leinninger et al. 2009). AGRP axons project widely across the LHA, with a particularly dense projection to the LHAs. Here, I tested whether this ARC^{AGRP}→LHAs circuit, and therefore, AGRP$_{LHAs}$ neuronal subpopulation, also plays a role in AGRP neuron-evoked feeding (Figure 5.3A-C). As with ARC^{AGRP}→PVH axonal activation, unilateral activation of ARC^{AGRP}→LHAs axon projections during light hours show an increase in feeding over baseline on both sessions tested (paired t-test, n=17, session 1: $p<0.001$, session 2: $p<0.001$; Fig 5.3D-E). Animals consumed, on average, 0.60 ± 0.05 g and 0.60 ± 0.07 g of food in a 1 hr stimulation period on the first and second sessions of testing, respectively. Average latency to initiate first bout was also within AGRP soma stimulation latencies (Figure 5.3F). Transgene penetrance indicates that ChR2-tdTomato was present in between 9.6% and 72.4% of AGRP neuron axons in the LHAs. Even under low penetrance, photostimulation was still capable of evoking a feeding response (Figure 5.3G-I). Abundant Fos expression was also observed in ChR2-tdTomato expressing AGRP neurons in the ARC, indicating that the photostimulation procedure employed was effective at activating ARC^{AGRP}→LHAs axonal projections. Therefore, the AGRP$_{LHAs}$ neuron subpopulation is a second group of AGRP neurons capable of independently evoke feeding.
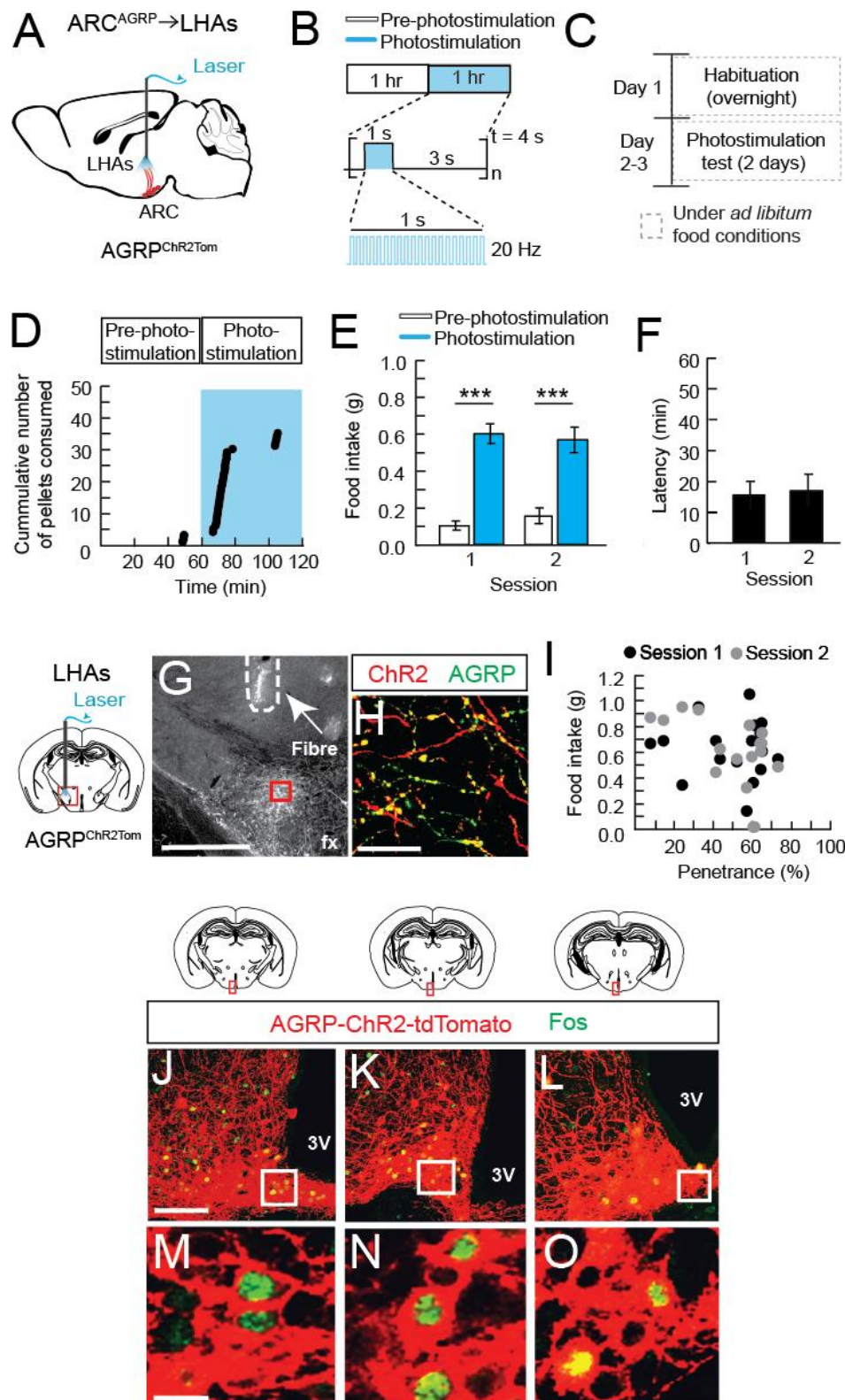
Figure 5.3 ARC^AGRP→LHAs circuit can independently evoke feeding. (A) Diagram of sagittal brain section depicting activation of ARC^AGRP→LHAs circuit in

AGRP^{ChR2Tom} animals. **(B)** Schematic of photostimulation test protocol. Food intake was measured for a one hour pre-photostimulation baseline (white) and during one hr ARC^{AGRP}→LHAs axonal photostimulation test (cyan). **(C)** Schematic of experimental design schedule. Animals received one overnight habituation session followed by 2 photostimulation tests conducted in 2 consecutive days. Photostimulation tests were conducted under *ad libitum* fed conditions during the light period. **(D)** Representative example of cumulative number of pellets (20 mg) consumed over time for pre-photostimulation baseline (1 hr, white shading) and ARC^{AGRP}→LHAs axonal photostimulation (1 hr, cyan shading). **(E)** Total food intake during pre-photostimulation baseline (white) and ARC^{AGRP}→LHAs axonal photostimulation (cyan) for each session tested. (n= 17 per session, paired t-test for each session). **(F)** Latency to initiate first bout of feeding after photostimulation onset for each session tested. (n= 17 per session). **(G)** Diagram and epifluorescence image of optical fibre placement (white dotted line) and ChR2-tdTomato-expressing ARC^{AGRP}→LHAs axon projections. Red box in coronal brain section diagram represents region shown. Scale bar, 500 μm. **(H)** Single plane confocal image showing AGRP (green) and ChR2-tdTomato (red) immunofluorescence containing boutons in the LHAs. Red box in (G) shows approximate imaging position for transgene penetrance analysis. Scale bar: 10 μm. **(I)** Food intake as a function of ChR2-tdTomato penetrance for each animal tested in each session (session 1: black, session 2: grey). **(J-L)** Diagrams and confocal images of a z-stack depicting ChR2-tdTomato (membrane-bound, red) and Fos (green) expression in AGRP neurons in (J) anterior, (K) medial, and (L) posterior ARC after one hr of ARC^{AGRP}→LHAs axon projection photostimulation. Red boxes in coronal brain section diagrams represent region shown. Scale bar: 200 μm. **(M-O)** Single plane confocal images of insets of (J-L), respectively, showing Fos (green) expression in ChR2-tdTomato (membrane-bound) expressing AGRP neurons (red). Scale bar 10 μm. Values are mean ± S.E.M. *** p<0.001. ARC: arcuate nucleus; LHAs: suprafornical subdivision of the lateral hypothalamic area; fx: fornix; 3V: third ventricle.

5.3.1.2 Role of extra-hypothalamic projecting AGRP neuron subpopulations in feeding

5.3.1.2.1 ARC^{AGRP}→aBNST circuit

The bed nucleus of stria terminalis (BNST) is part of the extended amygdala and receives significant projections from AGRP neurons across the anterior portion of the structure (aBNST). The BNST is most known to be involved in the regulation of stress and anxiety (Casada & Dafny 1991, Choi et al. 2008, Davis et al. 1997, Walker et al. 2003), though a recent study has shown that activation of BNST γ-aminobutyric acid (GABA) neuron projections to the LHA increases food consumption (Jennings et al. 2013), indicating that the BNST can play a role in feeding behaviour. Here I tested whether activation AGRP$_{aBNST}$ neurons can elicit feeding (Figure 5.4A-C). Unilateral stimulation of ARC^{AGRP}→aBNST axons in the aBNST showed significant increase in feeding (paired t test, n=15 session 1, 14 session 2, session 1 p<0.001, session 2 p 0.001; Figure 5.4D-E), with animals consuming 0.57 ± 0.06 g of food in 1 hr on the first tested session, when animals were naïve to photostimulation, and 0.62 ± 0.04 g of feeding on a second session. Again, latencies to first bout of feeding were on average within range of AGRP soma photostimulation latencies (Figure 5.4F). ChR2-tdTomato penetrance analysis indicates that even at low penetrance, photostimulation was able to induce elevated food consumption (Figure 5.4G-I). Fos immunoreactivity also indicated appropriate activation was achieved (Figure 5.4J-O). These data further supports the role of the BNST in the control of feeding behaviour.

Figure 5.4 Activation of ARC^AGRP→aBNST circuit is sufficient to coordinate food consumption. (A) Diagram of sagittal brain section depicting activation of
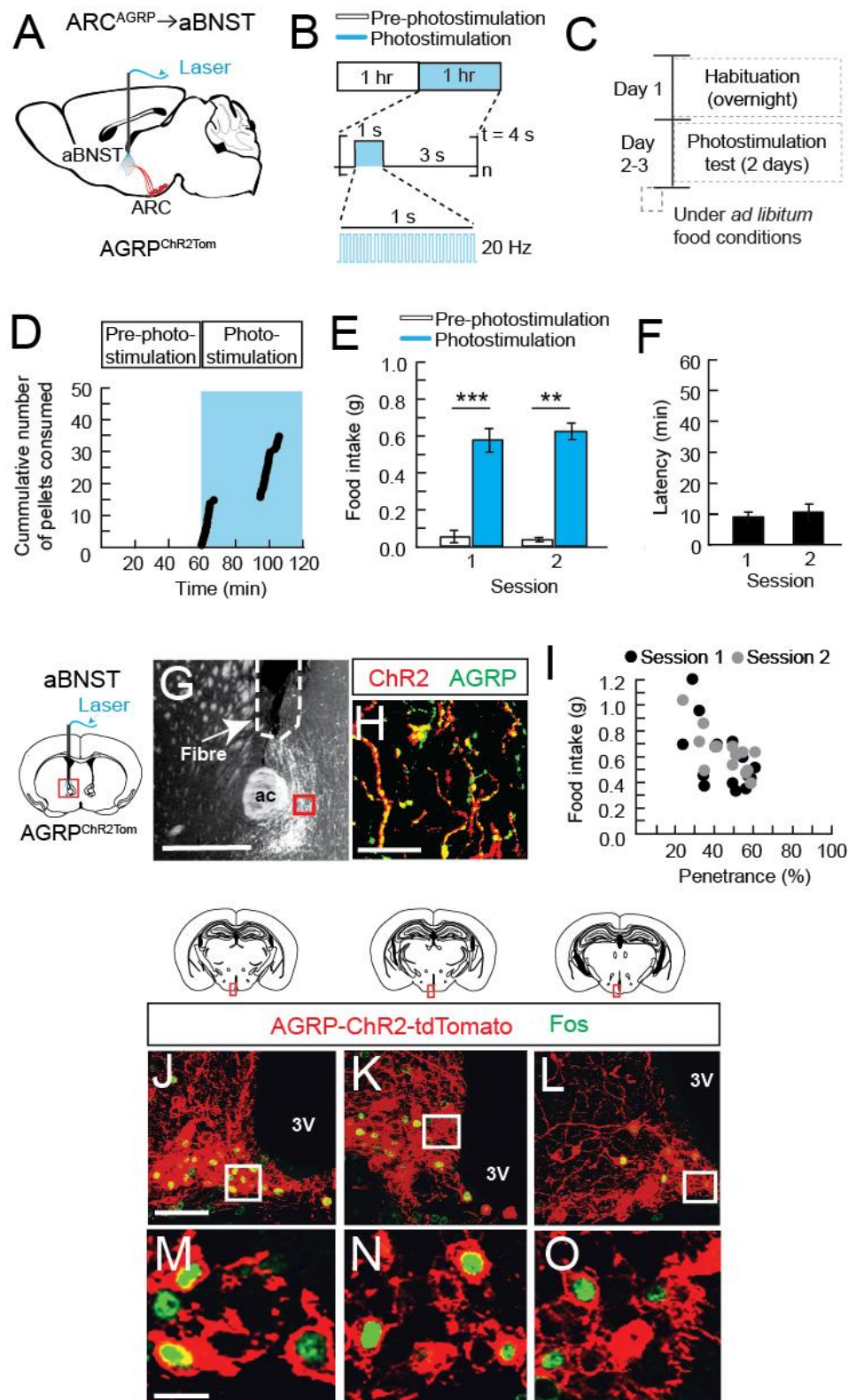
ARC^{AGRP}→aBNST circuit in AGRP^{ChR2Tom} animals. **(B)** Schematic of photostimulation test protocol. Food intake was measured for a one hour pre-photostimulation baseline (white) and during one hr ARC^{AGRP}→aBNST axonal photostimulation test (cyan). **(C)** Schematic of experimental design schedule. Animals received one overnight habituation session followed by 2 photostimulation tests conducted in 2 consecutive days. Photostimulation tests were conducted under *ad libitum* fed conditions during the light period. **(D)** Representative example of cumulative number of pellets (20 mg) consumed over time for pre-photostimulation baseline (1 hr, white shading) and ARC^{AGRP}→aBNST axonal photostimulation (1 hr, cyan shading). **(E)** Total food intake during pre-photostimulation baseline (white) and ARC^{AGRP}→aBNST axonal photostimulation (cyan) for each session tested. (n= 15 session 1, n= 14 session 2, paired t-test for each session). **(F)** Latency to initiate first bout of feeding after photostimulation onset for each session tested. (n= 15 session 1, n= 14 session 2). **(G)** Diagram and epifluorescence image of optical fibre placement (white dotted line) and ChR2-tdTomato-expressing ARC^{AGRP}→aBNST axon projections. Red box in coronal brain section diagram represents region shown. Scale bar, 500 µm. **(H)** Single plane confocal image showing AGRP (green) and ChR2-tdTomato (red) immunofluorescence containing boutons in the aBNST. Red box in (G) shows approximate imaging position for transgene penetrance analysis. Scale bar: 10 µm. **(I)** Food intake as a function of ChR2-tdTomato penetrance for each animal tested in each session (session 1: black, session 2: grey). **(J-L)** Diagrams and confocal images of a z-stack depicting ChR2-tdTomato (membrane-bound, red) and Fos (green) expression in AGRP neurons in (J) anterior, (K) medial, and (L) posterior ARC after one hr of ARC^{AGRP}→aBNST axon projection photostimulation. Red boxes in coronal brain section diagrams represent region shown. Scale bar: 200 µm. **(M-O)** Single plane confocal images of insets of (J-L), respectively, showing Fos (green) expression in ChR2-tdTomato (membrane-bound) expressing AGRP neurons (red). Scale bar 10 µm. Values are mean ± S.E.M. ** p<0.01; *** p<0.001. ARC: arcuate nucleus; aBNST: anterior subdivisions of the bed nucleus of stria terminalis; ac: anterior commissure; 3V: third ventricle.

5.3.1.2.2 ARC$^{AGRP}\rightarrow$PVT circuit

AGRP neurons also send projections throughout the PVT. The PVT has been previously shown to play a role in feeding as GABA-A receptor agonist microinjections into this area are reported to increase food consumption (Stratford & Wirtshafter 2013). Therefore, here, I investigated whether activation of ARC$^{AGRP}\rightarrow$PVT circuit would result in elevated food consumption (Figure 5.5A-C). Photostimulation of ARC$^{AGRP}\rightarrow$PVT projections in the posterior PVT significantly increase food consumption over 2 consecutive tests (paired t test, n=16, session 1 $p<0.001$, session 2 $p=0.001$; Figure 5.5D-E), with an average of 0.21 ± 0.04 g and 0.3 ± 0.05 g consumed on the first and second sessions of testing, respectively. Mean response latencies appear to be longer than for somatic stimulation, which is on average ~6 min (Aponte et al. 2011) (Figure 5.5F). In addition, transgene penetrance analysis indicates that despite high levels of infection (>50%), food consumption response observed was lower than those observed for PVH, LHAs and aBNST (Figure 5.5G-I). Although less prominent than under activation of ARC$^{AGRP}\rightarrow$PVH, ARC$^{AGRP}\rightarrow$LHAs, and ARC$^{AGRP}\rightarrow$aBNST axonal stimulation, Fos immunoreactivity was observed in ChR2-tdTomato-expressing AGRP neurons in the ARC, indicating that photostimulation was effective (Figure 5.5J-O). The lower number of observed Fos expressing AGRP neurons is not surprising, as anatomical studies indicate that AGRP$_{PVT}$ neuron subpopulation is smaller than AGRP$_{PVH}$ and AGRP$_{aBNST}$ subpopulations (Betley et al. 2013). Therefore, AGRP$_{PVT}$ neurons also contribute to AGRP neuron-mediated evoked feeding response, although the profile of the observed effect is not equivalent to that of other feeding-sufficient AGRP neuron subpopulations tested.
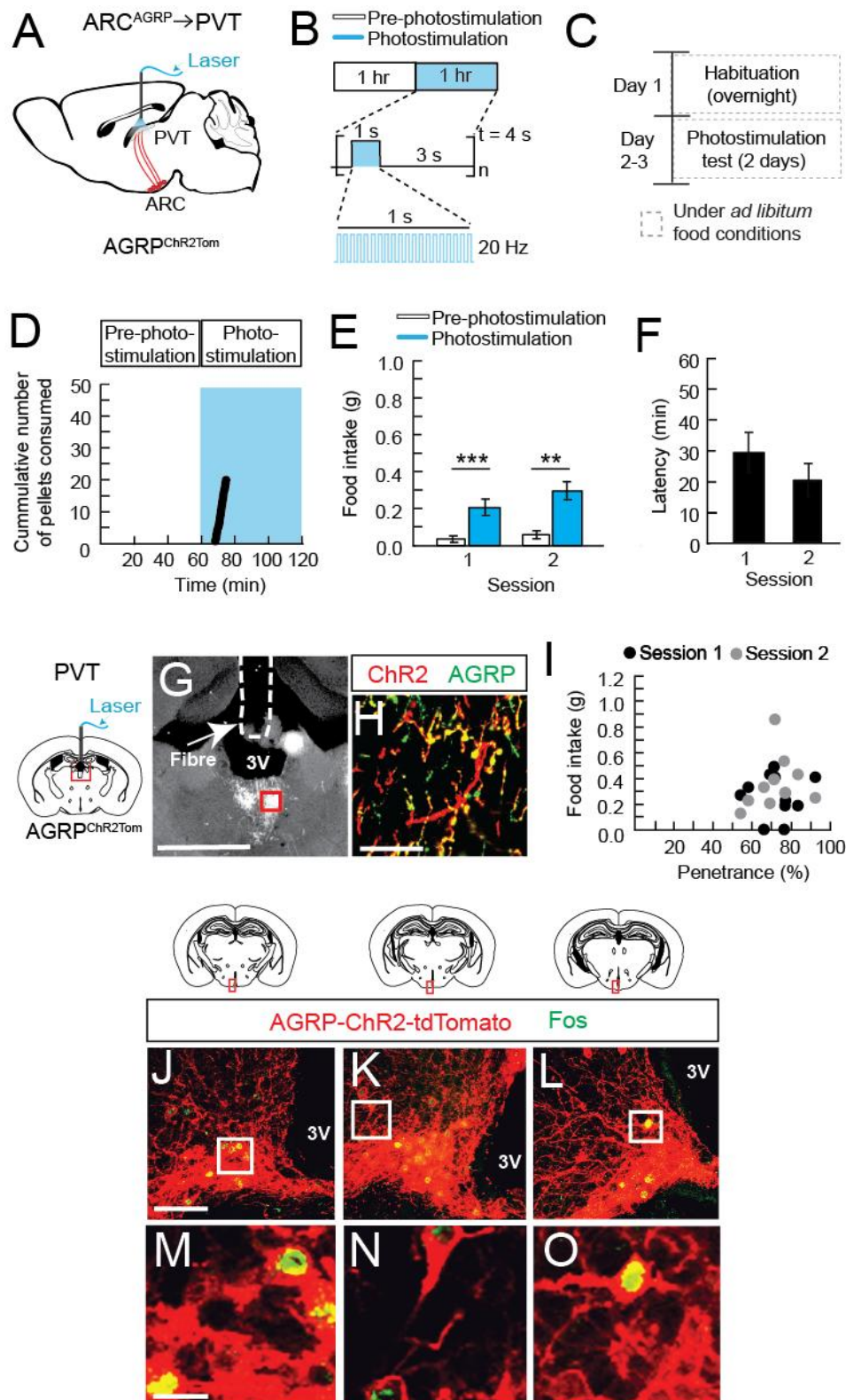
Figure 5.5 ARC^{AGRP}→PVT circuit is involved in the control of feeding behaviour. (A) Diagram of sagittal brain section depicting activation of

ARC^{AGRP}→PVT circuit in AGRP^{ChR2Tom} animals. **(B)** Schematic of photostimulation test protocol. Food intake was measured for a one hour pre-photostimulation baseline (white) and during one hr ARC^{AGRP}→PVT axonal photostimulation test (cyan). **(C)** Schematic of experimental design schedule. Animals received one overnight habituation session followed by 2 photostimulation tests conducted in 2 consecutive days. Photostimulation tests were conducted under *ad libitum* fed conditions during the light period. **(D)** Representative example of cumulative number of pellets (20 mg) consumed over time for pre-photostimulation baseline (1 hr, white shading) and ARC^{AGRP} PVT axonal photostimulation (1 hr, cyan shading). **(E)** Total food intake during pre-photostimulation baseline (white) and ARC^{AGRP}→PVT axonal photostimulation (cyan) for each session tested. (n= 16 per session, paired t-test for each session). **(F)** Latency to initiate first bout of feeding after photostimulation onset for each session tested. (n= 16 per session). **(G)** Diagram and epifluorescence image of optical fibre placement (white dotted line) and ChR2-tdTomato-expressing ARC^{AGRP}→PVT axon projections. Red box in coronal brain section diagram represents region shown. Scale bar, 500 μm. **(H)** Single plane confocal image showing AGRP (green) and membrane-bound ChR2-tdTomato (red) immunofluorescence containing boutons in the PVT. Red box in (G) shows approximate imaging position for transgene penetrance analysis. Scale bar: 10 μm. **(I)** Food intake as a function of ChR2-tdTomato penetrance for each animal tested in each session (session 1: black, session 2: grey). **(J-L)** Diagrams and confocal images of a z-stack depicting membrane-bound ChR2-tdTomato (red) and Fos (green) expression in AGRP neurons in (J) anterior, (K) medial, and (L) posterior ARC after one hr of ARC^{AGRP}→PVT axon projection photostimulation. Red boxes in coronal brain section diagrams represent region shown. Scale bar: 200 μm. **(M-O)** Single plane confocal images of insets of (J-L), respectively, showing Fos (green) expression in membrane bound ChR2-tdTomato expressing AGRP neurons (red). Scale bar 10 μm. Values are mean ± S.E.M. ** p<0.01; *** p<0.001. ARC: arcuate nucleus; PVT: paraventricular thalamic nucleus; 3V: third ventricle.

5.3.1.2.3 ARC^{AGRP}→CEA circuit

The amygdala has been implicated in having a role in the control of feeding by aversive learned cues (Petrovich et al. 2009). In particular, reduction of food consumption in the presence of an aversive learned cue was abolished in animals with CEA lesions (Petrovich et al. 2009). AGRP neuron projections to the amygdala are directed to the CEA. Here, I performed unilateral and bilateral activation of ARC^{AGRP}→CEA projections to evaluate their role in AGRP neuron evoked feeding (Figure 5.6A-C). Unilateral activation of CEA in photostimulation naïve animals (session 1) did not increase feeding significantly over pre-photostimulation periods (paired t-test, n=12, p=0.295; Figure 5.6D-E). Bilateral stimulation was conducted on the second session of testing, also showing no significant increase in feeding (paired t-test, n=12, p=0.0691; Figure 5.6E). In addition, feeding latencies were on average 44.06 ± 6.53 min and 38.01 ± 6.81 min under unilateral and bilateral photostimulation, respectively, indicating that any feeding observed is unlikely due to photostimulation (Figure 5.6F). Despite lack of evoked feeding response, transgene penetrance and FOS immunoreactivity analysis indicates high virus transduction levels (on average 61.81 ±4.55 %; Figure 5.6G-I) and presence of Fos expression in ChR2-tdTomato positive AGRP neurons in the ARC (Figure 5.6J-O). These results indicate that AGRP$_{CEA}$ neurons are not capable of independently evoke feeding under these testing conditions.
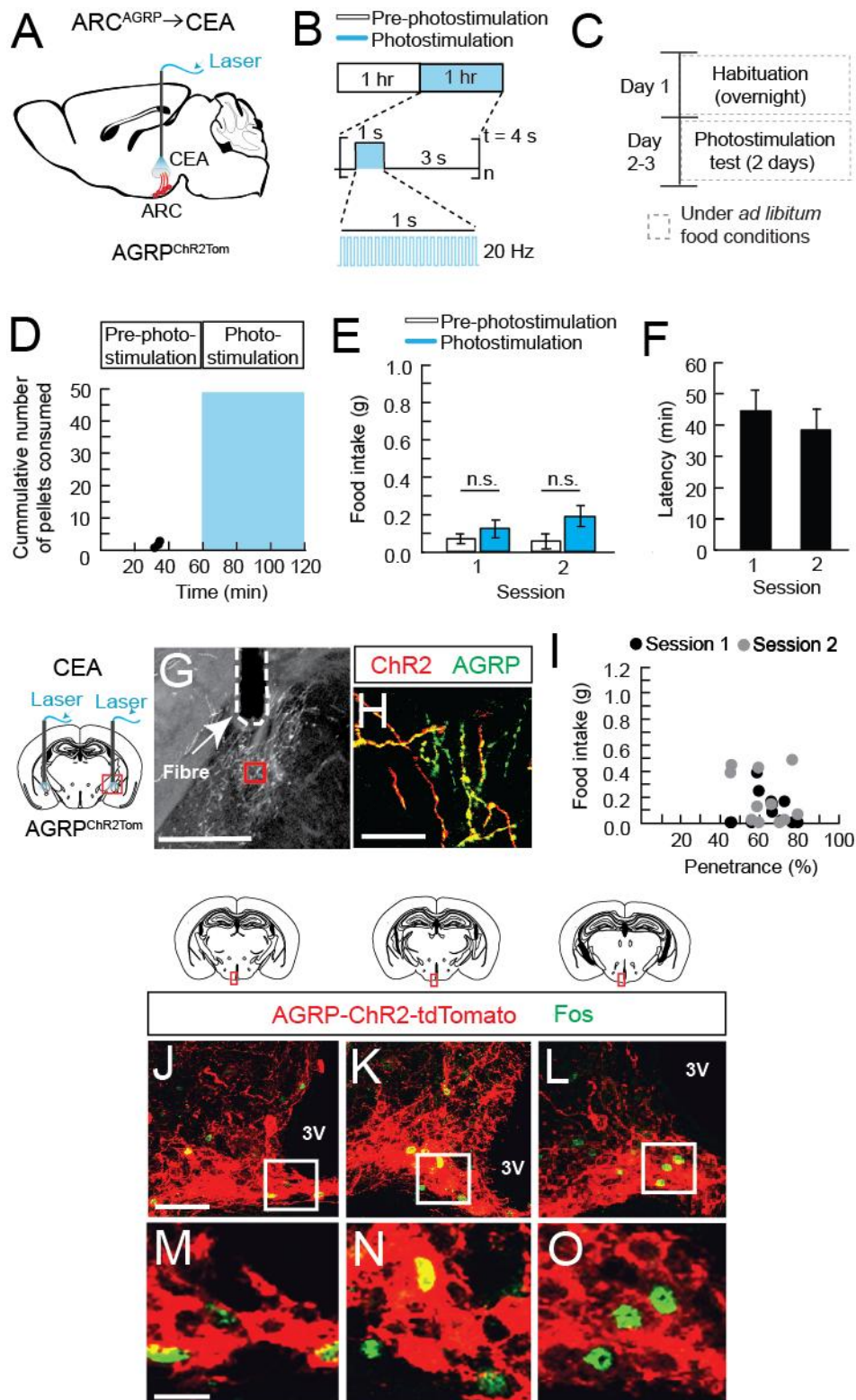
Figure 5.6 Elevated activity of ARC^AGRP→CEA circuit does not result in evoked feeding behaviour. (A) Diagram of sagittal brain section depicting activation of

ARC^{AGRP}→CEA circuit in AGRP^{ChR2Tom} animals. **(B)** Schematic of photostimulation test protocol. Food intake was measured for a one hour pre-photostimulation baseline (white) and during one hr ARC^{AGRP}→CEA axonal photostimulation test (cyan). **(C)** Schematic of experimental design schedule. Animals received one overnight habituation session followed by 2 photostimulation tests conducted in 2 consecutive days. Photostimulation tests were conducted under *ad libitum* fed conditions during the light period. **(D)** Representative example of cumulative number of pellets (20 mg) consumed over time for pre-photostimulation baseline (1 hr, white shading) and ARC^{AGRP}→CEA axonal photostimulation (1 hr, cyan shading). **(E)** Total food intake during pre-photostimulation baseline (white) and ARC^{AGRP}→CEA axonal photostimulation (cyan) for each session tested. (n= 12 per session, paired t-test for each session). **(F)** Latency to initiate first bout of feeding after photostimulation onset for each session tested. (n= 12 per session). **(G)** Diagram and epifluorescence image of optical fibre placement (white dotted line) and ChR2-tdTomato-expressing ARC^{AGRP}→CEA axon projections. Red box in coronal brain section diagram represents region shown. Scale bar, 500 µm. **(H)** Single plane confocal image showing AGRP (green) and ChR2-tdTomato (red) immunofluorescence containing boutons in the CEA. Red box in (G) shows approximate imaging position for transgene penetrance analysis. Scale bar: 10 µm. **(I)** Food intake as a function of ChR2-tdTomato penetrance for each animal tested in each session (session 1: black, session 2: grey). **(J-L)** Diagrams and confocal images of a z-stack depicting ChR2-tdTomato (membrane-bound, red) and Fos (green) expression in AGRP neurons in (J) anterior, (K) medial, and (L) posterior ARC after one hr of ARC^{AGRP}→CEA axon projection photostimulation. Red boxes in coronal brain section diagrams represent region shown. Scale bar: 200 µm. **(M-O)** Single plane confocal images of insets of (J-L), respectively, showing Fos (green) expression in ChR2-tdTomato (membrane-bound) expressing AGRP neurons (red). Scale bar 10 µm. Values are mean ± S.E.M. n.s. p>0.05. ARC: arcuate nucleus; CEA: central nucleus of the amygdala; 3V: third ventricle.

5.3.1.2.4 ARC^{AGRP}→PAG circuit

The PAG, a hindbrain structure mostly known for its function in the regulation of sympathetic systems (Johnson et al. 2004, Skultety 1958), has been indirectly associated with feeding. Anatomical studies of PAG inputs and outputs suggest this area may be involved in modulating motivation to hunt and forage (Comoli et al. 2003, Mota-Ortiz et al. 2012). In addition, morphine injections in the PAG blunt LHA electrical stimulation induced feeding (Jenck et al. 1986). AGRP neurons send dense projections to the ventromedial and ventrolateral portions of the PAG, with the densest projections observed in caudal regions. Photostimulation of AGRP$_{PAG}$ through activation of ARC^{AGRP}→PAG axons in the PAG did not show a significant increase in feeding over the pre-stimulation period on two consecutive sessions of testing (paired t test, n=18, session 1 p=0.341, session 2 p=0.256; Figure 5.7A-E). In addition, latencies were on average 43.29 ± 5.12 min and 46.44 ± 4.38 min each session of testing respectively, similar to those observed with ARC^{AGRP}→CEA activation (Figure 5.7F). Post-hoc immunohistological analysis also indicates that transgene penetrance were high (on average 65.14 ± 2.53 %; Figure 5.7G-I), and Fos expression was observed in AGRP ChR2-tdTomato positive neurons (Figure 5.7J-O), indicating lack of feeding is not due to improper manipulations. As with ARC^{AGRP}→CEA circuit activation, these results indicate that AGRP$_{PAG}$ neurons are also not sufficient to independently evoke feeding under the conditions tested.
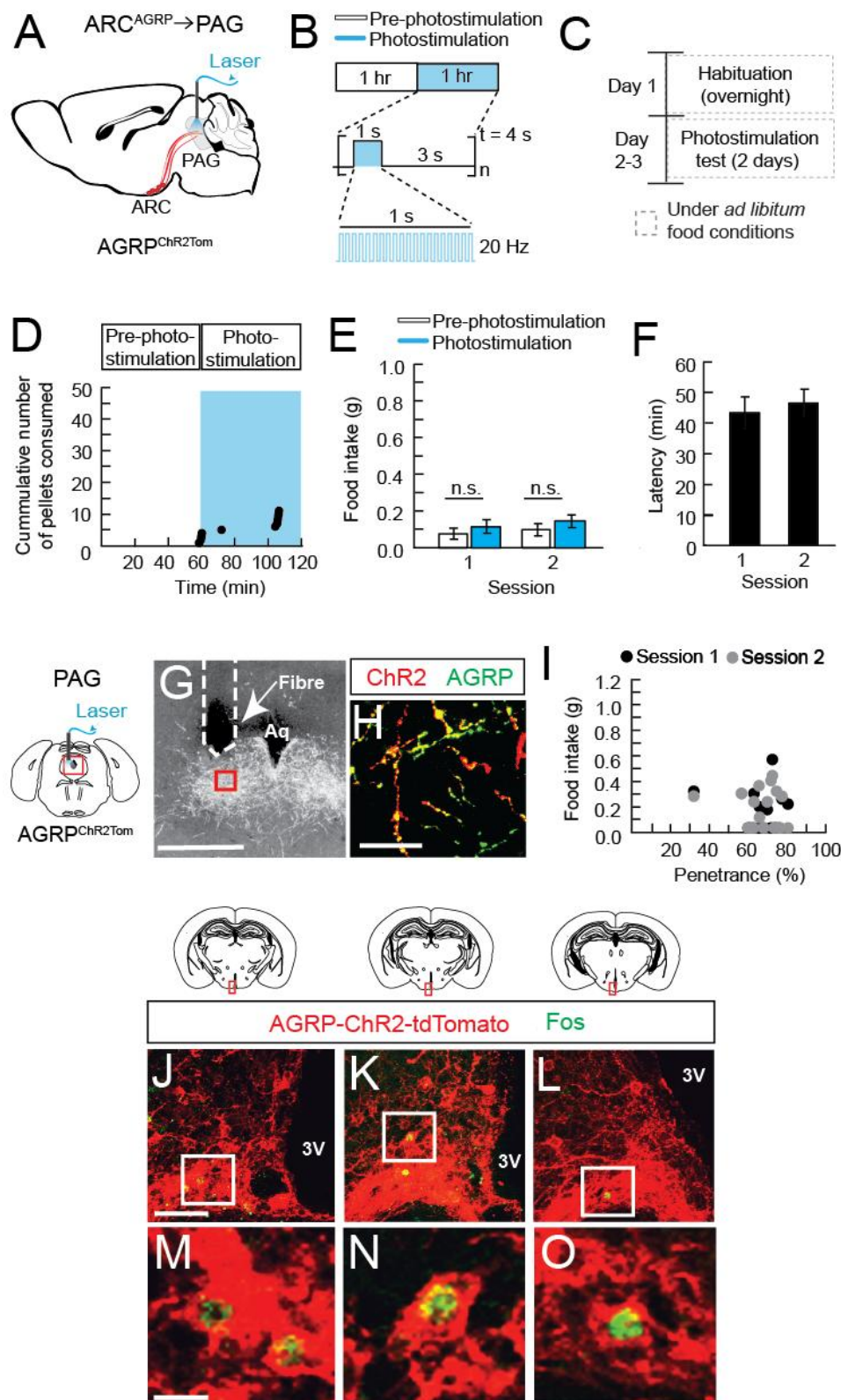
Figure 5.7 AGRP neuron evoked food consumption is not mediated by ARC^AGRP→PAG circuit. (A) Diagram of sagittal brain section depicting activation of

ARC^{AGRP}→PAG circuit in AGRP^{ChR2Tom} animals. **(B)** Schematic of photostimulation test protocol. Food intake was measured for a one hour pre-photostimulation baseline (white) and during one hr ARC^{AGRP}→PAG axonal photostimulation test (cyan). **(C)** Schematic of experimental design schedule. Animals received one overnight habituation session followed by 2 photostimulation tests conducted in 2 consecutive days. Photostimulation tests were conducted under *ad libitum* fed conditions during the light period. **(D)** Representative example of cumulative number of pellets (20 mg) consumed over time for pre- photostimulation baseline (1 hr, white shading) and ARC^{AGRP}→PAG axonal photostimulation (1 hr, cyan shading). **(E)** Total food intake during pre-photostimulation baseline (white) and ARC^{AGRP}→PAG axonal photostimulation (cyan) for each session tested. (n= 18 per session, paired t-test for each session). **(F)** Latency to initiate first bout of feeding after photostimulation onset for each session tested. (n= 18 per session). **(G)** Diagram and epifluorescence image of optical fibre placement (white dotted line) and ChR2-tdTomato-expressing ARC^{AGRP}→PAG axon projections. Red box in coronal brain section diagram represents region shown. Scale bar, 500 μm. **(H)** Single plane confocal image showing AGRP (green) and ChR2-tdTomato (red) immunofluorescence containing boutons in the PAG. Red box in (G) shows approximate imaging position for transgene penetrance analysis. Scale bar: 10 μm. **(I)** Food intake as a function of ChR2-tdTomato penetrance for each animal tested in each session (session 1: black, session 2: grey). **(J-L)** Diagrams and confocal images of a z-stack depicting ChR2-tdTomato (membrane-bound, red) and Fos (green) expression in AGRP neurons in (J) anterior, (K) medial, and (L) posterior ARC after one hr of ARC^{AGRP}→PAG axon projection photostimulation . Red boxes in coronal brain section diagrams represent region shown. Scale bar: 200 μm. **(M-O)** Single plane confocal images of insets of (J-L), respectively, showing Fos (green) expression in ChR2-tdTomato (membrane-bound) expressing AGRP neurons (red). Scale bar 10 μm. Values are mean ± S.E.M. n.s. p>0.05. ARC: arcuate nucleus; PAG: periaqueductal grey; Aq: aqueduct; 3V: third ventricle.

5.3.1.3 Verification of specificity of evoked feeding behaviour through activation of ARC^{AGRP}→LHAs and ARC^{AGRP}→aBNST axon projections

Although photostimulation offers cell type specific control of axonal activation, both the aBNST and LHAs are nearby regions containing AGRP axon projections, and light scattering could potentially result in activation of these neighbouring axons. The aBNST projections lie in close proximity of AGRP axons in the medial preoptic area and sparse lateral septum projections. For the LHAs, photostimulation could also activate projections in the dorsomedial nucleus of the hypothalamus (DMH). To address this possibility and improve spatial specificity for axon activation, I titrated light intensity to the threshold for ChR2 activation—50% activated at 1 mW/mm^2 (Lin et al. 2009)—in the vicinity of the projection field (calculated for distal portion of the target region), based on a theoretical model of light absorption and scattering in neural tissue (Aravanis et al. 2007) (Figure 5.8A-D, F). For ARC^{AGRP}→LHAs, irradiances at the target region larger than 1 mW/mm^2 significantly elevated feeding over pre-stimulation periods, while light power intensities below this level did not (paired t-tests, n=6, 0.4 mW/mm^2 p=0.856 ; 1.0 mW/mm^2 p=0.151; 1.9 mW/mm^2 p=0.033; 3.8 mW/mm^2 p=0.027; Figure 3.8E, Table 5.1). For ARC^{AGRP}→aBNST, irradiance at the target region of 0.5 mw/mm^2 and higher resulted in increased food intake (paired t-tests, n=6, 0.5 mW/mm^2 p=0.001; 1.1 mW/mm^2 p=0.012; 2.5 mW/mm^2 p<0.001; 5.0 mW/mm^2 p=0.008; Figure 5.8G, Table 5.1). The ability of lower irradiances increasing food intake in aBNST vs. LHAs may be due to the difference in density of fibres in the two areas, or might indicate increased sensitivity to feeding under activation in aBNST. These experiments further substantiate my findings indicating that activation of AGRP axons projecting to LHAs and aBNST are sufficient to evoke feeding.

Although PVT projections targeted lie directly above the PVH projections, calculations using the theoretical model of light scattering (Aravanis et al. 2007) indicate that at light powers used (between 10 mW and 15 mW), irradiance levels in the PVH are below ChR2 activation threshold (~0.3 mW/mm^2 at the most dorsal portion of the PVH, dorsal surface 4.5 mm). Thus, feeding responses observed by ARC^{AGRP}→PVT axonal activation are unlikely to be the result of potential activation of PVH projecting axons, and light intensity titration studies were not performed. AGRP projections to the PVH are also located near other brain regions with dense

AGRP neuron projections, such as the DMH. However, experiments on excitation of AGRP axonal projections in the PVH were performed primarily as a positive control for the experimental procedures used in these studies, as a prior study using the same experimental procedure demonstrated that excitation of these axons evokes feeding (Atasoy et al. 2012). Given that this prior study demonstrated that inhibition of post-synaptic PVH neurons recapitulates the behavioural response observed with $ARC^{AGRP} \rightarrow PVH$ axonal activation (Atasoy et al. 2012), therefore validating the role $ARC^{AGRP} \rightarrow PVH$ circuit in AGRP neuron-mediated evoked feeding, light intensity titration studies were not performed here either.
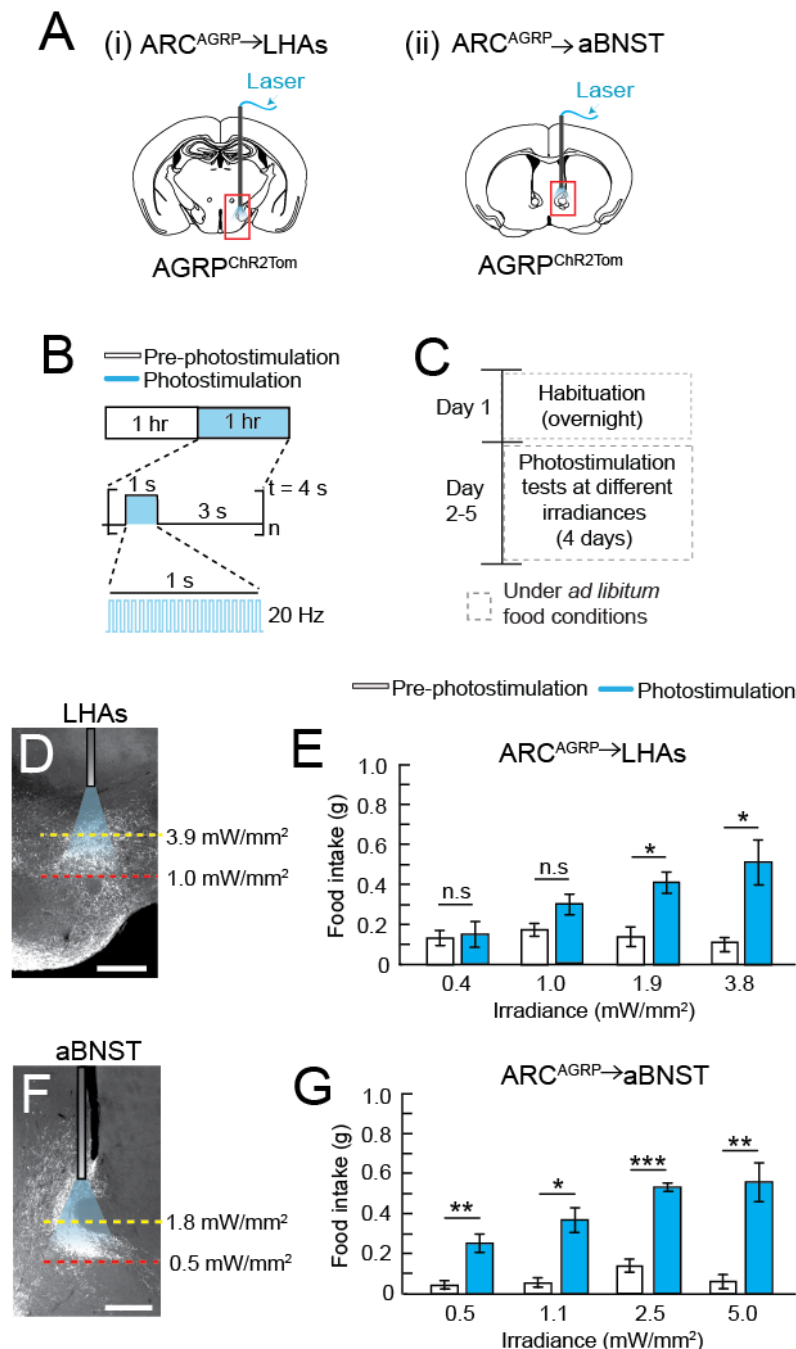
Figure 5.8 Increased food consumption under ARC^{AGRP}→LHAs and ARC^{AGRP}→aBNST circuit photostimulation is specific to activation of AGRP neuron axons in LHAs and aBNST. (A) Diagram of coronal brain section depicting fibre placement in AGRP^{ChR2Tom} animals for activation of (i) ARC^{AGRP} LHAs and (ii) ARC^{AGRP}→ aBNST axonal projections. **(B)** Schematic of photostimulation test protocol. Food intake was measured for a one hour pre-photostimulation baseline (white) and a 1 hr AGRP neuron axonal photostimulation (cyan). **(C)** Schematic of experimental design schedule. Animals received one overnight habituation session

followed by 4 photostimulation tests at different irradiances, conducted in 4 consecutive days. Photostimulation tests were conducted under *ad libitum* fed conditions during the light period. **(D, F)** Epifluorescent images depicting examples of estimated irradiance values at middle (yellow dashed lines) and most distal portion (red dashed lines) of area with observed AGRP neuron axons in targeted projection regions based on theoretical model (Aravanis et al. 2007) for (D) ARC^{AGRP}→ LHAs and (F) ARC^{AGRP}→ aBNST axonal activation. Red boxes in coronal brain section diagrams in (A) represent area shown in images of (D) and (F), respectively. Scale bar 500 µm. **(E, G)** Food intake during pre photostimulation baseline (white) and photostimulation (cyan) condition under (E) ARC^{AGRP}→ LHAs (n=6) and (G) ARC^{AGRP}→ aBNST (n=6) axon projection photostimulation at different irradiances (paired t-tests for each test session, see Table 5.1). Irradiance values calculated for most distal portion of area with observed AGRP neuron axons in target brain region (red dashed lines in (D) and (F), respectively). Values are mean ± S.E.M. n.s. p>0.05, * p<0.05, ** p<0.01, *** p<0.001. aBNST: anterior subdivisions of the bed nucleus of stria terminalis; LHAs: suprafornical subdivision of the lateral hypothalamic area; ARC: arcuate nucleus.

Figure Panel	Sample size	Statistical test	Values
E	6	Paired t-test	
		0.4 mW/mm^2	p=0.856
		1.0 mW/mm^2	p=0.151
		1.9 mW/mm^2	p=0.033
		3.8 mW/mm^2	p=0.027
G	6	Paired t-test	
		0.5 mW/mm^2	p=0.001
		1.1 mW/mm^2	p=0.012
		2.5 mW/mm^2	p<0.001
		5.0 mW/mm^2	p<0.001

Table 5.1 Statistical values for Figure 5.8

5.3.1.4 Similarities and differences of evoked-feeding behaviour by feeding-sufficient AGRP neuron subpopulations

The results presented above indicate that several AGRP neuron projection subpopulations and their circuits are capable of eliciting feeding (feeding-sufficient: $AGRP_{PVH}$, $AGRP_{LHAs}$, $AGRP_{aBNST}$, and $AGRP_{PVT}$), while others do not (feeding-insufficient: $AGRP_{CEA}$ and $AGRP_{PAG}$; Figure 5.9, Table 5.2). In addition, a prior study examining the role of $ARC^{AGRP} \rightarrow PBN$ circuit, which was not tested here, showed that activation of AGRP neuron axons in this region was also insufficient to elicit an acute feeding response (Atasoy et al. 2012). Analysis comparing food intake levels after photoactivation between feeding-sufficient subpopulations indicate that food consumption is significantly different between $AGRP_{PVT}$, and other subpopulations during both sessions tested (post hoc multiple comparisons with Holm-Sidak correction, $AGRP_{PVH}$, $AGRP_{LHAs}$, and $AGRP_{aBNST}$ vs. $AGRP_{PVT:}$ session 1 n= 7 $AGRP_{PVH}$, 17 $AGRP_{LHAs}$, 15 $AGRP_{aBNST}$, 16 $AGRP_{PVT}$ $p<0.001$ for all comparisons, session 2: n= 6 $AGRP_{PVH}$, 17 $AGRP_{LHAs}$, 14 $AGRP_{aBNST}$, 16 $AGRP_{PVT}$, p= 0.006, p=0.004, and p=0.001, respectively; Figure 5.9A, C, Table 5.3). In addition, statistical analysis of latencies to feed after photostimulation onset indicate that latency for $ARC^{AGRP} \rightarrow PVT$ axonal activation is significantly different from $ARC^{AGRP} \rightarrow aBNST$ (post hoc multiple comparisons with Holm-Sidak correction, n=15 $AGRP_{aBNST}$, 16 $AGRP_{PVT,}$ p=0.011; Figure 5.9B, Table 5.3) and $ARC^{AGRP} \rightarrow PVH$ (post hoc multiple comparisons with Holm-Sidak correction, n=7 $AGRP_{PVH}$, 16 $AGRP_{PVT,}$ p=0.040; Figure 5.9B, Table 5.3) but not $ARC^{AGRP} \rightarrow LHAs$ (post hoc multiple comparisons with Holm-Sidak correction, n=17 $AGRP_{LHAs}$, 16 $AGRP_{PVT,}$ p=0.095; Figure 5.9B, Table 5.3). This difference was not observed on session 2 (post hoc multiple comparisons with Holm-Sidak correction, $AGRP_{PVH}$, $AGRP_{LHAs}$, and $AGRP_{aBNST}$ vs. $AGRP_{PVT:}$ n= 6 $AGRP_{PVH}$, 17 $AGRP_{LHAs}$, 14 $AGRP_{aBNST}$, 16 $AGRP_{PVT}$, p= 0.417, p=0.279, and p=0.572, respectively; Figure 5.9D; Table 5.3). Therefore, the characteristics of $AGRP_{PVT}$ neuron-evoked food consumption is not equivalent to that of other feeding-sufficient AGRP neuron subpopulations tested.

Sub-population	Sample size	Session 1		Session 2	
		Food intake (g)	Latency (min)	Food intake (g)	Latency (min)
AGRP$_{aBNST}$	Session 1: 15 Session 2: 14	0.57 ± 0.06 p<0.001	8.53 ±1.46	0.62 ± 0.04 p=0.001	10.05 ± 2.54
AGRP$_{PVH}$	Session 1: 7 Session 2: 6	0.66 ± 0.06 p<0.001	7.48 ± 1.82	0.65 ± 0.07 p=0.003	3.46 ± 0.68
AGRP$_{LHAs}$	Both sessions: 17	0.6 ± 0.05 p<0.001	15.02 ± 4.07	0.60 ± 0.07 p<0.001	16.49 ± 4.98
AGRP$_{PVT}$	Both sessions: 16	0.21 ± 0.04 p<0.001	28.8 ± 6.4	0.30 ± 0.05 p=0.001	19.93 ± 5.34
AGRP$_{CEA}$	Both sessions: 12	0.12 ± 0.04 p=0.295	44.06 ± 6.53	0.19 ± 0.05 p=0.0691	38.01 ± 6.81
AGRP$_{PAG}$	Both Sessions: 18	0.11 ± 0.04 p=0.341	43.29 ± 5.12	0.14 ± 0.03 p=0.256	46.44 ± 4.38

Table 5.2 Food intake and latency to initiate feeding under activation of specific AGRP neuron projection subpopulations. Values are mean ± S.E.M. p-values reported are comparisons (paired t-tests) between pre-photostimulation and photostimulation periods.
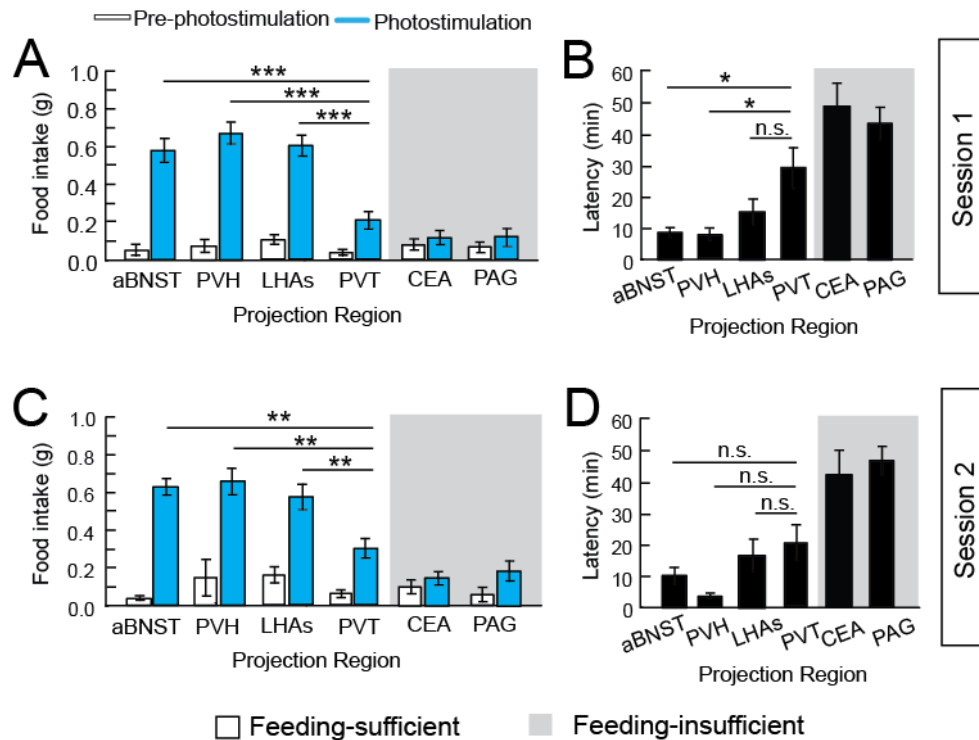
Figure 5.9 Multiple AGRP neuron projection subpopulations are capable of independently coordinate food consumption. (A, C) Food intake during pre-photostimulation baseline (white) and photostimulation (cyan) test for all AGRP neuron axonal projections tested for (A) session 1 and (C) session 2. **(B, D)** Latency to initiate first bout of feeding after photostimulation onset for all AGRP neuron axonal projections tested for (B) session 1 and (D) session 2. All data in this Figure is reproduced from Figures 5.2-5.7. All statistical comparisons are between groups, comparing food intake under photostimulation between feeding sufficient regions only (white background, see Table 5.3). Values are mean ± S.E.M. n.s. $p > 0.05$, * $p < 0.05$, ** $p < 0.01$, *** $p < 0.001$. aBNST: anterior subdivisions of the bed nucleus of stria terminalis; PVH: paraventricular nucleus of the hypothalamus; PVT: paraventricular thalamic nucleus; LHAs: suprafornical subdivision of the lateral hypothalamic area; CEA: central nucleus of the amygdala; PAG: periaqueductal grey.

Figure panel	Sample size	Statistical test	Values
A	aBNST: 15	One-Way RM ANOVA	$F_{(3, 51)}=13.9$, $p<0.001$
	PVH: 7	Post hoc multiple comparison with Holm-Sidak corrections	
	LHAs: 17	aBNST vs. PVH	p=0.734
		aBNST vs. LHAs	p=0.732
	PVT: 16	PVH vs. LHAs	p=0.753
		aBNST vs. PVT	p<0.001
		PVH vs. PVT	p<0.001
		LHAs vs. PVT	p<0.001
B	aBNST: 15	One-Way RM ANOVA	$F_{(3,51)}=4.5$, $p=0.007$
	PVH: 7	Post hoc multiple comparison with Holm-Sidak corrections	
	LHAs: 17	aBNST vs. PVH	p=0.893
		aBNST vs. LHAs	p=0.641
	PVT: 16	PVH vs. LHAs	p=0.552
		aBNST vs. PVT	p=0.011
		PVH vs. PVT	p=0.040
		LHAs vs. PVT	p=0.095
C	aBNST: 14	One-Way RM ANOVA	$F_{(3,49)}=7.5$, $p=0.002$
	PVH: 6	Post hoc multiple comparison with Holm-Sidak corrections	
	LHAs: 17	aBNST vs. PVH	p=0.789
		aBNST vs. LHAs	p=0.762
	PVT: 16	PVH vs. LHAs	p=0.825
		aBNST vs. PVT	p=0.001
		PVH vs. PVT	p=0.006
		LHAs vs. PVT	p=0.004
D	aBNST: 14	One-Way RM ANOVA	$F_{(3, 49)}=1.7$, $p=0.177$
	PVH: 6	Post hoc multiple comparison with Holm-Sidak corrections	
	LHAs: 17	aBNST vs. PVH	p=0.687
		aBNST vs. LHAs	p=0.670
	PVT: 16	PVH vs. LHAs	p=0.473
		aBNST vs. PVT	p=0.417
		PVH vs. PVT	p=0.279
		LHAs vs. PVT	p=0.572

Table 5.3 Statistical values for Figure 5.9

5.3.2 Feeding-insufficient AGRP neuron subpopulations do not potentiate feeding under states of increased food consumption probability

Daytime activation studies described above indicate that a subset of AGRP neuron circuits are capable of eliciting feeding under states of low feeding probability (ARC$^{AGRP}\rightarrow$PVH, ARC$^{AGRP}\rightarrow$LHAs, ARC$^{AGRP}\rightarrow$aBNST, and ARC$^{AGRP}\rightarrow$PVT). Other circuits (ARC$^{AGRP}\rightarrow$CEA and ARC$^{AGRP}\rightarrow$PAG), however, were insufficient to independently evoke feeding. There is, however, the possibility that these circuits may potentiate feeding under states of increased food consumption probability. To determine whether this is the case, I tested whether feeding can be potentiated by photostimulation of specific AGRP neurons projection subpopulations during the early dark period, where animals are more likely to initiate food consumption.

Food consumption was measured during the first hour of the dark period (6pm-7pm). Two baseline food consumption measurements were taken for comparison, one where animals received no photostimulation, and one where photostimulation was applied but light was prevented from entering the brain (mock stimulation). This second baseline was taken in order to control for any effects visible light emitted during stimulation might have on feeding irrespective of activation of AGRP neuron projections tested. On test day, AGRP neuron axonal photostimulation was applied for 1 hr and food consumption measured (Figure 5.10A-B). All projection areas tested during daytime stimulation studies were accessed in this paradigm (PVH, LHAs, aBNST, PVT, CEA, and PAG). During both baseline food consumption tests, animals across groups consumed approximately 0.2 g of food in 1 hr. Unsurprisingly, early dark period photostimulation of ARC$^{AGRP}\rightarrow$PVH, ARC$^{AGRP}\rightarrow$LHAs, ARC$^{AGRP}\rightarrow$aBNST, and ARC$^{AGRP}\rightarrow$PVT projections (target regions that elicited a significant increase in feeding under daytime photostimulation) resulted in increased feeding over no photostimulation and mock photostimulation baselines (post hoc multiple comparisons with Holm-Sidak correction, ARC$^{AGRP}\rightarrow$PVH: n=6 photostimulation vs. no photostimulation p=0.013, photostimulation vs. mock photostimulation p=0.013; ARC$^{AGRP}\rightarrow$LHAs n=7 photostimulation vs. no photostimulation p<0.001, photostimulation vs. mock photostimulation p<0.001; ARC$^{AGRP}\rightarrow$aBNST: n=6 photostimulation vs. no photostimulation p<0.001, photostimulation vs. mock photostimulation p=0.001;

ARC^{AGRP}→PVT n= 11 photostimulation vs. no photostimulation p=0.015, photostimulation vs. mock photostimulation p=0.002; Figure 5.10 C-F, Table 5.4).

In the same fashion as early light period stimulation, activation of feeding-insufficient AGRP neuron subpopulations (AGRP$_{CEA}$ and AGRP$_{PAG}$) did not potentiate feeding in the early dark period. Activation of ARC^{AGRP}→CEA projections did not lead to an increase in feeding over baseline conditions (post hoc multiple comparisons with Holm-Sidak correction, n= 6 photostimulation vs. no photostimulation p=0.896, photostimulation vs. mock photostimulation p=0.9; Figure 5.10G, Table 5.4). For ARC^{AGRP}→PAG projections, food consumption was elevated under photostimulation over the mock photostimulation baseline, but not over no stimulation baseline, and these two baselines were shown to be significantly different statistically (post hoc multiple comparisons with Holm-Sidak correction, n=11 photostimulation vs. no photostimulation p=0.395, photostimulation vs. mock photostimulation p=0.004, no photostimulation vs. mock photostimulation p=0.018; Figure 5.10H, Table 5.4). Significant differences between the two baselines were also observed under ARC^{AGRP}→aBNST projection activation, although the photostimulation session resulted in higher food consumption over both baseline sessions. However, given lack of differences between baselines for all other projections tested, I contend the differences observed are likely the result of overall variability in food consumption between animals, and therefore indicate that activation of ARC^{AGRP}→PAG projections are unlikely to potentiate feeding in the early light period. Further studies should be performed to confirm this.
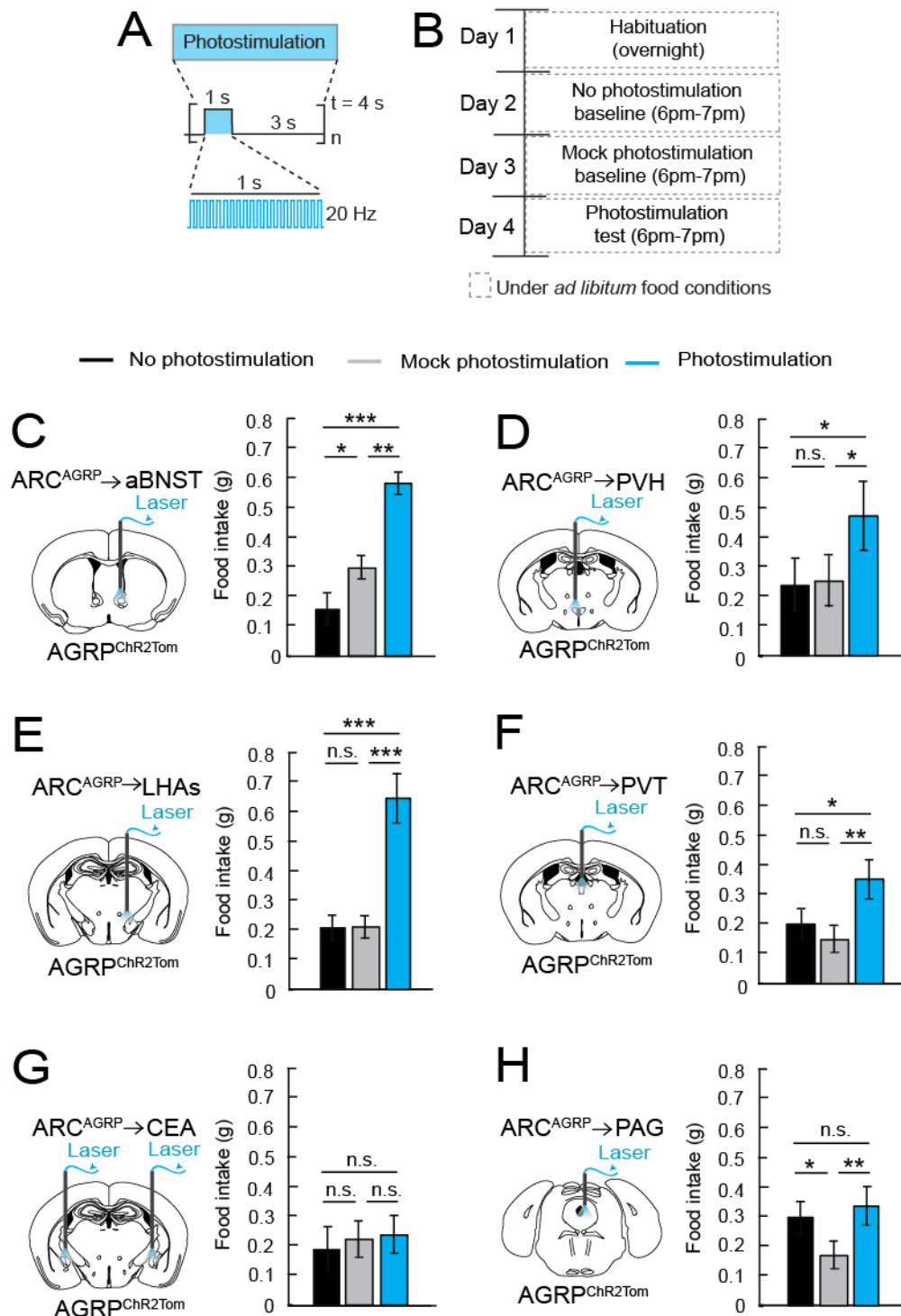
Figure 5.10 Activation of feeding-insufficient AGRP neuron subpopulations does not potentiate early night-time feeding. (A) Schematic of photostimulation protocol used. **(B)** Schematic of experimental design schedule. Animals received one overnight habituation session followed by a no photostimulation baseline test, a mock photostimulation baseline test, and a photostimulation test conducted in 3

consecutive days. All tests were conducted under *ad libitum* fed conditions, during the early dark period (6-7 pm). **(C-H)** Diagrams of fibre placement position in AGRP^{ChR2Tom} animals for AGRP neuron axonal photoactivation (left) and total food intake (right) during no photostimulation baseline (black), mock photostimulation baseline (grey), and photostimulation test (cyan) for axonal activation of (C) ARC^{AGRP}→ aBNST, (D) ARC^{AGRP}→ PVH, (E) ARC^{AGRP}→ LHAs, (F) ARC^{AGRP}→ PVT, (G) ARC^{AGRP}→ CEA and (H) ARC^{AGRP}→ PAG. All statistical comparisons are within groups (see Table 5.4). Values are mean ± S.E.M. n.s. $p>0.05$, * $p<0.05$, ** $p<0.01$, *** $p<0.001$. aBNST: anterior subdivisions of the bed nucleus of stria terminalis; PVH: paraventricular nucleus of the hypothalamus; PVT: paraventricular thalamic nucleus; LHAs: suprafornical subdivision of the lateral hypothalamic area; CEA: central nucleus of the amygdala; PAG: periaqueductal grey.

Figure panel	Sample size	Statistical Test	Values
C	6	One-Way RM ANOVA	$F(2,10)=28.8$, $p<0.001$
		Post hoc multiple comparison with Holm-Sidak corrections	
		No photostimulation vs. Mock photostimulation	$p=0.035$
		No photostimulation vs. photostimulation	$p<0.001$
		Mock photostimulation vs. Photostimulation	$p=0.001$
D	6	One-Way RM ANOVA	$F(2,10)=8.4$, $p=0.007$
		Post hoc multiple comparison with Holm-Sidak corrections	
		No photostimulation vs. Mock photostimulation	$p=0.839$
		No photostimulation vs. photostimulation	$p=0.013$
		Mock photostimulation vs. Photostimulation	$p=0.013$
E	7	One-Way RM ANOVA	$F(2,12)=19.0$ $p<0.001$
		Post hoc multiple comparison with Holm-Sidak corrections	
		No photostimulation vs. Mock photostimulation	$p=0.973$
		No photostimulation vs. photostimulation	$p<0.001$
		Mock photostimulation vs. Photostimulation	$p<0.001$
F	11	One-Way RM ANOVA	$F(2,20)=8.4$, $p=0.002$
		Post hoc multiple comparison with Holm-Sidak corrections	
		No photostimulation vs. Mock photostimulation	$p=0.336$
		No photostimulation vs. photostimulation	$p=0.015$
		Mock photostimulation vs. Photostimulation	$p=0.002$

Table 5.4 Statistical values for Figure 5.10. *Table continued on next page*

Figure panel	Sample size	Statistical test	Values
G	6	One-Way RM ANOVA	$F_{(2,10)}=0.2$, $p=0.808$
		Post hoc multiple comparison with Holm-Sidak corrections	
		No photostimulation vs. Mock photostimulation	$p=0.900$
		No photostimulation vs. photostimulation	$p=0.896$
		Mock photostimulation vs. Photostimulation	$p=0.821$
H	11	One-Way RM ANOVA	$F_{(3, 51)}=13.9$, $p<0.001$
		Post hoc multiple comparison with Holm-Sidak corrections	
		No photostimulation vs. Mock photostimulation	$p=0.018$
		No photostimulation vs. photostimulation	$p=0.395$
		Mock photostimulation vs. Photostimulation	$p=0.004$

Table 5.4 continued

5.3.3 AGRP neuron subpopulations are similarly regulated by states and signals of energy deficit

The observed differences in the functional efficacy in evoking food consumption under photoactivation of distinct AGRP neuron subpopulations in the studies above, both in daytime and the early dark period, suggest that distinct AGRP neuron subpopulations might be regulated differently under states of energy deficit. Food deprivation or ghrelin administration has been shown to lead to the induction of Fos in AGRP neurons. The intensity of Fos immunoreactivity, however, is variable across AGRP neurons (Betley et al. 2013). Differences in Fos expression intensity between AGRP neurons may indicate differential regulation between projection specific subpopulations. Therefore, I measured the induction of Fos in distinct AGRP neuron projection subpopulations after 24 hrs of food deprivation or i.p. ghrelin administration (1 mg/kg). To label distinct AGRP subpopulations, FG microinjections were performed in major AGRP projection areas (aBNST, PVH, LHAs, PVT, CEA, PAG, PBN, Figure 5.12A-G, Figure 5.13A-G) in AGRP^{ChR2EYFP} animals, where AGRP neurons were identified by the membrane-bound EYFP fluorophore.

After a 24 hours food deprivation, Fos immunoreactivity was observed in AGRP neurons in the ARC, including FG labelled projection subpopulation neurons. For all subpopulations tested, a range of Fos intensity was observed (Figure 5.12A-G). Statistical analysis of the distribution of Fos intensity for each projection subpopulation revealed that Fos activation was not significantly different across groups (Kruskal Wallis one one-way ANOVA on ranks, n= 25 PVH, 25 LHAs, 20 aBNST, 25 PVT, 25 CEA, 21 PAG, and 25 PBN, p=0.541; Figure 5.11H). Fos immunoreactivity after ghrelin administration showed similar patterns in all subpopulations as with food deprivation. As under food deprivation conditions, statistical analysis also show that all subpopulations are similarly regulated by ghrelin (Kruskal Wallis one one-way ANOVA on ranks, n= 25 PVH, 25 LHAs, 25 aBNST, 25 PVT, 25 CEA, 22 PAG, and 25 PBN, p=0.286; Figure 5.12H). These data indicated that despite observed differences in behavioural output (elevated food consumption), AGRP neuron subpopulations are similarly regulated under states of food deprivation, as well as by the orexigenic hormone ghrelin.
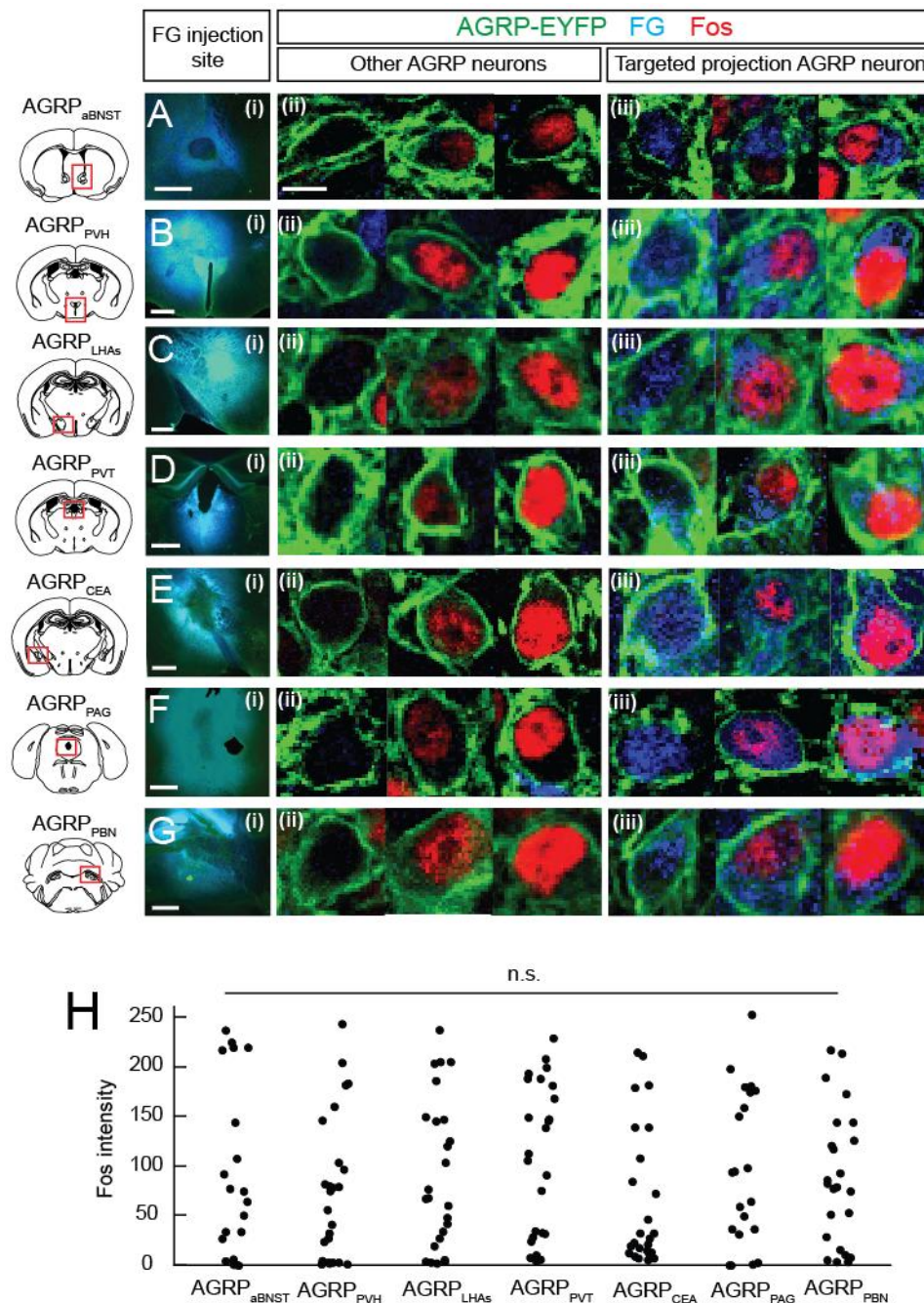
Figure 5.11 Food deprivation elicits comparable Fos expression levels across AGRP neuron subpopulations. (A-G) Fos (red) expression after 24 hrs of food deprivation in (A) AGRP$_{aBNST}$, (B) AGRP$_{PVH}$, (C) AGRP$_{LHAs}$, (D) AGRP$_{PVT}$, (E) AGRP$_{CEA}$, (F) AGRP$_{PAG}$, (G) AGRP$_{PBN}$ neuron subpopulations. (i) Epifluorescence example images showing FG (cyan) injection site in projection regions performed to label AGRP neuron subpopulation of interest. Red boxes in coronal brain section diagrams represent area shown. (ii) Single plane confocal example images of FG(-) AGRP neurons in the ARC (marked by membrane-bound EYFP, green) with no Fos

(left), low Fos (middle), and high Fos (right) expression. (iii) Single plane confocal example images of FG(+) (cyan) AGRP neurons in the ARC with no Fos (left), low Fos (middle), and high Fos (right) expression. **(H)** Scatter plots showing distribution of Fos immunofluorescence intensity measured in the nucleus of FG(+) AGRP-ChR2-EYFP neurons for all subpopulations tested (n= 25 PVH, 25 LHAs, 20 aBNST, 25 PVT, 25 CEA, 21 PAG, and 25 PBN, Kruskal Wallis one-way ANOVA on ranks). n.s. $p > 0.05$. aBNST: anterior subdivisions of the bed nucleus of stria terminalis; PVH: paraventricular nucleus of the hypothalamus; PVT: paraventricular thalamic nucleus; LHAs: suprafornical subdivision of the lateral hypothalamic area; ARC: arcuate nucleus; CEA: central nucleus of the amygdala; PAG: periaqueductal grey; PBN: parabrachial nucleus; FG: Fluoro-Gold.
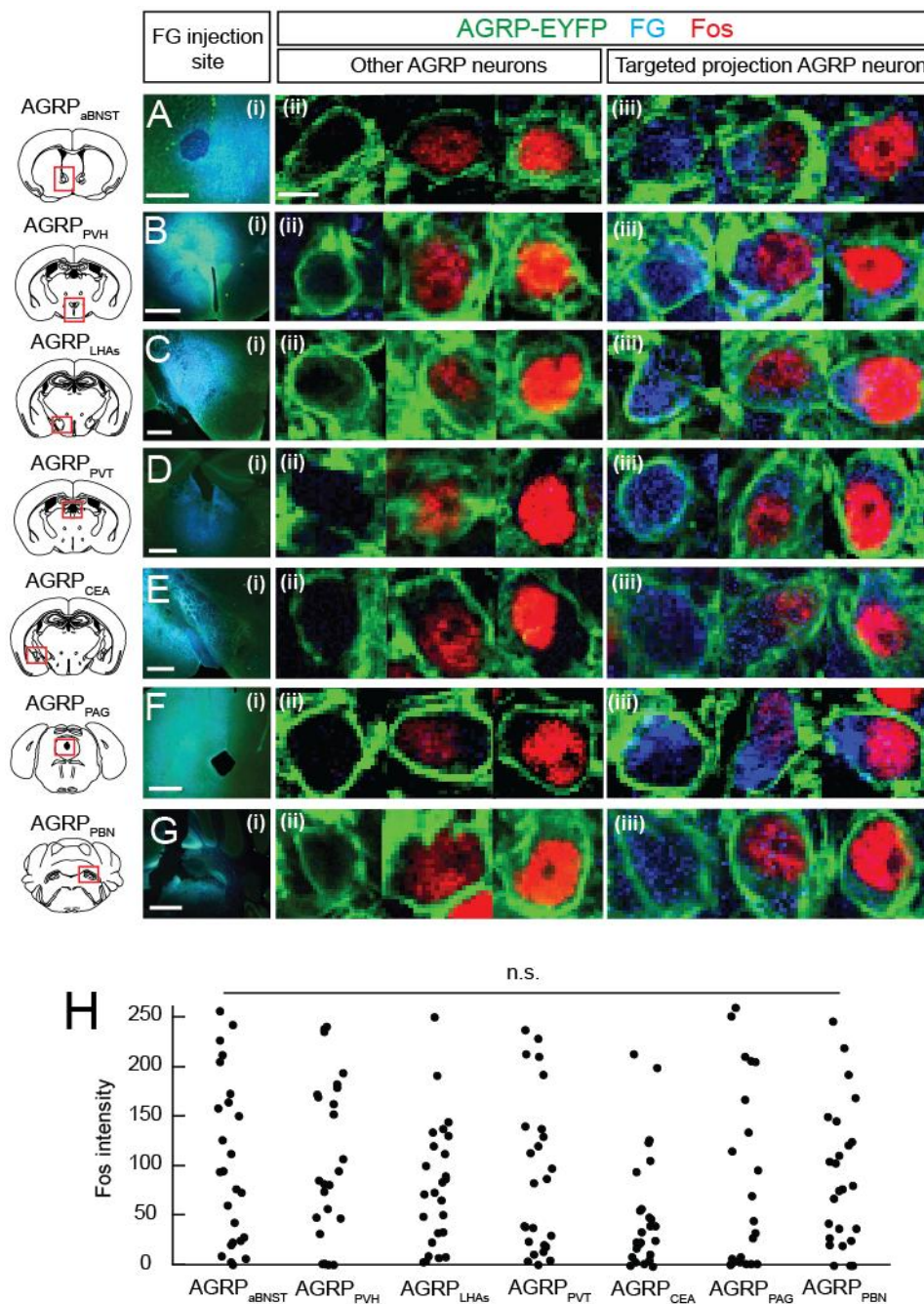
Figure 5.12 Fos expression is similar between AGRP neuron subpopulations under ghrelin administration. (A-G) Fos (red) expression 3 hrs after i.p administration of ghrelin (1 mg/kg) in (A) AGRP_aBNST, (B) AGRP_PVH, (C) AGRP_LHAs, (D) AGRP_PVT, (E) AGRP_CEA, (F) AGRP_PAG, (G) AGRP_PBN neuron subpopulations. (i) Epifluorescence example images showing FG (cyan) injection site in projection regions performed to label AGRP neuron subpopulation of interest. Red boxes in coronal brain section diagrams represent area shown. (ii) Single plane confocal example images of FG(-) AGRP neurons in the ARC (marked by membrane-bound

EYFP, green) with no Fos (left), low Fos (middle), and high Fos (right) expression. (iii) Single plane confocal example images of FG(+) (cyan) AGRP neurons in the ARC with no Fos (left), low Fos (middle), and high Fos (right) expression. **(H)** Scatter plots showing distribution of Fos immunofluorescence intensity measured in the nucleus of FG(+) AGRP-ChR2-EYFP neurons for all subpopulations tested (n= 25 PVH, 25 LHAs, 25 aBNST, 25 PVT, 25 CEA, 22 PAG, and 25 PBN, Kruskal Wallis one-way ANOVA on ranks). n.s. $p>0.05$. aBNST: anterior subdivisions of the bed nucleus of stria terminalis; PVH: paraventricular nucleus of the hypothalamus; PVT: paraventricular thalamic nucleus; LHAs: suprafornical subdivision of the lateral hypothalamic area; ARC: arcuate nucleus; CEA: central nucleus of the amygdala; PAG: periaqueductal grey; PBN: parabrachial nucleus; FG: Fluoro-Gold.

5.4 Discussion

Feeding behaviour is controlled and directed, in part, by homeostatic neural circuits that signal the energetic state of an animal. AGRP neurons are viewed as starvation sensitive neurons (Sternson 2013) capable of directing food-seeking and consumption behaviours (Aponte et al. 2011, Atasoy et al. 2012, Krashes et al. 2011). Studies by Betley et al. (2013) and studies presented in Chapter 4 indicate that AGRP neurons direct feeding behaviour through a negative reinforcement teaching mechanism. However, the downstream AGRP neuron circuits important in mediating this negative reinforcement process and food consumption are unclear. Since AGRP neurons are known to be further subdivided into projection specific subpopulations, here I systematically examined the functional significance of these subpopulations in AGRP neuron evoked feeding using cell-type specific axonal activation techniques in order to prioritize the downstream nodes for further examination in their role in AGRP neuron-mediated negative reinforcement.

5.4.1 Parallel and redundant circuit organization of AGRP neurons in the control of feeding behaviour

The studies using axonal activation of AGRP neurons in specific projections regions presented here indicate that AGRP neurons can elicit feeding behaviour through four distinct projection subpopulations to four separate forebrain regions: aBNST, PVH, PVT, and LHAs. Activation of two other projection subpopulations through axonal photostimulation in the CEA and PAG did not result in elevated food consumption. In addition, previous studies have shown that activation of AGRP neuron axons in the PBN was also insufficient to elicit feeding (Atasoy et al. 2012). Since circuit mapping studies indicated that no functional connectivity was observed between AGRP neurons in the ARC (Atasoy et al. 2012), activation of one subset of AGRP neurons should not activate other subpopulations through intra-ARC connectivity. No evidence of gap junctions between ARC^{AGRP} neurons have been found either (Magnus & Sternson, unpublished). In addition, anatomical techniques employed by Betley et al. (2013) could not determine whether AGRP neurons that project within the ARC to POMC neurons were distinct subpopulations from long-

range projecting AGRP neurons, or resulted from collaterals from these long-range projecting neurons. However, *in vivo* studies indicate that acute evoked feeding is not a result of POMC neuron inhibition by AGRP neurons, further validating the use of axonal activation techniques. Therefore, AGRP neuron circuit is configured with distinct parallel circuit elements, some of which have redundant capability to drive feeding behaviour.

Despite the differential ability to elicit feeding by distinct AGRP neuron projection subpopulations, no differences in neuronal activation by signals and states of energy deficit were observed. Regulation of neuron activity by ghrelin or food deprivation appears similar in anatomically and functionally separate subpopulations. In addition, previous work indicates that synaptic regulation can be consistent across most AGRP neurons (Yang et al. 2011). However, it has been demonstrated that there is differential expression of leptin receptors between AGRP neuron subpopulations. AGRP neuron subpopulations that project outside of the hypothalamus ($AGRP_{aBNST}$, $AGRP_{PVT}$, $AGRP_{CEA}$, $AGRP_{PAG}$, $AGRP_{PBN}$) but not within the hypothalamus ($AGRP_{PVH}$, $AGRP_{LHAs}$, $AGRP_{DMH}$) appear to express the receptor for the hormone leptin (Betley et al. 2013). Thus, AGRP neuron projection classes are regulated similarly by some hormonal signals and differently by others, indicating a previously unappreciated intricacy of physiological and neural control of AGRP neuron circuits. Although these subpopulations are distinguished by their projections, it is unclear whether they can be defined by their neuropeptide content. Further studies using single cell RNA sequencing methods (Jaitin et al. 2014) would be able to determine this.

5.4.2 Forebrain regions that control feeding

Most of the brain regions targeted by AGRP neuron projections have been only lightly characterized for their influence on feeding behaviour. Therefore following the axon projections of this interoceptive population helps identify brain areas sufficient to coordinate feeding behaviour. Although, prior work showed that $ARC^{AGRP} \rightarrow PVH$ projections evoke feeding (Atasoy et al. 2012), activation of distinct AGRP neuron subpopulations projecting to the aBNST, LHAs, and PVT reveal that these brain regions also have the capacity to orchestrate feeding behaviour.

The BNST has been implicated in a broad range of behavioural roles, including feeding (Jennings et al. 2013). Based on the selective anatomical connectivity of ARC^{AGRP}→aBNST axons, the aBNST is shown here to have functional properties that are sufficient to rapidly orchestrate feeding behaviour. Recently, Jennings et al. (2013) demonstrated that optogenetic activation of GABAergic BNST projections to the LHA is capable of rapidly inducing food consumption, further validating the role of BNST in the control of feeding behaviour. However, it is unlikely that ARC^{AGRP}→aBNST neurons directly regulate BNST^{GABA} neurons, as AGRP neurons are inhibitory (Atasoy et al. 2008, Atasoy et al. 2012).

The LHA is a loosely defined brain region that is associated with multiple behavioural and autonomic outputs. Previous studies using electrical stimulation in the LHA directly demonstrated a role for this region in feeding behaviour. However, studies showed both increases and decreases in feeding (Delgado & Anand 1953, Jennings et al. 2013). The LHAs is a subdivision of the LHA that receives robust AGRP neuron input. My studies indicate that activation of ARC^{AGRP}→LHAs projections can independently evoke feeding. These and prior studies (Jennings et al. 2013), then, indicate that LHA electrical stimulation induced elevated food consumption is due to activation of inhibitory inputs from AGRP$_{LHAs}$ and BNST^{GABA} neurons.

The PVT is an integratory area and GABA-A receptor agonist microinjections (Stratford & Wirtshafter 2013) are reported to increase food consumption. In my experiments, activation of GABAergic ARC^{AGRP}→PVT projections significantly increased food intake, albeit with characteristics distinct from other feeding-sufficient regions, as consumption was lower and latencies to initiate feeding longer.

5.4.3 A core forebrain feeding circuit

A major implication of my systematic examination of the functional role of AGRP neuron projections is that they point to a core forebrain feeding circuit involving the aBNST, PVH, LHAs, and to a lesser extent the PVT (Figure 5.13). The capability of multiple, independent projections to separately evoke a complex behavioural response such as feeding suggests that these second-order circuit

elements are likely functionally interconnected. The PVH is an integratory centre for the coordination of appetite (Swanson 2000) and multiple brain regions targeted by AGRP neurons might act through the PVH. Indeed, the PVH receives inputs from each of the feeding-sufficient regions identified here: BNST, LHA, and PVT (Cullinan et al. 1993, Hahn & Swanson 2010, Moga & Saper 1994, Prewitt & Herman 1998, Swanson & Sawchenko 1983). However, the PVH is unlikely to be the sole convergence point for these feeding circuits. Pharmacological blockade of $ARC^{AGRP} \rightarrow PVH$ connections during AGRP neuron activation suppressed food intake by only ~50% (Atasoy et al. 2012). This pharmacological manipulation likely also disrupts the overall function of the PVH, including afferent inputs from the aBNST and LHAs. Based on AGRP neuron projection stimulation experiments here, this suggests that feeding can also be separately coordinated by the aBNST and/or the LHAs when $ARC^{AGRP} \rightarrow PVH$ is blocked. Retrograde and anterograde anatomical studies also report strong bidirectional connectivity between the aBNST and the LHAs (Hahn & Swanson 2010, Shin et al. 2008) indicating a circuit involving these two brain areas that are targeted by AGRP neurons. The aBNST, but not the LHAs, is also reported to receive input from the PVH (Wittmann et al. 2009). In addition, the PVT is bi-directionally connected with both the aBNST and the LHAs (Hahn & Swanson 2010, Shin et al. 2008). Taken together, the independent projections from AGRP neuron subpopulations highlight a core set of interconnected brain regions that are sufficient to evoke feeding.
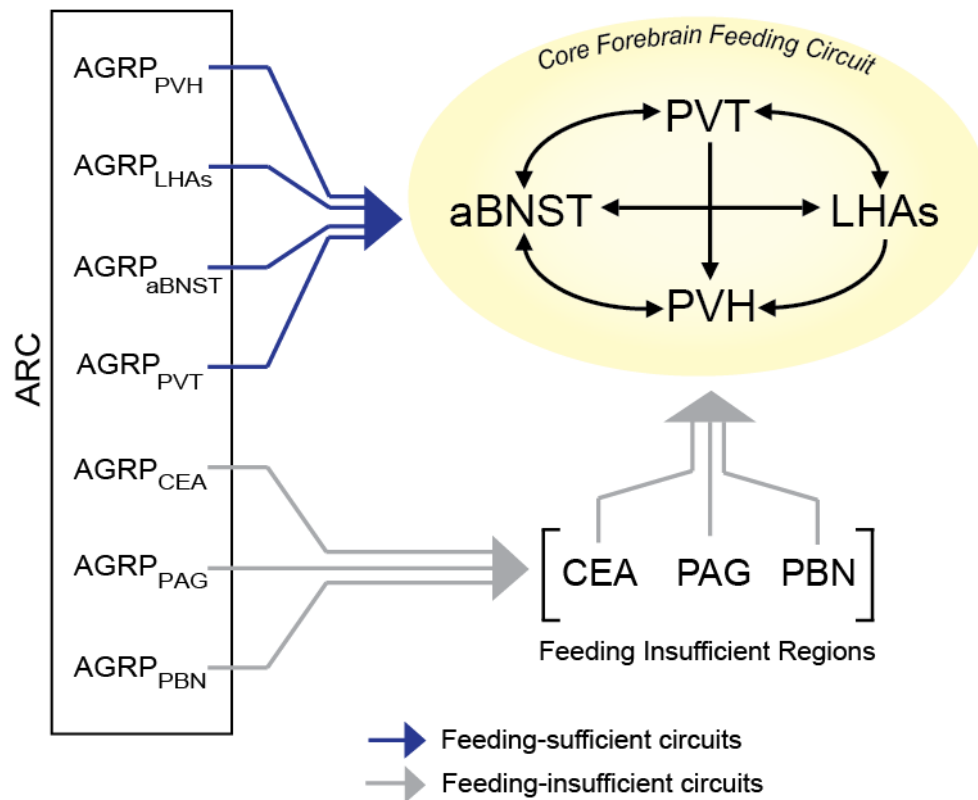
Figure 5.13 AGRP neuron modulation of a core forebrain feeding circuit. Activation of four distinct AGRP neuron subpopulations (AGRP$_{aBNST}$, AGRP$_{PVH}$, AGRP$_{LHAs}$, and AGRP$_{PVT}$) and their circuits can independently evoke food intake. Downstream projection regions of these circuits (aBNST, PVH, LHAs, and PVT) are anatomically interconnected between each other and comprise a core forebrain feeding circuit. Activation of three other AGRP neuron subpopulations (AGRP$_{CEA}$, AGRP$_{PAG}$, and AGRP$_{PBN}$) is not sufficient to elicit acute food intake nor potentiate food intake under states of increased food intake probability (early dark period). The downstream projection regions are considered feeding-insufficient regions. These regions project heavily to brain regions comprising the core forebrain feeding circuit and these inputs may play modulatory roles. Blue lines and arrow signify projections that are sufficient to evoke acute food consumption, while grey lines and arrows signify projections that are insufficient to increase acute food intake. aBNST: anterior subdivisions of the bed nucleus of stria terminalis; PVH: paraventricular nucleus of the hypothalamus; PVT: paraventricular thalamic nucleus; LHAs: suprafornical subdivision of the lateral hypothalamic area; ARC: Arcuate nucleus; CEA: central nucleus of the amygdala; PAG: periaqueductal grey; PBN: parabrachial nucleus.

5.4.4 Modulation of feeding behaviour by feeding-insufficient AGRP neuron projection regions

Daytime activation studies presented here of ARC$^{AGRP}\rightarrow$CEA and ARC$^{AGRP}\rightarrow$PAG circuits and prior studies on activation of ARC$^{AGRP}\rightarrow$PBN circuit (Atasoy et al. 2012) indicate that these downstream projection regions are not sufficient to independently evoke feeding. In addition, studies performed here probing the ability of ARC$^{AGRP}\rightarrow$CEA and ARC$^{AGRP}\rightarrow$PAG projections to potentiate feeding under states of increased food consumption probability (early dark period) also failed to show any effects in elevating feeding. Therefore, these regions do not directly contribute to AGRP neuron evoked feeding responses. However, these regions have been indirectly associated with the regulation of feeding behaviour. The CEA has been shown to be important in the suppression of feeding in the presence of learned aversive cues (Petrovich et al. 2009). The PBN has been demonstrated to play a role in modulation of food palatability and food choice (DiPatrizio & Simansky 2008, Ward & Simansky 2006) as well as aversive and appetitive gustatory conditioning (Reilly & Trifunovic 2000) and the regulation of visceral malaise (Luquet et al. 2005, Wu et al. 2009, Wu et al. 2012). The PAG has been suggested to modulate the motivational state during hunting and foraging behaviours (Comoli et al. 2003, Mota-Ortiz et al. 2012). In addition, all projection subpopulations were shown here to be similarly regulated by hormonal signals of hunger and negative energetic state, as food deprivation and ghrelin administration elicits similar Fos expression patterns in all subpopulations. Experiments with retrogradely transported dyes and viruses indicate that each of these regions also project to the PVH, aBNST and LHAs (Betley et al. 2013, Hahn & Swanson 2010, Shin et al. 2008). Therefore, these feeding-insufficient regions are gated or otherwise regulated by AGRP neurons and may modulate the output of the core forebrain feeding circuit (Figure 5.13). Behavioural modulation may be dependent on feeding contexts not present in current studies.

5.4.5 The role of AGRP neuron subpopulations in AGRP neuron mediated negative reinforcement teaching signal

The studies presented here allow us to prioritize AGRP neuron subpopulations and downstream circuit nodes important in the coordination of rapidly evoked, voracious feeding. This prioritization provides guidance for further investigation on the neuronal circuits involved in mediating previously reported negative reinforcement processes employed by AGRP neurons to control food seeking and food consumption behaviours (Betley et al. 2014). Feeding sufficient AGRP neuron projection regions (aBNST, PVH, LHAs, and PVT) are expected to be involved in this regulation. However, feeding insufficient regions may also modulate negative reinforcement processes, as elevation of willingness to work for food, such as in hyperdopaminergic animals, does not necessarily correlate with increase in overall food consumption (Beeler et al. 2010, Beeler et al. 2012a). Further studies using activation of AGRP neuron projections in conditioned place avoidance and operant studies can help elucidate which downstream brain regions may be involved in mediating the negative internal state and increased willingness to expend energy for food elicited under AGRP neuron somatic activation.

5.5 Conclusion

AGRP neurons can coordinate food seeking and food consumption behaviours, and its circuitry and downstream projection regions provide a blueprint for uncovering new nodes involved in the regulation of feeding behaviour. In this study, identification of multiple, distinct circuit projections with the capacity to evoke food consumption points to a core forebrain circuit in the regulation of feeding. These studies prioritize downstream circuit components to guide the study of their functional role in the modulation of feeding through negative reinforcement directed selection of behavioural output.

Publication arising from data from this chapter:

Chapter 6

General Discussion

6.1 Synopsis of findings

The studies presented in this dissertation extend our understanding of the role of homeostatic neurons in food consumption and uncovers the previously unappreciated functional organization and reinforcement mechanisms employed by neuronal circuits that control feeding behaviour. Studies probing the role of leptin receptor (LepRb) neurons in the lateral hypothalamic area (LHA) neurons in the control of food intake indicate that these neurons, comprised primarily of LHA^{GABA} low threshold-spiking (LTS) neurons, are homeostatic neurons capable of detecting and signalling information about body energy status and are capable of modulating body weight. In addition, examination of the underlying reinforcement mechanisms engaged by agouti-related peptide (AGRP) neurons to guide flexible goal-directed food-seeking and consumption behaviours indicate that these neurons employ a negative reinforcement teaching signal. Disruption of this teaching signal can lead to the disruption of formerly learned contingencies between actions and outcomes in relation to food consumption, in particular under high effort requirements. This demonstrates a prior unrecognized role for negative reinforcement in the regulation of behaviour under homeostatic hunger states. Furthermore, identification of multiple, distinct AGRP neuron subpopulations with the capacity to evoke food consumption points to a core forebrain circuit in the regulation of feeding. These studies prioritize downstream circuit components that may play a role in the modulation of feeding through negative reinforcement-directed selection of behavioural output, and highlight the complexity of the brain's control of feeding behaviour.

6.2 LepRb neurons in the control of food intake

Given that leptin is a signal of energetic state and is known to reduce feeding behaviour, leptin receptor neurons in the brain can act as homeostatic neurons that regulate food consumption behaviours. Major roles in feeding have been attributed to leptin receptor expressing neurons in the arcuate nucleus (ARC)—AGRP and proopiomelanocortin (POMC) neurons (Coll et al. 2007, Gao & Horvath 2007, 2008, Oswal & Yeo 2010, van Swieten et al. 2014). My studies on the role of LHA^{LepRb} neurons in feeding indicate that, in addition to leptin, they are also capable of

detecting changes in glucose concentration and modulate their activity accordingly, similar to orexin (OX), melanin-concentrating hormone (MCH), and other γ-aminobutyric acid (GABA) neurons in the LHA (Burdakov et al. 2005a, Karnani et al. 2013, Yamanaka et al. 2003). In addition, activation of these neurons led to a reduction in feeding, although not acutely, as when activating POMC neurons in the ARC (Aponte 2011). Therefore, leptin's activating effect on LHA^{LepRb} (Leinninger et al. 2009) in addition to POMC neurons in the ARC (Cowley et al. 2001), also underlie leptin's ability to reduce food intake. Although it is unclear whether they synapse onto LHA^{LepRb} neurons directly, LepRb expressing POMC neurons also project to the LHA (Betley et al. 2013), which could conceivably potentiate leptin's inhibition of food intake through the LHA. The downstream projections of LHA^{LepRb} neurons that might regulate this reduction in feeding are still unclear, as functional synaptic connectivity studies with two known downstream regions were ambiguous. In addition, studies examining whether inhibition of LHA^{LepRb} neurons can increase food intake have not been performed, so further studies should be carried out in order to determine the bidirectionality of feeding regulation by these neurons.

6.3 A core forebrain feeding circuit as an interaction hub for multiple modulatory inputs

Results presented here and by Atasoy et al (2012) systematically examining the role of projection based AGRP neuron subpopulations in evoked feeding indicate that AGRP neurons use a parallel and redundant functional circuit organization to coordinate food intake. Optogenetic activation of AGRP neuron axons in the paraventricular nucleus of the hypothalamus (PVH), suprafornical subdivision of the lateral hypothalamic area (LHAs), anterior subdivisions of the bed nucleus of stria terminalis (aBNST), and paraventricular thalamic nucleus (PVT) resulted in evoked feeding behaviour, while activation of axons in the central nucleus of the amygdala (CEA), periaqueductal grey (PAG), and parabrachial nucleus (PBN) did not. The exact cell-types in these downstream projection regions that mediate this effect are currently unknown and should be the subject of further investigation. Along with prior anatomical evidence of interconnectivity between feeding sufficient regions, these results highlight a core set of interconnected brain regions that are sufficient to evoke

feeding. This core forebrain feeding circuit is positioned to participate in an extended circuit that can be modulated by multiple cortical, hippocampal, hypothalamic and brainstem regions, including regions involved in homeostatic, cognitive, emotional and visceral control (Betley et al. 2013, Fanselow & Dong 2010, Hahn & Swanson 2010, Napadow et al. 2013, Risold et al. 1997, Shin et al. 2008, Swanson 2000). In addition, prior anatomical studies indicate that feeding insufficient regions also show second-order interactions with the core feeding circuit (Betley et al. 2013, Hahn & Swanson 2010, Shin et al. 2008). These regions are involved in processing visceral information (Wu et al. 2012), and AGRP neuron subpopulations targeting these regions are still modulated by states of energy deficit and signals of starvation. Therefore, in response to particular bodily or physiological stimuli, these regions may influence feeding behaviour by interactions with this core feeding circuit in a manner subject to modulation by AGRP neurons. The output connectivity of the core feeding circuit nodes is a key area for future research, with particular focus on the convergence points for the downstream projections of the PVH, aBNST, LHAs, and PVT.

6.4 Integration of AGRP neuron circuits with other known feeding circuits

As a whole, studies presented here and by others investigating other neuronal circuits have identified many new subpopulations of neurons and their downstream projections involved in the regulation of feeding behaviour. An emerging picture highlights many AGRP neuron projecting downstream regions as important brain area in the coordination of food intake. In addition, it also reveals the divergent role of distinct AGRP neuron circuits in the differential temporal regulation of feeding behaviour (Figure 6.1, see below for detailed descriptions of these circuits). However, much work remains to be done to determine how AGRP neuron circuits may interact with these other feeding circuits to coordinate food consumption.
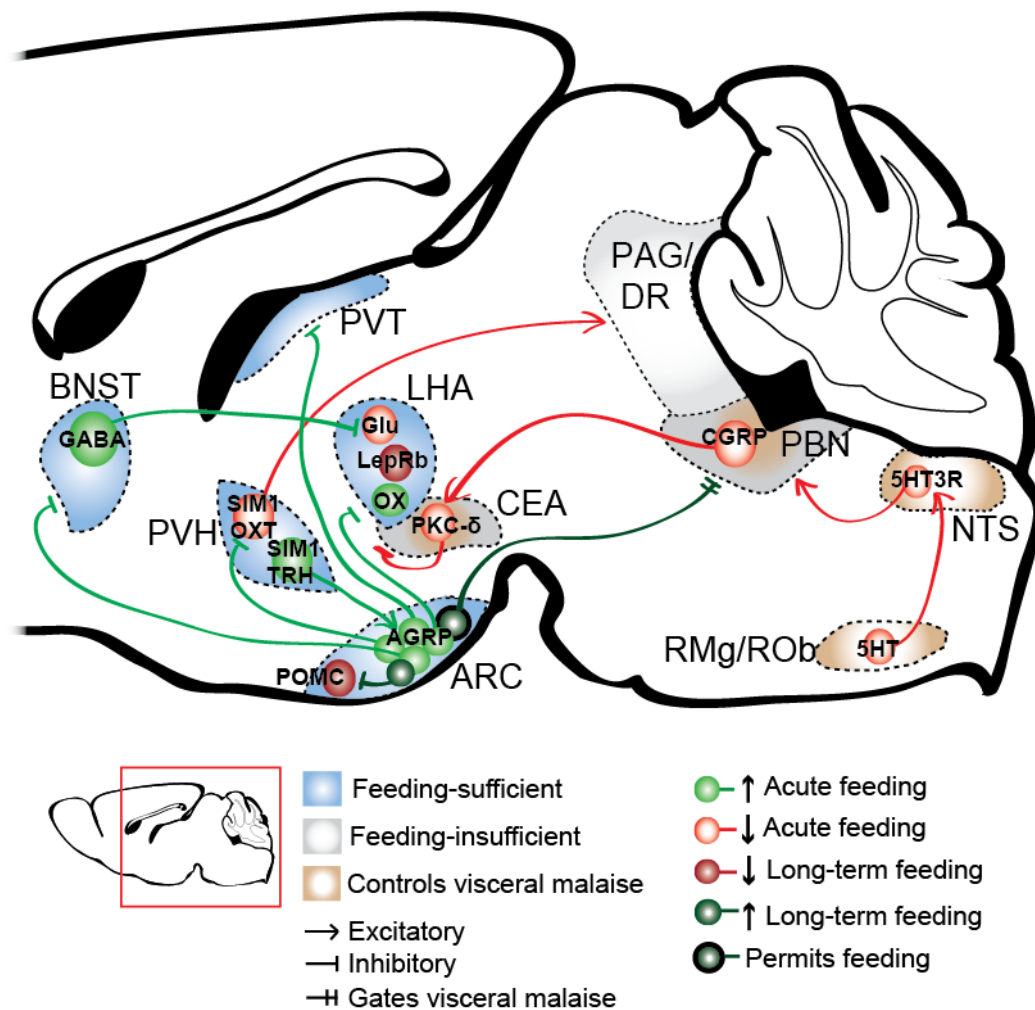
Figure 6.1 Cell types and circuits that influence appetite. Summary diagram illustrating cell types and circuits that control different aspects of food consumption behaviour. Red box in sagittal brain section diagram represents area depicted in this graphic. BNST: bed nucleus of stria terminalis; PVH: paraventricular nucleus of the hypothalamus; PVT: paraventricular thalamic nucleus; LHA: lateral hypothalamic area; ARC: arcuate nucleus; CEA: central nucleus of the amygdala; PAG: periaqueductal grey; DR: dorsal raphe; PBN: parabrachial nucleus; NTS: nucleus of the solitary tract; RMg: raphe magnus nucleus; ROb: raphe obscurus nucleus; AGRP: agouti-related peptide; POMC: proopiomelanocortin; GABA: gamma-aminobutyric acid SIM1: single-minded homolog 1 protein; OXT: oxytocin; TRH: thyrotrophin-releasing hormone; Glu: glutamate; LepRb: leptin receptor; OX: orexin; PKC-δ: protein kinase C- δ; 5HT: serotonin; 5HT3R: serotonin 3 receptor; CGRP: calcitonin gene related peptide.

6.4.1 Differential regulation of food intake by intra-ARC short-range and long-range AGRP neuron circuits

The combined interrogation of intra-ARC short-range and long-range AGRP neuron circuits presented here and in Atasoy et al. (2012) suggests different roles for different circuits. Acute activation of ARC$^{AGRP}\rightarrow$ARC^{POMC} projections inhibits POMC neurons, but this inhibition is unnecessary to evoke feeding behaviour. However, chronic inhibition of POMC neurons does reduce feeding over 24 hrs. In contrast, activation of long range projections to forebrain regions (aBNST, PVH, LHAs and PVT) was capable of recapitulating acute evoked feeding observed with somatic stimulation of AGRP neurons. This reveals differential control of feeding regulation by AGRP neurons, where ARC$^{AGRP}\rightarrow$ARC^{POMC} circuit regulates long term food consumption, while ARC$^{AGRP}\rightarrow$aBNST, ARC$^{AGRP}\rightarrow$PVH, ARC$^{AGRP}\rightarrow$LHAs and ARC$^{AGRP}\rightarrow$PVT exert acute control of appetite. Furthermore, activation of ARC$^{AGRP}\rightarrow$PBN did not elicit acute food consumption (Atasoy et al. 2012), but it is believed to play a permissive role in feeding by suppressing visceral malaise (Wu et al. 2009, Wu et al. 2012). Further examination of ARC$^{AGRP}\rightarrow$CEA and ARC$^{AGRP}\rightarrow$PAG feeding-insufficient circuits may reveal new regulatory roles for AGRP neurons.

6.4.2 Interactions between ARC$^{AGRP}\rightarrow$aBNST and ARC$^{AGRP}\rightarrow$LHA feeding circuits with BNST$^{Vgat}\rightarrow$LHA^{Vglut2} feeding circuit

Jennings et al. (2013) recently reported that inhibitory output from the bed nucleus of stria terminalis (BNST) to the LHA plays a role in feeding, since photostimulation of axonal projections in the LHA of vesicular GABA transporter (Vgat) expressing neurons in the BNST increased feeding in sated animals during the light period, while photoinhibition reduced feeding in food deprived mice. Interestingly, my studies here indicate that photoactivation of AGRP$_{aBNST}$ neurons, which should inhibit the aBNST as AGRP neurons are GABAergic, also induced feeding in well-fed animals. It is currently unclear what post-synaptic cell-types in the aBNST AGRP$_{aBNST}$ neurons might be acting on, whether ARC$^{AGRP}\rightarrow$aBNST circuit is connected to BNST$^{Vgat}\rightarrow$LHA circuit through intra-BNST connections, or whether ARC$^{AGRP}\rightarrow$aBNST evoked feeding is elicited through a separate downstream circuit.

In addition, Jennings et al. (2013) found that BNST^{Vgat} neurons exerted their orexigenic effects by inhibiting glutamatergic neurons in the LHA. Inhibition of vesicular glutamate transporter-2 (Vglut2) expressing neurons in the LHA led to an increase in feeding, while activation led to a decrease. It is also unclear whether AGRP$_{LHAs}$ neurons may act on these LHA^{Vglut2} neurons to evoke feeding. The differing timescales to elicit feeding between manipulations of activity of AGRP$_{aBNST}$, AGRP$_{LHAs}$, BNST^{Vgat}, and LHA^{Vglut2} neurons, however, suggest these might be different circuits. Feeding evoked by AGRP neuron stimulation displays latencies on average of ~6 min, while increase in food consumption by BNST^{Vgat} photostimulation and LHA^{Vglut2} photoinhibition was observed in under 1 min (Jennings et al. 2013). Inhibition of LHA^{LepRb} neurons can suppress food intake over longer timescales, but it is unlikely that LHA^{LepRb} neuron may directly modulate LHA^{Vglut2} neurons' ability to evoke feeding through intra-LHA connections, as LHA^{LepRb} neurons' output is believed to be inhibitory (Leinninger et al. 2009). Instead, anatomical studies indicate that LHA^{LepRb} projects significantly onto OX neurons in the LHA (Leinninger et al. 2011, Louis et al. 2010), which are glutamatergic (Rosin et al. 2003). However, functional connectivity has not yet been established between these two types of neurons, and the behavioural evaluation of this circuit has not been performed, so the role of this circuit is unknown. Although photoactivation of OX neurons does lead to an acute increase in food intake, it also elevated locomotor activity and drinking behaviour (Inutsuka et al. 2014), indicating increase in food intake is due to non-specific behavioural activation, supporting their role in arousal (Alexandre et al. 2013, Tsujino & Sakurai 2013). However, it is still possible that feeding might be under the control of a specific subset of OX neurons, potentially marked by the expression of other neurotransmitters, although this has not been investigated to date.

6.4.3 Potential modulation of PVH^{SIM1}→PAGvl/DR circuit by ARC^{AGRP}→PAG feeding-insufficient circuit

Atasoy et al. (2012) established that ARC^{AGRP}→PVH evoked feeding is mediated by single-minded homolog 1 protein (SIM1) neurons in the PVH, since chemogenetic inhibition of these neurons recapitulated the elevated feeding

observed by stimulation of ARC^{AGRP}→PVH axons. Further studies by the Sternson group investigating the relevant downstream projections of PVH^{SIM1} neurons in this evoked feeding behaviour using chemogenetic inhibition of their axons located a feeding hot spot centred in the caudal ventrolateral portion of the PAG (PAGvl) and the dorsal raphe (DR) (Stachniak et al. 2014). Although not directly tested, the group suggests that PVH^{SIM1}→PAGvl/DR may be excitatory, as many PVH neurons express Vglut2 and disruption of glutamate signalling by PVH^{SIM1} neurons can lead to hypophagia (Xu et al. 2013). Therefore, AGRP neurons induce feeding through the suppression of excitatory inputs to the hindbrain. It is also possible that this response might be mediated, at least partially, through oxytocin (OXT), as AGRP neurons are synaptically connected to PVH^{OXT} neurons and coactivation of these neurons with AGRP neuron axons in the region led to a reduction in AGRP neuron evoked-feeding (Atasoy et al. 2012). In the PAG, OXT was found to increase neuronal activity (Ogawa et al. 1992), and OXT receptors are known to be expressed in the DR (Spaethling et al. 2014). Interestingly, inhibition of the PAG through excitation of ARC^{AGRP}→PAG projections did not elicit feeding on its own. It is unclear whether PVH^{SIM1}→PAGvl/DR and ARC^{AGRP}→PAG projections converge onto the same post-synaptic targets, but significant levels of ARC^{AGRP}→PAG axons are found in the caudal ventromedial and ventrolateral portions of the PAG.

6.4.4 Opposing modulation of feeding from PVH efferent circuits

A study investigating the upstream circuits regulating AGRP neuron activity found that the PVH was a major source of glutamatergic input to AGRP neurons. This excitatory input to AGRP neurons was mediated by thyrotrophin-releasing hormone (TRH) expressing neurons and pituitary adenylate cyclase-activating polypeptide (PACAP) expressing neurons. Chemogenetic activation of either PVH^{TRH} or PVH^{PACAP} neurons (which might not represent completely distinct subpopulations) rapidly evoked feeding behaviour. In addition, PVH^{TRH} mediated evoked feeding was blunted by silencing of AGRP neurons, demonstrating an orexigenic PVH^{TRH}→ARC^{AGRP} circuit in the control of feeding (Krashes et al. 2014). These were unexpected results as silencing of SIM1 neurons, which are glutamatergic and comprises most PVH neurons, also evoked feeding. This might represent the

differing roles in feeding between cell-types within the PVH, where promotion of food intake is driven by PVH^{TRH} and PVH^{PACAP} neurons, while suppression is mediated by PVH^{OXT} neurons (Atasoy et al. 2012). It is unclear whether intra-PVH connectivity between these neurons exists to regulate these opposing circuits. In addition, it is possible that PVH^{THR}→ARC^{AGRP} circuit might not elicit feeding through downstream PVH silencing. Krashes et al. (2014) did not identify whether PVH^{TRH} and PVH^{PACAP} project specifically to AGRP$_{PVH}$ neurons, and activation of ARC^{AGRP}→aBNST, ARC^{AGRP}→LHAs, and to a lesser extent, ARC^{AGRP}→PVT circuits was also capable of evoking voracious food intake.

6.4.5 Prospective modulation of PBelo^{CGRP}→CEAlc$^{PKC-δ}$ circuit by feeding-insufficient ARC^{AGRP}→CEA circuit

Recent examination of the anorexia feeding circuit, which indicated that serotonergic output by the raphe magnus (RMg) and raphe obscurus (ROb) to the nucleus of the solitary tract (NTS) activates PBN neurons to reduce feeding through visceral malaise, revealed that excitatory output of PBN was mediated by calcitonin-gene related peptide (CGRP) neurons in the external lateral subdivision of the PBN (PBelo). Activation of PBelo^{CGRP} neurons was sufficient to suppress baseline feeding and feeding after 24 hrs of food deprivation. In addition, chronic chemogenetic inhibition of these neurons in AGRP neuron ablated mice prevented starvation in these animals. It was further determined that feeding suppression by activation of PBelo^{CGRP} neurons was mediated through projections to the lateral capsular division of the CEA (CEAlc), as photoactivation of PBelo^{CGRP}→CEAlc axons resulted in the same inhibition of feeding as PBelo^{CGRP} soma activation (Carter et al. 2013). A separate study demonstrated that PBelo^{CGRP} exert their anorexigenic effects through activation of protein kinase C-δ (PKC-δ) expressing neurons in the CEAlc, as optogenetic activation of CEAlc$^{PKC-δ}$ neurons inhibited food intake acutely. This effect is believed to be mediated through intra-CEA inhibition by CEAlc$^{PKC-δ}$ neurons (Cai et al. 2014). Although it is unclear whether inhibitory AGRP$_{CEA}$ neurons synapse with CEAlc$^{PKC-δ}$ neurons, inhibition of CEA through photoactivation of ARC^{AGRP}→CEA projections did not evoke feeding, similar to results observed with activation of ARC^{AGRP}→PBN projections. Therefore, the possibility that ARC^{AGRP}→CEA circuit

also plays a role in the gating of visceral malaise, like ARC^{AGRP}→PBN circuit, should be examined.

6.5 Negative reinforcement and its relevance to eating disorders

My studies on the reinforcement properties of AGRP neuron presented in chapter 4 indicate that these neurons employ a negative reinforcement teaching signal to direct feeding behaviour. Under homeostatic hunger, elevated AGRP neuron activity creates a negative internal affective state, eliciting food seeking and consumption, with the ultimate goal of ingesting nutrients to eliminate the aversive state. Furthermore, together with studies by Betley et al. (2014), this mechanism can direct action selection and food choice during consumption, where actions that lead to ingestion of nutrients capable of reducing AGRP neuron activity are maintained, while those that don't are discontinued. Energy deficit can also regulate behaviour through positive reinforcement or negative reinforcement mechanisms employed by other feeding circuits, as low effort actions were maintained under AGRP negative reinforcement signal disruption, and disruption of this signal alone under food deprivation did not extinguish previously reinforced actions. Therefore, under homeostatic hunger, negative and positive reinforcement processes are expected to operate in a concerted manner by controlling state-driven and incentive-driven responding, respectively. These results highlight the importance of homeostatic neuron circuits in the regulation of reinforcement learning.

The exact circuits mediating this negative reinforcement signal are unknown, although it is likely to be mediated through the DAergic system and other brain regions previously implicated in reinforcement learning, such as the basolateral amygdala (BLA) and the prelimbic cortex (Cardinal et al. 2002). Although AGRP neurons do not directly innervate many of these regions, it is possible that AGRP neurons influence these circuits through secondary nodes. Feeding-sufficient AGRP neuron projection regions (aBNST, PVH, LHAs, and PVT) are expected to be involved in this regulation. However, feeding-insufficient regions may also modulate negative reinforcement processes, as they may provide regulatory inputs to feeding-sufficient regions. Aberrations in negative reinforcement processes and downstream circuit function, therefore, can be the source of anomalous food consumption

behaviours leading to obesity or the development of other eating disorders such as anorexia. In drug addiction, negative affect associated with withdrawal symptoms, which are believed to be mediated in part by lowered dopamine (DA) signalling, are thought to negatively reinforce drug-seeking behaviours to relief the aversive feeling of decreased DA neuron function (Koob & Le Moal 1997). This reward deficiency theory (Figlewicz 2003, Kenny 2011) has also been proposed to be the source of "food addiction" (Randolph 1956, Smith & Robbins 2013) that leads to the development of obesity. Disregulation of the DAergic system is also believed to contribute to the behavioural profile of anorexia nervosa (Kaye et al. 2013). Understanding the neurocircuitry involved in regulating negative reinforcement, therefore, is consequential for the development of therapeutics for the treatment of eating disorders.

6.6 Utility of the distinction of positive and negative reinforcement processes of homeostatic hunger

The continued use of the distinction between negative and positive reinforcement processes to guide behaviour has been questioned throughout the years (Baron & Galizio 2005, Michael 1975). Traditionally, this distinction was created to accommodate the introduction of differing motivational variables (Hilgard & Marquis 1940, Mowrer 1960, Thorndike 1898) that either produced pleasure of satisfaction or reduced discomfort or distress (Baron & Galizio 2005). However, in both cases, actions produce a change from one condition to another (Michael 1975). Therefore, behaviour modulation by reinforcement can be explained by changes in expected outcomes, without the need for the distinction between positive and negative reinforcement, such as through prediction error theories (Schultz et al. 1997).

However, these psychological distinctions can be important in relation to the development of behavioural therapies for food consumption disorders. The negative characteristics of elevated AGRP neuron activity are also consistent with human self-reports of negative feelings associated with hunger arising from homeostatic deficits (Keys et al. 1950). The characteristics of AGRP neuron activity in mice, therefore, parallel some negative emotional aspects of diet restrictions in humans, which

contribute to low long-term behavioural compliance (Stunkard & Rush 1974, Wadden et al. 1986) and the failure to maintain weight loss. The negative reinforcement mechanism of directed food seeking and consumption discussed above may underlie the failure of continued compliance of dieting, where caloric intake is reduced or consumption of nutritive food is replaced by low or non-caloric substances. It has been shown, for example, that food deprived mice are unwilling to work (through lever presses), for saccharine and other sweet tasting non-caloric rewards, while lever presses for sucrose, which is both sweet and contains caloric value, is enhanced across days (Beeler et al. 2012b). The experiments presented here and conducted by other groups show that homeostatic neurons that control feeding behaviour, such as AGRP neurons, provide an entry point to investigate the relationship between metabolism and negative emotional states. Future studies using circuit mapping approaches to identify the downstream circuit elements mediating the negative emotional consequences of hunger should provide a platform for the development of therapies to combat obesity and other eating disorders.

6.7 Limitations of studies and techniques employed

The studies presented here are subject to a number of limitations. Most studies using optogenetic techniques are liable to general technical issues. In particular, light delivery to deep brain structures require the surgical implantation of optic fibres, which lead to damage of brain structures in the path of the implanted fibre, including cortical and thalamic regions. In addition, prolonged stimulation can lead to heating of brain tissue, which in turn can create tissue damage or produce non-specific behavioural effects (Yizhar et al. 2011). In order to control for any non-specific effects of damage due to fibre implantation, all control animals employed in my studies also received fibre implantation. In general, no obvious motor impairments were observed, but it is unclear how tissue damage from the implanted fibre and heating from photostimulation might affect behavioural output. Although the level of brain tissue damage in my experimental animals was not directly quantified, no overt anatomical changes, such as cell density and morphology, where observed in target regions. Some studies quantifying the level of tissue damage due to implantation of other similar devices in the brain, including electrodes

and prisms, indicate that small but significant changes in cell density are observed only within 150 μm of the implanted object (Andermann et al. 2013, Biran et al. 2005, Chia & Levene 2009). Better understanding of the extent of tissue damage due to the fibre implant and photostimulation induced heating can be acquired through more thorough histological evaluation, including haematoxylin, eosin, Nissl and DAPI stains, to understand cell density and morphology around the implant and in target regions. In addition, quantification of astrocyte and microglia density through G-FAP and CD11b can determine provide a sense of the level of tissue trauma in the vicinity of the implant and target regions. The development of light sensitive opsins in the far red spectrum are expected to eliminate some of these current issues, as they reduce the possibility of light-induced tissue damage and introduce the possibility of delivering light through the intact skull (Chuong et al. 2014).

In addition, optogenetic techniques employ bulk stimulation which synchronizes firing patterns in the target population, which may drive circuits into unphysiological patterns of activity (Hausser 2014). For AGRP neurons, for example, although Fos expression studies presented here show that signals of low energetic state activate projection-specific subpopulations in a similar manner, it is likely the actual firing pattern between and within subpopulations are variable. Furthermore, this technique employs the indiscriminate activation of a genetically defined population, which is problematic. This is particularly relevant to studies presented here on LHA^{LepRb} neurons. Although a large number of LHA^{LepRb} neurons where shown to depolarize in response to leptin, some LHA^{LepRb} neurons were either hyperpolarized by leptin, or showed no responses in slice recording (Leinninger et al. 2009). This suggest that this population of neurons can be further subdivided into distinct subpopulations, and therefore, optogenetic stimulation studies alone do not appropriately reflect activity patterns of this neuronal population under states of satiety, such as during elevated circulating leptin conditions. Future studies using single cell RNA sequencing methods (Jaitin et al. 2014) can help refine the definition of a neuronal population for more selective studies. In addition, *in vivo* calcium imaging and electrophysiological studies can help shed light into the physiological activity patterns of neurons studied, for further refinement of future activity manipulation studies.

Beyond the general caveats and limitations of optogenetic techniques themselves, there are several limitations in the experimental design of the studies presented here. First of all, the stimulation protocol employed here limits the interpretation of my results. The 20 Hz stimulation protocol used to stimulated AGRP neurons was employed in order to mimic activity of these neurons under 24 hr food deprivation conditions and under elevated levels of peripheral signals of energy deficit, such as ghrelin (Aponte et al. 2011, van den Top et al. 2004). Together with the prolonged stimulations employed in my studies (1-2 hrs), these manipulations more closely resemble states of chronic energy deficit and extreme starvation, rather than daily fluctuations of energetic state. Therefore, my results on the mechanisms by which AGRP neurons drive food seeking and consumption behaviours are limited to states of starvation, and might not appropriately explain food seeking and consumption choice under normal daily food intake conditions.

In addition, studies presented here investigating the reinforcement mechanisms of AGRP neurons suggest that the activity of these neurons serve as a teaching signal to direct action selection in food seeking. Operant studies demonstrated that disruption of this signal lead to a gradual reduction of previously reinforced food seeking actions (lever pressing). However, these studies did not investigate whether animals might engage in other actions to reduce AGRP neuron activity, as animals were not provided the opportunity to perform other tasks to reduce AGRP neuron activity. Future studies with more enriched environments would allow for better observation of behavioural flexibility and action selection. Likewise, this negative reinforcement model proposes that actions are selected based on their ability to inhibit AGRP neuron activity, but this was not directly investigated here. Operant studies in which animals perform a task to either shut-off AGRP neuron photostimulation under sated conditions or optogenetically inhibit AGRP neuron activity under hunger states can test this hypothesis. Furthermore, this AGRP neuron mediated negative reinforcement model assumes that the consumption of nutrients lead to the reduction of AGRP neuron activity through peripheral signals. However, this was not directly studied and it is still unclear whether AGRP neuron activity is truly modulated in this fashion *in vivo*. It is also possible the activity of these neurons might mediate conditioned anticipatory behaviour and be regulated by the presence of learned cues associated with food,

working as prediction error signals in a manner resembling VTA DA neurons (Schultz et al. 1997, van Zessen et al. 2012), or might be modulated by consummatory behaviour alone, or both. The *in vivo* activity of these neurons under difference energetic states and their change in activity patterns during feeding behaviour is an active area of investigation. Newly developed technologies in calcium imaging and electrophysiological recordings of deep brain structures in awake behaving animals should help determine whether the activity of these neurons is indeed modulated by nutrient ingestion.

Lastly, although the results of studies presented here support the hypothesis that AGRP neurons employ a negative reinforcement mechanism to drive feeding, the possibility that these neurons might also, to a lesser extent, employ positive reinforcement mechanisms cannot be ruled out. Disruption of this AGRP neuron mediated teaching signal under free food consumption conditions, for example, was not sufficient to reduce food intake, which suggest positive reinforcement based on the nutritive value of food is still present, and might be mediated by AGRP neuron activity. Therefore, taste reactivity studies (Grill & Norgren 1978, Schultz et al. 1997, van Zessen et al. 2012) can help understand how elevated AGRP neuron activity might modulate the perceived palatability of food. In addition, it is also unclear what effect diet composition or highly palatable foods, such as high fat high sugar diets, might shape the observed effects. Further studies addressing the issues highlighted here will therefore provide a more comprehensive understanding on the mechanisms in which AGRP neuron modulate and direct food seeking and consumption.

6.8 Concluding remarks

The experimental approaches used in studies presented in this dissertation, as well as in studies by others, to identify and evaluate the function of homeostatic feeding neurons and their circuits have significantly aided in the study of the control of feeding behaviour. As a whole, these studies have unravelled many circuits through which the brain controls food intake, providing an emerging picture of the organization and complexity of the regulation of survival driven behaviours such as feeding. Continued investigation will allow us to create a complete map of the brain processes that control feeding behaviour. This is an important step for the

development of treatments for eating disorders, as well as to uncover the psychological principles that guide behaviour for the purpose of survival.

List of References

Ackroff K, Dym C, Yiin YM, & Sclafani A. 2009. Rapid acquisition of conditioned flavor preferences in rats. *Physiology & Behavior* 97: 406-13

Adan RA, Cone RD, Burbach JP, & Gispen WH. 1994. Differential effects of melanocortin peptides on neural melanocortin receptors. *Molecular Pharmacology* 46: 1182-90

Ahima RS, Prabakaran D, Mantzoros C, Qu D, Lowell B, Maratos-Flier E, & Flier JS. 1996. Role of leptin in the neuroendocrine response to fasting. *Nature* 382: 250-2

Ahlskog JE, & Hoebel BG. 1973. Overeating and obesity from damage to a noradrenergic system in the brain. *Science* 182: 166-9

Albrecht J, Schreder T, Kleemann AM, Schopf V, Kopietz R, Anzinger A, Demmel M, Linn J, Kettenmann B, & Wiesmann M. 2009. Olfactory detection thresholds and pleasantness of a food-related and a non-food odour in hunger and satiety. *Rhinology* 47: 160-5

Alexander GM, Rogan SC, Abbas AI, Armbruster BN, Pei Y, Allen JA, Nonneman RJ, Hartmann J, Moy SS, Nicolelis MA, McNamara JO, & Roth BL. 2009. Remote control of neuronal activity in transgenic mice expressing evolved G protein-coupled receptors. *Neuron* 63: 27-39

Alexandre C, Andermann ML, & Scammell TE. 2013. Control of arousal by the orexin neurons. *Current Opinion in Neurobiology* 23: 752-9

Anand BK, & Brobeck JR. 1951a. Hypothalamic control of food intake in rats and cats. *The Yale Journal of Biology and Medicine* 24: 123-40

Anand BK, & Brobeck JR. 1951b. Localization of a "feeding center" in the hypothalamus of the rat. *Proceedings of The Society for Experimental Biology and Medicine* 77: 323-4

Andermann ML, Gilfoy NB, Goldey GJ, Sachdev RN, Wolfel M, McCormick DA, Reid RC, & Levene MJ. 2013. Chronic cellular imaging of entire cortical columns in awake mice using microprisms. *Neuron* 80: 900-13

Aponte Y, Atasoy D, & Sternson SM. 2011. AGRP neurons are sufficient to orchestrate feeding behavior rapidly and without training. *Nature Neuroscience* 14: 351-5

Aravanis AM, Wang LP, Zhang F, Meltzer LA, Mogri MZ, Schneider MB, & Deisseroth K. 2007. An optical neural interface: in vivo control of rodent motor cortex with integrated fiberoptic and optogenetic technology. *Journal of Neural Engineering* 4: S143-56

Aravich PF, & Sclafani A. 1983. Paraventricular hypothalamic lesions and medial hypothalamic knife cuts produce similar hyperphagia syndromes. *Behavioral Neuroscience* 97: 970-83

Armbruster BN, Li X, Pausch MH, Herlitze S, & Roth BL. 2007. Evolving the lock to fit the key to create a family of G protein-coupled receptors potently activated by an inert ligand. *Proceedings of the National Academy of Sciences of the United States of America* 104: 5163-8

Asakawa A, Inui A, Kaga T, Yuzuriha H, Nagata T, Ueno N, Makino S, Fujimiya M, Niijima A, Fujino MA, & Kasuga M. 2001. Ghrelin is an appetite-stimulatory signal from stomach with structural resemblance to motilin. *Gastroenterology* 120: 337-45

Atalayer D, Robertson KL, Haskell-Luevano C, Andreasen A, & Rowland NE. 2010. Food demand and meal size in mice with single or combined disruption of melanocortin type 3 and 4 receptors. *American Journal of Physiology. Regulatory, Integrative and Comparative Physiology* 298: R1667-74

Atasoy D, Aponte Y, Su HH, & Sternson SM. 2008. A FLEX switch targets Channelrhodopsin-2 to multiple cell types for imaging and long-range circuit mapping. *The Journal of Neuroscience* 28: 7025-30

Atasoy D, Betley JN, Li WP, Su HH, Scheffer L, Fetter R, & S.M. S. 2014. A genetically specified connectomics approach applied to long-range feeding regulatory circuits. *Nature Neuroscience* 17: 1830-39

Atasoy D, Betley JN, Su HH, & Sternson SM. 2012. Deconstruction of a neural circuit for hunger. *Nature* 488: 172-7

Balthasar N, Dalgaard LT, Lee CE, Yu J, Funahashi H, Williams T, Ferreira M, Tang V, McGovern RA, Kenny CD, Christiansen LM, Edelstein E, Choi B, Boss O, Aschkenasi C, Zhang CY, Mountjoy K, Kishi T, Elmquist JK, & Lowell BB. 2005. Divergence of melanocortin pathways in the control of food intake and energy expenditure. *Cell* 123: 493-505

Baron A, & Galizio M. 2005. Positive and negative reinforcement: Should the distinction be preserved? *The Behavior Analyst / MABA* 28: 85-98

Barsh GS, & Schwartz MW. 2002. Genetic approaches to studying energy balance: perception and integration. *Nature Review Genetics* 3: 589-600

Bass CE, Grinevich VP, Vance ZB, Sullivan RP, Bonin KD, & Budygin EA. 2010. Optogenetic control of striatal dopamine release in rats. *Journal of Neurochemistry* 114: 1344-52

Beeler JA, Daw N, Frazier CR, & Zhuang X. 2010. Tonic dopamine modulates exploitation of reward learning. *Frontiers in Behavioral Neuroscience* 4: 170

Beeler JA, Frazier CR, & Zhuang X. 2012a. Dopaminergic enhancement of local food-seeking is under global homeostatic control. *The European Journal of Neuroscience* 35: 146-59

Beeler JA, McCutcheon JE, Huang Cao ZF, Murakami M, Alexander E, Roitman MF, & Zhuang X. 2012b. Taste uncoupled from nutrition fails to sustain the reinforcing properties of food. *The European Journal of Neuroscience* 36: 2533-46

Bellinger LL, Mendel VE, Bernardis LL, & Castonguay TW. 1986. Meal patterns of rats with dorsomedial hypothalamic nuclei lesions or sham operations. *Physiology & Behavior* 36: 693-8

Bernard C. 1859. *Leçons sur les propriétés physiologiques et les altérations pathologiques des liquides de l'organisme*. Paris: Baillière.

Berridge KC. 2004. Motivation concepts in behavioral neuroscience. *Physiology & Behavior* 81: 179-209

Betley JN, Huang Cao ZF, Gong R, Magnus CJ, & Sternson SM. 2014. Homeostatic neurons for hunger and thirst transmit a negative reinforcement teaching signal. *In review*

Betley JN, Huang Cao ZF, Ritola KD, & Sternson SM. 2013. Parallel, redundant circuit organization for homeostatic control of feeding behavior. *Cell* 155: 1337-50

Betley JN, & Sternson SM. 2011. Adeno-associated viral vectors for mapping, monitoring, and manipulating neural circuits. *Human Gene Therapy* 22: 669-77

Bindra D. 1976. *A theory of intelligent behavior*. New York: Wiley. vii, p. 447

Binzegger T, Douglas RJ, & Martin KA. 2004. A quantitative map of the circuit of cat primary visual cortex. *The Journal of Neuroscience* 24: 8441-53

Biran R, Martin DC, & Tresco PA. 2005. Neuronal cell loss accompanies the brain tissue response to chronically implanted silicon microelectrode arrays. *Experimental Neurology* 195: 115-26

Bjorbaek C, Elmquist JK, Michl P, Ahima RS, van Bueren A, McCall AL, & Flier JS. 1998. Expression of leptin receptor isoforms in rat brain microvessels. *Endocrinology* 139: 3485-91

Bjorbak C, Lavery HJ, Bates SH, Olson RK, Davis SM, Flier JS, & Myers MG, Jr. 2000. SOCS3 mediates feedback inhibition of the leptin receptor via Tyr985. *The Journal of Biological Chemistry* 275: 40649-57

Boyden ES, Zhang F, Bamberg E, Nagel G, & Deisseroth K. 2005. Millisecond-timescale, genetically targeted optical control of neural activity. *Nature Neuroscience* 8: 1263-8

Branson K, Robie AA, Bender J, Perona P, & Dickinson MH. 2009. High-throughput ethomics in large groups of Drosophila. *Nature Methods* 6: 451-7

Bray GA. 2000. Afferent signals regulating food intake. *The Proceedings of the Nutrition Society* 59: 373-84

Brecher G, & Waxler SH. 1949. Obesity in albino mice due to single injections of goldthioglucose. *Proceedings of The Society for Experimental Biology and Medicine* 70: 498-501

Brief DJ, & Davis JD. 1984. Reduction of food intake and body weight by chronic intraventricular insulin infusion. *Brain Research Bulletin* 12: 571-5

Brobeck JR, Tepperman J, & Long CN. 1943. Experimental Hypothalamic Hyperphagia in the Albino Rat. *The Yale Journal of Biology and Medicine* 15: 831-53

Bromberg-Martin ES, Matsumoto M, & Hikosaka O. 2010. Dopamine in motivational control: rewarding, aversive, and alerting. *Neuron* 68: 815-34

Brosvic GM, & Hoey NE. 1990. Dietary sodium deprivation does not alter taste sensitivity in the rat. *Physiology & Behavior* 47: 881-8

Bullitt E. 1990. Expression of c-fos-like protein as a marker for neuronal activity following noxious stimulation in the rat. *The Journal of Comparative Neurology* 296: 517-30

Burdakov D, Gerasimenko O, & Verkhratsky A. 2005a. Physiological changes in glucose differentially modulate the excitability of hypothalamic melanin-concentrating hormone and orexin neurons in situ. *The Journal of neuroscience* 25: 2429-33

Burdakov D, Karnani MM, & Gonzalez A. 2013. Lateral hypothalamus as a sensor-regulator in respiratory and metabolic control. *Physiology & Behavior* 121: 117-24

Burdakov D, Luckman SM, & Verkhratsky A. 2005b. Glucose-sensing neurons of the hypothalamus. *Philosophical Transactions of the Royal Society of London. Series B, Biological Sciences* 360: 2227-35

Cai H, Haubensak W, Anthony TE, & Anderson DJ. 2014. Central amygdala PKC-delta neurons mediate the influence of multiple anorexigenic signals. *Nature Neuroscience* 9:1240-8

Cannon WB. 1915. *Bodily changes in pain, hunger, fear, and rage; an account of recent researches into the function of emotional excitement.* New York, London: D. Appleton and Company. xiii, p.311

Cannon WB. 1932. *The wisdom of the body.* New York: W.W. Norton & Company, Inc. xv p. 19-312

Cannon WB, & Washburn AL. 1912. An explanation of hunger. *American Journal of Physiology* 29: 441-54

Cardinal RN, Parkinson JA, Hall J, & Everitt BJ. 2002. Emotion and motivation: the role of the amygdala, ventral striatum, and prefrontal cortex. *Neuroscience and Biobehavioral Reviews* 26: 321-52

Caro JF, Kolaczynski JW, Nyce MR, Ohannesian JP, Opentanova I, Goldman WH, Lynn RB, Zhang PL, Sinha MK, & Considine RV. 1996. Decreased cerebrospinal-fluid/serum leptin ratio in obesity: a possible mechanism for leptin resistance. *Lancet* 348: 159-61

Carter ME, Soden ME, Zweifel LS, & Palmiter RD. 2013. Genetic identification of a neural circuit that suppresses appetite. *Nature* 503: 111-4

Casada JH, & Dafny N. 1991. Restraint and stimulation of bed nucleus of the stria terminalis produce similar stress-like behaviors. *Brain Research Bulletin* 27: 207-12

Chalasani SH, Kato S, Albrecht DR, Nakagawa T, Abbott LF, & Bargmann CI. 2010. Neuropeptide feedback modifies odor-evoked dynamics in Caenorhabditis elegans olfactory neurons. *Nature Neuroscience* 13: 615-21

Challis BG, Coll AP, Yeo GS, Pinnock SB, Dickson SL, Thresher RR, Dixon J, Zahn D, Rochford JJ, White A, Oliver RL, Millington G, Aparicio SA, Colledge WH, Russ AP, Carlton MB, & O'Rahilly S. 2004. Mice lacking pro-opiomelanocortin are sensitive to high-fat feeding but respond normally to the acute anorectic effects of peptide-YY(3-36). *Proceedings of the National Academy of Sciences of the United States of America* 101: 4695-700

Chen H, Charlat O, Tartaglia LA, Woolf EA, Weng X, Ellis SJ, Lakey ND, Culpepper J, Moore KJ, Breitbart RE, Duyk GM, Tepper RI, & Morgenstern JP. 1996. Evidence that the diabetes gene encodes the leptin receptor: identification of a mutation in the leptin receptor gene in db/db mice. *Cell* 84: 491-5

Chia TH, & Levene MJ. 2009. Microprisms for in vivo multilayer cortical imaging. *Journal of Neurophysiology* 102: 1310-4

Choi DC, Evanson NK, Furay AR, Ulrich-Lai YM, Ostrander MM, & Herman JP. 2008. The anteroventral bed nucleus of the stria terminalis differentially regulates hypothalamic-pituitary-adrenocortical axis responses to acute and chronic stress. *Endocrinology* 149: 818-26

Chow BY, Han X, Dobry AS, Qian X, Chuong AS, Li M, Henninger MA, Belfort GM, Lin Y, Monahan PE, & Boyden ES. 2010. High-performance genetically targetable optical neural silencing by light-driven proton pumps. *Nature* 463: 98-102

Chronwall BM. 1985. Anatomy and physiology of the neuroendocrine arcuate nucleus. *Peptides* 6 Suppl 2: 1-11

Chua SC, Jr., Chung WK, Wu-Peng XS, Zhang Y, Liu SM, Tartaglia L, & Leibel RL. 1996. Phenotypes of mouse diabetes and rat fatty due to mutations in the OB (leptin) receptor. *Science* 271: 994-6

Chuong AS, Miri ML, Busskamp V, Matthews GA, Acker LC, Sorensen AT, Young A, Klapoetke NC, Henninger MA, Kodandaramaiah SB, Ogawa M, Ramanlal SB, Bandler RC, Allen BD, Forest CR, Chow BY, Han X, Lin Y, Tye KM, Roska B, Cardin JA, & Boyden ES. 2014. Noninvasive optical inhibition with a red-shifted microbial rhodopsin. *Nature Neuroscience* 17: 1123-9

Clark JT, Kalra PS, Crowley WR, & Kalra SP. 1984. Neuropeptide Y and human pancreatic polypeptide stimulate feeding behavior in rats. *Endocrinology* 115: 427-9

Coleman DL, & Hummel KP. 1969. Effects of parabiosis of normal with genetically diabetic mice. *The American Journal of Physiology* 217: 1298-304

Coll AP, Farooqi IS, & O'Rahilly S. 2007. The hormonal control of food intake. *Cell* 129: 251-62

Comoli E, Ribeiro-Barbosa ER, & Canteras NS. 2003. Predatory hunting and exposure to a live predator induce opposite patterns of Fos immunoreactivity in the PAG. *Behavioural Brain Research* 138: 17-28

Conklin BR, Hsiao EC, Claeysen S, Dumuis A, Srinivasan S, Forsayeth JR, Guettier JM, Chang WC, Pei Y, McCarthy KD, Nissenson RA, Wess J, Bockaert J, & Roth BL. 2008. Engineering GPCR signaling pathways with RASSLs. *Nature Methods* 5: 673-8

Considine RV, Sinha MK, Heiman ML, Kriauciunas A, Stephens TW, Nyce MR, Ohannesian JP, Marco CC, McKee LJ, Bauer TL, & et al. 1996. Serum immunoreactive-leptin concentrations in normal-weight and obese humans. *The New England Journal of Medicine* 334: 292-5

Cools R, Nakamura K, & Daw ND. 2011. Serotonin and dopamine: unifying affective, activational, and decision functions. *Neuropsychopharmacology* 36: 98-113

Cowley MA, Smart JL, Rubinstein M, Cerdan MG, Diano S, Horvath TL, Cone RD, & Low MJ. 2001. Leptin activates anorexigenic POMC neurons through a neural network in the arcuate nucleus. *Nature* 411: 480-4

Cowley MA, Smith RG, Diano S, Tschop M, Pronchuk N, Grove KL, Strasburger CJ, Bidlingmaier M, Esterman M, Heiman ML, Garcia-Segura LM, Nillni EA, Mendez P, Low MJ, Sotonyi P, Friedman JM, Liu H, Pinto S, Colmers WF, Cone RD, & Horvath TL. 2003. The distribution and mechanism of action of ghrelin in the CNS demonstrates a novel hypothalamic circuit regulating energy homeostasis. *Neuron* 37: 649-61

Cullinan WE, Herman JP, & Watson SJ. 1993. Ventral subicular interaction with the hypothalamic paraventricular nucleus: evidence for a relay in the bed nucleus of the stria terminalis. *The Journal of Comparative Neurology* 332: 1-20

Czupryn A, Zhou YD, Chen X, McNay D, Anderson MP, Flier JS, & Macklis JD. 2011. Transplanted hypothalamic neurons restore leptin signaling and ameliorate obesity in db/db mice. *Science* 334: 1133-7

Date Y, Kojima M, Hosoda H, Sawaguchi A, Mondal MS, Suganuma T, Matsukura S, Kangawa K, & Nakazato M. 2000. Ghrelin, a novel growth hormone-releasing acylated peptide, is synthesized in a distinct endocrine cell type in the gastrointestinal tracts of rats and humans. *Endocrinology* 141: 4255-61

Davidson TL. 1987. Learning about deprivation intensity stimuli. *Behavioral Neuroscience* 101: 198-208

Davis JD, Gallagher RL, & Ladove R. 1967. Food intake controlled by a blood factor. *Science* 156: 1247-8

Davis JF, Choi DL, Schurdak JD, Fitzgerald MF, Clegg DJ, Lipton JW, Figlewicz DP, & Benoit SC. 2011. Leptin regulates energy balance and motivation through action at distinct neural circuits. *Biological Psychiatry* 69: 668-74

Davis M, Walker DL, & Lee Y. 1997. Amygdala and bed nucleus of the stria terminalis: differential roles in fear and anxiety measured with the acoustic startle reflex. *Philosophical Transactions of the Royal Society of London. Series B, Biological Sciences* 352: 1675-87

Dayan P, & Huys QJ. 2009. Serotonin in affective control. *Annual Review of Neuroscience* 32: 95-126

de Araujo IE, Oliveira-Maia AJ, Sotnikova TD, Gainetdinov RR, Caron MG, Nicolelis MA, & Simon SA. 2008. Food reward in the absence of taste receptor signaling. *Neuron* 57: 930-41

DeFalco J, Tomishima M, Liu H, Zhao C, Cai X, Marth JD, Enquist L, & Friedman JM. 2001. Virus-assisted mapping of neural inputs to a feeding center in the hypothalamus. *Science* 291: 2608-13

Delgado JM, & Anand BK. 1953. Increase of food intake induced by electrical stimulation of the lateral hypothalamus. *American Journal of Physiology* 172: 162-8

Dhillon H, Zigman JM, Ye C, Lee CE, McGovern RA, Tang V, Kenny CD, Christiansen LM, White RD, Edelstein EA, Coppari R, Balthasar N, Cowley MA, Chua S, Jr., Elmquist JK, & Lowell BB. 2006. Leptin directly activates SF1 neurons in the VMH, and this action by leptin is required for normal body-weight homeostasis. *Neuron* 49: 191-203

Dickinson AB, B. 2002. The Role of Learning in the Operation of Motivational Systems. Stevens' Handbook of Experimental Psychology Learning, Motivation, and Emotion. New York: John Wiley & Sons, p. 497-534

Dimicco JA, & Zaretsky DV. 2007. The dorsomedial hypothalamus: a new player in thermoregulation. *American Journal of Physiology. Regulatory, Integrative and Comparative Physiology* 292: R47-63

DiPatrizio NV, & Simansky KJ. 2008. Activating parabrachial cannabinoid CB1 receptors selectively stimulates feeding of palatable foods in rats. *The Journal of Neuroscience* 28: 9702-9

Dong HW, Petrovich GD, & Swanson LW. 2001. Topography of projections from amygdala to bed nuclei of the stria terminalis. *Brain research. Brain Research Reviews* 38: 192-246

Dornonville de la Cour C, Bjorkqvist M, Sandvik AK, Bakke I, Zhao CM, Chen D, & Hakanson R. 2001. A-like cells in the rat stomach contain ghrelin and do not operate under gastrin control. *Regulatory Peptides* 99: 141-50

Druce MR, Neary NM, Small CJ, Milton J, Monteiro M, Patterson M, Ghatei MA, & Bloom SR. 2006. Subcutaneous administration of ghrelin stimulates energy intake in healthy lean human volunteers. *International Journal of Obesity (London)* 30: 293-6

Eccles J. 1976. From electrical to chemical transmission in the central nervous system. *Notes and Records of the Royal Society of London* 30: 219-30

Eccles JC, Fatt P, & Koketsu K. 1954. Cholinergic and inhibitory synapses in a pathway from motor-axon collaterals to motoneurones. *The Journal of Physiology* 126: 524-62

Elias CF. 2014. A critical view of the use of genetic tools to unveil neural circuits: the case of leptin action in reproduction. *American Journal of Physiology. Regulatory, Integrative and Comparative Physiology* 306: R1-9

Elmquist JK, Coppari R, Balthasar N, Ichinose M, & Lowell BB. 2005. Identifying hypothalamic pathways controlling food intake, body weight, and glucose homeostasis. *The Journal of Comparative Neurology* 493: 63-71

Epstein AN. 1960. Reciprocal changes in feeding behavior produced by intrahypothalamic chemical injections. *The American Journal of Physiology* 199: 969-74

Erickson JC, Clegg KE, & Palmiter RD. 1996. Sensitivity to leptin and susceptibility to seizures of mice lacking neuropeptide Y. *Nature* 381: 415-21

Eskay RL, Giraud P, Oliver C, & Brown-Stein MJ. 1979. Distribution of alpha-melanocyte-stimulating hormone in the rat brain: evidence that alpha-MSH-containing cells in the arcuate region send projections to extrahypothalamic areas. *Brain Research* 178: 55-67

Fan W, Boston BA, Kesterson RA, Hruby VJ, & Cone RD. 1997. Role of melanocortinergic neurons in feeding and the agouti obesity syndrome. *Nature* 385: 165-8

Fanselow MS, & Dong HW. 2010. Are the dorsal and ventral hippocampus functionally distinct structures? *Neuron* 65: 7-19

Farooqi IS, Keogh JM, Yeo GS, Lank EJ, Cheetham T, & O'Rahilly S. 2003. Clinical spectrum of obesity and mutations in the melanocortin 4 receptor gene. *The New England Journal of Medicine* 348: 1085-95

Figlewicz DP. 2003. Adiposity signals and food reward: expanding the CNS roles of insulin and leptin. *American Journal of Physiology. Regulatory, Integrative and Comparative Physiology* 284: R882-92

Figlewicz DP, Bennett JL, Naleid AM, Davis C, & Grimm JW. 2006. Intraventricular insulin and leptin decrease sucrose self-administration in rats. *Physiology & Behavior* 89: 611-6

Figlewicz DP, & Benoit SC. 2009. Insulin, leptin, and food reward: update 2008. *American Journal of Physiology. Regulatory, Integrative and Comparative Physiology* 296: R9-R19

Finger BC, Dinan TG, & Cryan JF. 2010. Progressive ratio responding in an obese mouse model: Effects of fenfluramine. *Neuropharmacology* 59: 619-26

Fioramonti X, Contie S, Song Z, Routh VH, Lorsignol A, & Penicaud L. 2007. Characterization of glucosensing neuron subpopulations in the arcuate nucleus: integration in neuropeptide Y and pro-opio melanocortin networks? *Diabetes* 56: 1219-27

Freud S. 2001. Instincts and their Vicissitudes In *Standard Edition of the Complete Psychological Works of Sigmund Freud*, ed. J Strachey, London: Hogarth Press, p. 111-40

Frohlich A. 1901. *Ein Fall von Tumor der Hypophysis cerebri ohne Akromegalie*. Rundschau: Wien. klin. p. 883-86, 906-08

Fruhbeck G, Jebb SA, & Prentice AM. 1998. Leptin: physiology and pathophysiology. *Clinical Physiology and Functional Imaging* 18: 399-419

Gantz I, & Fong TM. 2003. The melanocortin system. *American Journal of Physiology. Endocrinology and Metabolism* 284: E468-74

Gao Q, & Horvath TL. 2007. Neurobiology of feeding and energy expenditure. *Annual Review of Neuroscience* 30: 367-98

Gao Q, & Horvath TL. 2008. Neuronal control of energy homeostasis. *FEBS Letters* 582: 132-41

Gee CE, Chen CL, Roberts JL, Thompson R, & Watson SJ. 1983. Identification of proopiomelanocortin neurones in rat hypothalamus by in situ cDNA-mRNA hybridization. *Nature* 306: 374-6

Geerling JC, Shin JW, Chimenti PC, & Loewy AD. 2010. Paraventricular hypothalamic nucleus: axonal projections to the brainstem. *The Journal of Comparative Neurology* 518: 1460-99

Gibbs J, Young RC, & Smith GP. 1973. Cholecystokinin elicits satiety in rats with open gastric fistulas. *Nature* 245: 323-5

Gilbert CD. 1983. Microcircuitry of the visual cortex. *Annual Review of Neuroscience* 6: 217-47

Gradinaru V, Mogri M, Thompson KR, Henderson JM, & Deisseroth K. 2009. Optical deconstruction of parkinsonian neural circuitry. *Science* 324: 354-9

Gradinaru V, Zhang F, Ramakrishnan C, Mattis J, Prakash R, Diester I, Goshen I, Thompson KR, & Deisseroth K. 2010. Molecular and cellular approaches for diversifying and extending optogenetics. *Cell* 141: 154-65

Granholm NH, Jeppesen KW, & Japs RA. 1986. Progressive infertility in female lethal yellow mice (Ay/a; strain C57BL/6J). *Journal of Reproduction and Fertility* 76: 279-87

Grill HJ, & Norgren R. 1978. The taste reactivity test. I. Mimetic responses to gustatory stimuli in neurologically normal rats. *Brain Research* 143: 263-79

Gropp E, Shanabrough M, Borok E, Xu AW, Janoschek R, Buch T, Plum L, Balthasar N, Hampel B, Waisman A, Barsh GS, Horvath TL, & Bruning JC. 2005. Agouti-related peptide-expressing neurons are mandatory for feeding. *Nature Neuroscience* 8: 1289-91

Grossman SP. 1960. Eating or drinking elicited by direct adrenergic or cholinergic stimulation of hypothalamus. *Science* 132: 301-2

Hagan MM, Rushing PA, Pritchard LM, Schwartz MW, Strack AM, Van Der Ploeg LH, Woods SC, & Seeley RJ. 2000. Long-term orexigenic effects of AgRP-(83---132) involve mechanisms other than melanocortin receptor blockade. *American Journal of Physiology. Regulatory, Integrative and Comparative Physiology* 279: R47-52

Hahn JD, & Swanson LW. 2010. Distinct patterns of neuronal inputs and outputs of the juxtaparaventricular and suprafornical regions of the lateral hypothalamic area in the male rat. *Brain Research Reviews* 64: 14-103

Hahn TM, Breininger JF, Baskin DG, & Schwartz MW. 1998. Coexpression of Agrp and NPY in fasting-activated hypothalamic neurons. *Nature Neuroscience* 1: 271-2

Halford JC, Harrold JA, Lawton CL, & Blundell JE. 2005. Serotonin (5-HT) drugs: effects on appetite expression and use for the treatment of obesity. *Current Drug Targets* 6: 201-13

Hara J, Beuckmann CT, Nambu T, Willie JT, Chemelli RM, Sinton CM, Sugiyama F, Yagami K, Goto K, Yanagisawa M, & Sakurai T. 2001. Genetic ablation of orexin neurons in mice results in narcolepsy, hypophagia, and obesity. *Neuron* 30: 345-54

Haskell-Luevano C, Chen P, Li C, Chang K, Smith MS, Cameron JL, & Cone RD. 1999. Characterization of the neuroanatomical distribution of agouti-related protein immunoreactivity in the rhesus monkey and the rat. *Endocrinology* 140: 1408-15

Hausser M. 2014. Optogenetics: the age of light. *Nature Methods* 11: 1012-4

Havel PJ. 1999. Mechanisms regulating leptin production: implications for control of energy balance. *The American Journal of Clinical Nutrition* 70: 305-6

Hegyi K, Fulop K, Kovacs K, Toth S, & Falus A. 2004. Leptin-induced signal transduction pathways. *Cell biology International* 28: 159-69

Heisler LK, Jobst EE, Sutton GM, Zhou L, Borok E, Thornton-Jones Z, Liu HY, Zigman JM, Balthasar N, Kishi T, Lee CE, Aschkenasi CJ, Zhang CY, Yu J, Boss O, Mountjoy KG, Clifton PG, Lowell BB, Friedman JM, Horvath T, Butler AA, Elmquist JK, & Cowley MA. 2006. Serotonin reciprocally regulates melanocortin neurons to modulate food intake. *Neuron* 51: 239-49

Hervey GR. 1959. The effects of lesions in the hypothalamus in parabiotic rats. *The Journal of Physiology* 145: 336-52

Hetherington AW, & Ranson SW. 1940. Hypothalamic lesions and adiposity in the rat. *Anatomical Record* 78: 149-72

Hetherington AW, & Ranson SW. 1942. The relation of various hypothalamic lesions to adiposity in the rat. *Journal of Comparative Neurology* 76: 475-99

Hilgard ER, & Marquis DG. 1940. *Conditioning and learning*. New York, London: D. Appleton-Century Company. xi p. 429

Hodos W. 1961. Progressive ratio as a measure of reward strength. *Science* 134: 943-4

Hoebel BG. 1971. Feeding: neural control of intake. *Annual Review of Physiology* 33: 533-68

Holloway BB, Stornetta RL, Bochorishvili G, Erisir A, Viar KE, & Guyenet PG. 2013. Monosynaptic glutamatergic activation of locus coeruleus and other lower brainstem noradrenergic neurons by the C1 cells in mice. *The Journal of Neuroscience* 33: 18792-805

Holmgren C, Harkany T, Svennenfors B, & Zilberter Y. 2003. Pyramidal cell communication within local networks in layer 2/3 of rat neocortex. *The Journal of Physiology* 551: 139-53

Hommel JD, Trinko R, Sears RM, Georgescu D, Liu ZW, Gao XB, Thurmon JJ, Marinelli M, & DiLeone RJ. 2006. Leptin receptor signaling in midbrain dopamine neurons regulates feeding. *Neuron* 51: 801-10

Horvath TL, Bechmann I, Naftolin F, Kalra SP, & Leranth C. 1997. Heterogeneity in the neuropeptide Y-containing neurons of the rat arcuate nucleus: GABAergic and non-GABAergic subpopulations. *Brain Research* 756: 283-6

Horvath TL, Naftolin F, Kalra SP, & Leranth C. 1992. Neuropeptide-Y innervation of beta-endorphin-containing cells in the rat mediobasal hypothalamus: a light and electron microscopic double immunostaining analysis. *Endocrinology* 131: 2461-7

Hull CL. 1943. *Principles of Behavior*. New York: D. Appleton-Century Co. p. 421

Hummel KP, Dickie MM, & Coleman DL. 1966. Diabetes, a new mutation in the mouse. *Science* 153: 1127-8

Inagaki HK, Ben-Tabou de-Leon S, Wong AM, Jagadish S, Ishimoto H, Barnea G, Kitamoto T, Axel R, & Anderson DJ. 2012. Visualizing neuromodulation in vivo: TANGO-mapping of dopamine signaling reveals appetite control of sugar sensing. *Cell* 148: 583-95

Ingalls AM, Dickie MM, & Snell GD. 1950. Obese, a new mutation in the house mouse. *The Journal of Heredity* 41: 317-8

Inutsuka A, Inui A, Tabuchi S, Tsunematsu T, Lazarus M, & Yamanaka A. 2014. Concurrent and robust regulation of feeding behaviors and metabolism by orexin neurons. *Neuropharmacology* 85: 451-60

Irving AJ, & Harvey J. 2014. Leptin regulation of hippocampal synaptic function in health and disease. *Philosophical Transactions of the Royal Society of London. Series B, Biological Sciences* 369: 20130155

Ishizuka T, Kakuda M, Araki R, & Yawo H. 2006. Kinetic evaluation of photosensitivity in genetically engineered neurons expressing green algae light-gated channels. *Neuroscience Research* 54: 85-94

Jacob NM, B.S.; Joel, K.; Elmquist, D.V.M. 2005. *Orexin Projections and Locatization of Orexin Receptors. The Orexin/Hypocretin System*. Totowa NJ: Humana Press Inc. p. 21-23.

Jaitin DA, Kenigsberg E, Keren-Shaul H, Elefant N, Paul F, Zaretsky I, Mildner A, Cohen N, Jung S, Tanay A, & Amit I. 2014. Massively parallel single-cell RNA-seq for marker-free decomposition of tissues into cell types. *Science* 343: 776-9

Jenck F, Gratton A, & Wise RA. 1986. Opposite effects of ventral tegmental and periaqueductal gray morphine injections on lateral hypothalamic stimulation-induced feeding. *Brain Research* 399: 24-32

Jennings JH, Rizzi G, Stamatakis AM, Ung RL, & Stuber GD. 2013. The inhibitory circuit architecture of the lateral hypothalamus orchestrates feeding. *Science* 341: 1517-21

Johnson PL, Lightman SL, & Lowry CA. 2004. A functional subset of serotonergic neurons in the rat ventrolateral periaqueductal gray implicated in the inhibition of sympathoexcitation and panic. *Annals of the New York Academy of Sciences* 1018: 58-64

Karnani MM, Apergis-Schoute J, Adamantidis A, Jensen LT, de Lecea L, Fugger L, & Burdakov D. 2011. Activation of central orexin/hypocretin neurons by dietary amino acids. *Neuron* 72: 616-29

Karnani MM, Szabo G, Erdelyi F, & Burdakov D. 2013. Lateral hypothalamic GAD65 neurons are spontaneously firing and distinct from orexin- and melanin-concentrating hormone neurons. *The Journal of Physiology* 591: 933-53

Kawai K, Sugimoto K, Nakashima K, Miura H, & Ninomiya Y. 2000. Leptin as a modulator of sweet taste sensitivities in mice. *Proceedings of the National Academy of Sciences of the United States of America* 97: 11044-9

Kaye WH, Wierenga CE, Bailer UF, Simmons AN, & Bischoff-Grethe A. 2013. Nothing tastes as good as skinny feels: the neurobiology of anorexia nervosa. *Trends in Neurosciences* 36: 110-20

Kempadoo KA, Tourino C, Cho SL, Magnani F, Leininger GM, Stuber GD, Zhang F, Myers MG, Deisseroth K, de Lecea L, & Bonci A. 2013. Hypothalamic neurotensin projections promote reward by enhancing glutamate transmission in the VTA. *The Journal of Neuroscience* 33: 7618-26

Kennedy GC. 1950. The hypothalamic control of food intake in rats. *Proceedings of The Royal Society of London. Series B, Biological Sciences* 137: 535-49

Kenny PJ. 2011. Reward mechanisms in obesity: new insights and future directions. *Neuron* 69: 664-79

Keys A, Brozek J, Henshel A, Mickelsen O, & Taylor HL. 1950. *The biology of human starvation*. Minneapolis: University of Minnesota Press. p. 1385

King T, Vera-Portocarrero L, Gutierrez T, Vanderah TW, Dussor G, Lai J, Fields HL, & Porreca F. 2009. Unmasking the tonic-aversive state in neuropathic pain. *Nature Neuroscience* 12: 1364-6

Kishi T, Aschkenasi CJ, Lee CE, Mountjoy KG, Saper CB, & Elmquist JK. 2003. Expression of melanocortin 4 receptor mRNA in the central nervous system of the rat. *The Journal of Comparative Neurology* 457: 213-35

Klebig ML, Wilkinson JE, Geisler JG, & Woychik RP. 1995. Ectopic expression of the agouti gene in transgenic mice causes obesity, features of type II diabetes, and yellow fur. *Proceedings of the National Academy of Sciences of the United States of America* 92: 4728-32

Kojima M, Hosoda H, Date Y, Nakazato M, Matsuo H, & Kangawa K. 1999. Ghrelin is a growth-hormone-releasing acylated peptide from stomach. *Nature* 402: 656-60

Konner AC, Janoschek R, Plum L, Jordan SD, Rother E, Ma X, Xu C, Enriori P, Hampel B, Barsh GS, Kahn CR, Cowley MA, Ashcroft FM, & Bruning JC. 2007. Insulin action in AgRP-expressing neurons is required for suppression of hepatic glucose production. *Cell Metabolism* 5: 438-49

Koob GF. 2013. Negative reinforcement in drug addiction: the darkness within. *Current Opinion in Neurobiology* 23: 559-63

Koob GF, & Le Moal M. 1997. Drug abuse: hedonic homeostatic dysregulation. *Science* 278: 52-8

Krashes MJ, Koda S, Ye C, Rogan SC, Adams AC, Cusher DS, Maratos-Flier E, Roth BL, & Lowell BB. 2011. Rapid, reversible activation of AgRP neurons drives feeding behavior in mice. *The Journal of Clinical Investigation* 121: 1424-8

Krashes MJ, Shah BP, Koda S, & Lowell BB. 2013. Rapid versus Delayed Stimulation of Feeding by the Endogenously Released AgRP Neuron Mediators GABA, NPY, and AgRP. *Cell Metabolism* 18: 588-95

Krashes MJ, Shah BP, Madara JC, Olson DP, Strochlic DE, Garfield AS, Vong L, Pei H, Watabe-Uchida M, Uchida N, Liberles SD, & Lowell BB. 2014. An excitatory paraventricular nucleus to AgRP neuron circuit that drives hunger. *Nature* 507: 238-42

Krasne FB. 1962. General Disruption Resulting from Electrical Stimulus of Ventromedial Hypothalamus. *Science* 138: 822-3

Krude H, Biebermann H, Luck W, Horn R, Brabant G, & Gruters A. 1998. Severe early-onset obesity, adrenal insufficiency and red hair pigmentation caused by POMC mutations in humans. *Nature Genetics* 19: 155-7

Laque A, Zhang Y, Gettys S, Nguyen TA, Bui K, Morrison CD, & Munzberg H. 2013. Leptin receptor neurons in the mouse hypothalamus are colocalized with the neuropeptide galanin and mediate anorexigenic leptin action. *American journal of physiology. Endocrinology and Metabolism* 304: E999-1011

Lechin F, van der Dijs B, & Hernandez-Adrian G. 2006. Dorsal raphe vs. median raphe serotonergic antagonism. Anatomical, physiological, behavioral, neuroendocrinological, neuropharmacological and clinical evidences: relevance for neuropharmacological therapy. *Progress in Neuro-psychopharmacology & Biological Psychiatry* 30: 565-85

Lee GH, Proenca R, Montez JM, Carroll KM, Darvishzadeh JG, Lee JI, & Friedman JM. 1996. Abnormal splicing of the leptin receptor in diabetic mice. *Nature* 379: 632-5

Leibowitz SF. 1970a. Hypothalamic beta-adrenergic "satiety" system antagonizes an alpha-adrenergic "hunger" system in the rat. *Nature* 226: 963-4

Leibowitz SF. 1970b. Reciprocal hunger-regulating circuits involving alpha- and beta-adrenergic receptors located, respectively, in the ventromedial and lateral hypothalamus. *Proceedings of the National Academy of Sciences of the United States of America* 67: 1063-70

Leibowitz SF. 1978. Adrenergic stimulation of the paraventricular nucleus and its effects on ingestive behavior as a function of drug dose and time of injection in the light-dark cycle. *Brain Research Bulletin* 3: 357-63

Leibowitz SF, Hammer NJ, & Chang K. 1981. Hypothalamic paraventricular nucleus lesions produce overeating and obesity in the rat. *Physiology & Behavior* 27: 1031-40

Leibowitz SF, Weiss GF, & Shor-Posner G. 1988. Hypothalamic serotonin: pharmacological, biochemical, and behavioral analyses of its feeding-suppressive action. *Clinical Neuropharmacology* 11 Suppl 1: S51-71

Leinninger GM, Jo YH, Leshan RL, Louis GW, Yang H, Barrera JG, Wilson H, Opland DM, Faouzi MA, Gong Y, Jones JC, Rhodes CJ, Chua S, Jr., Diano S, Horvath TL, Seeley RJ, Becker JB, Munzberg H, & Myers MG, Jr. 2009. Leptin acts via leptin receptor-expressing lateral hypothalamic neurons to modulate the mesolimbic dopamine system and suppress feeding. *Cell Metabolism* 10: 89-98

Leinninger GM, Opland DM, Jo YH, Faouzi M, Christensen L, Cappellucci LA, Rhodes CJ, Gnegy ME, Becker JB, Pothos EN, Seasholtz AF, Thompson RC, & Myers MG, Jr. 2011. Leptin action via neurotensin neurons controls orexin, the mesolimbic dopamine system and energy balance. *Cell metabolism* 14: 313-23

Leshan RL, Bjornholm M, Munzberg H, & Myers MG, Jr. 2006. Leptin receptor signaling and action in the central nervous system. *Obesity (Silver Spring)* 14 Suppl 5: 208S-12S

Lin JY, Lin MZ, Steinbach P, & Tsien RY. 2009. Characterization of engineered channelrhodopsin variants with improved properties and kinetics. *Biophysical Journal* 96: 1803-14

Lollmann B, Gruninger S, Stricker-Krongrad A, & Chiesi M. 1997. Detection and quantification of the leptin receptor splice variants Ob-Ra, b, and, e in different mouse tissues. *Biochemical and Biophysical Research Communications* 238: 648-52

Lott GK. 2010. gVision: Scientific video and image acquisition. http://gvision-hhmisourceforgenet/.

Louis GW, Leinninger GM, Rhodes CJ, & Myers MG, Jr. 2010. Direct innervation and modulation of orexin neurons by lateral hypothalamic LepRb neurons. *The Journal of Neuroscience* 30: 11278-87

Lu D, Willard D, Patel IR, Kadwell S, Overton L, Kost T, Luther M, Chen W, Woychik RP, Wilkison WO, & et al. 1994. Agouti protein is an antagonist of the melanocyte-stimulating-hormone receptor. *Nature* 371: 799-802

Luiten PG, & Room P. 1980. Interrelations between lateral, dorsomedial and ventromedial hypothalamic nuclei in the rat. An HRP study. *Brain Research* 190: 321-32

Luquet S, Perez FA, Hnasko TS, & Palmiter RD. 2005. NPY/AgRP neurons are essential for feeding in adult mice but can be ablated in neonates. *Science* 310: 683-5

Madisen L, Mao T, Koch H, Zhuo JM, Berenyi A, Fujisawa S, Hsu YW, Garcia AJ, 3rd, Gu X, Zanella S, Kidney J, Gu H, Mao Y, Hooks BM, Boyden ES, Buzsaki G, Ramirez JM, Jones AR, Svoboda K, Han X, Turner EE, & Zeng H. 2012. A toolbox of Cre-dependent optogenetic transgenic mice for light-induced activation and silencing. *Nature Neuroscience* 15: 793-802

Madisen L, Zwingman TA, Sunkin SM, Oh SW, Zariwala HA, Gu H, Ng LL, Palmiter RD, Hawrylycz MJ, Jones AR, Lein ES, & Zeng H. 2010. A robust and high-throughput Cre reporting and characterization system for the whole mouse brain. *Nature Neuroscience* 13: 133-40

Makara GB, & Hodacs L. 1975. Rostral projections from the hypothalamic arcuate nucleus. *Brain Research* 84: 23-9

Margolis EB, Lock H, Hjelmstad GO, & Fields HL. 2006. The ventral tegmental area revisited: is there an electrophysiological marker for dopaminergic neurons? *The Journal of Physiology* 577: 907-24

Margules DL. 1970. Alpha-adrenergic receptors in hypothalamus for the suppression of feeding behavior by satiety. *Journal of Comparative and Physiological Psychology* 73: 1-12

Margules DL, & Olds J. 1962. Identical "feeding" and "rewarding" systems in the lateral hypothalamus of rats. *Science* 135: 374-5

Marshall NB, Barrnett RJ, & Mayer J. 1955. Hypothalamic lesions in goldthioglucose injected mice. *Proceedings of The Society for Experimental Biology and Medicine* 90: 240-4

Mayer J. 1953. Glucostatic mechanism of regulation of food intake. *The New England Journal of Medicine* 249: 13-6

McCutcheon JE, Ebner SR, Loriaux AL, & Roitman MF. 2012. Encoding of aversion by dopamine and the nucleus accumbens. *Frontiers in Neuroscience* 6: 137

Michael A. 1975. Positive and negative reinforcement, a distinction that is no longer necessary; or a better way to talk about bad things. *Behaviorism* 3: 33-44

Miller MW, Duhl DM, Vrieling H, Cordes SP, Ollmann MM, Winkes BM, & Barsh GS. 1993. Cloning of the mouse agouti gene predicts a secreted protein ubiquitously expressed in mice carrying the lethal yellow mutation. *Genes & Development* 7: 454-67

Mistry AM, Swick AG, & Romsos DR. 1997. Leptin rapidly lowers food intake and elevates metabolic rates in lean and ob/ob mice. *The Journal of Nutrition* 127: 2065-72

Miyazaki J, Takaki S, Araki K, Tashiro F, Tominaga A, Takatsu K, & Yamamura K. 1989. Expression vector system based on the chicken beta-actin promoter directs efficient production of interleukin-5. *Gene* 79: 269-77

Moga MM, & Saper CB. 1994. Neuropeptide-immunoreactive neurons projecting to the paraventricular hypothalamic nucleus in the rat. *The Journal of Comparative Neurology* 346: 137-50

Montague CT, Farooqi IS, Whitehead JP, Soos MA, Rau H, Wareham NJ, Sewter CP, Digby JE, Mohammed SN, Hurst JA, Cheetham CH, Earley AR, Barnett AH, Prins JB, & O'Rahilly S. 1997. Congenital leptin deficiency is associated with severe early-onset obesity in humans. *Nature* 387: 903-8

Morton GJ, Meek TH, & Schwartz MW. 2014. Neurobiology of food intake in health and disease. *Nature Reviews Neuroscience* 15: 367-78

Mota-Ortiz SR, Sukikara MH, Bittencourt JC, Baldo MV, Elias CF, Felicio LF, & Canteras NS. 2012. The periaqueductal gray as a critical site to mediate reward seeking during predatory hunting. *Behavioural Brain Research* 226: 32-40

Mounzih K, Lu R, & Chehab FF. 1997. Leptin treatment rescues the sterility of genetically obese ob/ob males. *Endocrinology* 138: 1190-3

Mowrer OH. 1960. *Learnig theory and behavior*. New York: Wiley & Sons., xi p. 473

Myers MG, Jr., Munzberg H, Leininger GM, & Leshan RL. 2009. The geometry of leptin action in the brain: more complicated than a simple ARC. *Cell Metabolism* 9: 117-23

Nakazato M, Murakami N, Date Y, Kojima M, Matsuo H, Kangawa K, & Matsukura S. 2001. A role for ghrelin in the central regulation of feeding. *Nature* 409: 194-8

Napadow V, Sheehan JD, Kim J, Lacount LT, Park K, Kaptchuk TJ, Rosen BR, & Kuo B. 2013. The brain circuitry underlying the temporal evolution of nausea in humans. *Cerebral Cortex* 23: 806-13

Navratilova E, Xie JY, Okun A, Qu C, Eyde N, Ci S, Ossipov MH, King T, Fields HL, & Porreca F. 2012. Pain relief produces negative reinforcement through activation of mesolimbic reward-valuation circuitry. *Proceedings of the National Academy of Sciences of the United States of America* 109: 20709-13

Nichols CD, & Roth BL. 2009. Engineered G-protein Coupled Receptors are Powerful Tools to Investigate Biological Processes and Behaviors. *Frontiers in Molecular Neuroscience* 2: 16

Niwa H, Yamamura K, & Miyazaki J. 1991. Efficient selection for high-expression transfectants with a novel eukaryotic vector. *Gene* 108: 193-9

Ogawa S, Kow LM, & Pfaff DW. 1992. Effects of lordosis-relevant neuropeptides on midbrain periaqueductal gray neuronal activity in vitro. *Peptides* 13: 965-75

Olds J. 1969. The central nervous system and the reinforcement of behavior. *The American Psychologist* 24: 114-32

Olds J. 1976. Brain stimulation and the motivation of behavior. *Progress in Brain Research* 45: 401-26

Olds J, & Milner P. 1954. Positive reinforcement produced by electrical stimulation of septal area and other regions of rat brain. *Journal of Comparative and Physiological Psychology* 47: 419-27

Ollmann MM, Wilson BD, Yang YK, Kerns JA, Chen Y, Gantz I, & Barsh GS. 1997. Antagonism of central melanocortin receptors in vitro and in vivo by agouti-related protein. *Science* 278: 135-8

Olney JW. 1969. Brain lesions, obesity, and other disturbances in mice treated with monosodium glutamate. *Science* 164: 719-21

Olney JW, Adamo NJ, & Ratner A. 1971. Monosodium glutamate effects. *Science* 172: 294

Ostlund SB, Wassum KM, Murphy NP, Balleine BW, & Maidment NT. 2011. Extracellular dopamine levels in striatal subregions track shifts in motivation and response cost during instrumental conditioning. *The Journal of Neuroscience* 31: 200-7

Oswal A, & Yeo G. 2010. Leptin and the control of body weight: a review of its diverse central targets, signaling mechanisms, and role in the pathogenesis of obesity. *Obesity (Silver Spring)* 18: 221-9

Overduin J, Figlewicz DP, Bennett-Jay J, Kittleson S, & Cummings DE. 2012. Ghrelin increases the motivation to eat, but does not alter food palatability. *American Journal of Physiology. Regulatory, Integrative and Comparative Physiology* 303: R259-69

Pasquet P, Monneuse MO, Simmen B, Marez A, & Hladik CM. 2006. Relationship between taste thresholds and hunger under debate. *Appetite* 46: 63-6

Pei Y, Rogan SC, Yan F, & Roth BL. 2008. Engineered GPCRs as tools to modulate signal transduction. *Physiology (Bethesda)* 23: 313-21

Pelleymounter MA, Cullen MJ, Baker MB, Hecht R, Winters D, Boone T, & Collins F. 1995. Effects of the obese gene product on body weight regulation in ob/ob mice. *Science* 269: 540-3

Peng H, Ruan Z, Atasoy D, & Sternson S. 2010. Automatic reconstruction of 3D neuron structures using a graph-augmented deformable model. *Bioinformatics* 26: i38-46

Petreanu L, Huber D, Sobczyk A, & Svoboda K. 2007. Channelrhodopsin-2-assisted circuit mapping of long-range callosal projections. *Nature Neuroscience* 10: 663-8

Petrovich GD, Ross CA, Mody P, Holland PC, & Gallagher M. 2009. Central, but not basolateral, amygdala is critical for control of feeding by aversive learned cues. *The Journal of Neuroscience* 29: 15205-12

Plata-Salaman CR, & Oomura Y. 1986. Effect of intra-third ventricular administration of insulin on food intake after food deprivation. *Physiology & Behavior* 37: 735-9

Prewitt CM, & Herman JP. 1998. Anatomical interactions between the central amygdaloid nucleus and the hypothalamic paraventricular nucleus of the rat: a dual tract-tracing analysis. *Journal of Chemical Neuroanatomy* 15: 173-85

Pronchuk N, Beck-Sickinger AG, & Colmers WF. 2002. Multiple NPY receptors Inhibit GABA(A) synaptic responses of rat medial parvocellular effector neurons in the hypothalamic paraventricular nucleus. *Endocrinology* 143: 535-43

Qian S, Chen H, Weingarth D, Trumbauer ME, Novi DE, Guan X, Yu H, Shen Z, Feng Y, Frazier E, Chen A, Camacho RE, Shearman LP, Gopal-Truter S, MacNeil DJ, Van der Ploeg LH, & Marsh DJ. 2002. Neither agouti-related protein nor neuropeptide Y is critically required for the regulation of energy homeostasis in mice. *Molecular and Cellular Biology* 22: 5027-35

Quiros-Gonzalez I, & Yadav VK. 2014. Central genes, pathways and modules that regulate bone mass. *Archives of Biochemistry and Biophysics* 651: 130-6

Ramos EJ, Meguid MM, Campos AC, & Coelho JC. 2005. Neuropeptide Y, alpha-melanocyte-stimulating hormone, and monoamines in food intake regulation. *Nutrition* 21: 269-79

Randolph TG. 1956. The descriptive features of food addiction; addictive eating and drinking. *Quarterly Journal of Studies on Alcohol* 17: 198-224

Reilly S, & Trifunovic R. 2000. Lateral parabrachial nucleus lesions in the rat: aversive and appetitive gustatory conditioning. *Brain Research Bulletin* 52: 269-78

Richter CP. 1943. Total self regulatory functions in animals and human beings. *Harvey Lectures* 38: 63-103

Risold PY, Thompson RH, & Swanson LW. 1997. The structural organization of connections between hypothalamus and cerebral cortex. *Brain Research Reviews* 24: 197-254

Rodgers RJ, Halford JC, Nunes de Souza RL, Canto de Souza AL, Piper DC, Arch JR, & Blundell JE. 2000. Dose-response effects of orexin-A on food intake and the behavioural satiety sequence in rats. *Regulatory Peptides* 96: 71-84

Rodgers RJ, Halford JC, Nunes de Souza RL, Canto de Souza AL, Piper DC, Arch JR, Upton N, Porter RA, Johns A, & Blundell JE. 2001. SB-334867, a selective orexin-1 receptor antagonist, enhances behavioural satiety and blocks the hyperphagic effect of orexin-A in rats. *The European Journal of Neuroscience* 13: 1444-52

Rolls ET, Rolls BJ, & Rowe EA. 1983. Sensory-specific and motivation-specific satiety for the sight and taste of food and water in man. *Physiology & Behavior* 30: 185-92

Rolls ET, & Rolls JH. 1997. Olfactory sensory-specific satiety in humans. *Physiology & Behavior* 61: 461-73

Root CM, Ko KI, Jafari A, & Wang JW. 2011. Presynaptic facilitation by neuropeptide signaling mediates odor-driven food search. *Cell* 145: 133-44

Rosin DL, Weston MC, Sevigny CP, Stornetta RL, & Guyenet PG. 2003. Hypothalamic orexin (hypocretin) neurons express vesicular glutamate transporters VGLUT1 or VGLUT2. *The Journal of Comparative Neurology* 465: 593-603

Salamone JD, Correa M, Farrar AM, Nunes EJ, & Pardo M. 2009. Dopamine, behavioral economics, and effort. *Frontiers in Behavioral Neuroscience* 3: 13

Salamone JD, Cousins MS, & Bucher S. 1994. Anhedonia or anergia? Effects of haloperidol and nucleus accumbens dopamine depletion on instrumental response selection in a T-maze cost/benefit procedure. *Behavioural Brain Research* 65: 221-9

Salamone JD, Cousins MS, & Snyder BJ. 1997. Behavioral functions of nucleus accumbens dopamine: empirical and conceptual problems with the anhedonia hypothesis. *Neuroscience and Biobehavioral Reviews* 21: 341-59

Samano C, Cifuentes F, & Morales MA. 2012. Neurotransmitter segregation: functional and plastic implications. *Progress in Neurobiology* 97: 277-87

Saper CB, Chou TC, & Elmquist JK. 2002. The need to feed: homeostatic and hedonic control of eating. *Neuron* 36: 199-211

Savigner A, Duchamp-Viret P, Grosmaitre X, Chaput M, Garcia S, Ma M, & Palouzier-Paulignan B. 2009. Modulation of spontaneous and odorant-evoked activity of rat olfactory sensory neurons by two anorectic peptides, insulin and leptin. *Journal of Neurophysiology* 101: 2898-906

Schnutgen F, Doerflinger N, Calleja C, Wendling O, Chambon P, & Ghyselinck NB. 2003. A directional strategy for monitoring Cre-mediated recombination at the cellular level in the mouse. *Nature Biotechnology* 21: 562-5

Schoenenberger P, Scharer YP, & Oertner TG. 2011. Channelrhodopsin as a tool to investigate synaptic transmission and plasticity. *Experimental Physiology* 96: 34-9

Schone C, Apergis-Schoute J, Sakurai T, Adamantidis A, & Burdakov D. 2014. Coreleased orexin and glutamate evoke nonredundant spike outputs and computations in histamine neurons. *Cell Reports* 7: 697-704

Schone C, Huang Cao ZF, Apergis-Schoute J, Adamantidis A, Sakurai T, & Burdakov D. 2012. Optogenetic probing of fast glutamatergic transmission from hypocretin/orexin to histamine neurons in situ. *The Journal of Neuroscience* 32: 12437-43

Schultz W. 2006. Behavioral theories and the neurophysiology of reward. *Annual Review of Psychology* 57: 87-115

Schultz W, Dayan P, & Montague PR. 1997. A neural substrate of prediction and reward. *Science* 275: 1593-9

Schwartz MW, Woods SC, Porte D, Jr., Seeley RJ, & Baskin DG. 2000. Central nervous system control of food intake. *Nature* 404: 661-71

Sclafani A, & Berner CN. 1977. Hyperphagia and obesity produced by parasagittal and coronal hypothalamic knife cuts: further evidence for a longitudinal feeding inhibitory pathway. *Journal of Comparative and Physiological Psychology* 91: 1000-18

Sclafani A, Berner CN, & Maul G. 1975. Multiple knife cuts between the medial and lateral hypothalamus in the rat: a reevaluation of hypothalamic feeding circuitry. *Journal of Comparative and Physiological Psychology* 88: 201-7

Sclafani A, & Nissenbaum JW. 1988. Robust conditioned flavor preference produced by intragastric starch infusions in rats. *The American Journal of Physiology* 255: R672-5

Scott MM, Lachey JL, Sternson SM, Lee CE, Elias CF, Friedman JM, & Elmquist JK. 2009. Leptin targets in the mouse brain. *The Journal of Comparative Neurology* 514: 518-32

Seeley RJ, & Woods SC. 2003. Monitoring of stored and available fuel by the CNS: implications for obesity. *Nature Reviews Neuroscience* 4: 901-9

Sengupta P. 2013. The belly rules the nose: feeding state-dependent modulation of peripheral chemosensory responses. *Current Opinion in Neurobiology* 23: 68-75

Shapiro MG, Frazier SJ, & Lester HA. 2012. Unparalleled control of neural activity using orthogonal pharmacogenetics. *ACS Chemical Neuroscience* 3: 619-29

Shin JW, Geerling JC, & Loewy AD. 2008. Inputs to the ventrolateral bed nucleus of the stria terminalis. *The Journal of Comparative Neurology* 511: 628-57

Skinner BF. 1938. *The behavior of organisms : an experimental analysis.* New York, London: D. Appleton-Century Company, Inc. ix, p. 457

Skultety FM. 1958. The behavioral effects of destructive lesions of the periaqueductal gray matter in adult cats. *The Journal of Comparative Neurology* 110: 337-65

Small CJ, Kim MS, Stanley SA, Mitchell JR, Murphy K, Morgan DG, Ghatei MA, & Bloom SR. 2001. Effects of chronic central nervous system administration of agouti-related protein in pair-fed animals. *Diabetes* 50: 248-54

Smith DG, & Robbins TW. 2013. The neurobiological underpinnings of obesity and binge eating: a rationale for adopting the food addiction model. *Biological Psychiatry* 73: 804-10

Smith GP, & Epstein AN. 1969. Increased feeding in response to decreased glucose utilization in the rat and monkey. *The American Journal of Physiology* 217: 1083-7

Sohn JW, Elmquist JK, & Williams KW. 2013. Neuronal circuits that regulate feeding behavior and metabolism. *Trends in Neurosciences* 36: 504-12

Spaethling JM, Piel D, Dueck H, Buckley PT, Morris JF, Fisher SA, Lee J, Sul JY, Kim J, Bartfai T, Beck SG, & Eberwine JH. 2014. Serotonergic neuron regulation informed by in vivo single-cell transcriptomics. *FASEB Journal* 28: 771-80

Spanswick D, Smith MA, Groppi VE, Logan SD, & Ashford ML. 1997. Leptin inhibits hypothalamic neurons by activation of ATP-sensitive potassium channels. *Nature* 390: 521-5

Stachniak TJ, Ghosh A, & Sternson SM. 2014. Chemogenetic synaptic silencing of neural circuits localizes a hypothalamus-->midbrain pathway for feeding behavior. *Neuron* 82: 797-808

Stafford LD, & Welbeck K. 2011. High hunger state increases olfactory sensitivity to neutral but not food odors. *Chemical Senses* 36: 189-98

Stamatakis AM, & Stuber GD. 2012. Activation of lateral habenula inputs to the ventral midbrain promotes behavioral avoidance. *Nature Neuroscience* 15: 1105-7

Stanley BG, & Leibowitz SF. 1984. Neuropeptide Y: stimulation of feeding and drinking by injection into the paraventricular nucleus. *Life Sciences* 35: 2635-42

Sternson SM. 2013. Hypothalamic survival circuits: blueprints for purposive behaviors. *Neuron* 77: 810-24

Sternson SM, Nicholas Betley J, & Huang Cao ZF. 2013. Neural circuits and motivational processes for hunger. *Current Opinion in Neurobiology* 23: 353-60

Stoeckel LE, Cox JE, Cook EW, 3rd, & Weller RE. 2007. Motivational state modulates the hedonic value of food images differently in men and women. *Appetite* 48: 139-44

Stratford TR, & Wirtshafter D. 2013. Injections of muscimol into the paraventricular thalamic nucleus, but not mediodorsal thalamic nuclei, induce feeding in rats. *Brain Research* 1490: 128-33

Strubbe JH, & Mein CG. 1977. Increased feeding in response to bilateral injection of insulin antibodies in the VMH. *Physiology & Behavior* 19: 309-13

Stuart GJ, & Hausser M. 2001. Dendritic coincidence detection of EPSPs and action potentials. *Nature Neuroscience* 4: 63-71

Stuber GD, Hnasko TS, Britt JP, Edwards RH, & Bonci A. 2010. Dopaminergic terminals in the nucleus accumbens but not the dorsal striatum corelease glutamate. *The Journal of Neuroscience* 30: 8229-33

Stunkard AJ, & Rush J. 1974. Dieting and depression reexamined. A critical review of reports of untoward responses during weight reduction for obesity. *Annals of Internal Medicine* 81: 526-33

Sun Y, Ahmed S, & Smith RG. 2003. Deletion of ghrelin impairs neither growth nor appetite. *Molecular and Cellular Biology* 23: 7973-81

Swanson LW. 2000. Cerebral hemisphere regulation of motivated behavior. *Brain Research* 886: 113-64

Swanson LW, & Sawchenko PE. 1983. Hypothalamic integration: organization of the paraventricular and supraoptic nuclei. *Annual Review of Neuroscience* 6: 269-324

Takahashi KA, & Cone RD. 2005. Fasting induces a large, leptin-dependent increase in the intrinsic action potential frequency of orexigenic arcuate nucleus neuropeptide Y/Agouti-related protein neurons. *Endocrinology* 146: 1043-7

Tartaglia LA, Dembski M, Weng X, Deng N, Culpepper J, Devos R, Richards GJ, Campfield LA, Clark FT, Deeds J, Muir C, Sanker S, Moriarty A, Moore KJ, Smutko JS, Mays GG, Wool EA, Monroe CA, & Tepper RI. 1995. Identification and expression cloning of a leptin receptor, OB-R. *Cell* 83: 1263-71

Tecuapetla F, Patel JC, Xenias H, English D, Tadros I, Shah F, Berlin J, Deisseroth K, Rice ME, Tepper JM, & Koos T. 2010. Glutamatergic signaling by mesolimbic dopamine neurons in the nucleus accumbens. *The Journal of Neuroscience* 30: 7105-10

Thomson AM, West DC, Wang Y, & Bannister AP. 2002. Synaptic connections and small circuits involving excitatory and inhibitory neurons in layers 2-5 of adult rat and cat neocortex: triple intracellular recordings and biocytin labelling in vitro. *Cerebral Cortex* 12: 936-53

Thorndike EL. 1898. *Animal intelligence, an experimental study of the associative processes in animals*. New York: Macmillan. p. 100

Tinbergen N. 1989. *The study of instinct*. Oxford England: Oxford University Press; New York: Clarendon Press; xxii, p. 228

Tong Q, Ye CP, Jones JE, Elmquist JK, & Lowell BB. 2008. Synaptic release of GABA by AgRP neurons is required for normal regulation of energy balance. *Nature Neuroscience* 11: 998-1000

Tschop M, Smiley DL, & Heiman ML. 2000. Ghrelin induces adiposity in rodents. *Nature* 407: 908-13

Tsujino N, & Sakurai T. 2013. Role of orexin in modulating arousal, feeding, and motivation. *Frontiers in Behavioral Neuroscience* 7: 28

Ungerstedt U. 1971. Adipsia and aphagia after 6-hydroxydopamine induced degeneration of the nigro-striatal dopamine system. *Acta Physiologica Scandinavica. Supplementum* 367: 95-122

Valassi E, Scacchi M, & Cavagnini F. 2008. Neuroendocrine control of food intake. *Nutrition, Metabolism, and Cardiovascular Diseases : NMCD* 18: 158-68

van den Pol AN, Acuna-Goycolea C, Clark KR, & Ghosh PK. 2004. Physiological properties of hypothalamic MCH neurons identified with selective expression of reporter gene after recombinant virus infection. *Neuron* 42: 635-52

van den Top M, Lee K, Whyment AD, Blanks AM, & Spanswick D. 2004. Orexigen-sensitive NPY/AgRP pacemaker neurons in the hypothalamic arcuate nucleus. *Nature Neuroscience* 7: 493-4

van Swieten MM, Pandit R, Adan RA, & van der Plasse G. 2014. The neuroanatomical function of leptin in the hypothalamus. *Journal of Chemical Neuroanatomy* 61-62: 207-20

van Zessen R, Phillips JL, Budygin EA, & Stuber GD. 2012. Activation of VTA GABA neurons disrupts reward consumption. *Neuron* 73: 1184-94

Volman SF, Lammel S, Margolis EB, Kim Y, Richard JM, Roitman MF, & Lobo MK. 2013. New insights into the specificity and plasticity of reward and aversion encoding in the mesolimbic system. *The Journal of Neuroscience* 33: 17569-76

Wadden TA, Stunkard AJ, & Smoller JW. 1986. Dieting and depression: a methodological study. *Journal of Consulting and Clinical Psychology* 54: 869-71

Walker DL, Toufexis DJ, & Davis M. 2003. Role of the bed nucleus of the stria terminalis versus the amygdala in fear, stress, and anxiety. *European Journal of Pharmacology* 463: 199-216

Wang H, Peca J, Matsuzaki M, Matsuzaki K, Noguchi J, Qiu L, Wang D, Zhang F, Boyden E, Deisseroth K, Kasai H, Hall WC, Feng G, & Augustine GJ. 2007. High-speed mapping of synaptic connectivity using photostimulation in Channelrhodopsin-2 transgenic mice. *Proceedings of the National Academy of Sciences of the United States of America* 104: 8143-8

Ward HG, & Simansky KJ. 2006. Chronic prevention of mu-opioid receptor (MOR) G-protein coupling in the pontine parabrachial nucleus persistently decreases consumption of standard but not palatable food. *Psychopharmacology* 187: 435-46

Webb WB. 1955. Drive stimuli as cues. *Psychological Reports* 1: 287-98

Williams DL, & Cummings DE. 2005. Regulation of ghrelin in physiologic and pathophysiologic states. *The Journal of Nutrition* 135: 1320-5

Williams RH, Morton AJ, & Burdakov D. 2011. Paradoxical function of orexin/hypocretin circuits in a mouse model of Huntington's disease. *Neurobiology of Disease* 42: 438-45

Williams SR, & Mitchell SJ. 2008. Direct measurement of somatic voltage clamp errors in central neurons. *Nature Neuroscience* 11: 790-8

Williams SR, & Stuart GJ. 2003. Role of dendritic synapse location in the control of action potential output. *Trends in Neurosciences* 26: 147-54

Wise RA. 1974. Lateral hypothalamic electrical stimulation: does it make animals 'hungry'? *Brain Research* 67: 187-209

Wittmann G, Fuzesi T, Singru PS, Liposits Z, Lechan RM, & Fekete C. 2009. Efferent projections of thyrotropin-releasing hormone-synthesizing neurons residing in the anterior parvocellular subdivision of the hypothalamic paraventricular nucleus. *The Journal of Comparative Neurology* 515: 313-30

Woods SC, Lotter EC, McKay LD, & Porte D, Jr. 1979. Chronic intracerebroventricular infusion of insulin reduces food intake and body weight of baboons. *Nature* 282: 503-5

Wren AM, Seal LJ, Cohen MA, Brynes AE, Frost GS, Murphy KG, Dhillo WS, Ghatei MA, & Bloom SR. 2001. Ghrelin enhances appetite and increases food intake in humans. *The Journal of Clinical Endocrinology and Metabolism* 86: 5992

Wu Q, Boyle MP, & Palmiter RD. 2009. Loss of GABAergic signaling by AgRP neurons to the parabrachial nucleus leads to starvation. *Cell* 137: 1225-34

Wu Q, Clark MS, & Palmiter RD. 2012. Deciphering a neuronal circuit that mediates appetite. *Nature* 483: 594-7

Wu Q, Howell MP, Cowley MA, & Palmiter RD. 2008. Starvation after AgRP neuron ablation is independent of melanocortin signaling. *Proceedings of the National Academy of Sciences of the United States of America* 105: 2687-92

Xia Y, Driscoll JR, Wilbrecht L, Margolis EB, Fields HL, & Hjelmstad GO. 2011. Nucleus accumbens medium spiny neurons target non-dopaminergic neurons in the ventral tegmental area. *The Journal of Neuroscience* 31: 7811-6

Xu L. 2014. Leptin action in the midbrain: From reward to stress. *Journal of Chemical Neuroanatomy* 61-62: 256-65

Xu Y, Wu Z, Sun H, Zhu Y, Kim ER, Lowell BB, Arenkiel BR, & Tong Q. 2013. Glutamate mediates the function of melanocortin receptor 4 on Sim1 neurons in body weight regulation. *Cell Metabolism* 18: 860-70

Yamanaka A, Beuckmann CT, Willie JT, Hara J, Tsujino N, Mieda M, Tominaga M, Yagami K, Sugiyama F, Goto K, Yanagisawa M, & Sakurai T. 2003. Hypothalamic orexin neurons regulate arousal according to energy balance in mice. *Neuron* 38: 701-13

Yang Y, Atasoy D, Su HH, & Sternson SM. 2011. Hunger states switch a flip-flop memory circuit via a synaptic AMPK-dependent positive feedback loop. *Cell* 146: 992-1003

Yang YK, Thompson DA, Dickinson CJ, Wilken J, Barsh GS, Kent SB, & Gantz I. 1999. Characterization of Agouti-related protein binding to melanocortin receptors. *Molecular Endocrinology* 13: 148-55

Yaswen L, Diehl N, Brennan MB, & Hochgeschwender U. 1999. Obesity in the mouse model of pro-opiomelanocortin deficiency responds to peripheral melanocortin. *Nature Medicine* 5: 1066-70

Yaxley S, Rolls ET, & Sienkiewicz ZJ. 1988. The responsiveness of neurons in the insular gustatory cortex of the macaque monkey is independent of hunger. *Physiology & Behavior* 42: 223-9

Yaxley S, Rolls ET, Sienkiewicz ZJ, & Scott TR. 1985. Satiety does not affect gustatory activity in the nucleus of the solitary tract of the alert monkey. *Brain Research* 347: 85-93

Yeomans MR, & Mobini S. 2006. Hunger alters the expression of acquired hedonic but not sensory qualities of food-paired odors in humans. *Journal of Experimental Psychology. Animal Behavior Processes* 32: 460-6

Yiin YM, Ackroff K, & Sclafani A. 2005. Flavor preferences conditioned by intragastric nutrient infusions in food restricted and free-feeding rats. *Physiology & Behavior* 84: 217-31

Yizhar O, Fenno LE, Davidson TJ, Mogri M, & Deisseroth K. 2011. Optogenetics in neural systems. *Neuron* 71: 9-34

Young A, & Sun QQ. 2009. GABAergic inhibitory interneurons in the posterior piriform cortex of the GAD67-GFP mouse. *Cerebral Cortex* 19: 3011-29

Yulyaningsih E, Zhang L, Herzog H, & Sainsbury A. 2011. NPY receptors as potential targets for anti-obesity drug development. *British Journal of Pharmacology* 163: 1170-202

Zhang F, Gradinaru V, Adamantidis AR, Durand R, Airan RD, de Lecea L, & Deisseroth K. 2010. Optogenetic interrogation of neural circuits: technology for probing mammalian brain structures. *Nature Protocols* 5: 439-56

Zhang F, Wang LP, Brauner M, Liewald JF, Kay K, Watzke N, Wood PG, Bamberg E, Nagel G, Gottschalk A, & Deisseroth K. 2007. Multimodal fast optical interrogation of neural circuitry. *Nature* 446: 633-9

Zhang Y, Proenca R, Maffei M, Barone M, Leopold L, & Friedman JM. 1994. Positional cloning of the mouse obese gene and its human homologue. *Nature* 372: 425-32

Zhao S, Cunha C, Zhang F, Liu Q, Gloss B, Deisseroth K, Augustine GJ, & Feng G. 2008. Improved expression of halorhodopsin for light-induced silencing of neuronal activity. *Brain Cell Biology* 36: 141-54

Zverev YP. 2004. Effects of caloric deprivation and satiety on sensitivity of the gustatory system. *BMC Neuroscience* 5: 5